

A microscopic view of cells, likely a petri dish, with a pipette tip visible in the upper left. The background is a vibrant orange-red color with a blue circular arc on the right side.

# Reviews of Physiology, Biochemistry and Pharmacology 171

# Reviews of Physiology, Biochemistry and Pharmacology

More information about this series at <http://www.springer.com/series/112>

Bernd Nilius · Pieter de Tombe ·  
Thomas Gudermann · Reinhard Jahn ·  
Roland Lill · Ole H. Petersen  
Editors

Reviews of Physiology,  
Biochemistry and  
Pharmacology  
171

 Springer

*Editor in Chief*

Bernd Nilius  
KU Leuven  
Leuven  
Belgium

*Editors*

Pieter de Tombe  
Cardiovascular Research Center  
Loyola University Chicago  
Maywood, Illinois  
USA

Thomas Gudermann  
Walther-Straub-Institut für  
Pharmakologie und Toxikologie  
München, Bayern  
Germany

Reinhard Jahn  
Department of Neurobiology  
Max-Planck-Institute  
Göttingen, Niedersachsen  
Germany

Roland Lill  
Department of Cytobiology  
University of Marburg  
Marburg  
Germany

Ole H. Petersen  
Cardiff School of Biosciences  
Cardiff University  
Cardiff  
United Kingdom

ISSN 0303-4240

ISSN 1617-5786 (electronic)

Reviews of Physiology, Biochemistry and Pharmacology

ISBN 978-3-319-43813-9

ISBN 978-3-319-43814-6 (eBook)

DOI 10.1007/978-3-319-43814-6

© Springer International Publishing Switzerland 2016

This work is subject to copyright. All rights are reserved by the Publisher, whether the whole or part of the material is concerned, specifically the rights of translation, reprinting, reuse of illustrations, recitation, broadcasting, reproduction on microfilms or in any other physical way, and transmission or information storage and retrieval, electronic adaptation, computer software, or by similar or dissimilar methodology now known or hereafter developed.

The use of general descriptive names, registered names, trademarks, service marks, etc. in this publication does not imply, even in the absence of a specific statement, that such names are exempt from the relevant protective laws and regulations and therefore free for general use.

The publisher, the authors and the editors are safe to assume that the advice and information in this book are believed to be true and accurate at the date of publication. Neither the publisher nor the authors or the editors give a warranty, express or implied, with respect to the material contained herein or for any errors or omissions that may have been made.

Printed on acid-free paper

This Springer imprint is published by Springer Nature

The registered company is Springer International Publishing AG Switzerland

# Contents

<b>Curcumin as a MicroRNA Regulator in Cancer: A Review</b> .....	1
Amir Abbas Momtazi, Fahimeh Shahabipour, Sepideh Khatibi, Thomas P. Johnston, Matteo Pirro, and Amirhossein Sahebkar	
<b>Functional Impact of Ryanodine Receptor Oxidation on Intracellular Calcium Regulation in the Heart</b> .....	39
Aleksy V. Zima and Stefan R. Mazurek	
<b>Electromagnetic Fields and Stem Cell Fate: When Physics Meets Biology</b> .....	63
Sara Hassanpour Tamrin, Fatemeh Sadat Majedi, Mahdi Tondar, Amir Sanati-Nezhad, and Mohammad Mahdi Hasani-Sadrabadi	
<b>The Zebrafish Heart as a Model of Mammalian Cardiac Function</b> .....	99
Christine E. Genge, Eric Lin, Ling Lee, XiaoYe Sheng, Kaveh Rayani, Marvin Gunawan, Charles M. Stevens, Alison Yueh Li, Sanam Shafaat Talab, Thomas W. Claydon, Leif Hove-Madsen, and Glen F. Tibbits	

# Curcumin as a MicroRNA Regulator in Cancer: A Review

**Amir Abbas Momtazi, Fahimeh Shahabipour, Sepideh Khatibi, Thomas P. Johnston, Matteo Pirro, and Amirhossein Sahebkar**

**Abstract** Curcumin is a natural dietary polyphenol for which anti-tumor effects have been documented. Anti-inflammatory and antioxidant properties of curcumin, along with its immunomodulatory, proapoptotic, and antiangiogenic properties, are often referred to as the main mechanisms underlying the anti-tumor effects. At the molecular level, inhibition of NF- $\kappa$ B, Akt/PI3K, and MAPK pathways and enhancement of p53 are among the most important anticancer alterations induced

---

A.A. Momtazi

Student Research Committee, Department of Medical Biotechnology, School of Medicine, Mashhad University of Medical Sciences, Mashhad, Iran

Nanotechnology Research Center, Bu-Ali Research Institute, Mashhad University of Medical Sciences, Mashhad, Iran

F. Shahabipour

National Cell Bank of Iran, Pasteur Institute of Iran, Tehran, Iran

S. Khatibi

Neurogenic Inflammation Research Center, Department of Medical Biotechnology, Mashhad University of Medical Sciences, Mashhad, Iran

T.P. Johnston

Division of Pharmaceutical Sciences, School of Pharmacy, University of Missouri-Kansas City, Kansas City, MO, USA

M. Pirro

Unit of Internal Medicine, Angiology and Arteriosclerosis Diseases, Department of Medicine, University of Perugia, Perugia, Italy

A. Sahebkar (✉)

Biotechnology Research Center, Mashhad University of Medical Sciences, Mashhad 91779-48564, Iran

Metabolic Research Centre, Royal Perth Hospital, School of Medicine and Pharmacology, University of Western Australia, Perth, WA, Australia

e-mail: [sahebkar@mums.ac.ir](mailto:sahebkar@mums.ac.ir); [amir\\_saheb2000@yahoo.com](mailto:amir_saheb2000@yahoo.com); [amirhossein.sahebkar@uwa.edu.au](mailto:amirhossein.sahebkar@uwa.edu.au)

by curcumin. Recent evidence has suggested that epigenetic alterations are also involved in the anti-tumor properties of curcumin. Among these curcumin-induced epigenetic alterations is modulation of the expression of several oncogenic and tumor suppressor microRNAs (miRNAs). Suppression of oncomiRs such as miR-21, miR-17-5p, miR-20a, and miR-27a and over-expression of miR-34 a/c and epithelial-mesenchymal transition-suppressor miRNAs are among the most important effects of curcumin on miRNA homeostasis. The present review will summarize the findings of in vitro and experimental studies on the impact of curcumin and its analogues on the expression of miRNAs involved in different stages of tumor initiation, growth, metastasis, and chemo-resistance.

**Keywords** Cancer • Curcumin • Epigenetics • miRNA • Turmeric

## Contents

1	Curcumin .....	3
2	Anticancer and Cancer Chemo-Preventive Properties of Curcumin .....	7
3	Role of Epigenetics in Cell Homeostasis and Cancer .....	8
4	Role of miRNAs in Cell Homeostasis and Cancer .....	9
5	Search Strategy .....	10
6	Modulation of miRNAs in Different Types of Cancer: The Influence of Curcumin .....	14
6.1	Colon Cancer .....	14
6.2	Pancreatic Cancer .....	20
6.3	Lung Cancer .....	23
6.4	Breast Cancer .....	24
6.5	Prostate Cancer .....	26
6.6	Melanoma .....	27
6.7	Other Types of Cancers .....	28
7	Concluding Remarks .....	31
	References .....	32

## Abbreviations

5FUR	5-Fluorouracil resistant
Bcl-2	B cell lymphoma 2
CAM	Chick chorioallantoic membrane
CDF	Difluorinated-curcumin
ChIP	Chromatin immuno precipitation
CR	Chemo-resistant
CS	Chemo-sensitive
CSC	Cancer stem cells
EMT	Epithelial-mesenchymal transition
ESR1	Estrogen receptor 1
MDR1	Multidrug resistance protein 1
OSCC	Oral squamous-cell carcinoma

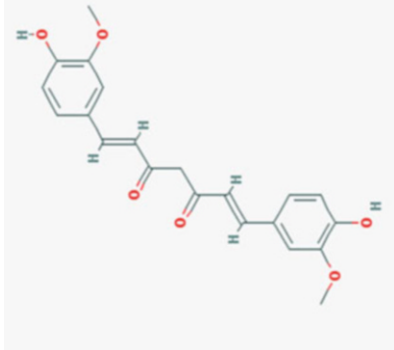
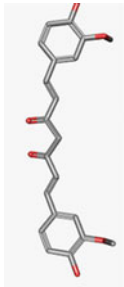
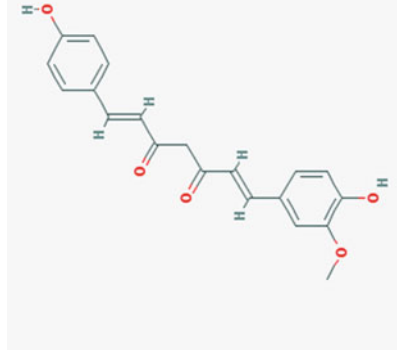
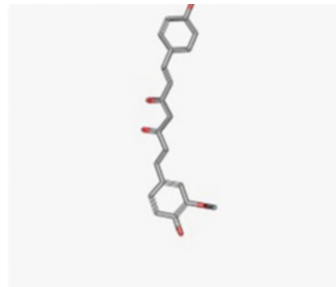


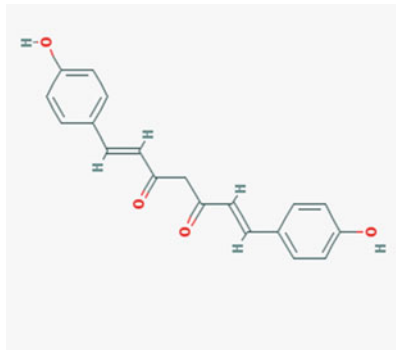
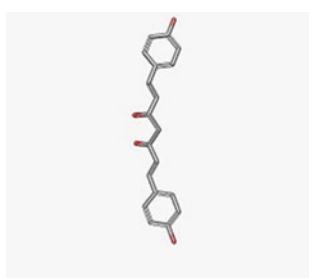
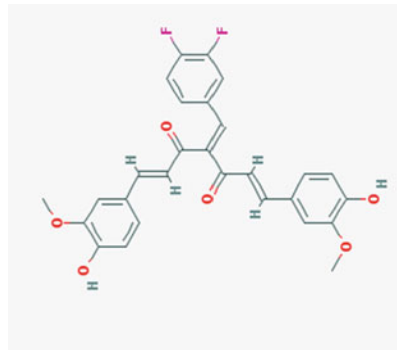
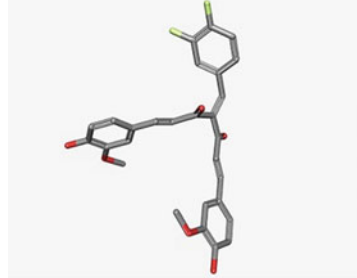
PCNA	Proliferating cell nuclear antigen
PDCD4	Programmed cell death protein 4
PRC	Polycomb repressive complexes
PTEN	Phosphatase and tensin homolog deleted on chromosome 10
Sp	Specificity protein
WT1	Wilm's tumor 1

## 1 Curcumin

*Curcuma longa* (turmeric) is a medicinal plant cultivated across the Indian subcontinent and in tropical countries, particularly in Southeast Asia. In addition to its use as a food additive and dietary spice, the plant has a long record in several traditional systems of medicine such as Ayurvedic medicine and Traditional Chinese Medicine (Strimpakos and Sharma 2008). Curcuminoids are pigments present in dried rhizomes of *C. longa* and are responsible for the yellow color of the plant. There are three compounds known as curcuminoids: curcumin, demethoxycurcumin, and bis-demethoxycurcumin (Strimpakos and Sharma 2008). Chemical structure and physicochemical properties of curcuminoids and curcumin analogues are presented in Table 1. Curcumin is structurally a polyphenolic compound, existing in at least two turmeric forms, keto and enol. The latter form is more chemically stable (Akram et al. 2010). Curcumin and turmeric products meet the safety standard of health authorities such as the Food and Drug Administration (FDA) of the USA, the Natural Health Products Directorate of Canada, and also the Expert Joint Committee of the Food and Agriculture Organization/World Health Organization (FAO/WHO) on food additives (JECFA). Additionally, a daily curcumin intake (ADI) of 0.1–3 mg/kg-body weight has been accepted by the Joint FAO/WHO Expert Committee on Food Additives (NCI 1996). Curcumin possesses numerous biological and pharmacological properties such as anti-inflammatory (Ganjali et al. 2014; Gupta et al. 2010; Panahi et al. 2012b, 2014a, b, 2016; Sahebkar 2014; Sahebkar et al. 2013), antioxidant (Panahi et al. 2012a; Sahebkar et al. 2013, 2015; Sharma 1976), anti-ischemic (Sahebkar 2010), hepatoprotective (Rahmani et al. 2016), anti-diabetic (Nishiyama et al. 2005; Sharma et al. 2006), anti-arthritis (Kumar and Rai 2012; Kuncha et al. 2014; Panahi et al. 2014a, 2016; Yang et al. 2015), analgesic (Sahebkar and Henrotin 2015), neuroprotective (Chen et al. 2015; Sahebkar 2013; Shen et al. 2015; Wang et al. 2015), lipid-modifying (Panahi et al. 2016; Sahebkar et al. 2014; Arafa 2005; Asai and Miyazawa 2001; Fan et al. 2006; Mohammadi et al. 2013; Um et al. 2014; Wang et al. 2014), immunomodulatory (Ganjali et al. 2014; Sahebkar et al. 2016; Sankar et al. 2013; Seyedzadeh et al. 2014), cognitive-enhancing and anti-Alzheimer (Sahebkar 2016; Shakeri and Sahebkar 2016), anti-depressant (Esmaily et al. 2015; Panahi et al. 2015), wound-healing (Sidhu et al. 1998), and antimicrobial (Jordan and Drew 1996; Kim et al. 2003; Mahady et al. 2001; Negi et al. 1999; Reddy et al. 2005) effects. Such a diversity in the biological effects of curcumin is due to the capacity of this compound to interact with numerous molecular targets

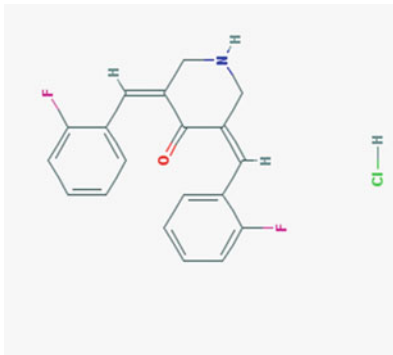
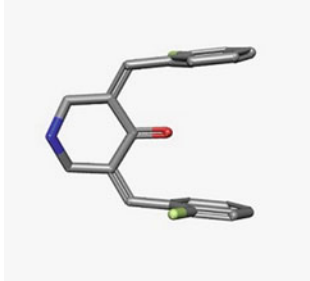
**Table 1** Chemical structure and physicochemical properties of curcumin and its analogues

Compound properties	2D structure	3D Structure
<p><i>Chemical names:</i> Curcumin; Diferuloylmethane; Natural yellow 3; Turmeric yellow</p> <p><i>Molecular formula:</i> C<sub>21</sub>H<sub>20</sub>O<sub>6</sub></p> <p><i>Molecular weight:</i> 368.3799 g/mol</p> <p><i>PubChem CID:</i> 969516</p>		
<p><i>Chemical names:</i> Demethoxycurcumin; Curcumin II; Monodemethoxycurcumin; BHC FM; 4-Hydroxycinnamoyl(feroyl)methane</p> <p><i>Molecular formula:</i> C<sub>20</sub>H<sub>18</sub>O<sub>5</sub></p> <p><i>Molecular weight:</i> 338.35392 g/mol</p> <p><i>PubChem CID:</i> 5469424</p>		

<p><i>Chemical names:</i> Bisdemethoxycurcumin; Curcumin III; Bis (4-hydroxycinnamoyl)methane; Didemethoxycurcumin; (1E,6E)-1,7-bis (4 hydroxyphenyl)hepta-1,6-diene-3,5-dione  <i>Molecular formula:</i> C<sub>19</sub>H<sub>16</sub>O<sub>4</sub>  <i>Molecular weight:</i> 308.32794 g/mol  <i>PubChem CID:</i> 5315472</p>		
<p><i>Chemical names:</i> Difluorinated-Curcumin (CDF)  <i>Molecular formula:</i> C<sub>28</sub>H<sub>22</sub>F<sub>2</sub>O<sub>6</sub>  <i>Molecular weight:</i> 492.467486 g/mol  <i>PubChem CID:</i> 54597187</p>		

(continued)

**Table 1** (continued)

Compound properties	2D structure	3D Structure
<p><i>Chemical names:</i> EF-24; (3E,5E)-3,5-bis[(2-fluorophenyl)methylene]-4-piperidinone</p> <p><i>Molecular formula:</i> C<sub>19</sub>H<sub>16</sub>ClF<sub>2</sub>NO</p> <p><i>Molecular weight:</i> 347.786246 g/mol</p> <p><i>PubChem CID:</i> 71311883</p>		

including receptors, cytokines, hormones, growth factors, transcription factors, enzymes, and cell adhesion molecules (Jurenka 2009). Several studies have shown that curcumin inhibits the growth of different types of cancer cells by exerting effects on genes and cell-signaling pathways at multiple levels (Mirzaei et al. 2016; Momtazi and Sahebkar 2016; Akram et al. 2010; Strimpakos and Sharma 2008). The cellular processes targeted by curcumin occur at three stages of carcinogenesis: initiation, promotion, and progression. These processes regulate gene expression, transcription factors, growth factors and their receptors, nuclear factors, and hormones and hormone receptors together with other potential regulators including miRNA and various epigenetic events (Momtazi et al. 2016; Li et al. 2010; Teiten et al. 2013).

## 2 Anticancer and Cancer Chemo-Preventive Properties of Curcumin

One of the central nuclear factors regulated by curcumin is nuclear factor kappa B (NF- $\kappa$ B). NF- $\kappa$ B potentially serves as an important link between inflammatory conditions and the pathogenesis of many types of malignancies. NF- $\kappa$ B can be activated by any stimulus that can trigger tumor necrosis factor (TNF), including free radicals, inflammatory cytokines, endotoxins, ionizing radiation, ultraviolet light, and carcinogens. Curcumin has been shown to be a strong suppressor of NF- $\kappa$ B. Additionally, curcumin inhibits the activation of I $\kappa$ B kinase (IKK) and, thus, prevents the phosphorylation of I $\kappa$ B and the subsequent translocation of NF- $\kappa$ B to the nucleus (Aggarwal et al. 2004). Curcumin inhibits some signaling pathways, such as the Akt/PI3K pathway and the mitogen-activating protein kinases (MAPKs) pathway, involved in cancer and inflammation. With respect to the inhibition of the Akt/PI3K pathway, which transmits signals received by the epidermal growth factor receptor (EGFR) tyrosine kinase, curcumin suppresses cell growth by interference with EGFR signaling (Chen et al. 2006). Moreover, curcumin enhances cell death or apoptosis via inhibition of the MAPKs pathway, which includes c-Jun N-terminal kinases (JNKs), extracellular signal-regulated kinases (ERKs), p38 kinases, and stress-activated protein kinases (SAPKs) (Aggarwal and Shishodia 2006; Strimpakos and Sharma 2008). This process is regulated by inducing JNK and subsequent activation of c-jun and c-abl, which, after phosphorylation, creates a homodimer or a heterodimer with c-fos. This hetero/homodimer is then attached to the activator protein-1 (AP-1) response elements in the promoters of target genes such as bax, B-cell lymphoma-2 (Bcl-2), and Bcl-XL, which then leads to cell death or apoptosis (Collett and Campbell 2004). Curcumin can alter the expression of genes involved in tumor growth and apoptosis, namely oncogenes and tumor suppressor genes. p53 is a well-known tumor suppressor. Loss-of-function mutations in this gene may cause several types of cancers, as well as resistance to chemotherapy (Mao et al. 1994; Sun 2006). p53 can be modulated by curcumin in several ways. Curcumin induces

apoptosis selectively in different malignant cell lines, such as human mammary epithelial carcinoma cells, prostate cancer cells, and B-lymphoma cells, by increasing p53 expression at the G2 phase of the cell cycle (Choudhuri et al. 2005). In addition, p73 is a member of the p53 family which encodes both a tumor suppressor (transcription-competent p73 – TAp73) and a putative oncogene (dominant-negative p73 – DNp73). Recently, Wang et al. (2016) found that curcumin induced DNA damage, increased TAp73/DNp73 ratio, and also led to apoptosis in p53-deficient Hep3B cells.

### 3 Role of Epigenetics in Cell Homeostasis and Cancer

Epigenetics refers to a reversible change in gene expression and chromatin organization without any alteration in DNA sequences, leading to silencing or activation of multiple genes. Epigenetic alterations occur mainly through changes in histone modifications, DNA methylation, or miRNA expression (Sawan et al. 2008). Histone modifications include lysine acetylation, ADP-ribosylation, ubiquitination, and sumoylation that affect chromatin structure and function. Histone acetylation is well-studied among histone modifications, and is regulated by two types of enzymes, namely histone acetyl transferases (HATs) and histone deacetylases (Grunstein 1997). While hyperacetylation of histones leads to an open and transcriptionally active chromatin, deacetylation of histones causes a closed chromatin conformation (Steger and Workman 1996). DNA methylation is catalyzed by a family of enzymes called DNA methyltransferases (DNMTs) at the 5' position of the cytosine within the context of CpG sequences. In cancer cells, two different patterns related to DNA methylation can be observed, hypomethylation and hypermethylation. Hypomethylation of DNA causes the activation of proto-oncogenes or cancer-related genes, while tumor suppressor genes are silenced with hypermethylation of their promoter regions (Mani and Herceg 2010). Epigenetic silencing of tumor suppressor genes with DNA methylation leads to oncogenic processes. Hence, reactivation of tumor suppressor genes by DNA hypomethylation has emerged as a molecular target for cancer therapy (Das and Singal 2004). Several lines of evidence have shown that curcumin regulates gene expression in various cancers through modulation of epigenetic mechanisms. Three epigenetic mechanisms are regulated by curcumin to selectively activate or inactivate genes implicated in cancer (Teiten et al. 2013). Curcumin can inhibit acetyltransferase activity in cervical HeLa cancer cells, and this inhibition leads to apoptosis with abrogation of p300-mediated p53 acetylation (Balasubramanyam et al. 2004). Moreover, curcumin induces apoptosis in LNCaP prostate cancer cells treated at a dose of 10–30  $\mu\text{M}$ . In addition, acetylation of histone H3 and H4 by curcumin has been observed over the same dose range (Shankar and Srivastava 2007). In medulloblastoma cells, curcumin reduced histone deacetylase 4 (HDAC4) expression and activity when applied over the concentration range of 5–40  $\mu\text{M}$ , thereby inducing apoptosis and cell cycle arrest at the G2/M phase (Lee et al. 2011).

With respect to an inhibitory effect on DNA methylation, curcumin covalently blocks the catalytic thiolate of DNMT1. This epigenetic event may be achieved through different mechanisms, including disruption of an NF- $\kappa$ B/Sp1 complex bound to the promoter region of DNMT1, and reversal of the CpG methylation of the promoter region of a cancer methylation marker. For example, curcumin, at a concentration of 5  $\mu$ m, is capable of reversing DNA methylation in the promoter region of the Neurog1 gene whose expression is silenced due to extensive methylation in prostate cancer LNCaP cells (Shu et al. 2011). Additionally, curcumin reactivated silenced tumor suppressor gene retinoic acid receptor  $\beta$  (RAR $\beta$ ) by reducing DNA methylation (Jiang et al. 2015). The third layer of epigenetic modification is controlled by miRNAs, which represent a promising target for the prevention and treatment of cancer.

## 4 Role of miRNAs in Cell Homeostasis and Cancer

miRNAs are endogenous RNAs of about 22 nucleotides in length that belong to family of small noncoding single-stranded regulatory RNAs. miRNAs regulate gene expression through multiple mechanisms, and could serve as either oncogenic or tumor-suppressive factors. Over 2,000 miRNAs have been discovered in humans which are involved in the regulation of many physiological and pathological processes (Hammond 2015). Hence, miRNAs could be used as biomarkers for diagnosis and prognosis of disease, and also as targets for cancer therapy (Li et al. 2010). Biogenesis of miRNAs involves transcription by RNA polymerase II in the nucleus to form the long primary transcripts (pri-miRNA) which have hundreds to thousands of nucleotides (Lee et al. 2004). Pri-miRNAs consist of a hairpin stem of 33 base-pairs, a terminal loop, and two single-stranded flanking regions upstream and downstream of the hairpin which are processed in several modification steps. Initially, the pri-miRNA is cleaved by the RNase III (Drosha) and the DGCR8 (DiGeorge critical region 8) protein to form a 70-nucleotide precursor miRNA (pre-miRNA). In the next step, pre-miRNA is transported by nuclear export factor, Exportin 5, to the cytoplasm where another RNase III (Dicer) cleaves the pre-miRNA hairpin and generates an RNA duplex of about 22 nucleotides. Mature miRNA is then incorporated into the RNA-induced silencing complex (RISC) and guides RISC to target mRNA. The level of complementarity between the guide strand and mRNA target determines which silencing mechanism will be employed (Winter et al. 2009). miRNAs regulate the gene expression at the level of messenger RNA degradation and translation. The mature miRNA which binds perfectly to the 3'UTR of mRNA induces targeted mRNA cleavage, while miRNA that binds imperfectly to mRNA leads to translational suppression (Williams and Spencer 2012). As mentioned above, changes in miRNAs expression profiles may be associated with human diseases such as the progression and metastasis of cancer, skeletal muscle diseases, and cardiovascular diseases (Ambros 2003; Wang and Lee 2009). Alterations in miRNA expression are not only an effect

of tumorigenesis, but might have a causative role in cancer development by affecting the initiation, progression, and dissemination of tumors. To date, numerous miRNAs have been identified and implicated as either tumor suppressor or promoters (Brighenti 2015). A well-established example of miRNAs with tumor suppressor activity is the let7 family, which consists of let-7, miR-48, miR-84, and miR-241. Many studies have demonstrated that this miRNA cluster is down-regulated in various cancers, especially in lung cancer. The tumor suppressor effect of let7 miRNAs is mediated by targeting human Ras 3'UTRs. miR-34 is another notable cancer-associated miRNA that has been found to possess tumor suppressor activity. Studies have shown that this miRNA may be induced by p53 signaling (Chang et al. 2007; Corney et al. 2007). Consequently, the high expression of mir-34a leads to increased apoptosis and changes in the expression of genes related to cell cycle progression, apoptosis, DNA repair, and angiogenesis (Chang et al. 2007). Among oncogenic miRNAs, miR-21 has been shown to be up-regulated in several malignancies such as colorectal and breast cancers. Up-regulation of miR-21 is associated with tumor cell proliferation, migration, invasion, metastasis, and suppression of apoptosis by down-regulating the tumor suppressors phosphatase and tensin homolog (PTEN) and programmed cell death protein 4 (PDCD4) (Asangani et al. 2008).

Inflammation, oxidative stress, apoptosis, and angiogenesis have a strong impact on tumorigenesis. Most of these processes have been shown to be regulated through a complex network of epigenetic mechanisms, in which miRNAs play an important role. By acting on several of the above-mentioned pathways, curcumin can mitigate tumorigenesis. A schematic highlighting of the anticancer effects of curcumin is presented in Fig. 1. Specifically, modulation of miRNA expression might explain a significant amount of the tumor-suppressive effects of curcumin. Patterns of miRNA expression which are modulated by curcumin are presented in different human cancer cell lines (Table 2) and types of cancer (Table 3 and Fig. 2).

## 5 Search Strategy

A systematic literature search was performed in Scopus (<http://www.scopus.com>) and Medline (<http://www.ncbi.nlm.nih.gov/pubmed>), without any language restriction, to identify all published articles dealing with curcumin-modulated Micro RNAs in different cancer cells. The search terms included ["curcumin" AND "cancer" AND "Micro RNA"] in titles and abstracts. The search was performed from inception to March, 2016.



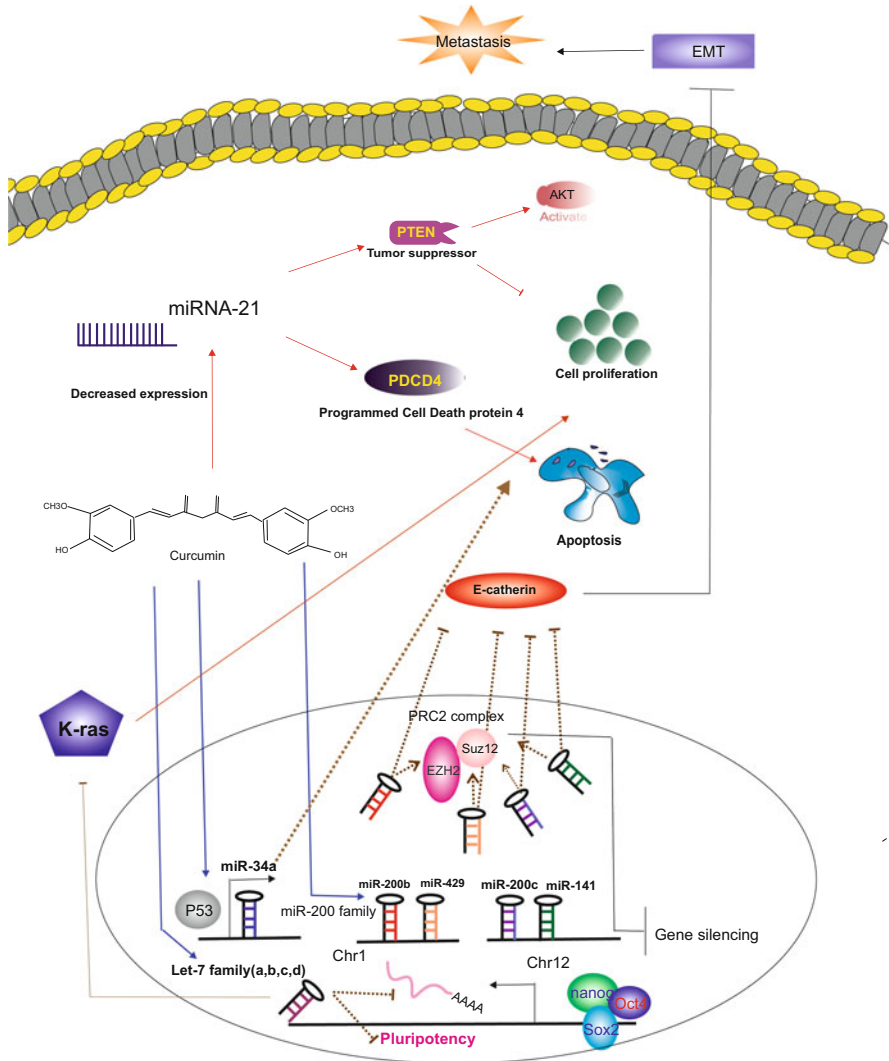


**Fig. 1** Schematic highlighting of the anticancer effects of curcumin. Curcumin suppresses cell proliferation by decreasing the expression of miR-21, which then leads to up-regulation of PTEN and activation of the Akt signaling pathway. Curcumin also stimulates apoptosis by up-regulation of miR-21, which targets programmed cell death protein 4 (PDCD4) and up-regulates miR-34a by activation of p53. Moreover, curcumin exerts inhibitory effects on metastasis by causing over-expression of the miR-200 family, which suppresses the expression of the polycomb repressive complexes (PRCs) including EZH2, SUZ12, and EMT. Curcumin inhibits Ras activity through up-regulation of tumor-suppressive microRNAs such as let-7a/b/c/d that target cancer stem cell (CSC) marker genes such as Nanog, Sox2, and Oct4

**Table 2** Modulation of miRNA expression by curcumin and its analogues in different human cancer cell lines

Cancer type	Curcumin type	Cell line	Regulated miRNA by curcumin	References
Colon cancer	CDF	CR HCT-116, CR HT-29, the metastatic SW620	miR-21(-)	Roy et al. (2013)
	Curcumin	Rko, HCT116	miR-21 (-)	Mudduluru et al. (2011)
	CDF	CR HCT-116, CR SW620	miR-3a/c (+)	Roy et al. (2012)
	Curcuminoid	SW-480	miR-27a (-)	Noratto et al. (2013)
	Curcumin	HCT1160-5FUR, SW480-5FUR	miR-200b (+) miR-200c (+) miR-141 (+) miR-429 (+) miR-101 (+) miR-34a (+) <sup>a</sup>	Toden et al. (2015)
	Curcumin	RKO	miR-27a (-) miR-20a (-) miR-17-5p (-)	Gandhy et al. (2012)
Pancreatic cancer	Curcumin, liposomal curcumin	BxPC-3	miR-22 (+)	Sun et al. (2008)
			miR-199a* (-)	
	Curcumin, CDF	MIAPaCa-E, MIAPaCa-M	miR-21 (--)	Ali et al. (2010)
		BxPC-3	miR-21 (-)	
	CDF	MIAPaCa-E, MIAPaCa-M, BxPC-3	miR-200b/c (++)	
	Curcumin	MIAPaCa-E, MIAPaCa-M, BxPC-3	miR-200b/c (+)	
	CDF	AsPC-1, MiaPaCa-2	let-7a/b/c/d (+) miR-26a (+) miR-101 (+) miR-146a (+) miR-200b (+)	Bao et al. (2012)
			miR-21 (-)	
CDF	COLO-357, BxPC-3, MIAPaCa-2	miR-21 (-)	Ali et al. (2012)	
	MIAPaCa-2	miR-143 (+)		
Curcumin	AsPC-1, BxPC-3	miR-7 (+)	Ma et al. (2014)	
Melanoma	EF24	B16	miR-21 (-)	Yang et al. (2013)

(continued)

**Table 2** (continued)

Cancer type	Curcumin type	Cell line	Regulated miRNA by curcumin	References
	Curcumin	Murine B78H1, human SK-MEL-28	mmu-miR-205-5p (++) mmu -miR-205-3p (+) mmu-miR-142-5p (+) mmu-miR-130b-3p (-)	Dahmke et al. (2013)
	EF24	Lu1205, A375	miR-33b (+)	Zhang et al. (2015)
		Lu1205	Let-7 (+)	
		A375	Let-7 (=) <sup>b</sup>	
		Lu1205, A375	miR-200a (=) miR-98 (=) miR-145 (=) miR-26a (=)	
Lung cancer	Curcumin	A549	miR-21 (-)	Zhang et al. (2010b)
		The p53 wild-type H460, A427, A549	miR-192-5p (+) miR-215 (+)	Ye et al. (2015)
		p53-null H1299	miR-192-5p (=) miR-215 (=)	
		A549	miR-186* (-)	Tang et al. (2010) and Zhang et al. (2010a, b)
	Curcumin, CDF	A549, H1299	miR-874 (+)	Ahmad et al. (2015)
Breast cancer	Curcumin	MCF-7	miR-15a (+) miR-16 (+)	Yang et al. (2010)
			miR-19a (-) miR-19b (-)	Li et al. (2014)
		MDA-MB 231	miR181b (+)	Kronski et al. (2014)
		MDA-MB-231, MDA-MB-435	miR-34a (+)	Guo et al. (2013)
Prostate cancer	Poly(lactic-coglycolic acid)-curcumin nanoparticles	C4-2, DU-145 and PC-3	miR-21 (-) miR-205 (+)	Yallapu et al. (2014)
	EF24	DU145	miR-21 (-)	Yang et al. (2013)
Bladder cancer	Curcumin	T24, J82, TCCSUP	miR-203 (+)	Saini et al. (2011)
Retinoblastoma	Curcumin	Y79	let-7 g* (+) miR-22 (+)	Sreenivasan et al. (2012)

(continued)

**Table 2** (continued)

Cancer type	Curcumin type	Cell line	Regulated miRNA by curcumin	References
			miR-503 (+) miR-200c (+)	
			miR-135b (-) miR-210 (-) miR-25* (-) miR- 95 (-) miR-514 (-) miR-106b* (-) miR-34c-3p (-) miR-92a-1* (-)	

<sup>a</sup>miR-34a expression was the only up-regulated in HCT116-5FUR cells

<sup>b</sup>Not changed

## 6 Modulation of miRNAs in Different Types of Cancer: The Influence of Curcumin

### 6.1 Colon Cancer

The miR-17-5p, mir-20a, miR-21, miR-27a, miR-34a/c, miR-101, miR-141, miR-200b/c, and miR-429 have roles in curcumin-mediated treatment of the human colon cancer (Tables 2 and 3).

Expression of miR-21 has been found to increase in colon cancer cells. One of the most important miR-21 targets in human colon cancer cells is the PTEN, a tumor-suppressive gene that is involved in the regulation of the cell cycle, as well as preventing cells from proliferation. Difluorinated-curcumin (CDF), a safe analog of the curcumin with a greater bioavailability than the parent compound, has been shown to prevent growth of chemo-resistant colon cancer cells (Kanwar et al. 2011). Roy et al. studied the effect of CDF on miR-21 expression in the chemo-resistant (CR) HCT116 and HT29, and the metastatic SW620 human colon cancer cell lines. Target of miR-21 was experimentally validated by luciferase assay, qRT-PCR, and western-blot analysis. As determined by qRT-PCR, the expression of miR-21 in CR HCT116, HT29, and the metastatic SW620 cells was markedly decreased when they were incubated with 100 nM CDF. This was associated with increased expression of PTEN in CDF-treated cancer cells. The results suggest that CDF-induced growth and metastasis inhibition of colon cancer cells by a decrease in miR-21 lead to an increase in PTEN and subsequent activation of the Akt signaling pathway (Roy et al. 2013). Another target of miR-21 in human colon cancer cells is the PDCD4, which is a tumor suppressor that is involved in apoptosis. Mudduluru et al. investigated the effect of curcumin on miR-21 expression in Rko and HCT116 human colon cancer cell lines and in vivo using the chick chorioallantoic membrane (CAM) assay. As determined by qRT-PCR, both Rko and HCT116 cells, and primary tumors showed a significant

**Table 3** Modulation of miRNA expression by curcumin in vivo

Disease	Animal model	Dosage	Duration of treatment	Curcumin type	OncomiR/tumor suppressor	Regulated miRNA	miRNA expression	References
Pancreatic cancer	Female CB17 SCID mice	5 mg/mouse/day	Once daily for 12 day	CDF	OncomiR	miR-21	Decreased	Bao et al. (2011)
					Tumor suppressor	miR-200b/200c	Increased	
Melanoma	Male C57BL/6 mice,	8 g/kg b.w. or 160 mg/day	Two weeks	Curcumin	Tumor suppressor	miR-21	Decreased	Dahmke et al. (2013)
					Tumor suppressor	miR-200b/200c	Increased	
Prostate and melanoma cancer	NSG mice	EF24 (200 mg/kg body weight)	Daily intraperitoneal injections	EF24	OncomiR	miR-21.	Decreased	Yang et al. (2013)
Colorectal cancer	Male athymic nude mice	Curcumin (50 mg/kg intraperitoneally daily)	40 days	Curcumin	Tumor suppressor	miR-200b, miR-200c	Increased	Toden et al. (2015)
					Tumor suppressor	miR-141	Decreased	
					Tumor suppressor	miR-429	Decreased	
					Tumor suppressor	mir101	Decreased	
Nasopharyngeal carcinoma	Athymic nu/nu mice	150 mg/kg	Three times a week for 30 days	Curcumin	Tumor suppressor	mir34	Decreased	Gao et al. (2014)

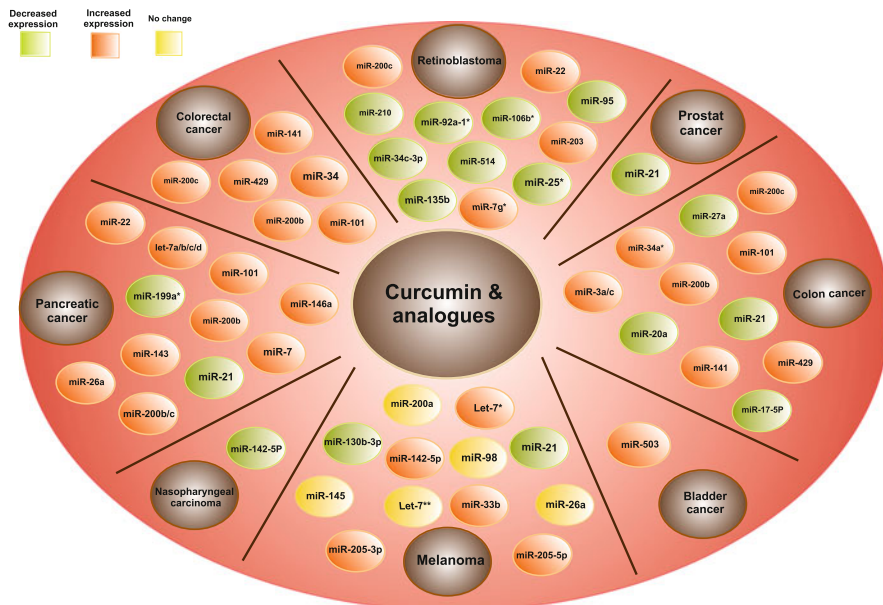


**Fig. 2** Modulation of miRNAs in different types of cancer by curcumin and its analogues

reduction in pre-miR and miR-21 expression after curcumin treatment in a dose-dependent manner. It was suggested that this finding resulted from the inhibition of the transcription factor AP-1 binding to the promoter and induction in the expression of the tumor suppressor PDCD4, which is a target of miR-21. The target of miR-21 was experimentally confirmed by transfection and a luciferase assay, ChIP assay, qRT-PCR, and western-blot analysis. The findings suggest that curcumin-induced tumor suppression, and inhibition of migration, invasion, and in vivo metastasis might at least in part be mediated by miR-21-triggered, PDCD4-dependent mechanisms (Mudduluru et al. 2011).

The miR-34 target in human colon cancer cells is Notch-1 that functions as a receptor for membrane-bound ligands, and has multiple roles during development. Roy et al. investigated the effect of CDF on miR-34a/c expression in CR HCT116 and SW620 human colon cancer cell lines. As determined by qRT-PCR, the expression of miR-34a/c in both CR HCT116 and SW620 cells was significantly induced when they were incubated with 100 nM CDF. The target of miR-34 was experimentally confirmed by methylation-specific PCR and western-blot analysis. The re-expression of miR-34 led to a marked reduction in the expression of its target gene, Notch-1. The loss of expression of miR-34 in colon cancer is, in part, due to promoter hypermethylation of miR-34, which can be re-expressed with CDF. This suggests that CDF could be a novel demethylating agent for restoring the expression of miR-34 family (Roy et al. 2012).

miR-27a is a target in human colon cancer SW480 cells, which suppresses transcription of specificity protein (Sp) transcription factors that regulate the

multidrug resistance protein 1 (MDR1) and have an important role in the growth and metastasis of colon cancer cells. Noratto et al. investigated the effect of curcuminoids on miR-27a expression in the SW480 human colon cancer cell line. As determined by qRT-PCR, the expression of miR-27a in SW480 cells was decreased by 70–93% when they were incubated with 2.5–10 g/mL curcuminoids. The target of miR-27a was experimentally confirmed by a luciferase assay and western-blot analysis. The suppression of miR-27a led to a 2.5-fold increase in the expression of its target gene, ZBTB10. The results showed that curcuminoid-induced growth inhibition of colon cancer cells is mediated by disruption of the miR-27a-ZBTB10-Sp axis (Noratto et al. 2013).

The target of epithelial-mesenchymal transition (EMT)-suppressive miRNAs (miR-200b, miR-200c, miR-34a, miR-141, miR-429, and miR-101) in colon cancer cells are the polycomb repressive complexes (PRCs), including BMI1, SUZ12, and EZH2, which have a crucial role in development through epigenetic silencing of genes. EMT is responsible for progression and metastasis of cancer, and is also accountable for chemo-resistance. Toden et al. evaluated the effect of curcumin on the expression pattern of EMT-suppressive miRNAs in HCT1160-5-fluorouracil (FUR) and SW480-5FUR cell lines, as well as in a mouse xenograft tumor model. As determined by qRT-PCR, the expression of EMT-suppressive miRNAs in the curcumin-treated HCT116-5FUR and SW480-5FUR cells was up-regulated. miR-34a expression was the only one up-regulated in HCT116-5FUR cells, but not in the SW480-5FUR cell line. Since SW480 is p53-mutated and miR-34a is primarily up-regulated by p53, it follows that curcumin up-regulates miR-34a through p53 activation. miR-200c expression was increased in the mouse xenograft treated with 50 mg/kg/day of curcumin. It was demonstrated that over-expression of miR-200c, a key EMT-suppressive miRNA, was accompanied with reduced tumor growth in the xenograft model. The target of EMT-suppressive miRNAs was experimentally confirmed by western-blot analysis. In conclusion, curcumin suppressed tumor growth in human colon cancer cells through the suppression of EMT and PRC due to the up-regulation of EMT-suppressive miRNAs (Toden et al. 2015).

The miR-27a, miR-20a, and miR-17-5p targets in the human colon cancer cells are ZBTB10 and ZBTB4, Sp repressors. Gandhi et al. examined the effect of curcumin on miR-27a, miR-20a, and miR-17-5p expression in the RKO colon cancer cell line. The qRT-PCR analysis revealed that curcumin (10  $\mu$ M) decreased the expression of miR-27a and also miR-20a/miR-17-5p, which inhibit the expression of ZBTB10 and ZBTB4, respectively. The target of miR-27a, miR-20a, and miR-17-5p was experimentally confirmed by western-blot analysis. The induction of transcriptional repressors ZBTB10 and ZBTB4 was accompanied by decreased expression of Sp1, Sp3, Sp4, and Sp-regulated gene mRNA levels that play a role in cell proliferation (EGFR, cMET, and cyclin D1), survival (survivin and Bcl-2), inflammation (p65 and p50), and metabolism/drug transport (fatty acid synthase) (Gandhy et al. 2012). To summarize, curcumin and CDF can exert anti-proliferative and proapoptotic effects and reduce chemo-resistance in colorectal cancer cell lines by modulation of the expression/activity of PTEN, Notch1, PDCD4, Sp repressors (ZBTB4, ZBTB10), and PRCs-related pathways (Table 4). These curcumin-

**Table 4** Biological relevance and targets of miRNAs regulated by curcumin and its analogues in different types of cancer

Regulated miRNA	OncomiR/ tumor suppressive	Cancer type	Target gene	miRNA effects on target biological function	Target validation method	References
miR-21	OncomiR	Colon cancer	PTEN	Cell cycle regulation and proliferation	Luciferase assay	Roy et al. (2013)
			PDCD4	Apoptosis	Luciferase assay and western-blot analysis	Mudduluru et al. (2011)
		Pancreatic cancer	PTEN	Cell cycle regulation and proliferation	Luciferase assay	Ali et al. (2010)
			K-Ras	Cell cycle regulation and proliferation	Western-blot analysis	Ali et al. (2012)
		Melanoma	PTEN, PDCD4 and Bcl-2	Cell cycle regulation and apoptosis	Data not showed	Yang et al. (2013)
miR-34 a/c	Tumor suppressive	Colon cancer	Notch-1	Cell development regulation	Methylation-specific PCR and western- blot analysis	Roy et al. (2012)
miR-27a	OncomiR	Colon cancer	ZBTBs10	Cell growth regulation and metastasis	Luciferase assay and western-blot analysis	Noratto et al. (2013) and Gandhy et al. (2012)
miR-20a, miR-17-5p	OncomiR	Colon cancer	ZBTB10 and ZBTB4	Cell growth regulation and metastasis	Western-blot analysis	Gandhy et al. (2012)
EMT-suppressive miRNAs	Tumor suppressive	Colon cancer	BMI1, SUZ12 and EZH2	Cell growth regulation and metastasis	Western-blot analysis	Toden et al. (2015)
miR-22	Tumor suppressive	Pancreatic cancer	ESR1, Sp1 transcription factors	Cell cycle regulation, apoptosis, and DNA repair	miRNA transfection and flow cytometry analysis	Sun et al. (2008)
		Retinoblastoma tumor	ErbB3	Proliferation, differ- entiation, cell motil- ity, and survival	Western-blot analysis	Sreenivasan et al. (2012)



let-7family	Tumor suppressive	Pancreatic cancer	CSC marker genes (EZH2, EpCAM, Nanog, Sox2, Oct4) and K-Ras gene	Cell growth regulation and proliferation	Western-blot analysis	Bao et al. (2012) and Ali et al. (2012)
miR-143	Tumor suppressive	Pancreatic cancer	K-Ras gene	Cell cycle regulation and proliferation	Western-blot analysis	Ali et al. (2012)
miR-26a, miR-101, miR-146a and miR-200b	Tumor suppressive	Pancreatic cancer	CSC marker genes (EZH2, EpCAM, Nanog, Sox2, Oct4)	Cell growth regulation and proliferation	Western-blot analysis	Bao et al. (2012)
miR-7	Tumor suppressive	Pancreatic cancer	Histone-lysine N-methyltransferase SETD8	Cell proliferation and apoptosis	qRT-PCR and western-blot analysis	Ma et al. (2014)
mmu-miR-205-5p	Tumor suppressive	Melanoma	Bcl-2, PCNA	Cell proliferation and apoptosis	Western-blot analysis	Dahmke et al. (2013)
miR-33b	Tumor suppressive	Melanoma	HMGGA2	Mediator of EMT	Dual-luciferase assay and western-blot analysis	Zhang et al. (2015)
miR-203	Tumor suppressive	Bladder cancer	Akt2 and Src oncogenes	Cell proliferation and apoptosis	Western-blot analysis	Saini et al. (2011)

induced pathway modulations in colorectal cancer are likely to be mediated by changes in the expression of miR-17-5p, miR-20a, miR-21, miR-27a, miR-34a/c, miR-101, miR-141, miR-200b/c, and miR-429 (Fig. 2).

## 6.2 Pancreatic Cancer

miR-7, miR-21, miR-22, miR-26a, miR-101, miR-146a, miR-199a\*, miR-200b/c, let-7a,b,c,d,i, and miR-221 have roles in curcumin-mediated effects on human pancreatic cancer (Tables 2 and 3). The target of miR-22 in human pancreatic cancer cells are estrogen receptor1 (ESR1) and Sp1 transcription factor genes. Over-expression of ESRs leads to interruption of the cell cycle, apoptosis, and DNA repair, and finally, tumorigenesis. Sun et al. (2008) investigated the effect of curcumin and liposomal curcumin on miR-22 and miR-199a\* expression in the BxPC-3 human pancreatic cancer cell line at concentrations of 10  $\mu\text{mol/L}$ . Liposomal encapsulated curcumin enhanced absorption properties when compared to non-liposomal encapsulated curcumin administered orally (Kurzrock and Li 2005; Li et al. 2007); hence, its effect on pancreatic cancer was evaluated. As determined by microarray analysis and qRT-PCR, the expression of miR-22 was up-regulated by 10  $\mu\text{mol/L}$  curcumin and 10  $\mu\text{mol/L}$  liposomal curcumin by 60.3% and 68.6%, respectively, whereas miR-199a\* was down-regulated by 25.1% and 36.40%, respectively (Sun et al. 2008). The target of miR-22 was predicted by PicTar and TargetScan software, and experimentally validated by miRNA transfection and flow cytometry analysis. miRNA-22 down-regulated ESR1 and Sp1 in BxPC-3 cells treated with curcumin. The attenuation in ESR1 and Sp1 expression resulted in alteration of miR-22 and miR-199a\* expression and liposomal-based, curcumin-treated BxPC-3 cells demonstrated inhibited cell growth and proliferation (Sun et al. 2008).

miR-21 is an oncogenic miRNA and has been shown to have anti-apoptotic activity in various cancer cell lines. Its target in pancreatic cancer cells is PTEN. On the contrary, miR-200b/c led to the reversal of the oncogenic EMT phenotype. Ali et al. investigated the effect of CDF, curcumin, or gemcitabine on the expression of miR-200 and miR-21 in human pancreatic cancer cell lines MIAPaCa-E (relatively resistant to gemcitabine), MIAPaCa-M (highly resistant to gemcitabine), and BxPC-3 (gemcitabine-sensitive). As determined by qRT-PCR, the expression of miR-21 was significantly decreased in both MIAPaCa-E and MIAPaCa-M cells compared with BxPC-3 cells after treatment with either CDF alone, or in combination with gemcitabine. The target of miR-21 was experimentally validated by PTEN cDNA transfection, antisense miR-21 oligonucleotide transfection, and western-blot analysis. BxPC-3, MIAPaCa-E, and MIAPaCa-M cells treated with CDF, curcumin, or gemcitabine and various combinations of these compounds for 72 h showed increased expression of miR-200b and miR-200c, but the effect was much more pronounced in CDF-treated cells, suggesting the superiority of CDF when compared to curcumin. In conclusion, inhibition of miR-21 led to the

reactivation of PTEN, resulting in the inactivation of phosphorylated Akt. In addition, reactivation of miR-200b/c, which may, in turn, result in the reversal of the EMT phenotype and, thus, sensitize gemcitabine-resistant pancreatic cancer cells to gemcitabine (Ali et al. 2010). In another different *in vivo* study, the role of miR-21 and miR-200b/200c was evaluated in curcumin and a CDF-treated animal model. Bao et al. investigated the effect of curcumin and its synthetic analogue, CDF, on miR-21 and miR-200b/c expression in pancreatic tumors *in vivo* using a mouse xenograft model following curcumin (5 mg/mouse/day) and/or CDF (5 mg/mouse/day) treatment, administered intragastrically once daily for 12 days. As determined by qRT-PCR, the expression of miR-21 in the mouse xenograft model was significantly decreased after CDF treatment, but was only slightly decreased after curcumin treatment. In contrast, CDF treatment increased the expression of both miR-200b and miR-200c, but the effect on these miRNAs with curcumin was minimal. The targets of miR-21, miR-200b, and 200c were experimentally validated by western-blot analysis. Importantly, results of these studies have suggested superiority of CDF, as opposed to curcumin, in suppressing the expression of miR-21, which results in the re-expression of PTEN and re-expression of miR-200. Consequently, the re-expression of both PTEN and miR-200 could be responsible for the reversal of the EMT phenotype and the reduction in tumor growth observed in the xenograft model treated with CDF (Bao et al. 2011).

MicroRNAs belonging to the let-7 family, miR-26a, miR-101, miR-146a, and miR-200b are a panel of tumor-suppressive microRNAs that target cancer stem cells (CSC) marker genes such as EZH2, EpCAM, Nanog, Sox2, and Oct4. Bao et al. investigated the effect of CDF on the panel of tumor-suppressive microRNAs and miR-21 expression in human pancreatic cancer cell lines AsPC-1 and MiaPaCa-2, and *in vivo* using a xenograft mouse model following CDF (2.5 mg/mouse/d) treatment, administered intragastrically once daily for 3 weeks. The target of tumor-suppressive microRNAs was experimentally validated by transfection of a miRNA precursor and western-blot analysis. As determined by qRT-PCR, CDF treatment caused re-expression of tumor-suppressive microRNAs such as let-7a/b/c/d, miR-26a, miR-101, miR-146a, and miR-200b that are lost in AsPC-1 and MiaPaCa-2 cells. miR-21 expression was substantially greater in the AsPC-1 and MiaPaCa-2 cells and CDF was able to down-regulate its expression. Similarly, in the orthotopic xenograft model of human pancreatic cancer, administration of CDF inhibited tumor growth in a manner associated with reduced expression of EZH2, Notch-1, CD44, EpCAM, and Nanog, and increased expression of let-7, miR-26a, and miR-101 (Bao et al. 2012).

let-7 family, miR-143, and miR-21 target in pancreatic cancer cells is K-Ras gene that produces ras kinase with GTPase activity. The Ras kinase is implicated in cellular signal transduction. It is found to regulate cell proliferation and differentiation in many types of cancer cells, such as pancreatic cancer. The expression of the let-7 family and miR-143 is attenuated in MIA PaCa-2 cells compared to COLO-357 and BxPC-3 cells. However, miR-21 is up-regulated in MIA PaCa-2 cells. Ali et al. (2012) examined the effect of CDF on the expression of the miRNAs

mentioned above in human pancreatic cancer cell lines COLO-357, MIAPaCa-2, and BxPC-3, and in a tumor model treated by CDF (5 mg/mice/day) intragastrically once daily for 12 days. As shown by qRT-PCR data, let-7i expression was significantly up-regulated and miR-21 was down-regulated in all three cell lines, and miR-143 was up-regulated in MIAPaCa-2 cells following treatment with 0.5  $\mu$ M-1  $\mu$ M of CDF for 48 h. In vivo studies showed a similar result; miR-143 and let-7i were up-regulated and miR-21 was down-regulated in CDF-treated mouse models. miRNAs targets were experimentally validated by antisense oligonucleotide transfection and western-blot analysis. let-7i and miR-141 over-expression and reduced miR-21 expression induced by CDF reduced Ras expression and its GTPase activity. Inhibition of Ras activity through up-regulation and down-regulation of the above-mentioned miRNAs by CDF treatment resulted in decreased tumor growth in vivo and inhibited cell proliferation in vitro (Ali et al. 2012).

The miR-7 target in human pancreatic cancer cells is histone-lysine *N*-methyltransferase SETD8, which plays an important role in epigenetic gene regulation. Ma et al. investigated the effect of curcumin on miR-7 expression in human AsPC-1 and BxPC-3 pancreatic cancer cells. As determined by qRT-PCR, the expression of miR-7 was significantly increased after curcumin treatment (6  $\mu$ M) for 72 h in both AsPC-1 and BxPC-3 cells. The target of miR-7 was experimentally validated using an invasion assay, miR-7 mimic transfection, qRT-PCR, and western-blot analysis. The findings demonstrated that curcumin suppressed cell proliferation, induced cell apoptosis, and inhibited cell migration in pancreatic cancer cells partly through up-regulation of miR-7 and subsequent down-regulation of SET8 and its downstream effectors, including p53 (Gleissner et al. 2014).

Finally, expression of miR-221 is up-regulated in pancreatic cell lines and tumor tissues compared to normal pancreatic duct epithelial cells and normal pancreas tissues (Sarkar et al. 2013). Also, pancreatic cancer patients with high miR-221 expression had a shorter survival compared to those with lower expression. Interestingly, treatment of pancreatic cancer cells with CDF down-regulates the expression of miR-221 and up-regulates the expression of PTEN, p27(kip1), p57(kip2), and p53 up-regulated modulator of apoptosis (PUMA), leading to the inhibition of cell proliferation and migration of MiaPaCa-2 and Panc-1 cells (Sarkar et al. 2013).

In conclusion, curcumin, liposomal curcumin, and CDF can induce anti-proliferative and proapoptotic effects and decrease chemo-resistance in pancreatic cancer cells through modulation of the expression of ESR1 and Sp1 transcription factors, PTEN, CSC marker genes, K-Ras, and SETD8-related pathways (Table 4). Changes in the expression of miR-7, miR-21, miR-22, miR-143, miR-199a\*, miR-200c, tumor-suppressive microRNAs (let-7a,b, c,d,i, miR-26a, miR-101, miR-146a, and miR-200b), and miR-221 occur as a result of these curcumin-induced pathway modulations in pancreatic cancer cells.

### 6.3 Lung Cancer

It has been shown that miR-21, miR-192-5p, miR-215, miR-186, miR-186\*, and miR-874 have crucial roles in curcumin-treated lung cancer cells (Tables 2 and 3). The miR-21 target in lung cancer cells treated by curcumin is PTEN and this can mediate the anticancer activities of curcumin in non-small cell lung cancer (NSCLC) cells. Zhang and Bai (2014) evaluated miR-21 modulation by curcumin in the lung cancer cell line A549. qRT-PCR analysis showed dose-dependent and significant suppression of mir-21 expression in the A549 cell line exposed to 20–40  $\mu$ M of curcumin. There was approximately a 60% reduction in the miR-21 expression in cells exposed to 40  $\mu$ M of curcumin. The expression of mir-21 was measured by qRT-PCR. Curcumin at 20–40  $\mu$ M inhibited cell proliferation and induced apoptosis in A549 cells. Flow cytometric analysis of A549 cells exposed to 20–40  $\mu$ M of curcumin showed that curcumin significantly increased the proportion of apoptotic annexin V-positive cells by approximately two- to fivefold, compared to untreated control (Zhang and Bai 2014). The miR-192-5p and miR-215 are among the most responsive miRs to curcumin treatment, and they have been identified as putative anti-oncogenic miR in NSCLC cells. Ye et al. (2015) investigated the effect of curcumin on the expression of miR-192-5p/215 in the p53 wild-type H460, A427, and A549 cell lines, as well as the p53-null H1299 cell line. The tumor suppressor p53 is frequently inactivated by mutations or deletions in cancer. As revealed by miR microarray and qRT-PCR, miR-192-5p/215 expression was up-regulated in curcumin (15  $\mu$ M) treated A549 cells (p53 wild type), but not in H1299 cells (p53-null). The functional studies demonstrated that the proapoptotic effect of curcumin was related to over-expression of miR-192-5p/215 in H460, A427, and A549 cells. Curcumin up-regulated and activated p53 in the p53 wild-type H460, A427, and A549 NSCLC cells, while lack of p53 in H1299 cells impaired the response of miR-192-5p/215 to curcumin treatment. As predicted by miRBase, TargetScan, PicTar, and miRDB in silico miRNA target databases, and also confirmed by a dual-luciferase activity assay, XIAP is a target of miR-192-5p/215. The result showed that curcumin induced apoptosis through activation of the p53-miR-192-5p/215-XIAP pathway in NSCLC cells. In summary, the p53-miR-192-5p/215-XIAP pathway may be a feasible therapeutic target for NSCLC (Ye et al. 2015).

Recently, Jin et al. (2015) confirmed that curcumin treatment effectively increased the relative miR-192-5p expression and suppressed the PI3K/Akt signaling pathway; these effects were paralleled by inhibition of cell proliferation and increased apoptosis of human NSCLC cells, and were reversed by anti-miR-192-5p mimics.

The miR-186\* exerts an oncogenic role in human lung cancer cells by down-regulating proapoptotic genes. Tang et al. (2010) and Zhang et al. (2010a, b) investigated the effect of curcumin on the expression of miR-186\* in A549/DDP human lung cancer cells. Microarray analysis and qRT-PCR revealed that curcumin could induce apoptosis by down-regulating miR-186\* expression in A549/DDP

cells. The target of miR-186\* was predicted using the Miranda database and was confirmed by using dual-luciferase reporter assays and western-blot analysis. Caspase-10, as a target of miR-186\*, was significantly increased in curcumin-treated lung cancer cells. Caspase-10 is believed to be an initiator caspase in death receptor signaling that is crucial for apoptotic signaling. These results demonstrate that curcumin induces A549 cell apoptosis through the miR-186\* pathway in a dose- and time-dependent manner. In conclusion, curcumin can suppress A549 cell proliferation and induce apoptosis by increasing caspase-10 through down-regulation of miRNA-186\* expression (Tang et al. 2010; Zhang et al. 2010a, b).

The miR-874 is a tumor-suppressive miR which has been shown to target matrix metalloproteinase-2 (MMP-2) in NSCLC cell lines. Ahmad et al. (2015) found that CDF could inhibit MMP-2 expression and activity in A549 and H1299 NSCLC cells much more effectively than curcumin and resulted in up-regulation of miR-874, validating molecular modeling results. Additionally, CDF was found to be much more effective in down-regulating MMP-2 secretion, relative to curcumin, at all the time periods and in both A549 and H1299 cell lines (Ahmad et al. 2015).

In summary, the anti-apoptotic and anti-proliferative effect of curcumin in lung cancer cells is related to modulation of PTEN, Caspase-10, and MMP-2 gene expression. It has been shown that curcumin exerted its effects by modulating the expression of miR-21, miR-192-5p, miR-215, miR-186, miR-186\*, and miR-874.

## 6.4 Breast Cancer

Curcumin has significant effects on the expression of miR-15a, miR-16, miR-19, miR181b, and miR-34a in breast cancer cells (Tables 2 and 3). Both miR-15a and miR-16 may inhibit the expression of anti-apoptotic Bcl-2, thereby inducing apoptosis. Bcl-2 is a key factor in inhibiting apoptosis in eukaryotic cells. Yang et al. investigated the expression of miR-15a and miR-16 in curcumin-treated MCF-7 human breast cancer cells. Curcumin reduced the expression of Bcl-2 by up-regulating the expression of miR-15a and miR-16 in MCF-7 cells. Different concentrations of curcumin (10–60  $\mu$ M) had a dose-dependent cytotoxic effect on MCF-7 cells as revealed by the annexin V/propidium iodide staining assay. Treatment with 30–60  $\mu$ M curcumin for 24 h induced significant cell apoptosis compared with controls. The results of this study indicate that miR-15a and miR-16 can most likely serve as potential gene therapy targets for Bcl-2-overexpressing tumors (Yang et al. 2010).

In the miR-17-92 cluster, miR-19 has been identified as a key oncomiR that exerts oncogenic function by targeting several critical tumor suppressor genes such as PTEN. Li et al. studied the effect of curcumin on the expression of miR-19a and miR-19b in bisphenol A (BPA)-induced MCF-7 cells. BPA, a known endocrine disrupter, is closely related to the development of breast cancer. As demonstrated by qRT-PCR, curcumin decreased the gene expression of oncogenic miR-19a and miR-19b in BPA-induced MCF-7 cells. Using western blotting, PTEN, p-AKT, and

p53 were confirmed as targets of miR-19a and miR-19b based on expression patterns. Curcumin was able to increase the expression of miR-19-related downstream proteins, including PTEN, p-AKT, p-MDM2, p53, and proliferating cell nuclear antigen (PCNA). By modulating the miR-19/PTEN/AKT/p53 axis, curcumin inhibited the proliferative effects of BPA on MCF-7 cells (Li et al. 2014).

miR-181b induces apoptosis and necrosis in breast cancer cells by targeting the chemokine (C-X-C motif) ligand 1 (CXCL1) and 2. Apoptosis/necrosis assays revealed that miR181b over-expression led to enhanced apoptosis, as well as necrosis. miR-181b down-regulates CXCL1 and -2 through direct binding to their 3-UTR. As studied by Kronski et al. (2014) microarray miR expression analyses and qRT-PCR showed that curcumin induces miR-181b expression in metastatic breast cancer MDA-MB 231 cells. The curcumin-induced up-regulation of miR181b led to reduced expression of the prometastatic cytokines CXCL1 and -2, thus, repressing the potential for metastasis. Therefore, the inhibitory effect of curcumin on the expression of CXCL1 and 2 would suggest that it has great potential in anti-metastatic treatment of cancer (Kronski et al. 2014).

miR-34a has been described as a miRNA with anti-tumorigenic properties. Bcl-2 and Bmi-1 play important roles in tumorigenesis and have been shown to be regulated by miR-34a. Guo et al. (2013) reported that curcumin decreases the expression of Bcl-2 and Bmi-1 by up-regulating miR-34a in MDA-MB-231 and MDA-MB-435 cells. As determined by qRT-PCR, miR-34a is normally expressed at low levels, however, treatment of both cell lines with curcumin (30 and 35  $\mu$ M) significantly increased the expression of miR-34a. Bcl-2 and Bmi-1 were analyzed by western blot, and it would appear based on previous studies that curcumin inhibits cell proliferation and invasion, and induces cell cycle arrest and apoptosis, by inhibiting the expression of SIRT1, Bcl-2, and Fra-1. Curcumin inhibits breast cancer cell growth and invasion by regulating of miR-34a (Guo et al. 2013).

The tumor suppressor p16(INK4A) protein inhibits the pro-carcinogenic effects of breast stromal fibroblast by repressing IL-6 expression and secretion. This effect is mediated by miR-146b-5p, that inhibits IL-6 expression through a specific sequence at the IL-6 3'UTR. Treatment of active breast stromal fibroblasts with curcumin increased the level of p16(INK4A) and miR-146b-5p and suppressed IL-6 (Al-Ansari and Aboussekhra 2015).

To summarize, curcumin demonstrated an inhibitory effect on breast cancer proliferation and metastasis by inducing cell cycle arrest and apoptosis by modulating the expression of Bcl-2, Bmi-1, CXCL1 and -2, PTEN, p-AKT, p-MDM2, p53, p16(INK4A) and PCNA-related pathways (Table 4). The modified expression of miR-15a, miR-16, miR-19, miR181b, miR-34a and miR-146b-5p would seem to account for these curcumin-induced pathway modulations in breast cancer.



## 6.5 Prostate Cancer

miR-21, miR-205, miR-141, miR-183, miR-152, and miR-208 have been shown to exert an important role in curcumin-treated prostate cancer cells (Tables 2 and 3). miR-205 is down-regulated in prostate cancer and exerts tumor-suppressive functions, but miR-21 in this cancer seems to be associated with oncogenic effects. Yallapu et al. (2014) investigated the gene expression of miR-21 and miR-205 in prostate cancer cells C4-2, DU-145, and PC-3 that were treated with PLGA-CUR NPs, which are a novel formulation of poly(lactic-co-glycolic acid)-curcumin nanoparticles. As determined by qRT-PCR, significant down-regulation of oncogenic miR-21 and up-regulation of miR-205 was observed when prostate cancer cells were treated with PLGA-CUR NPs (4 and 6  $\mu\text{M}$ ). PLGA-CUR NPs caused a ninefold reduction in the expression of miR-21 and a tenfold increase in miR-205 levels. PLGA-CUR NPs were capable of modifying both *in vitro* and *in vivo* prostate cancer cell growth, as well as molecular pathways involved in apoptosis, oncogenic signaling pathways, and the tumor microenvironment (Yallapu et al. 2014). Some properties of curcumin such as a low bioavailability, rapid metabolism, and dose-limiting toxicities resulted in structural analogs of curcumin being designed. EF24 (diphenyl difluoroketone), a curcumin analogue, can improve the therapeutic effects of curcumin by increasing potency, decreasing side-effects, and increasing the bioavailability (Adams et al. 2004; Reid et al. 2014). Yang et al. (2013) evaluated the effect of EF24 (5  $\mu\text{M}$ ) on the gene expression of miR-21 in DU145 prostate tumor tissue. As revealed by qRT-PCR, EF24 was able to suppress the expression of miR-21 in prostate cancer cells both *in vitro* and *in vivo*. The targets of miR-21 in prostate cancer cells have been experimentally validated by qRT-PCR and immunoblotting. EF24 increased the expression of the miR-21 target genes, PTEN, and PDCD4 in DU145 tumor tissue, and suppressed the expression of markers of proliferating cells (cyclin D1 and Ki67). Expression profiling of miRs regulated by EF24 *in vitro* and *in vivo* showed that the anti-tumor activity of EF24 reflected the enhanced expression of potential tumor suppressor miRs, as well as the suppressed expression of oncomiRs, including miR-21. In conclusion, EF24 may induce apoptosis and inhibit cell growth in prostate cancer cells by suppression of miR-21 and, as a consequence, the up-regulation of PTEN and PDCD4 (Yang et al. 2013).

The bioinformatics analyses highlighted three miRs, which included miR-141, -183, and -152 that may be regulated by curcumin in prostate cancer cells. miR-141 is an androgen-regulated circulating miR that is involved in the progression of prostate cancer through its regulation (inhibition) of apoptosis. miR-141 is up-regulated in cancer primarily through the effects of zinc finger transcription factor Trps1, which is involved in oxidative stress and in DU145 cell death by apoptosis. miR-183 was reported to be up-regulated in prostate cancer and Dkk-3/SMAD4 were identified as potential target genes of miR-183 (Ueno et al. 2013). Two-dimensional gel electrophoresis (2D-DIGE) has identified miR-152 to be a tumor-suppressive miR due to its regulatory effects on DNMT1.



Recently, Guo et al. (2015) found that curcumin (from 0.2 to 0.8  $\mu\text{mol/L}$ ) dose-dependently inhibited the proliferation of prostate cancer cells, increased the cell cycle suppressor CDKN1A at protein level but not mRNA levels, and inhibited miR-208. These data suggest that curcumin inhibits growth of prostate cancer cells via miR-208-mediated CDKN1A activation (Guo et al. 2015).

Finally, proteins modulated by curcumin are implicated in protein folding (such as heat-shock protein PPP2R1A; RNA splicing proteins RBM17, DDX39; cell death proteins HMGB1 and NPM1; proteins involved in androgen receptor signaling, NPM1 and FKBP4 FKBP52), and curcumin could have an effect on miR-141, miR-152, and miR-183 expression (Table 4) (Teiten et al. 2012).

## 6.6 Melanoma

miR-21, miR-33b, mmu-miR-205-5p have roles in curcumin-mediated treatment of melanoma cells (Tables 2 and 3). miR-21 targets in melanoma cells are PTEN, PDCD4, and Bcl-2, which are involved in cell cycle regulation and apoptotic pathways. Yang et al. (2013) studied the effect of EF24 on miR-21 expression in a B16 melanoma cell line treated with EF24 (5  $\mu\text{M}$ ) for 24 h. qRT-PCR analysis demonstrated the expression level of miR-21 in EF24 treated cells was down-regulated by more than 70%. Down-regulation of miR-21 in EF24-treated melanoma cells led to a significant increase in the expression of PTEN and PDCD4, but had no effect on Bcl-2. Thus, EF24 can suppress the growth of melanoma cells through cell cycle arrest by inhibiting the expression of miR-21, which results in up-regulation of tumor suppressor genes (Yang et al. 2013).

The miR-33b target is the high mobility group AT-hook 2 (HMGA2), a key mediator of tumor-EMT. Zhang et al. (2015) investigated the effect of EF24 on the expression of miR-33b, miR-200a, Let-7, miR-98, miR-145, and miR-26a in the melanoma cell lines Lu1205 and A375. As determined by qRT-PCR, EF24 treatment conferred a 10.5- and 6.6-fold increase in miR-33b expression in Lu1205 and A375 cells, respectively. Furthermore, EF24 treatment up-regulated Let-7 by 2.9-fold in Lu1205 cells, while it did not result in a significant change in Let-7 expression in A375 cells. Importantly, all other miRNA levels were insensitive to EF24 treatment. The miR-33b target was predicted by three major prediction software programs; namely, TargetScan, PicTar, and miRandam, and experimentally validated by a dual-luciferase assay and western-blot analysis. In summary, EF24 limits melanoma metastasis and EMT by mediating the suppression of miR-33b-dependent HMGA2 (Zhang et al. 2015).

mmu-miR-205-5p targets in melanoma are anti-apoptotic Bcl-2 and PCNA proteins. Dahmke et al. (2013) evaluated the effect of dietary curcumin (consisting of 77% curcumin, 17% demethoxycurcumin, and 3% bis-demethoxycurcumin) consumption (160 mg/day) on the miRNA expression signature of a mouse melanoma model, and of murine B78H1 cells, human SK-MEL-28, and MeWo cells (treated with 20  $\mu\text{M}$  curcumin): in vivo and in vitro results were similar.

A microarray analysis revealed 147 miRNAs were markedly regulated following the administration of curcumin. The twenty most up-regulated and down-regulated miRNAs were identified. Among these miRNAs, the expression level of miRNAs that previously showed anticancer properties, including mmu-miR-205-5p, mmu-miR-205-3p, mmu-miR-142-5p, and mmu-miR-130b-3p, were confirmed by qRT-PCR. The most up-regulated miRNA, mmu-miR-205-5p, was expressed 135-fold greater in curcumin-treated samples. Also, mmu-miR-205-3p and mmu-miR-142-5p were up-regulated, but mmu-miR-130b-3p was down-regulated in murine B78H1 and human SK-MEL-28 cells. MeWo cells, derived from melanoma lymph node metastases, did not show an effective regulation of these miRNAs. The miRNA targets were predicted by the online analysis-tool called *GeneTrail*, and were experimentally validated by western-blot analysis. Bcl-2 and PCNA, which participate in cancer-related pathways including apoptosis and proliferation, were identified as targets of mmu-miR-205-5p. The expression of Bcl-2 and PCNA were significantly down-regulated by curcumin treatment. Finally, curcumin inhibited melanoma by modulating both proliferation and apoptosis pathways (Dahmke et al. 2013). In summary, curcumin and EF24 may inhibit melanoma growth and metastasis by inducing cell cycle arrest and apoptosis by modulating the expression of PCNA, PDCD4, PTEN, and Bcl-2-related pathways. The modified expression of miR-21, miR-33b, and mmu-miR-205-5p may possibly account for these curcumin-induced pathway modulations in melanoma cells (Table 4).

## 6.7 Other Types of Cancers

miR-31 has been found to be up-regulated in oral squamous-cell carcinoma (OSCC) and to act as an oncogenic miRNA. There is up-regulation of miR-31, miR-181b, and miR-222 in OSCC cells following EGF treatment. Up-regulation of miR-31 induced by EGF was abrogated by either AKT inhibition, or by the knockdown of C/EBP $\beta$  expression. Lu et al. investigated the effect of curcumin (6, 12, and 24  $\mu$ M) on miR-31 expression in three different OSCC cell lines: SAS, OECM-1, and HSC-3. The miR-31 expression was found to be down-regulated in a dose-dependent manner in SAS cells. As revealed by western-blot analysis, curcumin attenuated AKT activation and down-regulated C/EBP $\beta$  in response to miR-31 inhibition (Lu et al. 2014). In another study, Xiao et al. evaluated the effects of curcumin on the expression of miR-9 in OSCC cells and explored the potential relationships between miR-9 and the Wnt/ $\beta$ -catenin pathway in curcumin-mediated OSCC inhibition in vitro. qRT-PCR analysis suggested that curcumin treatment (20, 40, and 60  $\mu$ M) caused a significant elevation in the expression of miR-9 in SCC-9 cells in a dose-dependent manner. In conclusion, curcumin inhibited SCC-9 cell proliferation by up-regulating miR-9 expression and suppressing Wnt/ $\beta$ -catenin signaling. These effects were thought to result from the increase in

the expression levels of GSK-3b, phosphorylated GSK-3b, and  $\beta$ -catenin, and by a decrease in the cyclin D1 level (Xiao et al. 2014).

miR-203 is the only miR that has been studied in relation to curcumin's effects in bladder cancer. miR-203 is tumor suppressive, and DNA hypermethylation of its promoter has been shown to be down-regulated in bladder cancer. Its targets in bladder cancer are Akt2 and Src oncogenes, which have important roles in proliferation and apoptosis pathways. Saini et al. (2011) examined the effect of curcumin on miR-203 expression in bladder cancer cell lines (T24, J82, and TCCSUP) treated with 10  $\mu$ M curcumin. As determined by qRT-PCR, curcumin up-regulated the expression level of miR-203 nearly twofold in bladder cancer cells. miRANDA and TargetScan softwares were used to predict miR-203 targets. The targets were experimentally validated by western-blot analysis. Result showed that increased miR-203 expression led to down-regulation of its target oncogenes, Akt2 and Src, which resulted in inhibition of proliferation and induction of apoptosis in bladder cancer cells. In summary, curcumin directly induces hypomethylation of the miR-203 promoter, and subsequently, suppresses cellular proliferation, migration, and invasion of bladder cancer (Saini et al. 2011).

miR-22 is down-regulated in the human retinoblastoma (RB) tumor. Its target in human RB cells is the erythroblastic leukemia viral oncogene homolog 3 (ErbB3) that is involved in diverse biological responses, including proliferation, differentiation, cell motility, and survival. Sreenivasan et al. evaluated the effect of curcumin on the expression profile of miRNAs in the Y79 RB cell line. miRNA microarray analysis of curcumin-treated Y79 RB cells showed significant up-regulation of four tumor suppressor miRNAs (let-7 g\*, miR-22, 503, and 200c) and significant down-regulation of eight oncomiRs (miR-135b, 210, 25\*, 95, 514, 106b\*, 34c-3p, and 92a-1\*). The altered miRNA expression after curcumin treatment was confirmed by qRT-PCR. The targets of the miRNAs were predicted using miRBase, TargetScan, and the PicTar database algorithms, and subsequently validated by western-blot analysis. Results showed that the expression of the miR-22 target, ErbB3, was reduced as a function of miR-22 over-expression in curcumin-treated Y79 RB cells. In short, curcumin most likely inhibited cell proliferation, as well as diminished migration, through up-regulation of tumor-suppressive miRNAs; specifically, miR-22, and thereby caused inhibition of ErbB3 (Sreenivasan et al. 2012).

It has been reported that miR-9 inhibits ovarian cancer cell proliferation, migration, and invasion through suppression of the talin1/FAK/Akt pathway. Zhao et al. (2014) investigated the effect of curcumin (10–60  $\mu$ M) on miR-9 expression in SKOV3 ovarian cancer cells. qRT-PCR analysis revealed that curcumin treatment caused a significant increase in the expression of miR-9 in SKOV3 cells. Flow cytometric analysis demonstrated that exposure to 60  $\mu$ M curcumin for 72 h resulted in a significant increase in the percentage of apoptosis as a consequence of miR-9 up-regulation (Zhao et al. 2014).

In stem cells, miR-145 induces differentiation by suppressing the promoter of OCT4 and SOX-2. Additionally, miR-145 directly targets OCT4 and SOX-2 3'-UTR. Down-regulation of miR-145 in a wide range of tumors suggests that this miRNA acts as a tumor suppressor. Mirgani et al. (2014) studied the effect of

dendrosomal curcumin (DNC) on miR-145 expression in U87MG glioblastoma cells. DNC was prepared as 142 nm spherical structures with consistent physical and chemical stability. As demonstrated by qRT-PCR, miR-145 expression was significantly increased in U87MG cells treated with DNC (17.5 mM). DNC decreased the expression of OCT4A, OCT4B1, and SOX-2 in a miR-145-dependent manner. Transcription factors, OCT4 (octamer binding protein 4), SOX-2 (SRY [sex determining region Y]-box 2), and Nanog play crucial roles in the maintenance of stemness in both embryonic and somatic stem cells (Mirgani et al. 2014).

In nasopharyngeal carcinoma (NPC), miR-125a-5p targets the expression of tumor protein 53 (TP53). Gao et al. (2014) studied hsa-miR-125a-5p, hsa-miR-574-3p, and hsa-miR-210 expression in the HONE1 NPC cell line treated with curcumin. Curcumin treatment down-regulated the expression of hsa-miR-125a-5p, hsa-miR-574-3p, and hsa-miR-210 as determined by miR microarray analysis and qRT-PCR. Expression of hsa-miR-125a-5p has been shown to enhance proliferation, migration, and invasion of HONE1 cells. Curcumin caused inhibitory effects on HONE1 cells by inhibiting the expression of hsa-miR-125a-5p, and subsequently, enhancing the expression of TP53. Curcumin may provide a novel strategy to block hsa-miR-125a-5p for miR-based gene therapies in NPC (Gao et al. 2014). In another study, Gao et al. (2012) found that miR-15a/16-1 mediates the down-regulation of Wilm's tumor 1 gene (WT1), which plays an important role in the anti-proliferative effect of curcumin in leukemic cells (Gao et al. 2012). Pure curcumin up-regulated the expression of miR-15a/16-1 and down-regulated the expression of WT1 in leukemic cells and primary acute myeloid leukemia (AML) cells. The mRNA and protein levels of WT1 were detected by qRT-PCR and western blotting, respectively, after K562 and HL-60 cells were treated with pure curcumin.

Recently, Taverna et al. (2015) found that addition of curcumin to chronic ML cells caused a dose-dependent increase of PTEN, target of miR-21, and also down-regulated Bcr-Abl expression through the cellular increase of miR-196b. In vivo, curcumin-mediated selective packaging of miR-21 in exosomes is associated with an antileukemic effect in chronic ML.

miR-21 is up-regulated in esophageal cancer. Another important miR is miR-34, which has been found to participate in the regulation of p53 and Notch pathways consistent with tumor suppressor activity. Notch signaling and its regulations are critically important at the level of post-transcriptional and/or translational regulation of genes by miRNAs in esophagus. Subramaniam et al. (2012) showed curcumin treatment down-regulated the expression of Notch-1 specific microRNAs, miR-21, and miR-34a, and up-regulated tumor suppressor let-7a miRNA in esophageal cancer cell lines TE-7, TE-10, and Eso-1, as determined by qRT-PCR. Curcumin treatment resulted in a dose- and time-dependent inhibition of proliferation and colony formation in esophageal cancer cell lines. Curcumin significantly suppressed the proliferation of esophageal cancer cell lines together with modulation of the above-mentioned miRNAs and their targets (Subramaniam et al. 2012).

Finally, MEG3 is a tumor suppressor long noncoding RNA, whose methylation in its promoter region elicits the decrease in its expression in hepatocellular cancer (HCC) cells. Zamani et al. (2015) found that DNMT dependent over-expression of miR-29a and miR-185 can down-regulate the expression of DNMT1 and subsequently over-expresses MEG3. Also, the expression levels of miR-200a/b might determine the therapeutic efficacy of curcumin in HCC cells (Liang et al. 2013).

## 7 Concluding Remarks

Curcumin and its analogues, CDF, EF24, as well as nanoparticle formulations incorporating these agents, can exert anticancer effects by modulating the expression of oncomiRs and tumor-suppressive miRNAs in different cancer cells both in vitro and in vivo (Tables 2 and 3). Among various cancers, colon and pancreatic cancers have been the most extensively studied ones. Curcumin suppresses the progression and metastasis of chemo-resistant colon cancer cells through down-regulation of oncomiRs, including miR-27a, miR-20a, and miR-17-5p and up-regulation of EMT-suppressive miRNAs including miR-200b/c, miR-34a, miR-141, miR-429, and miR-101 (Fig. 2). Interestingly, CDF can demethylate the promoter of the miR-34 family that causes re-expression of these miRNAs in colon cancer cells. Additionally, down-regulation of miR-21 expression mediated by curcumin and/or CDF induces tumor suppression, and inhibition of migration, invasion, and metastasis of colon cancer cells. Curcumin and/or liposomal curcumin down-regulates miR-199a\* expression and up-regulates miR-22 expression, which subsequently leads to inhibited cell growth and induces pancreatic cancer cells to undergo apoptosis. Also, in pancreatic CSCs, CDF up-regulates the expression of miR-143 and a panel of tumor-suppressive microRNAs (let-7 family, miR-26a, miR-101, miR-146a, and miR-200b) that targets CSC marker genes. Finally, curcumin suppressed cell proliferation, induced cell apoptosis, and inhibited cell migration in pancreatic cancer cells due, in part, to up-regulation of miR-7. In summary, among oncomiRs that are modulated by exposure to curcumin, miR-21 seems to be targeted in a variety of cancer cells. However, some oncomiRs, including miR-17-5p, miR-20a, and miR-27a, were specifically down-regulated in colon cancer cells. Additionally, tumor-suppressive miRNAs, including miR-34 a/c and EMT-suppressive miRNAs, were specifically up-regulated in colon cancer. With regard to previous studies, it is suggested that the suppression of miR-21, miR-17-5p, miR-20a, and miR-27a and the over-expression of miR-34a/c and EMT-suppressive miRNAs, might offer a promising strategy forward in terms of inhibiting tumor progression.

**Conflict of Interests** The authors have no competing interests to declare.

## References

- Adams BK, Ferstl EM, Davis MC, Herold M, Kurtkaya S, Camalier RF, Hollingshead MG, Kaur G, Sausville EA, Rickles FR (2004) Synthesis and biological evaluation of novel curcumin analogs as anti-cancer and anti-angiogenesis agents. *Bioorg Med Chem* 12:3871–3883
- Aggarwal BB, Shishodia S (2006) Molecular targets of dietary agents for prevention and therapy of cancer. *Biochem Pharmacol* 71:1397–1421
- Aggarwal S, Takada Y, Singh S, Myers JN, Aggarwal BB (2004) Inhibition of growth and survival of human head and neck squamous cell carcinoma cells by curcumin via modulation of nuclear factor- $\kappa$ B signaling. *Int J Cancer* 111:679–692
- Ahmad A, Sayed A, Ginnebaugh KR, Sharma V, Suri A, Saraph A, Padhye S, Sarkar FH (2015) Molecular docking and inhibition of matrix metalloproteinase-2 by novel difluorinatedbenzylidene curcumin analog. *Am J Transl Res* 7:298–308
- Akram M, Shahab-Uddin AA, Usmanghani K, Hannan A, Mohiuddin E, Asif M (2010) Curcuma longa and curcumin: a review article. *Rom J Biol Plant Biol* 55:65–70
- Al-Ansari MM, Aboussekhra A (2015) miR-146b-5p mediates p16-dependent repression of IL-6 and suppresses paracrine procarcinogenic effects of breast stromal fibroblasts. *Oncotarget* 6:30006–30016
- Ali S, Ahmad A, Banerjee S, Padhye S, Dominiak K, Schaffert JM, Wang Z, Philip PA, Sarkar FH (2010) Gemcitabine sensitivity can be induced in pancreatic cancer cells through modulation of miR-200 and miR-21 expression by curcumin or its analogue CDF. *Cancer Res* 70:3606–3617
- Ali S, Ahmad A, Aboukameel A, Bao B, Padhye S, Philip PA, Sarkar FH (2012) Increased Ras GTPase activity is regulated by miRNAs that can be attenuated by CDF treatment in pancreatic cancer cells. *Cancer Lett* 319:173–181
- Ambros V (2003) MicroRNA pathways in flies and worms: growth, death, fat, stress, and timing. *Cell* 113:673–676
- Arafa HM (2005) Curcumin attenuates diet-induced hypercholesterolemia in rats. *Med Sci Monit* 11:BR228–BR234
- Asai A, Miyazawa T (2001) Dietary curcuminoids prevent high-fat diet-induced lipid accumulation in rat liver and epididymal adipose tissue. *J Nutr* 131:2932–2935
- Asangani IA, Rasheed SA, Nikolova DA, Leupold JH, Colburn NH, Post S, Allgayer H (2008) MicroRNA-21 (miR-21) post-transcriptionally downregulates tumor suppressor Pcd4 and stimulates invasion, intravasation and metastasis in colorectal cancer. *Oncogene* 27:2128–2136
- Balasubramanyam K, Varier RA, Altaf M, Swaminathan V, Siddappa NB, Ranga U, Kundu TK (2004) Curcumin, a novel p300/CREB-binding protein-specific inhibitor of acetyltransferase, represses the acetylation of histone/nonhistone proteins and histone acetyltransferase-dependent chromatin transcription. *J Biol Chem* 279:51163–51171
- Bao B, Ali S, Kong D, Sarkar SH, Wang Z, Banerjee S, Aboukameel A, Padhye S, Philip PA, Sarkar FH (2011) Anti-tumor activity of a novel compound-CDF is mediated by regulating miR-21, miR-200, and PTEN in pancreatic cancer. *PLoS One* 6, e17850
- Bao B, Ali S, Banerjee S, Wang Z, Logna F, Azmi AS, Kong D, Ahmad A, Li Y, Padhye S (2012) Curcumin analogue CDF inhibits pancreatic tumor growth by switching on suppressor microRNAs and attenuating EZH2 expression. *Cancer Res* 72:335–345
- Brighenti M (2015) MicroRNA and MET in lung cancer. *Ann Transl Med* 3:68
- Chang TC, Wentzel EA, Kent OA, Ramachandran K, Mullendore M, Lee KH, Feldmann G, Yamakuchi M, Ferlito M, Lowenstein CJ, Arking DE, Beer MA, Maitra A, Mendell JT (2007) Transactivation of miR-34a by p53 broadly influences gene expression and promotes apoptosis. *Mol Cell* 26:745–752

- Chen A, Xu J, Johnson A (2006) Curcumin inhibits human colon cancer cell growth by suppressing gene expression of epidermal growth factor receptor through reducing the activity of the transcription factor Egr-1. *Oncogene* 25:278–287
- Chen K, An Y, Tie L, Pan Y, Li X (2015) Curcumin protects neurons from glutamate-induced excitotoxicity by membrane anchored AKAP79-PKA interaction network. *Evid Based Complement Alternat Med* 2015:706207
- Choudhuri T, Pal S, Das T, Sa G (2005) Curcumin selectively induces apoptosis in deregulated cyclin D1-expressed cells at G2 phase of cell cycle in a p53-dependent manner. *J Biol Chem* 280:20059–20068
- Collett GP, Campbell FC (2004) Curcumin induces c-jun N-terminal kinase-dependent apoptosis in HCT116 human colon cancer cells. *Carcinogenesis* 25:2183–2189
- Corney DC, Flesken-Nikitin A, Godwin AK, Wang W, Nikitin AY (2007) MicroRNA-34b and MicroRNA-34c are targets of p53 and cooperate in control of cell proliferation and adhesion-independent growth. *Cancer Res* 67:8433–8438
- Dahmke IN, Backes C, Rudzitis-Auth J, Laschke MW, Leidinger P, Menger MD, Meese E, Mahlknecht U (2013) Curcumin intake affects miRNA signature in murine melanoma with mmu-miR-205-5p most significantly altered. *PLoS One* 8, e81122
- Das PM, Singal R (2004) DNA methylation and cancer. *J Clin Oncol* 22:4632–4642
- Esmaily H, Sahebkar A, Iranshahi M, Ganjali S, Mohammadi A, Ferns G, Ghayour-Mobarhan M (2015) An investigation of the effects of curcumin on anxiety and depression in obese individuals: a randomized controlled trial. *Chin J Integr Med* 21:332–338
- Fan C, Wo X, Qian Y, Yin J, Gao L (2006) Effect of curcumin on the expression of LDL receptor in mouse macrophages. *J Ethnopharmacol* 105:251–254
- Gandhy SU, Kim K, Larsen L, Rosengren RJ, Safe S (2012) Curcumin and synthetic analogs induce reactive oxygen species and decreases specificity protein (Sp) transcription factors by targeting microRNAs. *BMC Cancer* 12:564
- Ganjali S, Sahebkar A, Mahdipour E, Jamialahmadi K, Torabi S, Akhlaghi S, Ferns G, Parizadeh SMR, Ghayour-Mobarhan M (2014) Investigation of the effects of curcumin on serum cytokines in obese individuals: a randomized controlled trial. *ScientificWorldJournal* 2014:898361
- Gao SM, Yang JJ, Chen CQ, Chen JJ, Ye LP, Wang LY, Wu JB, Xing CY, Yu K (2012) Pure curcumin decreases the expression of WT1 by upregulation of miR-15a and miR-16-1 in leukemic cells. *J Exp Clin Cancer Res* 31:27
- Gao W, Chan JY-W, Wong T-S (2014) Curcumin exerts inhibitory effects on undifferentiated nasopharyngeal carcinoma by inhibiting the expression of miR-125a-5p. *Clin Sci* 127:571–579
- Gleissner CA, Erbel C, Haeussler J, Akhavanpoor M, Domschke G, Linden F, Doesch AO, Conradson G, Buss SJ, Hofmann NP, Gitsioudis G, Katus HA, Korosoglou G (2014) Low levels of natural IgM antibodies against phosphorylcholine are independently associated with vascular remodeling in patients with coronary artery disease. *Clin Res Cardiol* 104:13–22
- Grunstein M (1997) Histone acetylation in chromatin structure and transcription. *Nature* 389:349–352
- Guo J, Li W, Shi H, Xie X, Li L, Tang H, Wu M, Kong Y, Yang L, Gao J (2013) Synergistic effects of curcumin with emodin against the proliferation and invasion of breast cancer cells through upregulation of miR-34a. *Mol Cell Biochem* 382:103–111
- Guo H, Xu Y, Fu Q (2015) Curcumin inhibits growth of prostate carcinoma via miR-208-mediated CDKN1A activation. *Tumour Biol* 36(11):8511–8517. doi:10.1007/s13277-015-3592-y
- Gupta SC, Kim JH, Prasad S, Aggarwal BB (2010) Regulation of survival, proliferation, invasion, angiogenesis, and metastasis of tumor cells through modulation of inflammatory pathways by nutraceuticals. *Cancer Metastasis Rev* 29:405–434
- Hammond SM (2015) An overview of microRNAs. *Adv Drug Deliv Rev* 87:3–14
- Jiang A, Wang X, Shan X, Li Y, Wang P, Jiang P, Feng Q (2015) Curcumin reactivates silenced tumor suppressor gene RARbeta by reducing DNA methylation. *Phytother Res* 29:1237–1245

- Jin H, Qiao F, Wang Y, Xu Y, Shang Y (2015) Curcumin inhibits cell proliferation and induces apoptosis of human non-small cell lung cancer cells through the upregulation of miR-192-5p and suppression of PI3K/Akt signaling pathway. *Oncol Rep* 34:2782–2789
- Jordan W, Drew C (1996) Curcumin—a natural herb with anti-HIV activity. *J Natl Med Assoc* 88:333
- Jurenka JS (2009) Anti-inflammatory properties of curcumin, a major constituent of *Curcuma longa*: a review of preclinical and clinical research. *Altern Med Rev* 14:277
- Kanwar SS, Yu Y, Nautiyal J, Patel BB, Padhye S, Sarkar FH, Majumdar AP (2011) Difluorinated-curcumin (CDF): a novel curcumin analog is a potent inhibitor of colon cancer stem-like cells. *Pharm Res* 28:827–838
- Kim M-k, G-j C, Lee H-s (2003) Fungicidal property of *Curcuma longa* L. rhizome-derived curcumin against phytopathogenic fungi in a greenhouse. *J Agric Food Chem* 51:1578–1581
- Kronski E, Fiori ME, Barbieri O, Astigiano S, Mirisola V, Killian PH, Bruno A, Pagani A, Rovera F, Pfeffer U (2014) miR181b is induced by the chemopreventive polyphenol curcumin and inhibits breast cancer metastasis via down-regulation of the inflammatory cytokines CXCL1 and-2. *Mol Oncol* 8:581–595
- Kumar K, Rai AK (2012) Proniosomal formulation of curcumin having anti-inflammatory and anti-arthritic activity in different experimental animal models. *Pharmazie* 67:852–857
- Kuncha M, Naidu VG, Sahu BD, Gadepalli SG, Sistla R (2014) Curcumin potentiates the anti-arthritic effect of prednisolone in Freund's complete adjuvant-induced arthritic rats. *J Pharm Pharmacol* 66:133–144
- Kurzrock R, Li L (2005) Liposome-encapsulated curcumin: in vitro and in vivo effects on proliferation, apoptosis, signaling, and angiogenesis. In: ASCO annual meeting proceedings, p 4091
- Lee Y, Kim M, Han J, Yeom KH, Lee S, Baek SH, Kim VN (2004) MicroRNA genes are transcribed by RNA polymerase II. *EMBO J* 23:4051–4060
- Lee SJ, Krauthauser C, Maduskuie V, Fawcett PT, Olson JM, Rajasekaran SA (2011) Curcumin-induced HDAC inhibition and attenuation of medulloblastoma growth in vitro and in vivo. *BMC Cancer* 11:144
- Li L, Ahmed B, Mehta K, Kurzrock R (2007) Liposomal curcumin with and without oxaliplatin: effects on cell growth, apoptosis, and angiogenesis in colorectal cancer. *Mol Cancer Ther* 6:1276–1282
- Li Y, Kong D, Wang Z, Sarkar FH (2010) Regulation of microRNAs by natural agents: an emerging field in chemoprevention and chemotherapy research. *Pharm Res* 27:1027–1041
- Li X, Xie W, Xie C, Huang C, Zhu J, Liang Z, Deng F, Zhu M, Zhu W, Wu R (2014) Curcumin modulates miR-19/PTEN/AKT/p53 axis to suppress bisphenol A-induced MCF-7 breast cancer cell proliferation. *Phytother Res* 28:1553–1560
- Liang HH, Wei PL, Hung CS, Wu CT, Wang W, Huang MT, Chang YJ (2013) MicroRNA-200a/b influenced the therapeutic effects of curcumin in hepatocellular carcinoma (HCC) cells. *Tumour Biol* 34:3209–3218
- Lu W-C, Kao S-Y, Yang C-C, Tu H-F, Wu C-H, Chang K-W, Lin S-C (2014) EGF up-regulates miR-31 through the C/EBP $\beta$  signal cascade in oral carcinoma. *PLoS One* 9, e108049
- Ma J, Fang B, Zeng F, Pang H, Zhang J, Shi Y, Wu X, Cheng L, Ma C, Xia J (2014) Curcumin inhibits cell growth and invasion through up-regulation of miR-7 in pancreatic cancer cells. *Toxicol Lett* 231:82–91
- Mahady G, Pendland S, Yun G, Lu Z (2001) Turmeric (*Curcuma longa*) and curcumin inhibit the growth of *Helicobacter pylori*, a group 1 carcinogen. *Anticancer Res* 22:4179–4181
- Mani S, Herceg Z (2010) DNA demethylating agents and epigenetic therapy of cancer. *Adv Genet* 70:327–340
- Mao L, Hruban RH, Boyle JO, Tockman M, Sidransky D (1994) Detection of oncogene mutations in sputum precedes diagnosis of lung cancer. *Cancer Res* 54:1634–1637



- Mirgani MT, Isacchi B, Sadeghizadeh M, Marra F, Bilia AR, Mowla SJ, Najafi F, Babaei E (2014) Dendrosomal curcumin nanoformulation downregulates pluripotency genes via miR-145 activation in U87MG glioblastoma cells. *Int J Nanomedicine* 9:403
- Mirzaei H, Naseri G, Rezaee R, Mohammadi M, Banikazemi Z, Reza Mirzaei H, Salehi H, Peyvandi M, Pawelek JM, Sahebkar A (2016) Curcumin: a new candidate for melanoma therapy? *Int J Cancer*. doi:[10.1002/ijc.30224](https://doi.org/10.1002/ijc.30224)
- Mohammadi A, Sahebkar A, Iranshahi M, Amini M, Khojasteh R, Ghayour-Mobarhan M, Ferns GA (2013) Effects of supplementation with curcuminoids on dyslipidemia in obese patients: a randomized crossover trial. *Phytother Res* 27:374–379
- Montazi AA, Sahebkar A (2016) Difluorinated curcumin: a promising curcumin analogue with improved anti-tumor activity and pharmacokinetic profile. *Curr Pharm Des*. doi:[10.2174/1381612822666160527113501](https://doi.org/10.2174/1381612822666160527113501)
- Montazi AA, Derosa G, Maffioli P, Banach M, Sahebkar A (2016) Role of microRNAs in the therapeutic effects of curcumin in non-cancer diseases. *Mol Diagn Ther*. doi:[10.1007/s40291-016-0202-7](https://doi.org/10.1007/s40291-016-0202-7)
- Mudduluru G, George-William J, Muppala S, Asangani I, Kumarswamy R, Nelson L, Allgayer H (2011) Curcumin regulates miR-21 expression and inhibits invasion and metastasis in colorectal cancer. *Biosci Rep* 31:185–197
- NCI D (1996) Clinical development plan: curcumin. *J Cell Biochem Suppl* 26:72–85
- Negi P, Jayaprakasha G, Jagan Mohan Rao L, Sakariah K (1999) Antibacterial activity of turmeric oil: a byproduct from curcumin manufacture. *J Agric Food Chem* 47:4297–4300
- Nishiyama T, Mae T, Kishida H, Tsukagawa M, Mimaki Y, Kuroda M, Sashida Y, Takahashi K, Kawada T, Nakagawa K (2005) Curcuminoids and sesquiterpenoids in turmeric (*Curcuma longa* L.) suppress an increase in blood glucose level in type 2 diabetic KK-Ay mice. *J Agric Food Chem* 53:959–963
- Noratto GD, Jutooru I, Safe S, Angel-Morales G, Mertens-Talcott SU (2013) The drug resistance suppression induced by curcuminoids in colon cancer SW-480 cells is mediated by reactive oxygen species-induced disruption of the microRNA-27a-ZBTB10-Sp axis. *Mol Nutr Food Res* 57:1638–1648
- Panahi Y, Sahebkar A, Amiri M, Davoudi SM, Beiraghdar F, Hoseininejad SL, Kolivand M (2012a) Improvement of sulphur mustard-induced chronic pruritus, quality of life and antioxidant status by curcumin: results of a randomised, double-blind, placebo-controlled trial. *Br J Nutr* 108:1272–1279
- Panahi Y, Sahebkar A, Parvin S, Saadat A (2012b) A randomized controlled trial on the anti-inflammatory effects of curcumin in patients with chronic sulphur mustard-induced cutaneous complications. *Ann Clin Biochem* 49:580–588
- Panahi Y, Rahimnia AR, Sharafi M, Alishiri G, Saburi A, Sahebkar A (2014a) Curcuminoid treatment for knee osteoarthritis: a randomized double-blind placebo-controlled trial. *Phytother Res* 28:1625–1631
- Panahi Y, Saadat A, Beiraghdar F, Sahebkar A (2014b) Adjuvant therapy with bioavailability-boosted curcuminoids suppresses systemic inflammation and improves quality of life in patients with solid tumors: a randomized double-blind placebo-controlled trial. *Phytother Res* 28:1461–1467
- Panahi Y, Badeli R, Karami GR, Sahebkar A (2015) Investigation of the efficacy of adjunctive therapy with bioavailability-boosted curcuminoids in major depressive disorder. *Phytother Res* 29:17–21
- Panahi Y, Alishiri GH, Parvin S, Sahebkar A (2016) Mitigation of systemic oxidative stress by curcuminoids in osteoarthritis: results of a randomized controlled trial. *J Diet Suppl* 13:209–220
- Panahi Y, Kianpour P, Mohtashami R, Jafari R, Simental-Mendía LE, Sahebkar A (2016) Curcumin lowers serum lipids and uric acid in subjects with non-alcoholic fatty liver disease: a randomized controlled trial. *J Cardiovasc Pharmacol*. doi:[10.1097/FJC.0000000000000406](https://doi.org/10.1097/FJC.0000000000000406)

- Rahmani S, Asgary S, Askari G, Keshvari M, Hatamipour M, Feizi A, Sahebkar A (2016) Treatment of non-alcoholic fatty liver disease with curcumin: a randomized placebo-controlled trial. *Phytother Res*. doi:[10.1002/ptr.5659](https://doi.org/10.1002/ptr.5659)
- Reddy RC, Vatsala PG, Keshamouni VG, Padmanaban G, Rangarajan PN (2005) Curcumin for malaria therapy. *Biochem Biophys Res Commun* 326:472–474
- Reid JM, Buhrow SA, Gilbert JA, Jia L, Shoji M, Snyder JP, Ames MM (2014) Mouse pharmacokinetics and metabolism of the curcumin analog, 4-piperidinone, 3,5-bis [(2-fluorophenyl)methylene]-acetate (3E, 5E)(EF-24; NSC 716993). *Cancer Chemother Pharmacol* 73:1137–1146
- Roy S, Levi E, Majumdar A, Sarkar FH (2012) Expression of miR-34 is lost in colon cancer which can be re-expressed by a novel agent CDF. *J Hematol Oncol* 5:58
- Roy S, Yu Y, Padhye SB, Sarkar FH, Majumdar AP (2013) Difluorinated-curcumin (CDF) restores PTEN expression in colon cancer cells by down-regulating miR-21. *PLoS One* 8, e68543
- Sahebkar A (2010) Molecular mechanisms for curcumin benefits against ischemic injury. *Fertil Steril* 94:e75–e76; author reply e77
- Sahebkar A (2013) Why it is necessary to translate curcumin into clinical practice for the prevention and treatment of metabolic syndrome? *Biofactors* 39:197–208
- Sahebkar A (2014) Are curcuminoids effective C-reactive protein-lowering agents in clinical practice? Evidence from a meta-analysis. *Phytother Res* 28:633–642
- Sahebkar A (2016) Autophagic activation: a key piece of the puzzle for the curcumin-associated cognitive enhancement? *J Psychopharmacol* 30:93–94
- Sahebkar A, Henrotin Y (2015) Analgesic efficacy and safety of curcuminoids in clinical practice: a systematic review and meta-analysis of randomized controlled trials. *Pain Med*
- Sahebkar A, Mohammadi A, Atabati A, Rahiman S, Tavallaie S, Iranshahi M, Akhlaghi S, Ferns GA, Ghayour-Mobarhan M (2013) Curcuminoids modulate pro-oxidant–antioxidant balance but not the immune response to heat shock protein 27 and oxidized LDL in obese individuals. *Phytother Res* 27:1883–1888
- Sahebkar A, Chew GT, Watts GF (2014) Recent advances in pharmacotherapy for hypertriglyceridemia. *Prog Lipid Res* 56:47–66
- Sahebkar A, Serban MC, Ursioniu S, Banach M (2015) Effect of curcuminoids on oxidative stress: a systematic review and meta-analysis of randomized controlled trials. *J Funct Foods* 18:898–909
- Sahebkar A, Cicero AF, Simental-Mendia LE, Aggarwal BB, Gupta SC (2016) Curcumin downregulates human tumor necrosis factor- $\alpha$  levels: a systematic review and meta-analysis of randomized controlled trials. *Pharmacol Res* 107:234–242
- Saini S, Arora S, Majid S, Shahryari V, Chen Y, Deng G, Yamamura S, Ueno K, Dahiya R (2011) Curcumin modulates microRNA-203-mediated regulation of the Src-Akt axis in bladder cancer. *Cancer Prev Res (Phila)* 4:1698–1709
- Sankar P, Telang AG, Suresh S, Kesavan M, Kannan K, Kalaivanan R, Sarkar SN (2013) Immunomodulatory effects of nanocurcumin in arsenic-exposed rats. *Int Immunopharmacol* 17:65–70
- Sarkar S, Dubaybo H, Ali S, Goncalves P, Kollepara SL, Sethi S, Philip PA, Li Y (2013) Down-regulation of miR-221 inhibits proliferation of pancreatic cancer cells through up-regulation of PTEN, p27(kip1), p57(kip2), and PUMA. *Am J Cancer Res* 3:465–477
- Sawan C, Vaissière T, Murr R, Herceg Z (2008) Epigenetic drivers and genetic passengers on the road to cancer. *Mutat Res* 642:1–13
- Seyedzadeh MH, Safari Z, Zare A, Gholizadeh Navashenaq J, Razavi SA, Kardar GA, Khorramzadeh MR (2014) Study of curcumin immunomodulatory effects on reactive astrocyte cell function. *Int Immunopharmacol* 22:230–235
- Shakeri A, Sahebkar A (2016) Optimized curcumin formulations for the treatment of Alzheimer's disease: a patent evaluation. *J Neurosci Res* 94:111–113

- Shankar S, Srivastava RK (2007) Involvement of Bcl-2 family members, phosphatidylinositol 3'-kinase/AKT and mitochondrial p53 in curcumin (diferulolylmethane)-induced apoptosis in prostate cancer. *Int J Oncol* 30:905–918
- Sharma O (1976) Antioxidant activity of curcumin and related compounds. *Biochem Pharmacol* 25:1811–1812
- Sharma S, Kulkarni SK, Chopra K (2006) Curcumin, the active principle of turmeric (*Curcuma longa*), ameliorates diabetic nephropathy in rats. *Clin Exp Pharmacol Physiol* 33:940–945
- Shen LL, Jiang ML, Liu SS, Cai MC, Hong ZQ, Lin LQ, Xing YY, Chen GL, Pan R, Yang LJ, Xu Y, Dong J (2015) Curcumin improves synaptic plasticity impairment induced by HIV-1gp120 V3 loop. *Neural Regen Res* 10:925–931
- Shu L, Khor TO, Lee J-H, Boyanapalli SS, Huang Y, Wu T-Y, Saw CL-L, Cheung K-L, Kong A-NT (2011) Epigenetic CpG demethylation of the promoter and reactivation of the expression of *Neurog1* by curcumin in prostate LNCaP cells. *AAPS J* 13:606–614
- Sidhu GS, Singh AK, Thaloor D, Banaudha KK, Patnaik GK, Srimal RC, Maheshwari RK (1998) Enhancement of wound healing by curcumin in animals. *Wound Repair Regen* 6:167–177
- Sreenivasan S, Thirumalai K, Danda R, Krishnakumar S (2012) Effect of curcumin on miRNA expression in human Y79 retinoblastoma cells. *Curr Eye Res* 37:421–428
- Steger DJ, Workman JL (1996) Remodeling chromatin structures for transcription: what happens to the histones? *Bioessays* 18:875–884
- Strimpakos AS, Sharma RA (2008) Curcumin: preventive and therapeutic properties in laboratory studies and clinical trials. *Antioxid Redox Signal* 10:511–546
- Subramaniam D, Ponnuram S, Ramamoorthy P, Standing D, Battafarano RJ, Anant S, Sharma P (2012) Curcumin induces cell death in esophageal cancer cells through modulating Notch signaling. *PLoS One* 7, e30590
- Sun Y (2006) p53 and its downstream proteins as molecular targets of cancer. *Mol Carcinog* 45:409–415
- Sun M, Estrov Z, Ji Y, Coombes KR, Harris DH, Kurzrock R (2008) Curcumin (diferulolylmethane) alters the expression profiles of microRNAs in human pancreatic cancer cells. *Mol Cancer Ther* 7:464–473
- Tang N, Zhang J, Du Y (2010) [Curcumin promoted the apoptosis of cisplatin-resistant human lung carcinoma cells A549/DDP through down-regulating miR-186\*]. *Zhongguo Fei Ai Za Zhi* 13:301–306
- Taverna S, Giallombardo M, Pucci M, Flugy A, Manno M, Raccosta S, Rolfo C, De Leo G, Alessandro R (2015) Curcumin inhibits in vitro and in vivo chronic myelogenous leukemia cells growth: a possible role for exosomal disposal of miR-21. *Oncotarget* 6:21918–21933
- Teiten M-H, Gaigneaux A, Chateauvieux S, Billing AM, Planchon S, Fack F, Renaut J, Mack F, Muller CP, Dicato M (2012) Identification of differentially expressed proteins in curcumin-treated prostate cancer cell lines. *OMICS* 16:289–300
- Teiten MH, Dicato M, Diederich M (2013) Curcumin as a regulator of epigenetic events. *Mol Nutr Food Res* 57:1619–1629
- Toden S, Okugawa Y, Jascur T, Wodarz D, Komarova NL, Buhrmann C, Shakibaei M, Boland CR, Goel A (2015) Curcumin mediates chemosensitization to 5-fluorouracil through miRNA-induced suppression of epithelial-to-mesenchymal transition in chemoresistant colorectal cancer. *Carcinogenesis* 36:355–367
- Ueno K, Hirata H, Shahryari V, Deng G, Tanaka Y, Tabatabai ZL, Hinoda Y, Dahiya R (2013) microRNA-183 is an oncogene targeting *Dkk-3* and *SMAD4* in prostate cancer. *Br J Cancer* 108:1659–1667
- Um MY, Hwang KH, Choi WH, Ahn J, Jung CH, Ha TY (2014) Curcumin attenuates adhesion molecules and matrix metalloproteinase expression in hypercholesterolemic rabbits. *Nutr Res* 34:886–893
- Wang Y, Lee CG (2009) MicroRNA and cancer-focus on apoptosis. *J Cell Mol Med* 13:12–23

- Wang Y, Li J, Zhuge L, Su D, Yang M, Tao S (2014) Comparison between the efficacies of curcumin and puerarin in C57BL/6 mice with steatohepatitis induced by a methionine- and choline-deficient diet. *Exp Ther Med* 7:663–668
- Wang BF, Cui ZW, Zhong ZH, Sun YH, Sun QF, Yang GY, Bian LG (2015) Curcumin attenuates brain edema in mice with intracerebral hemorrhage through inhibition of AQP4 and AQP9 expression. *Acta Pharmacol Sin* 36:939–948
- Wang J, Xie H, Gao F, Zhao T, Yang H, Kang B (2016) Curcumin induces apoptosis in p53-null Hep3B cells through a TAp73/DNp73-dependent pathway. *Tumour Biol* 37:4203–4212
- Williams RJ, Spencer JP (2012) Flavonoids, cognition, and dementia: actions, mechanisms, and potential therapeutic utility for Alzheimer disease. *Free Radic Biol Med* 52:35–45
- Winter J, Jung S, Keller S, Gregory RI, Diederichs S (2009) Many roads to maturity: microRNA biogenesis pathways and their regulation. *Nat Cell Biol* 11:228–234
- Xiao C, Wang L, Zhu L, Zhang C, Zhou J (2014) Curcumin inhibits oral squamous cell carcinoma SCC-9 cells proliferation by regulating miR-9 expression. *Biochem Biophys Res Commun* 454:576–580
- Yallapu MM, Khan S, Maher DM, Ebeling MC, Sundram V, Chauhan N, Ganju A, Balakrishna S, Gupta BK, Zafar N (2014) Anti-cancer activity of curcumin loaded nanoparticles in prostate cancer. *Biomaterials* 35:8635–8648
- Yang J, Cao Y, Sun J, Zhang Y (2010) Curcumin reduces the expression of Bcl-2 by upregulating miR-15a and miR-16 in MCF-7 cells. *Med Oncol* 27:1114–1118
- Yang CH, Yue J, Sims M, Pfeffer LM (2013) The curcumin analog EF24 targets NF-kappaB and miRNA-21, and has potent anticancer activity in vitro and in vivo. *PLoS One* 8, e71130
- Yang Y, Wu X, Wei Z, Dou Y, Zhao D, Wang T, Bian D, Tong B, Xia Y, Xia Y, Dai Y (2015) Oral curcumin has anti-arthritis efficacy through somatostatin generation via cAMP/PKA and Ca(2+)-CaMKII signaling pathways in the small intestine. *Pharmacol Res* 95–96:71–81
- Ye M, Zhang J, Miao Q, Yao L (2015) Curcumin promotes apoptosis by activating the p53-miR-192-5p/215-XIAP pathway in non-small cell lung cancer. *Cancer Lett* 357:196–205
- Zamani M, Sadeghizadeh M, Behmanesh M, Najafi F (2015) Dendrosomal curcumin increases expression of the long non-coding RNA gene MEG3 via up-regulation of epi-miRs in hepatocellular cancer. *Phytomedicine* 22:961–967
- Zhang W, Bai W (2014) MiR-21 suppresses the anticancer activities of curcumin by targeting PTEN gene in human non-small cell lung cancer A549 cells. *Clin Transl Oncol* 16:708–713
- Zhang J, Du Y, Wu C, Ren X, Ti X, Shi J, Zhao F, Yin H (2010a) Curcumin promotes apoptosis in human lung adenocarcinoma cells through miR-186\* signaling pathway. *Oncol Rep* 24:1217–1223
- Zhang J, Zhang T, Ti X, Shi J, Wu C, Ren X, Yin H (2010b) Curcumin promotes apoptosis in A549/DDP multidrug-resistant human lung adenocarcinoma cells through an miRNA signaling pathway. *Biochem Biophys Res Commun* 399:1–6
- Zhang P, Bai H, Liu G, Wang H, Chen F, Zhang B, Zeng P, Wu C, Peng C, Huang C (2015) MicroRNA-33b, upregulated by EF24, a curcumin analog, suppresses the epithelial-to-mesenchymal transition (EMT) and migratory potential of melanoma cells by targeting HMGA2. *Toxicol Lett* 234:151–161
- Zhao S-F, Zhang X, Zhang X-J, Shi X-Q, Yu Z-J, Kan Q-C (2014) Induction of microRNA-9 mediates cytotoxicity of curcumin against SKOV3 ovarian cancer cells. *Asian Pac J Cancer Prev* 15:3363–3368

# Functional Impact of Ryanodine Receptor Oxidation on Intracellular Calcium Regulation in the Heart

Aleksey V. Zima and Stefan R. Mazurek

**Abstract** Type 2 ryanodine receptor (RyR2) serves as the major intracellular  $\text{Ca}^{2+}$  release channel that drives heart contraction. RyR2 is activated by cytosolic  $\text{Ca}^{2+}$  via the process of  $\text{Ca}^{2+}$ -induced  $\text{Ca}^{2+}$  release (CICR). To ensure stability of  $\text{Ca}^{2+}$  dynamics, the self-reinforcing CICR must be tightly controlled. Defects in this control cause sarcoplasmic reticulum (SR)  $\text{Ca}^{2+}$  mishandling, which manifests in a variety of cardiac pathologies that include myocardial infarction and heart failure. These pathologies are also associated with oxidative stress. Given that RyR2 contains a large number of cysteine residues, it is no surprise that RyR2 plays a key role in the cellular response to oxidative stress. RyR's many cysteine residues pose an experimental limitation in defining a specific target or mechanism of action for oxidative stress. As a result, the current understanding of redox-mediated RyR2 dysfunction remains incomplete. Several oxidative modifications, including *S*-glutathionylation and *S*-nitrosylation, have been suggested playing an important role in the regulation of RyR2 activity. Moreover, oxidative stress can increase RyR2 activity by forming disulfide bonds between two neighboring subunits (intersubunit cross-linking). Since intersubunit interactions within the RyR2 homotetramer complex dictate the channel gating, such posttranslational modification of RyR2 would have a significant impact on RyR2 function and  $\text{Ca}^{2+}$  regulation. This review summarizes recent findings on oxidative modifications of RyR2 and discusses contributions of these RyR2 modifications to SR  $\text{Ca}^{2+}$  mishandling during cardiac pathologies.

**Keywords** Ca release • Glutathione • Heart • Reactive oxygen species • Ryanodine receptor • Sarcoplasmic reticulum

---

A.V. Zima (✉) and S.R. Mazurek

Department of Cell and Molecular Physiology, Loyola University Chicago, Stritch School of Medicine, 2160 South First Avenue, Maywood, IL 60153, USA

e-mail: [azima@luc.edu](mailto:azima@luc.edu)

## Contents

1	Excitation-Contraction Coupling and SR Ca <sup>2+</sup> Cycling .....	40
1.1	Molecular Components of Ca <sup>2+</sup> Cycling .....	41
1.2	Ryanodine Receptor Complex .....	42
1.3	Ca <sup>2+</sup> -Induced Ca <sup>2+</sup> Release .....	44
1.4	Luminal Ca <sup>2+</sup> and Inter-RyR2 Regulation of CICR .....	44
1.5	SR Ca <sup>2+</sup> Leak .....	45
2	SR Ca <sup>2+</sup> Cycling in Heart Disease .....	46
2.1	Ischemia/Reperfusion .....	46
2.2	Heart Failure .....	47
3	Oxidative Stress .....	48
3.1	Acute Oxidative Stress in Ischemia/Reperfusion Injury .....	49
3.2	Chronic Oxidative Stress in Heart Failure .....	49
4	Oxidative Posttranslational Modifications of RyR2 .....	50
4.1	S-Glutathionylation .....	51
4.2	S-Nitrosylation .....	52
4.3	Intersubunit Cross-Linking .....	53
5	Conclusion .....	55
	References .....	56

## 1 Excitation-Contraction Coupling and SR Ca<sup>2+</sup> Cycling

Excitation-contraction coupling (ECC) is the cellular mechanism that connects the electrical stimulus to the contraction of the heart. During the action potential (AP), a small Ca<sup>2+</sup> influx via L-type Ca<sup>2+</sup> channels (LTCCs) causes a massive Ca<sup>2+</sup> release from the sarcoplasmic reticulum (SR). This global rise in cytosolic Ca<sup>2+</sup> concentration ([Ca<sup>2+</sup>]<sub>i</sub>) triggers cell contraction with the binding of Ca<sup>2+</sup> to the myofilament protein troponin C. This induces an allosteric change in the troponin-tropomyosin complex, allowing for myosin heads to form a cross bridge interaction with actin. Once this Ca<sup>2+</sup>-dependent interaction takes place, mechanical force is generated with the hydrolysis of ATP by the actomyosin ATPase. These cycles will persist as long as ATP and Ca<sup>2+</sup> are present in sufficient concentration (Goldman 1987). Thus, Ca<sup>2+</sup> transport systems involved in the movement of Ca<sup>2+</sup> into and out of the cytosolic milieu contribute directly to the activation and relaxation of the myofilaments. In adult ventricular myocytes, Ca<sup>2+</sup> released from the SR plays a particularly important role in cell contraction. The cardiac SR is equipped with Ca<sup>2+</sup> handling machinery that is perfectly designed to regularly repeat the major steps of the cardiac cycle: Ca<sup>2+</sup> release and uptake (Zima et al. 2014). SR Ca<sup>2+</sup> release predominantly occurs via the type 2 ryanodine receptors (RyR2), whereas SR Ca<sup>2+</sup> uptake is entirely mediated by the type 2a SR Ca-ATPase (SERCA) (Bers 2001).

## 1.1 Molecular Components of $Ca^{2+}$ Cycling

Activated by  $Ca^{2+}$  influx via LTCCs, RyR2 mediates a massive  $Ca^{2+}$  release during systole. This mechanism is known as  $Ca^{2+}$ -induced  $Ca^{2+}$  release (CICR) (Fabiato 1983). In order for membrane excitation to simultaneously activate SR  $Ca^{2+}$  release in ventricular myocytes, sarcolemmal invaginations called transverse tubules (T-tubules) descend deep into the myocyte (Fig. 1). The SR forms a junction with the T-tubule creating a specialized subcellular microdomain called the dyadic cleft that allows for efficient activation of CICR (Soeller and Cannell 1999). Within the dyadic cleft, RyR2s and LTCCs interact in a highly organized lattice forming the  $Ca^{2+}$  release unit (CRU; Fig. 1) (Cheng and Lederer 2008). It has been estimated that CRU comprises a cluster of  $\sim 100$  RyRs (Franzini-Armstrong et al. 1999). However, the exact value currently remains a debated issue. Other investigators have estimated RyR2 cluster number to be smaller in size (Baddeley et al. 2009; Hayashi et al. 2009). These RyR2 clusters align with LTCCs in the dyadic cleft via junctophilins (Garbino et al. 2009). Activation of single CRU (spontaneously or by LTCC  $Ca^{2+}$  current) produced a local increase of  $[Ca^{2+}]_i$  called  $Ca^{2+}$  spark (Cheng et al. 1993). The global  $Ca^{2+}$  release is the result of the spatiotemporal activation of thousands of individual CRU or  $Ca^{2+}$  sparks (Fig. 1). Thus, the amplitude of the global  $Ca^{2+}$  transient during systole is the result of local subcellular recruitment of CRUs (Stern 1992).

During diastole, there are two major  $Ca^{2+}$  transport systems that compete for cytosolic  $Ca^{2+}$ : SERCAa and the sarcolemmal  $Na^+$ - $Ca^{2+}$  exchanger (NCX). The sarcolemmal  $Ca^{2+}$ -ATPase and the mitochondrial  $Ca^{2+}$  uniporter compete as well, but are considered to be minor components (Bassani et al. 1992). Immediately after the global rise in cytosolic  $Ca^{2+}$ , the majority of  $Ca^{2+}$  is sequestered back into the SR by SERCA and to a lesser extent is extruded from the cell by NCX (Fig. 1). The contribution of SERCA and NCX to decreasing  $[Ca^{2+}]_i$  during diastole is variable among animal species. It has been estimated that NCX contributes only 7% to  $Ca^{2+}$  removal in small rodent myocardium (Bers 2001). Whereas in rabbit, dog, and human myocardium, SERCA and NCX contribute approximately 70% and 30% to cardiac relaxation, respectively. There are two major contributors to the  $Ca^{2+}$  transient in the heart: LTCC-mediated  $Ca^{2+}$  current and SR  $Ca^{2+}$  release. While  $Ca^{2+}$  current contributes approximately 30% to the  $Ca^{2+}$  transient in the rabbit ventricle, the majority of  $Ca^{2+}$  comes from SR  $Ca^{2+}$  release by RyR2 (Bers 2001). At steady state,  $Ca^{2+}$  current and SR  $Ca^{2+}$  release must be balanced by  $Ca^{2+}$  extrusion and SR  $Ca^{2+}$  reuptake. Therefore, any changes in sarcolemmal  $Ca^{2+}$  current, SR  $Ca^{2+}$  release, SR  $Ca^{2+}$  uptake, or sarcolemmal  $Ca^{2+}$  extrusion can have a profound effect on  $Ca^{2+}$ -dependent inotropy (force) and lusitropy (relaxation) (Eisner et al. 1998).

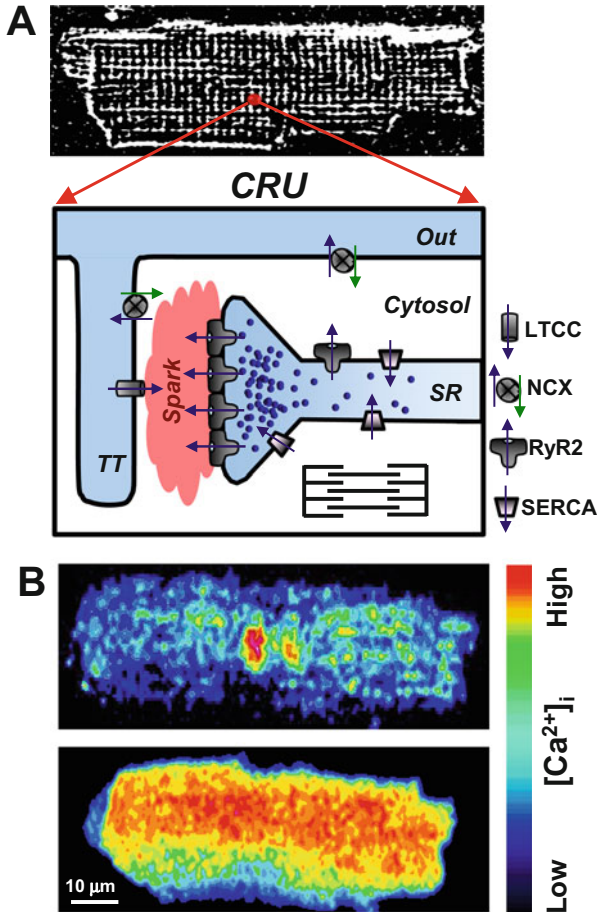


**Fig. 1** Intracellular  $\text{Ca}^{2+}$  regulation in adult ventricular myocytes. (**a**, *top panel*) a representative confocal image of rabbit ventricular myocytes loaded with the voltage-sensitive fluorescent dye Di-8-ANEPPS. Di-8-ANEPPS was used to label the T-tubular system. (**a**, *bottom panel*) the diagram illustrates the main components of  $\text{Ca}^{2+}$  release unit (CRU) in ventricular myocytes. A significant fraction of L-type  $\text{Ca}^{2+}$  channels (LTCC) is localized in the T-tubule (TT), whereas the majority of ryanodine receptors (RyR2) is concentrated in the junctional SR.  $\text{Ca}^{2+}$ -ATPase (SERCA) pumps cytosolic  $\text{Ca}^{2+}$  back into the SR, and the  $\text{Na}^{+}$ - $\text{Ca}^{2+}$  exchanger (NCX) removes  $\text{Ca}^{2+}$  from the cell. The plasmalemmal  $\text{Ca}^{2+}$ -ATPase and mitochondria play a minor role in cardiac relaxation. (**b**) Confocal images of diastolic  $\text{Ca}^{2+}$  spark (*top*) and an action potential-induced  $\text{Ca}^{2+}$  transient (*bottom*). Activation of a single CRU generates a  $\text{Ca}^{2+}$  spark, whereas simultaneous activation of thousands of these individual release units generates a global  $\text{Ca}^{2+}$  transient

## 1.2 Ryanodine Receptor Complex

Predominantly expressed in cardiac muscle, the type 2 RyR is a tetrameric channel with a total molecular weight of approximately 564 kDa. RyR2 has a relatively low selectivity given its permeability to many different divalent and monovalent



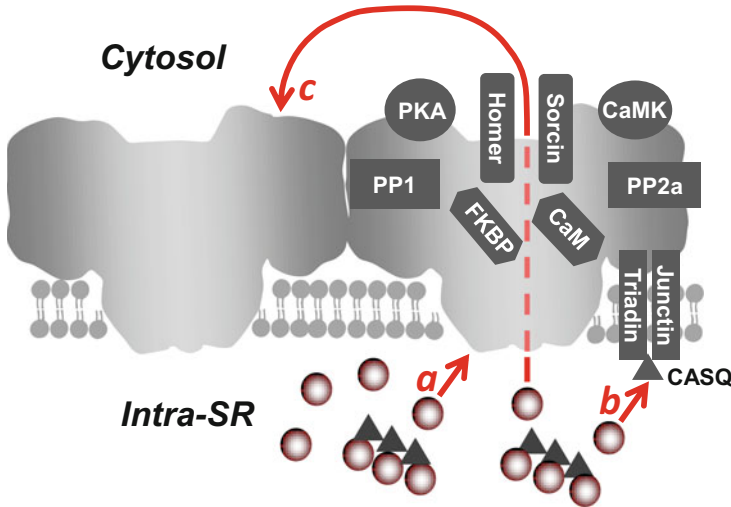


**Fig. 2** Regulation of cardiac ryanodine receptor. On the cytosolic side, RyR2 interacts with calmodulin (CaM), FK-506-binding proteins (FKBP), homer, sorcin, two major protein kinases (PKA and CaMKII), and two phosphatases (PP1 and PP2A). Luminal Ca<sup>2+</sup> regulates RyR2 activity by directly binding to the luminal side of the channel (*a*). Moreover, triadin and junctin form the luminal Ca<sup>2+</sup> sensor via interactions with the SR Ca<sup>2+</sup>-buffering protein calsequestrin (CASQ; *b*). Luminal Ca<sup>2+</sup> can also indirectly regulate RyR2 by acting on the cytosolic Ca<sup>2+</sup> activation site of neighboring channels by a “feed-through” mechanism (*c*)

cations. Furthermore, the channel has a very high conductance of approximately 100 pS for divalent cations (Fill and Copello 2002). Its characteristically low selectivity for Ca<sup>2+</sup> is suggested to be fundamental to its physiological role to produce a fast and large Ca<sup>2+</sup> release event. While Ca<sup>2+</sup> needs to compete with other cations for occupancy of the channel pore, it has been proposed that RyR2 has surface or vestibule charges that may enhance the permeation of Ca<sup>2+</sup> (Gillespie 2008; Mead-Savery et al. 2009). Although cytosolic Ca<sup>2+</sup> is the central physiological activator of RyR2, other free ions and small molecules can alter its activity including caffeine, Mg<sup>2+</sup>, H<sup>+</sup>, and ATP (Eager and Dulhunty 1998; Masumiya et al. 2001; Fill and Copello 2002). There are a number of proteins that interact with RyR2 as well, each of which can modulate the channel’s activity (Fig. 2). Proteins that interact on the cytosolic side of RyR2 include calmodulin (CaM), FK-506-binding proteins (FKBP), sorcin, and Homer-1 (for reviews, see (Bers 2004; Meissner 2004; Marx et al. 2000)). The two known kinases that are scaffolded on RyR2, protein kinase A (PKA), and calcium-/calmodulin-dependent kinase (CaMKII) have been shown to phosphorylate RyR2 at Ser-2809 and Ser-2815, respectively (Marx et al. 2000; Wehrens et al. 2004). Also, there are two known protein phosphatases that play a role in regulating RyR2 phosphorylation, including PP1 and PP2A. Spanning the SR membrane, but also associated with RyR2, are the auxiliary proteins junctin and triadin. Their function is thought to be important for RyR’s ability to sense luminal Ca<sup>2+</sup> ([Ca<sup>2+</sup>]<sub>SR</sub>) via interactions with the SR Ca<sup>2+</sup>-binding protein calsequestrin (CASQ). All of the aforementioned

proteins that make up the RyR2 complex are necessary for proper function of RyR2 channel activity.

### ***1.3 $Ca^{2+}$ -Induced $Ca^{2+}$ Release***

Unlike ECC in skeletal muscle, local  $Ca^{2+}$  entry from LTCC is an absolute requirement for SR  $Ca^{2+}$  release in cardiac muscle. Fabiato and Fabiato were the first to characterize cardiac CICR (Fabiato and Fabiato 1975). They showed that SR  $Ca^{2+}$  release by CICR was graded, having a dependence on both time and trigger. Moreover, it was shown that the introduction of high  $[Ca^{2+}]_i$  immediately after the  $Ca^{2+}$  pulse trigger would cause a decrease in SR  $Ca^{2+}$  release. It was concluded that this characteristic was due to a  $Ca^{2+}$ -dependent inactivation site on the cytosolic side of RyR2 (Fabiato 1985). While the activation characteristics of RyR2 have since been confirmed, inactivation of RyR2 or termination of CICR still remains controversial (Stern and Cheng 2004). A more recent study was unable to show that high  $[Ca^{2+}]_i$  promotes inactivation of CICR (Nabauer and Morad 1990; Stevens et al. 2009). Their results suggest the existence of other CICR termination mechanisms. In vitro and in vivo studies have shown that RyR2 channel activity and CICR termination are indeed dependent on  $[Ca^{2+}]_{SR}$  (Sitsapesan and Williams 1994; Terentyev et al. 2002; Gyorke et al. 2004; Qin et al. 2008). Furthermore, it has been demonstrated that SR  $Ca^{2+}$  release terminates at a critical level of  $[Ca^{2+}]_{SR}$ , which is dependent on RyR2 channel gating (Zima et al. 2008). For example, RyR2 sensitization to cytosolic  $Ca^{2+}$  by the presence of caffeine results in a lower SR termination level, increased SR  $Ca^{2+}$  fractional release, and increased cytosolic  $Ca^{2+}$  transient (Domeier et al. 2009). These characteristics of increased RyR2 activity are suggested to have pathological significance in the event of arrhythmogenic spontaneous  $Ca^{2+}$  waves and promoting abnormally low SR  $Ca^{2+}$  content as seen in the failing heart (Zima et al. 2014).

### ***1.4 Luminal $Ca^{2+}$ and Inter-RyR2 Regulation of CICR***

While Fabiato was the first to suggest an inactivation mechanism for RyR2 ( $[Ca^{2+}]_i$ -dependent), a number of other mechanisms have since been proposed that implicate luminal  $Ca^{2+}$  regulation ( $[Ca^{2+}]_{SR}$ -dependent) of RyR2 in the termination of CICR. Without changes in RyR2 channel activity, SR  $Ca^{2+}$  release terminates at a critical level that remains constant on a beat-to-beat basis (Domeier et al. 2009). Moreover, the termination level observed from a single RyR cluster (during  $Ca^{2+}$  spark events) also remains constant (Zima et al. 2008). This intrinsic property of RyR2 implies that there is the potential for a  $Ca^{2+}$  sensor to exist on the luminal side of the channel (Fig. 2a). While few argue the existence of a luminal  $Ca^{2+}$  binding site on RyR2 that acts as the primary  $[Ca^{2+}]_{SR}$  sensor (Chen et al. 2014), multiple studies claim that

the luminal  $\text{Ca}^{2+}$  sensing mechanism is solely regulated by a complex made up of junctin, triadin, and calsequestrin (Gyorke et al. 2004; Qin et al. 2008) (Fig. 2b). Furthermore, evidence linking the naturally occurring mutations in calsequestrin and triadin to catecholaminergic polymorphic ventricular tachycardia (CPVT) provide further support for the latter mechanism (Liu et al. 2006; Roux-Buisson et al. 2012).

While the dependence of SR  $\text{Ca}^{2+}$  release on SR  $\text{Ca}^{2+}$  load is widely accepted as fact, the theory that RyR2 activity is solely regulated by a luminal  $\text{Ca}^{2+}$  mechanism remains highly debatable. Other mechanisms have been proposed that explain termination of SR  $\text{Ca}^{2+}$  release as a RyR2 current-dependent process (Guo et al. 2012; Cannell et al. 2013; Bovo et al. 2015b). Recently proposed mechanism called induction decay (Cannell et al. 2013) or pernicious attrition (Guo et al. 2012) explains the local CICR dependence on SR  $\text{Ca}^{2+}$  load by the magnitude of the trans-SR  $\text{Ca}^{2+}$  driving force. This simply means that as RyR2  $\text{Ca}^{2+}$  current increases with increasing SR  $\text{Ca}^{2+}$  load, inter-RyR2 CICR within a cluster will facilitate  $\text{Ca}^{2+}$  release (Fig. 2c). Intuitively, as SR  $\text{Ca}^{2+}$  load falls, local  $\text{Ca}^{2+}$  release will fail to sustain inter-RyR2 CICR leading to the termination of SR  $\text{Ca}^{2+}$  release. While RyR2 gating is stochastic in nature, the decreased local  $[\text{Ca}^{2+}]_i$  will no longer be sufficient to activate channels that have spontaneously closed. Therefore, any modifications that promote the open conformation of RyR2 or enhance the channel's sensitivity to  $[\text{Ca}^{2+}]_i$  would likely hinder this termination process and, therefore, allow for a greater amount of SR  $\text{Ca}^{2+}$  release (Domeier et al. 2009; Bovo et al. 2015b).

## 1.5 SR $\text{Ca}^{2+}$ Leak

The RyR2, being the main  $\text{Ca}^{2+}$  release channel in the SR, is responsible for triggered  $\text{Ca}^{2+}$  release during systole as well as non-triggered  $\text{Ca}^{2+}$  release during diastole. Non-triggered  $\text{Ca}^{2+}$  release events are referred to as SR  $\text{Ca}^{2+}$  leak.  $\text{Ca}^{2+}$  leak mediated by RyR2 can occur as spontaneous  $\text{Ca}^{2+}$  sparks as well as non-spark-mediated  $\text{Ca}^{2+}$  leak (Zima et al. 2010).  $\text{Ca}^{2+}$  sparks are observed as spatially restricted rises in  $[\text{Ca}^{2+}]_i$  that predominantly occur at junctional SR, which lie adjacent to the z-lines of sarcomeres. Cheng and colleagues were the first to visualize  $\text{Ca}^{2+}$  sparks in 1993 (Cheng et al. 1993). Soon after, a growing body of work described the average  $\text{Ca}^{2+}$  spark to increase local  $[\text{Ca}^{2+}]_i$  by approximately 300–500 nM and have a spatial width of about 2  $\mu\text{m}$  (Lopez-Lopez et al. 1994; Cannell et al. 1995; Satoh et al. 1997). While  $\text{Ca}^{2+}$  sparks occur at a very low frequency in a healthy myocyte, a significantly increased  $\text{Ca}^{2+}$  sparks propensity during diastole observed during sympathetic stimulation with  $\beta$ -adrenergic receptor ( $\beta$ -AR) agonists (Bovo et al. 2012; Santiago et al. 2013) or in failing heart (Kubalova et al. 2005; Domeier et al. 2009). As the frequency of  $\text{Ca}^{2+}$  sparks during diastole increases over time,  $\text{Ca}^{2+}$  sparks can summate, causing local  $[\text{Ca}^{2+}]_i$  to rise to a level at which neighboring clusters become activated. Consequently, the

subsequent activation of several RyR2 clusters within a small region can propagate an asynchronous global SR  $\text{Ca}^{2+}$  release event known as a spontaneous  $\text{Ca}^{2+}$  wave.  $\text{Ca}^{2+}$  waves are a form of SR  $\text{Ca}^{2+}$  leak that is sufficient to induce spontaneous APs and is therefore considered an important trigger for cardiac arrhythmias (Schlotthauer and Bers 2000; Xie and Weiss 2009; Shiferaw et al. 2012). Although the majority of SR  $\text{Ca}^{2+}$  leak arises via RyR2 clusters that are responsible for the spark generation, sparks are very rare events during rest in healthy ventricular myocytes (Bovo et al. 2014). The absence of  $\text{Ca}^{2+}$  sparks can be explained if SR  $\text{Ca}^{2+}$  leak is mainly composed of unsynchronized openings of individual RyRs in a release cluster (non-spark-mediated  $\text{Ca}^{2+}$  leak) (Zima et al. 2010; Santiago et al. 2010).

## 2 SR $\text{Ca}^{2+}$ Cycling in Heart Disease

In the healthy myocardium, SR  $\text{Ca}^{2+}$  handling is robust and dynamic in nature, allowing the molecular machinery of the sarcomere to respond in an appropriate fashion. In fact, the intrinsic ability of the myocardium to modify amplitude and duration of each  $\text{Ca}^{2+}$  transient is fundamental property of the heart so that it can match cardiac output with the demand of the body (Lakatta 2004). In both ischemic and non-ischemic etiologies of heart disease, the heart undergoes a large number of changes that contribute to the disease phenotype as well as to the progression into heart failure (HF). In these pathophysiological states, both the contractile function and the electrical properties of the myocardium become dysfunctional. Abnormal  $\text{Ca}^{2+}$  handling is considered to be a major downstream effect that ultimately promotes the cardiac disease phenotypes. The inability of the failing heart to maintain an adequate SR  $\text{Ca}^{2+}$  load is an important contributor to the hearts' lack of capacity to meet cardiac demand (Houser et al. 2000; Bers 2001; Zima et al. 2014). Another consequence of impaired SR  $\text{Ca}^{2+}$  handling is the increased risk for cardiac arrhythmias. For instance, the abrupt increase in  $[\text{Ca}^{2+}]_i$  as a result of stress (e.g.,  $\beta$ -AR activation) can cause the formation of pro-arrhythmic  $\text{Ca}^{2+}$  waves (Bers 2001; Janse 2004; Pogwizd and Bers 2004; Eisner et al. 2009).

### 2.1 *Ischemia/Reperfusion*

In the event that a coronary artery becomes obstructed as a result of atherosclerotic plaques, the downstream blood flow slows or completely ceases, creating a hypoxic environment for the non-perfused myocardium. In the ischemic environment, metabolites build up within the interstitium and intracellularly due to the energy consumption of the working myocardium and the lack of blood perfusion. Commonly associated with ischemia/reperfusion (I/R) injury are complex cellular metabolic changes including a decrease in [ATP] and a subsequent increase in

free  $[Mg^{2+}]$ , [ADP], and inorganic phosphate ([Pi]) as well as a drop in intracellular pH (Opie and Clusin 1990; Opie 1993). Furthermore, increased reactive oxygen species (ROS) generation is prominent as a result of I/R injury (Misra et al. 2009). All the aforementioned factors are known to modulate the activity of the proteins required for intracellular  $Ca^{2+}$  cycling, particularly RyR2. Consequently, the enhanced RyR2-mediated  $Ca^{2+}$  leak results in the occurrence of pro-arrhythmic  $Ca^{2+}$  waves (Belevych et al. 2009, 2012). As a result, a major complication associated with reperfusing blood to the ischemic region is the increased risk of arrhythmogenesis (Yavuz 2008). These bouts of arrhythmias have the potential of initiating reentrant tachyarrhythmias, which can devolve into fibrillation and ultimately sudden cardiac death (Bunch et al. 2007).

## 2.2 Heart Failure

Congestive HF can be simply defined as the inability for cardiac output to meet the metabolic demand from the body. Today, HF remains the leading cause of hospitalization for ages 65 and older in the United States and Europe. Researchers have documented different cellular changes of the myocardium that prove to be dependent on the etiology of HF (Sen et al. 2000). Cardiovascular disease risk factors can promote a variety of cellular changes in the myocardium, which ultimately affect the development of HF. Myocardial infarction (MI), due to coronary artery disease, is the leading cause of ischemic HF, while increased cardiac afterload (e.g., hypertension) is a common cause of non-ischemic HF (Cowburn et al. 1998). Due to progressive cardiac remodeling, patients who suffer from HF have a poor prognosis as well as a low quality of life. In patients suffering from end-stage HF, death either results from cardiac pump failure or arrhythmias (Lane et al. 2005).

SR  $Ca^{2+}$  mishandling is one of the hallmark changes that take place in HF. This SR dysfunction is an important contributor to the heart's depressed contractile function and the increased incidence of arrhythmias, implicating RyR2 and SERCA dysfunction as the primary cause. In a majority of studies, HF is associated with increased SR  $Ca^{2+}$  leak and decreased SR  $Ca^{2+}$  reuptake mediated by RyR2 and SERCA, respectively. However, there is conflicting evidence with respect to the contribution of RyR2 to impaired SR  $Ca^{2+}$  cycling. Furthermore, pathophysiological differences have been observed between ischemic and idiopathic HF with regard to SR  $Ca^{2+}$  cycling dysfunction. A study by Sen et al. found that impaired SERCA activity was the primary impairment in ischemic HF, whereas SERCA activity in idiopathic HF was not significantly different when compared to healthy myocardium (Sen et al. 2000). Furthermore, impaired SR  $Ca^{2+}$  release was only observed in idiopathic HF. These results suggest that the underlying mechanisms responsible for SR  $Ca^{2+}$  cycling dysfunction may depend on the etiology of HF.

Moreover, HF is commonly defined as a condition of chronic oxidative stress due to compromised energetics. The impaired cardiac metabolism is considered to play an important role in the progression of disease (Mak and Newton 2001;

Ventura-Clapier et al. 2004; Santos et al. 2011). As the disease progresses, oxidative stress worsens due to the increasing energy demand and workload of the failing heart, thus perpetuating a deleterious cycle (Seddon et al. 2007). Although HF is associated with a large number of complex changes, the focus of this review is directed at understanding the role oxidative stress on SR  $\text{Ca}^{2+}$  regulation and RyR2 function. To date, RyR2 has been characterized in HF as having an increased phosphorylation level, an increased oxidation level, and a decreased association of auxiliary proteins. All of the aforementioned have been associated with increased channel activity. While functionally important phosphorylation sites on RyR2 have been characterized (Marx et al. 2000; Wehrens et al. 2004; Xiao et al. 2006), the specific mechanisms of oxidative modifications of RyR2 and their contribution to defective SR  $\text{Ca}^{2+}$  cycling remain incomplete.

### 3 Oxidative Stress

Oxidative stress is a prominent feature in the onset and progression of a number of disease states, including cardiovascular disease. Although the generation of ROS has been shown to play an important role in normal cell signaling, during periods of oxidative stress, excessive ROS production can have detrimental effects on normal protein function and cell viability. Furthermore, increased ROS production can induce lipid peroxidation and DNA damage that can compromise the structural and genetic integrity of the cell.

In order to counteract any ROS produced, the cell has an intrinsic antioxidant system that allows for the breakdown of ROS into nontoxic molecules. Some of the major components of the cellular antioxidant system include superoxide dismutase (SOD), catalase, and glutathione peroxidase (Turrens 2003; Yamawaki et al. 2003; Slodzinski et al. 2008), which act as selective scavenging enzymes. The nonspecific antioxidants include glutathione and thioredoxin systems. Reduced glutathione (GSH), a highly abundant low-molecular-weight thiol, is considered the largest of antioxidant pools and is arguably the most important antioxidant system in the myocardium. GSH is considered the main line of defense against ROS, because it is ubiquitous throughout all cellular compartments.

Thus, oxidative stress can be simply defined as increased ROS production that overwhelms the cellular antioxidant defense (Giordano 2005). Depending on the etiology of disease, oxidative stress can manifest at different time points and from different sources. The following will briefly review acute oxidative stress in I/R as well as chronic oxidative stress in HF.

### ***3.1 Acute Oxidative Stress in Ischemia/Reperfusion Injury***

It has been well characterized that restoring blood flow to the ischemic region drastically increases ROS production, which further increases oxidative stress. The generation of ROS, due to an increased supply of oxygen to ischemic myocardium, has been implicated as the underlying factor that promotes I/R injury (Vanden Hoek et al. 1996; Zweier et al. 1987). In this condition, the electron transport chain (ETC) in the mitochondria becomes uncoupled, producing superoxide anion ( $O_2^{\cdot-}$ ) (Turrens 1997). This sudden burst of ROS overwhelms the intrinsic antioxidant system. The GSH/GSSG ratio can decrease considerably during I/R (Ceconi et al. 1988; Werns et al. 1992), which can contribute to mitochondrial ROS spill over (Aon et al. 2007, 2010; Brown et al. 2010). Other sources of ROS, including NADPH oxidase (NOX), uncoupled nitric oxide synthase (NOS), and xanthine oxidase (XO), are also believed to play a role in I/R injury (Becker 2004; Zweier and Talukder 2006; Angelos et al. 2006). A recent study implicated  $Ca^{2+}$ -dependent delayed after depolarizations (DADs) as the major mechanism of arrhythmogenesis in a dog model of acute MI (Belevych et al. 2012). It has been shown that the occurrence of DADs could be prevented with intravenous perfusion of the ROS scavenger Tempol (Xing et al. 2009). The results from these studies implicate oxidative stress as a major factor in the generation of cardiac arrhythmias after MI.

During MI, excessive  $\beta$ -AR stimulation manifests in the ischemic region due to elevated concentrations of catecholamines (Lameris et al. 2000). Both ex vivo and in vivo I/R studies have shown that the main source of endogenous catecholamines is in fact from nonexocytotic release at sympathetic nerve endings that innervate the myocardium (Lameris et al. 2000; Kurz et al. 1995).  $\beta$ -AR stimulation is considered to be an important contributor in I/R injury. Increased  $\beta$ -AR stimulation can further increase energy demand and intracellular ROS production (Christensen and Videbaek 1974; Bovo et al. 2015a). Studies that block PKA activation via beta blockers or direct inhibition of PKA has proven to be effective in reducing infarct size (Makaula et al. 2005; Spear et al. 2007). A recent study done by Nagasaka et al. showed that mitochondrial ROS production was significantly increased in the presence of PKA catalytic subunit in permeabilized myocytes (Nagasaka et al. 2007).

### ***3.2 Chronic Oxidative Stress in Heart Failure***

The mechanisms that are responsible for the progression of heart failure are very complex and have been under intensive investigation for many years. However, one of the common features that have been implicated to play an important role in the pathophysiology of HF is chronic oxidative stress (Belch et al. 1991; Hill and Singal 1997). Both experimental and clinical studies have measured an increase in ROS production in HF (Mak and Newton 2001; Ventura-Clapier et al. 2004;



Giordano 2005; Santos et al. 2011). HF is commonly associated with morphological and functional abnormalities in mitochondria (Schaper et al. 1991). While compromised mitochondrial function is considered a significant cause of oxidative stress (Balaban et al. 2005; Turrens 2003; Giordano 2005), the molecular mechanisms of this defect in HF are not fully understood. In a mouse model of MI-induced HF, an increase in ROS production and lipid oxidation were associated with impaired mitochondrial function (Ide et al. 2001). Furthermore, in a canine model of HF, the mitochondrial ETC was significantly more prone to uncoupling and subsequent ROS production (Ide et al. 1999). These results also provide evidence for a positive correlation between depressed contractility and the level of ROS production.

Moreover, it has been shown that antioxidant activity progressively deteriorates in HF (Hill and Singal 1997). During HF progression, myocardium switches energy substrate from fatty acids to glucose. These adaptive changes in cellular metabolism are associated with decreased expression of mitochondrial transcription factors and proteins (Ventura-Clapier et al. 2004; Santos et al. 2011). In our recent studies, we found that the mitochondrial ROS defense is substantially reduced in HF, especially at the mitochondrial type 2 SOD (SOD-2) level (unpublished results). While the impaired SOD-2 function has been implicated in numerous diseases (including Parkinson, cancer, diabetes) (Turrens 2003; Miao and St Clair 2009), its role in HF has never been explored. We suggest that the SOD-2 decline is the critical step in a chain of events that lead to oxidative stress and HF progression. Foremost, SOD-2 is the only defense line against mitochondrial  $O_2^{\cdot-}$ , whereas  $H_2O_2$  can be neutralized by several enzymes (including peroxidase, peroxiredoxin, and catalase). Thus, SOD-2 downregulation would have more significant impact on ROS level than downregulation of any other ROS-scavenging enzyme. Second,  $O_2^{\cdot-}$  reacts extremely rapidly with nitric oxide (NO) forming highly reactive peroxynitrite ( $ONOO^{\cdot-}$ ) (Ferdinandy and Schulz 2003). Thus, the downregulation of SOD-2 in HF would have the significant impact on nitroso-redox balance: an increase of reactive  $ONOO^{\cdot-}$  production and a decrease of cardioprotective NO. In support of this hypothesis, *Sod2*<sup>-/-</sup> knockout mice are characterized by a maladaptive cardiac hypertrophy and cardiomyopathy (Makino et al. 2011; Lebovitz et al. 1996). Thus, restoring SOD-2 defense can be an effective strategy to improve cardiac function and delay HF progression.

## 4 Oxidative Posttranslational Modifications of RyR2

Recent emphasis has been placed on the study of oxidative posttranslational modifications (PTMs) and their important role in the regulation of heart function. Among all cardiac ion transporters and channels, RyR2 appears to be the most sensitive to redox modification (Zima and Blatter 2006; Hool and Corry 2007), thus linking oxidative stress to  $Ca^{2+}$  regulation. RyR2 has approximately 360 cysteine residues per tetrameric channel, with an estimated 84 of those are in a reduced free



thiol state (Xu et al. 1998). Each free thiol residue can serve as a target for a number of oxidative modifications including *S*-nitrosylation, *S*-glutathionylation, or disulfide cross bridge formation. To date, a number of in vitro studies have shown that both ROS and other free radicals can induce changes in RyR2 channel activity. Bilayer studies have shown that RyR2 channel activity is increased in the presence of ROS, whereas reducing agents decrease the RyR2 activity (for review, see Zima and Blatter (2006)). Elevated ROS production, which is associated with increased cardiac demand, has been suggested to play a role in the augmentation of SR  $\text{Ca}^{2+}$  release (Heinzel et al. 2006). Therefore, oxidative PTMs of RyR2 may function as a mechanism for positive inotropy in the healthy heart. However, in the case of MI or HF, abnormally elevated ROS level can cause irregular  $\text{Ca}^{2+}$  cycling and, therefore, contractile dysfunction and arrhythmias. It has been shown that abnormal SR  $\text{Ca}^{2+}$  release in myocytes from infarcted (Belevych et al. 2009) and failing (Terentyev et al. 2008) heart was associated with an increase in RyR2 oxidation.

#### 4.1 *S*-Glutathionylation

In the presence of oxidative stress, free thiols of cysteine residues are the first subjected to oxidation. Depending on the degree of oxidative stress, protein free thiols can be oxidized by ROS to form sulfenic (R-SOH), sulfinic (R-SO<sub>2</sub>H), or sulfonic (R-SO<sub>3</sub>H) acid products (Giles and Jacob 2002). GSH attenuates ROS production during oxidative stress either by directly scavenging free radicals or acting as a substrate for the major antioxidant enzyme glutathione peroxidase. Also, GSH can readily react with protein sulfenic acids forming the reversible *S*-glutathionylation of RyR2. The reversible reduction of *S*-glutathionylation is carried out mainly by the enzyme glutaredoxin. The formation of sulfinic and sulfonic acids, however, are considered biologically irreversible. Thus, the formation of the protein-glutathione-mixed disulfide is thought to have a protective role during changes in cellular redox state (Townsend 2007). However, it has been proposed that *S*-glutathionylation may play a role in promoting protein disulfide formation of both intra- and intermolecular species (Bass et al. 2004; Cumming et al. 2004; Brennan et al. 2004).

In all tissues, the ratio between oxidized and reduced GSH (GSSG/GSH) is an important indicator of the redox state. Changes in cellular redox environment potentially affects the activity of many proteins, including RyR2 (Zima and Blatter 2006). As a result, oxidative stress can potentially promote abnormally elevated  $[\text{Ca}^{2+}]_i$  in the myocardium during diastole (Kourie 1998). In cardiomyocytes, cytosolic glutathione is mainly reduced under normal physiological conditions. During oxidative stress, however, the GSSG/GSH ratio can increase significantly (Ceconi et al. 1988; Werns et al. 1992) as well as total protein-glutathione-mixed disulfides (Tang et al. 2011). The increased formation of glutathione-mixed disulfides is a common feature of oxidative stress due to the abundance of glutathione and the ready conversion of reactive thiols. Recent studies have been

implicated glutathione mixed disulfides as a critical signaling mechanism that plays a causative role, rather than a protective role, in cardiovascular disease. With respect to SR  $\text{Ca}^{2+}$  cycling, however, it is unclear if increased glutathione-mixed disulfide is beneficial or detrimental. *S*-glutathionylation of RyR2 is also thought to play a role in myocardial preconditioning before an ischemic insult. For example, tachycardia-induced preconditioning was proven to reduce the infarct size after ischemia (Domenech et al. 1998). It was later identified that tachycardia stimulated NADPH oxidase-dependent *S*-glutathionylation of RyR2, increasing RyR2  $\text{Ca}^{2+}$  release and decreasing SR  $\text{Ca}^{2+}$  leak in SR microsomal preparations (Sanchez et al. 2005). It still remains controversial whether or not increased single-channel activity or increased  $\text{Ca}^{2+}$  release from SR microsomes can also coincide with decreased SR  $\text{Ca}^{2+}$  leak within a cellular milieu.

## 4.2 *S*-Nitrosylation

The vast body of research studying ischemic preconditioning has yielded many different molecular mechanisms (Zaugg et al. 2003). Given its complex nature, the crucial downstream targets that give a tissue the ability to resist ischemic injury make up a sizeable list that has steadily grown over the recent years. NO signaling, an important regulator in many physiologic processes, and subsequent protein *S*-nitrosylation is commonly identified as an important molecular intermediate allowing for ischemic preconditioning. Several cardioprotection studies defined many downstream targets of NO, having identified the cardioprotective effect as the result of covalently linked NO with reactive protein thiols (*S*-nitrosylation). These downstream targets include proteins that are involved in mitochondrial metabolism, apoptosis, ROS defense, protein trafficking, myofilament contraction, and  $\text{Ca}^{2+}$  handling. Overall, increased *S*-nitrosylation in the myocardium can be antiapoptotic and anti-inflammatory (Sun and Murphy 2010; Lima et al. 2010). As mentioned previously, the reperfusion of blood or reintroduction of  $\text{O}_2$  to the ischemic tissue stimulates oxidative phosphorylation in impaired mitochondria, which results in a burst of ROS production. Recent studies have found that *S*-nitrosylation of mitochondrial protein complexes (I and IV) of the ETC inhibits their activity, which limits oxidative phosphorylation (Zhang et al. 2005; Sun et al. 2007; Rassaf et al. 2014). Furthermore, *S*-nitrosylation of myofilament proteins decreases their sensitivity to  $\text{Ca}^{2+}$ , decreasing myofilament cross bridge formation, which subsequently reduces ATP consumption (Nogueira et al. 2009). By promoting energy conservation in the myocardium, *S*-nitrosylation limits ROS production from uncoupled mitochondria during I/R.

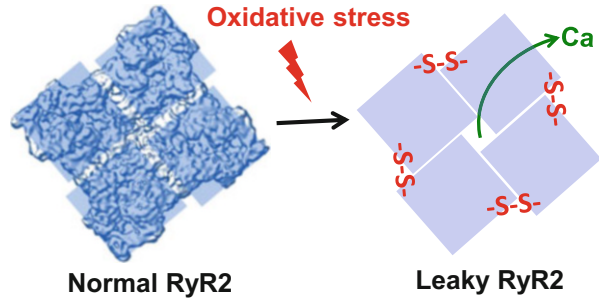
The cardioprotective effects of *S*-nitrosylation on  $\text{Ca}^{2+}$  machinery, although independent, complements the effect seen in the mitochondria. In both I/R and HF, impaired  $\text{Ca}^{2+}$  cycling commonly leads to an increase in diastolic  $[\text{Ca}^{2+}]_i$  as well as depleted  $[\text{Ca}^{2+}]_{\text{SR}}$ . In a state of  $[\text{Ca}^{2+}]_i$  overload, the diastolic function of the heart is impaired, and the likelihood of arrhythmogenesis is increased. Evidence of

*S*-nitrosylation-dependent cardioprotection has been documented for the major components of  $\text{Ca}^{2+}$  cycling, preventing  $[\text{Ca}^{2+}]_i$  overload (Loyer et al. 2008). For LTCC, *S*-nitrosylation of the channel has been shown to reduce the channel activity. Also, SERCA activity has been reported to increase in response to *S*-nitrosylation. Paradoxically, RyR2 activity has been shown to increase in response to *S*-nitrosylation (Zima and Blatter 2006; Gonzalez et al. 2009). Other studies, however, showed that hyponitrosylation of RyR2 caused the channel to be more susceptible to oxidation by ROS, leading to increased SR  $\text{Ca}^{2+}$  leak and arrhythmogenesis (Gonzalez et al. 2010). Moreover, it has been suggested that *S*-nitrosylation can potentially prevent irreversible oxidation of cysteine residues (Sun and Murphy 2010). Thus, *S*-nitrosylation of RyR2 may act as a protective PTM against oxidative stress and detrimental SR  $\text{Ca}^{2+}$  leak. By maintaining SR  $\text{Ca}^{2+}$  load and preventing  $[\text{Ca}^{2+}]_i$  overload, *S*-nitrosylation plays a very important role in cardiac function during periods of oxidative stress. Recent work from Gonzalez et al. identified that enhanced xanthine oxidase superoxide production caused a decrease in cardiac RyR2 *S*-nitrosylation with an overall decrease in free thiols, promoting SR  $\text{Ca}^{2+}$  leak in heart failure rats (Gonzalez et al. 2010).

### 4.3 Intersubunit Cross-Linking

The protein-protein interaction between RyR2 subunits has been implicated in channel gating (Abramson and Salama 1989; Kimlicka et al. 2013; Strauss and Wagenknecht 2013) and, therefore, likely plays an important role in regulating SR  $\text{Ca}^{2+}$  release. In the past decade, there has been a great amount of progress in defining the quaternary structure of RyR (Serysheva et al. 2008; Cornea et al. 2009; Tung et al. 2010; Zalk et al. 2015), particularly for the skeletal type 1 isoform (RyR1). Although only a small portion of the cytosolic domain has been crystalized to date, high-resolution cryo-EM studies have provided insight into conformational changes that occur as a result of channel activation. By superimposing the 3-D crystal structure of the N-terminal domain (1–532 amino acids) of RyR within the 3-D matrix created using images from cryo-EM, it was determined that the intersubunit gap between N-terminal domains becomes widened by  $\sim 7 \text{ \AA}$  in the open conformation. These results suggest that any protein-protein interactions that are taking place in the closed conformation are likely disrupted as the result of channel opening (van Petegem 2015). Although the N-terminal domain is only responsible for a small portion of the intersubunit interaction, it is of particular interest because a large number of disease mutations have been found to localize within it. In fact, a majority of these mutations were found facing the intersubunit boundary. Thus, it is highly plausible that these mutations affect the channel function by disrupting normal interdomain interactions. Moreover, the mutations were all associated with a gain-of-function phenotype (increased RyR channel activity) (Kimlicka et al. 2013). These functional results are consistent with the

**Fig. 3** Oxidative stress can increase diastolic SR  $\text{Ca}^{2+}$  leak by inducing intersubunit cross-linking within the ryanodine receptor complex. The RyR2 tetramer is shown as viewed from the cytoplasmic face



structural evidence, supporting the claim that RyR channel activity is indeed affected by changes in the intersubunit interactions.

Recent work by Han et al. demonstrated that in the presence of an oxidant, RyR1 undergoes covalent disulfide cross-linking between neighboring subunits (intersubunit cross-linking) that is reversible with the reducing agent dithiothreitol. In parallel, cryo-EM images showed that RyR1, which normally has a cytosolic structure that resembles a pinwheel (Fig. 3), undergoes major morphological changes as a result of  $\text{H}_2\text{O}_2$  treatment. These morphological changes, however, are reversible with the treatment of dithiothreitol (Han et al. 2006). A different cryo-EM study used a nonselective cross-linking agent (glutaraldehyde) to induce intersubunit cross-linking. In these conditions, RyR1 adopted a conformation that resembled that of the open state. In both these studies, the authors suggest that intersubunit cross-linking leads to activation of RyR1 as a result of structural changes that directly affect gating of the channel (Aghdasi et al. 1997; Strauss and Wagenknecht 2013).

Abramson and Salama were the first to suggest that intersubunit cross-linking is involved in the gating of RyR1 (Abramson and Salama 1989). They argue that thiol oxidation is a necessary requirement for RyR1 channel opening. In order for this hypothesis to be correct, the transition from conducting to nonconducting states would have to coincide with the reduction of the principal disulfides regulating gating. Furthermore, because the cytosolic environment is maintained at a highly reduced state, this proposed gating mechanism assumes that dynamic disulfide formation is present without oxidative stress. Recently, a study done by Zissimopoulos et al. provides some biochemical evidence to support this hypothesis for both RyR1 and RyR2. The major limitation to this study, however, was that full-length RyR was not used in the experimental approach (Zissimopoulos et al. 2013). Their work shows that N-terminal fragments of RyR2 self-assemble into oligomers similar to that of RyR1. Interestingly, unlike RyR1, N-terminal fragments of RyR2 were covalently linked by endogenous disulfide bonds in ambient conditions (absence of exogenous ROS treatment). Even though both RyR1 and RyR2 N-terminal fragments formed disulfide-linked oligomers with  $\text{H}_2\text{O}_2$  in a dose-dependent manner, the authors suggest that a difference in sequence homology between isoforms may explain the disparity in disulfide bond formation. Alternatively, if the requisite cysteine residues are in fact conserved between isoforms,

other oxidative PTMs (e.g., glutathionylation, nitrosylation) that resist disulfide formation may be unique to RyR1.

In light of recent work, the susceptibility for intersubunit cross-linking appears to be increased for the cardiac isoform of RyR2 (Zissimopoulos et al. 2013). Although some work has been done to examine the effects of intersubunit cross-linking on RyR2 function, no studies have examined its role in SR  $\text{Ca}^{2+}$  cycling within the cellular environment. We have recently discovered that the redox-mediated RyR2 cross-linking has a significant impact on the channel activity and SR  $\text{Ca}^{2+}$  release (Mazurek et al. 2014). We found that the RyR2 cross-linking increased the open probability of RyR2 measured in lipid bilayers and RyR2-mediated  $\text{Ca}^{2+}$  leak in isolated ventricular myocytes. Lastly, we found a positive correlation between the cross-linking level and SR  $\text{Ca}^{2+}$  leak. When the cross-linking reached the maximum level, further oxidation of RyR2 did not enhance SR  $\text{Ca}^{2+}$  leak. These results clearly demonstrate that the intersubunit cross-linking is a strong regulator of cardiac RyR2 function *in vivo* and *in vitro* (Fig. 3).

## 5 Conclusion

$\text{Ca}^{2+}$  released through RyR2 is essential for initiating a robust myocardial contraction. Consequently, defects in RyR2 regulation contribute to contractile dysfunction in a variety of cardiac pathologies (Janssen and de Tombe 1997; Marks 2000; Gyorke and Carnes 2008; Yano 2008; Zima and Terentyev 2013). In particular, abnormal RyR2 activity due to cysteine oxidation (Zima and Blatter 2006; Hool and Corry 2007) causes SR  $\text{Ca}^{2+}$  mishandling, arrhythmias, and contractile dysfunction in infarcted (Belevych et al. 2009) and failing hearts (Mochizuki et al. 2007; Terentyev et al. 2008; Domeier et al. 2009; Belevych et al. 2011). Since RyR2 cysteine oxidation is implicated in the progression of cardiac disease, these cysteine residues are promising targets for therapeutic intervention. RyR2 contains as many as 90 cysteine residues per monomer, and the redox status of these residues can affect RyR2 function (Zima and Blatter 2006). However, the functionally important redox-sensing sites on RyR2 have yet to be characterized. As a result, RyR2 oxidation has always been treated as a nonselective PTM. In contrast, three functionally important phosphorylation sites on RyR2 have been characterized (Marx et al. 2000; Wehrens et al. 2004; Xiao et al. 2006), and clinical studies targeting these sites are currently underway (Lehnart 2007; Lompre et al. 2010; van Oort et al. 2010). Thus, identifying the functionally important RyR2 cysteines is essential for understanding the molecular mechanisms of RyR2 regulation and SR  $\text{Ca}^{2+}$  mishandling during oxidative stress.

**Acknowledgments** This work was supported by the NIH Grant (R01HL130231), the Research Career Development Award from the Scheweppe Foundation, and the RFC grant from Loyola University Chicago to A.V.Z.

## References

- Abramson JJ, Salama G (1989) Critical sulfhydryls regulate calcium release from sarcoplasmic reticulum. *J Bioenerg Biomembr* 21:283–294
- Aghdasi B, Zhang JZ, Wu Y, Reid MB, Hamilton SL (1997) Multiple classes of sulfhydryls modulate the skeletal muscle  $\text{Ca}^{2+}$  release channel. *J Biol Chem* 272:3739–3748
- Angelos MG, Kutala VK, Torres CA, He G, Stoner JD, Mohammad M, Kuppusamy P (2006) Hypoxic reperfusion of the ischemic heart and oxygen radical generation. *Am J Physiol Heart Circ Physiol* 290:H341–H347
- Aon MA, Cortassa S, Maack C, O'Rourke B (2007) Sequential opening of mitochondrial ion channels as a function of glutathione redox thiol status. *J Biol Chem* 282:21889–21900
- Aon MA, Cortassa S, O'Rourke B (2010) Redox-optimized ROS balance: a unifying hypothesis. *Biochim Biophys Acta* 1797:865–877
- Baddeley D, Jayasinghe ID, Lam L, Rossberger S, Cannell MB, Soeller C (2009) Optical single-channel resolution imaging of the ryanodine receptor distribution in rat cardiac myocytes. *Proc Natl Acad Sci U S A* 106:22275–22280
- Balaban RS, Nemoto S, Finkel T (2005) Mitochondria, oxidants, and aging. *Cell* 120:483–495
- Bass R, Ruddock LW, Klappa P, Freedman RB (2004) A major fraction of endoplasmic reticulum-located glutathione is present as mixed disulfides with protein. *J Biol Chem* 279:5257–5262
- Bassani RA, Bassani JW, Bers DM (1992) Mitochondrial and sarcolemmal  $\text{Ca}^{2+}$  transport reduce  $[\text{Ca}^{2+}]_i$  during caffeine contractures in rabbit cardiac myocytes. *J Physiol* 453:591–608
- Becker LB (2004) New concepts in reactive oxygen species and cardiovascular reperfusion physiology. *Cardiovasc Res* 61:461–470
- Belch JJ, Bridges AB, Scott N, Chopra M (1991) Oxygen free radicals and congestive heart failure. *Br Heart J* 65:245–248
- Belevych AE, Terentyev D, Viatchenko-Karpinski S, Terentyeva R, Sridhar A, Nishijima Y, Wilson LD, Cardounel AJ, Laurita KR, Carnes CA, Billman GE, Gyorke S (2009) Redox modification of ryanodine receptors underlies calcium alternans in a canine model of sudden cardiac death. *Cardiovasc Res* 84:387–395
- Belevych AE, Terentyev D, Terentyeva R, Nishijima Y, Sridhar A, Hamlin RL, Carnes CA, Gyorke S (2011) The relationship between arrhythmogenesis and impaired contractility in heart failure: role of altered ryanodine receptor function. *Cardiovasc Res* 90:493–502
- Belevych AE, Terentyev D, Terentyeva R, Ho HT, Gyorke I, Bonilla IM, Carnes CA, Billman GE, Gyorke S (2012) Shortened  $\text{Ca}^{2+}$  signaling refractoriness underlies cellular arrhythmogenesis in a postinfarction model of sudden cardiac death. *Circ Res* 110:569–577
- Bers DM (2001) Excitation-contraction coupling and cardiac contractile force. Kluwer Academic Publishers, Dordrecht
- Bers DM (2004) Macromolecular complexes regulating cardiac ryanodine receptor function. *J Mol Cell Cardiol* 37:417–429
- Bovo E, Lipsius SL, Zima AV (2012) Reactive oxygen species contribute to the development of arrhythmogenic  $\text{Ca}^{2+}$  waves during beta-adrenergic receptor stimulation in rabbit cardiomyocytes. *J Physiol* 590:3291–3304
- Bovo E, de Tombe PP, Zima AV (2014) The role of dyadic organization in regulation of sarcoplasmic reticulum  $\text{Ca}^{2+}$  handling during rest in rabbit ventricular myocytes. *Biophys J* 106:1902–1909
- Bovo E, Mazurek SR, de Tombe PP, Zima AV (2015a) Increased Energy Demand during Adrenergic Receptor Stimulation Contributes to  $\text{Ca}^{2+}$  Wave Generation. *Biophys J* 109:1583–1591
- Bovo E, Mazurek SR, Fill M, Zima AV (2015b) Cytosolic  $\text{Ca}^{2+}$  buffering determines the intracellular  $\text{Ca}^{2+}$  concentration at which cardiac  $\text{Ca}^{2+}$  sparks terminate. *Cell Calcium* 58:246–253

- Brennan JP, Wait R, Begum S, Bell JR, Dunn MJ, Eaton P (2004) Detection and mapping of widespread intermolecular protein disulfide formation during cardiac oxidative stress using proteomics with diagonal electrophoresis. *J Biol Chem* 279:41352–41360
- Brown DA, Aon MA, Frasier CR, Sloan RC, Maloney AH, Anderson EJ, O'Rourke B (2010) Cardiac arrhythmias induced by glutathione oxidation can be inhibited by preventing mitochondrial depolarization. *J Mol Cell Cardiol* 48:673–679
- Bunch TJ, Hohnloser SH, Gersh BJ (2007) Mechanisms of sudden cardiac death in myocardial infarction survivors: insights from the randomized trials of implantable cardioverter-defibrillators. *Circulation* 115:2451–2457
- Cannell MB, Cheng H, Lederer WJ (1995) The control of calcium release in heart muscle. *Science* 268:1045–1049
- Cannell MB, Kong CH, Imtiaz MS, Laver DR (2013) Control of sarcoplasmic reticulum  $\text{Ca}^{2+}$  release by stochastic RyR gating within a 3D model of the cardiac dyad and importance of induction decay for CICR termination. *Biophys J* 104:2149–2159
- Cecconi C, Curello S, Cargnoni A, Ferrari R, Albertini A, Visioli O (1988) The role of glutathione status in the protection against ischaemic and reperfusion damage: effects of N-acetyl cysteine. *J Mol Cell Cardiol* 20:5–13
- Chen W, Wang R, Chen B, Zhong X, Kong H, Bai Y, Zhou Q, Xie C, Zhang J, Guo A, Tian X, Jones PP, O'Mara ML, Liu Y, Mi T, Zhang L, Bolstad J, Semeniuk L, Cheng H, Zhang J, Chen J, Tieleman DP, Gillis AM, Duff HJ, Fill M, Song LS, Chen SR (2014) The ryanodine receptor store-sensing gate controls  $\text{Ca}^{2+}$  waves and  $\text{Ca}^{2+}$ -triggered arrhythmias. *Nat Med* 20:184–192
- Cheng H, Lederer WJ (2008) Calcium sparks. *Physiol Rev* 88:1491–1545
- Cheng H, Lederer WJ, Cannell MB (1993) Calcium sparks: elementary events underlying excitation-contraction coupling in heart muscle. *Science* 262:740–744
- Christensen NJ, Videbaek J (1974) Plasma catecholamines and carbohydrate metabolism in patients with acute myocardial infarction. *J Clin Invest* 54:278–286
- Cornea RL, Nitu F, Gruber S, Kohler K, Satzer M, Thomas DD, Fruen BR (2009) FRET-based mapping of calmodulin bound to the RyR1  $\text{Ca}^{2+}$  release channel. *Proc Natl Acad Sci U S A* 106:6128–6133
- Cowburn PJ, Cleland JG, Coats AJ, Komajda M (1998) Risk stratification in chronic heart failure. *Eur Heart J* 19:696–710
- Cumming RC, Andon NL, Haynes PA, Park M, Fischer WH, Schubert D (2004) Protein disulfide bond formation in the cytoplasm during oxidative stress. *J Biol Chem* 279:21749–21758
- Domeier TL, Blatter LA, Zima AV (2009) Alteration of sarcoplasmic reticulum  $\text{Ca}^{2+}$  release termination by ryanodine receptor sensitization and in heart failure. *J Physiol* 587:5197–5209
- Domenech RJ, Macho P, Velez D, Sanchez G, Liu X, Dhalla N (1998) Tachycardia preconditions infarct size in dogs: role of adenosine and protein kinase C. *Circulation* 97:786–794
- Eager KR, Dulhunty AF (1998) Activation of the cardiac ryanodine receptor by sulfhydryl oxidation is modified by  $\text{Mg}^{2+}$  and ATP. *J Membr Biol* 163:9–18
- Eisner DA, Trafford AW, Diaz ME, Overend CL, O'Neill SC (1998) The control of Ca release from the cardiac sarcoplasmic reticulum: regulation versus autoregulation. *Cardiovasc Res* 38:589–604
- Eisner DA, Kashimura T, Venetucci LA, Trafford AW (2009) From the ryanodine receptor to cardiac arrhythmias. *Circ J* 73:1561–1567
- Fabiato A (1983) Calcium-induced release of calcium from the cardiac sarcoplasmic reticulum. *Am J Physiol* 245:C1–C14
- Fabiato A (1985) Time and calcium dependence of activation and inactivation of calcium-induced release of calcium from the sarcoplasmic reticulum of a skinned canine cardiac Purkinje cell. *J Gen Physiol* 85:247–289
- Fabiato A, Fabiato F (1975) Contractions induced by a calcium-triggered release of calcium from the sarcoplasmic reticulum of single skinned cardiac cells. *J Physiol* 249:469–495

- Ferdinandy P, Schulz R (2003) Nitric oxide, superoxide, and peroxyxynitrite in myocardial ischaemia-reperfusion injury and preconditioning. *Br J Pharmacol* 138:532–543
- Fill M, Copello JA (2002) Ryanodine receptor calcium release channels. *Physiol Rev* 82:893–922
- Franzini-Armstrong C, Protasi F, Ramesh V (1999) Shape, size, and distribution of Ca(2+) release units and couplons in skeletal and cardiac muscles. *Biophys J* 77:1528–1539
- Garbino A, van Oort RJ, Dixit SS, Landstrom AP, Ackerman MJ, Wehrens XH (2009) Molecular evolution of the junctophilin gene family. *Physiol Genomics* 37:175–186
- Giles GI, Jacob C (2002) Reactive sulfur species: an emerging concept in oxidative stress. *Biol Chem* 383:375–388
- Gillespie D (2008) Energetics of divalent selectivity in a calcium channel: the ryanodine receptor case study. *Biophys J* 94:1169–1184
- Giordano FJ (2005) Oxygen, oxidative stress, hypoxia, and heart failure. *J Clin Invest* 115:500–508
- Goldman YE (1987) Kinetics of the actomyosin ATPase in muscle fibers. *Annu Rev Physiol* 49:637–654
- Gonzalez DR, Treuer A, Sun QA, Stamler JS, Hare JM (2009) S-Nitrosylation of cardiac ion channels. *J Cardiovasc Pharmacol* 54:188–195
- Gonzalez DR, Treuer AV, Castellanos J, Dulce RA, Hare JM (2010) Impaired S-nitrosylation of the ryanodine receptor caused by xanthine oxidase activity contributes to calcium leak in heart failure. *J Biol Chem* 285:28938–28945
- Guo T, Gillespie D, Fill M (2012) Ryanodine receptor current amplitude controls Ca<sup>2+</sup> sparks in cardiac muscle. *Circ Res* 111:28–36
- Gyorke S, Cames C (2008) Dysregulated sarcoplasmic reticulum calcium release: potential pharmacological target in cardiac disease. *Pharmacol Ther* 119:340–354
- Gyorke I, Hester N, Jones LR, Gyorke S (2004) The role of calsequestrin, triadin, and junctin in conferring cardiac ryanodine receptor responsiveness to luminal calcium. *Biophys J* 86:2121–2128
- Han HM, Wei RS, Lai FA, Yin CC (2006) Molecular nature of sulfhydryl modification by hydrogen peroxide on type 1 ryanodine receptor. *Acta Pharmacol Sin* 27:888–894
- Hayashi T, Martone ME, Yu Z, Thor A, Doi M, Holst MJ, Ellisman MH, Hoshijima M (2009) Three-dimensional electron microscopy reveals new details of membrane systems for Ca<sup>2+</sup> signaling in the heart. *J Cell Sci* 122:1005–1013
- Heinzel FR, Luo Y, Dodoni G, Boengler K, Petrat F, Di LF, de GH, Schulz R, Heusch G (2006) Formation of reactive oxygen species at increased contraction frequency in rat cardiomyocytes. *Cardiovasc Res* 71:374–382
- Hill MF, Singal PK (1997) Right and left myocardial antioxidant responses during heart failure subsequent to myocardial infarction. *Circulation* 96:2414–2420
- Hool LC, Corry B (2007) Redox control of calcium channels: from mechanisms to therapeutic opportunities. *Antioxid Redox Signal* 9:409–435
- Houser SR, Piacentino V III, Weisser J (2000) Abnormalities of calcium cycling in the hypertrophied and failing heart. *J Mol Cell Cardiol* 32:1595–1607
- Ide T, Tsutsui H, Kinugawa S, Utsumi H, Kang D, Hattori N, Uchida K, Arimura K, Egashira K, Takeshita A (1999) Mitochondrial electron transport complex I is a potential source of oxygen free radicals in the failing myocardium. *Circ Res* 85:357–363
- Ide T, Tsutsui H, Hayashidani S, Kang D, Suematsu N, Nakamura K, Utsumi H, Hamasaki N, Takeshita A (2001) Mitochondrial DNA damage and dysfunction associated with oxidative stress in failing hearts after myocardial infarction. *Circ Res* 88:529–535
- Janse MJ (2004) Electrophysiological changes in heart failure and their relationship to arrhythmogenesis. *Cardiovasc Res* 61:208–217
- Janssen PM, de Tombe PP (1997) Uncontrolled sarcomere shortening increases intracellular Ca<sup>2+</sup> transient in rat cardiac trabeculae. *Am J Physiol* 272:H1892–H1897
- Kimlicka L, Lau K, Tung CC, Van PF (2013) Disease mutations in the ryanodine receptor N-terminal region couple to a mobile intersubunit interface. *Nat Commun* 4:1506



- Kourie JI (1998) Interaction of reactive oxygen species with ion transport mechanisms. *Am J Physiol* 275:C1–C24
- Kubalova Z, Terentyev D, Viatchenko-Karpinski S, Nishijima Y, Gyorke I, Terentyeva R, da Cunha DN, Sridhar A, Feldman DS, Hamlin RL, Carnes CA, Gyorke S (2005) Abnormal intrastore calcium signaling in chronic heart failure. *Proc Natl Acad Sci U S A* 102:14104–14109
- Kurz T, Offner B, Schrieck J, Richardt G, Tolg R, Schomig A (1995) Nonexocytotic noradrenaline release and ventricular fibrillation in ischemic rat hearts. *Naunyn Schmiedebergs Arch Pharmacol* 352:491–496
- Lakatta EG (2004) Beyond Bowditch: the convergence of cardiac chronotropy and inotropy. *Cell Calcium* 35:629–642
- Lameris TW, de ZS, Alberts G, Boomsma F, Duncker DJ, Verdouw PD, Veld AJ, van den Meiracker AH (2000) Time course and mechanism of myocardial catecholamine release during transient ischemia in vivo. *Circulation* 101:2645–2650
- Lane RE, Cowie MR, Chow AW (2005) Prediction and prevention of sudden cardiac death in heart failure. *Heart* 91:674–680
- Lebovitz RM, Zhang H, Vogel H, Cartwright J Jr, Dionne L, Lu N, Huang S, Matzuk MM (1996) Neurodegeneration, myocardial injury, and perinatal death in mitochondrial superoxide dismutase-deficient mice. *Proc Natl Acad Sci U S A* 93:9782–9787
- Lehnart SE (2007) Novel targets for treating heart and muscle disease: stabilizing ryanodine receptors and preventing intracellular calcium leak. *Curr Opin Pharmacol* 7:225–232
- Lima B, Forrester MT, Hess DT, Stamler JS (2010) S-nitrosylation in cardiovascular signaling. *Circ Res* 106:633–646
- Liu N, Colombi B, Memmi M, Zissimopoulos S, Rizzi N, Negri S, Imbriani M, Napolitano C, Lai FA, Priori SG (2006) Arrhythmogenesis in catecholaminergic polymorphic ventricular tachycardia: insights from a RyR2 R4496C knock-in mouse model. *Circ Res* 99:292–298
- Lompre AM, Hajjar RJ, Harding SE, Kranias EG, Lohse MJ, Marks AR (2010) Ca<sup>2+</sup> cycling and new therapeutic approaches for heart failure. *Circulation* 121:822–830
- Lopez-Lopez JR, Shacklock PS, Balke CW, Wier WG (1994) Local, stochastic release of Ca<sup>2+</sup> in voltage-clamped rat heart cells: visualization with confocal microscopy. *J Physiol* 480 (Pt 1):21–29
- Loyer X, Gomez AM, Milliez P, Fernandez-Velasco M, Vangheluwe P, Vinet L, Charue D, Vaudin E, Zhang W, Sainte-Marie Y, Robidel E, Marty I, Mayer B, Jaissier F, Mercadier JJ, Richard S, Shah AM, Benitah JP, Samuel JL, Heymes C (2008) Cardiomyocyte overexpression of neuronal nitric oxide synthase delays transition toward heart failure in response to pressure overload by preserving calcium cycling. *Circulation* 117:3187–3198
- Mak S, Newton GE (2001) The oxidative stress hypothesis of congestive heart failure: radical thoughts. *Chest* 120:2035–2046
- Makaula S, Lochner A, Genade S, Sack MN, Awan MM, Opie LH (2005) H-89, a non-specific inhibitor of protein kinase A, promotes post-ischemic cardiac contractile recovery and reduces infarct size. *J Cardiovasc Pharmacol* 45:341–347
- Makino N, Maeda T, Oyama J, Sasaki M, Higuchi Y, Mimori K, Shimizu T (2011) Antioxidant therapy attenuates myocardial telomerase activity reduction in superoxide dismutase-deficient mice. *J Mol Cell Cardiol* 50:670–677
- Marks AR (2000) Cardiac intracellular calcium release channels: role in heart failure. *Circ Res* 87:8–11
- Marx SO, Reiken S, Hisamatsu Y, Jayaraman T, Burkhoff D, Rosembli N, Marks AR (2000) PKA phosphorylation dissociates FKBP12.6 from the calcium release channel (ryanodine receptor): defective regulation in failing hearts. *Cell* 101:365–376
- Masumiya H, Li P, Zhang L, Chen SR (2001) Ryanodine sensitizes the Ca(2+) release channel (ryanodine receptor) to Ca(2+) activation. *J Biol Chem* 276:39727–39735
- Mazurek SR, Bovo E, Zima AV (2014) Regulation of sarcoplasmic reticulum Ca(2+) release by cytosolic glutathione in rabbit ventricular myocytes. *Free Radic Biol Med* 68:159–167

- Mead-Savery FC, Wang R, Tanna-Topan B, Chen SR, Welch W, Williams AJ (2009) Changes in negative charge at the luminal mouth of the pore alter ion handling and gating in the cardiac ryanodine-receptor. *Biophys J* 96:1374–1387
- Meissner G (2004) Molecular regulation of cardiac ryanodine receptor ion channel. *Cell Calcium* 35:621–628
- Miao L, St Clair DK (2009) Regulation of superoxide dismutase genes: implications in disease. *Free Radic Biol Med* 47:344–356
- Misra MK, Sarwat M, Bhakuni P, Tuteja R, Tuteja N (2009) Oxidative stress and ischemic myocardial syndromes. *Med Sci Monit* 15:RA209–RA219
- Mochizuki M, Yano M, Oda T, Tateishi H, Kobayashi S, Yamamoto T, Ikeda Y, Ohkusa T, Ikemoto N, Matsuzaki M (2007) Scavenging free radicals by low-dose carvedilol prevents redox-dependent  $\text{Ca}^{2+}$  leak via stabilization of ryanodine receptor in heart failure. *J Am Coll Cardiol* 49:1722–1732
- Nabauer M, Morad M (1990)  $\text{Ca}^{2+}$ -induced  $\text{Ca}^{2+}$  release as examined by photolysis of caged  $\text{Ca}^{2+}$  in single ventricular myocytes. *Am J Physiol* 258:C189–C193
- Nagasaka S, Katoh H, Niu CF, Matsui S, Urushida T, Satoh H, Watanabe Y, Hayashi H (2007) Protein kinase A catalytic subunit alters cardiac mitochondrial redox state and membrane potential via the formation of reactive oxygen species. *Circ J* 71:429–436
- Nogueira L, Figueiredo-Freitas C, Casimiro-Lopes G, Magdesian MH, Assreuy J, Sorenson MM (2009) Myosin is reversibly inhibited by S-nitrosylation. *Biochem J* 424:221–231
- Opie LH (1993) The mechanism of myocyte death in ischaemia. *Eur Heart J* 14 Suppl G:31–33
- Opie LH, Clusin WT (1990) Cellular mechanism for ischemic ventricular arrhythmias. *Annu Rev Med* 41:231–238
- Pogwizd SM, Bers DM (2004) Cellular basis of triggered arrhythmias in heart failure. *Trends Cardiovasc Med* 14:61–66
- Qin J, Valle G, Nani A, Nori A, Rizzi N, Priori SG, Volpe P, Fill M (2008) Luminal  $\text{Ca}^{2+}$  regulation of single cardiac ryanodine receptors: insights provided by calsequestrin and its mutants. *J Gen Physiol* 131:325–334
- Rassaf T, Totzeck M, Hendgen-Cotta UB, Shiva S, Heusch G, Kelm M (2014) Circulating nitrite contributes to cardioprotection by remote ischemic preconditioning. *Circ Res* 114:1601–1610
- Roux-Buisson N, Cacheux M, Fourest-Lieuvain A, Fauconnier J, Brocard J, Denjoy I, Durand P, Guicheney P, Kyndt F, Leenhardt A, Le MH, Lucet V, Mabo P, Probst V, Monnier N, Ray PF, Santoni E, Tremaux P, Lacampagne A, Faure J, Lunardi J, Marty I (2012) Absence of triadin, a protein of the calcium release complex, is responsible for cardiac arrhythmia with sudden death in human. *Hum Mol Genet* 21:2759–2767
- Sanchez G, Pedrozo Z, Domenech RJ, Hidalgo C, Donoso P (2005) Tachycardia increases NADPH oxidase activity and RyR2 S-glutathionylation in ventricular muscle. *J Mol Cell Cardiol* 39:982–991
- Santiago DJ, Curran JW, Bers DM, Lederer WJ, Stern MD, Rios E, Shannon TR (2010) Ca sparks do not explain all ryanodine receptor-mediated SR Ca leak in mouse ventricular myocytes. *Biophys J* 98:2111–2120
- Santiago DJ, Rios E, Shannon TR (2013) Isoproterenol increases the fraction of spark-dependent RyR-mediated leak in ventricular myocytes. *Biophys J* 104:976–985
- Santos CX, Anilkumar N, Zhang M, Brewer AC, Shah AM (2011) Redox signaling in cardiac myocytes. *Free Radic Biol Med* 50:777–793
- Satoh H, Blatter LA, Bers DM (1997) Effects of  $[\text{Ca}^{2+}]_i$ , SR  $\text{Ca}^{2+}$  load, and rest on  $\text{Ca}_2+$  spark frequency in ventricular myocytes. *Am J Physiol* 272:H657–H668
- Schaper J, Froede R, Hein S, Buck A, Hashizume H, Speiser B, Friedl A, Bleese N (1991) Impairment of the myocardial ultrastructure and changes of the cytoskeleton in dilated cardiomyopathy. *Circulation* 83:504–514
- Schlotthauer K, Bers DM (2000) Sarcoplasmic reticulum  $\text{Ca}^{2+}$  release causes myocyte depolarization. Underlying mechanism and threshold for triggered action potentials. *Circ Res* 87:774–780

- Seddon M, Looi YH, Shah AM (2007) Oxidative stress and redox signalling in cardiac hypertrophy and heart failure. *Heart* 93:903–907
- Sen L, Cui G, Fonarow GC, Laks H (2000) Differences in mechanisms of SR dysfunction in ischemic vs. idiopathic dilated cardiomyopathy. *Am J Physiol Heart Circ Physiol* 279:H709–H718
- Serysheva II, Ludtke SJ, Baker ML, Cong Y, Topf M, Eramian D, Sali A, Hamilton SL, Chiu W (2008) Subnanometer-resolution electron cryomicroscopy-based domain models for the cytoplasmic region of skeletal muscle RyR channel. *Proc Natl Acad Sci U S A* 105:9610–9615
- Shiferaw Y, Aistrup GL, Wasserstrom JA (2012) Intracellular  $Ca^{2+}$  waves, afterdepolarizations, and triggered arrhythmias. *Cardiovasc Res* 95:265–268
- Sitsapesan R, Williams AJ (1994) Regulation of the gating of the sheep cardiac sarcoplasmic reticulum  $Ca(2+)$ -release channel by luminal  $Ca^{2+}$ . *J Membr Biol* 137:215–226
- Slodzinski MK, Aon MA, O'Rourke B (2008) Glutathione oxidation as a trigger of mitochondrial depolarization and oscillation in intact hearts. *J Mol Cell Cardiol* 45:650–660
- Soeller C, Cannell MB (1999) Examination of the transverse tubular system in living cardiac rat myocytes by 2-photon microscopy and digital image-processing techniques. *Circ Res* 84:266–275
- Spear JF, Prabu SK, Galati D, Raza H, Anandatheerthavarada HK, Avadhani NG (2007) beta1-Adrenoreceptor activation contributes to ischemia-reperfusion damage as well as playing a role in ischemic preconditioning. *Am J Physiol Heart Circ Physiol* 292:H2459–H2466
- Stern MD (1992) Theory of excitation-contraction coupling in cardiac muscle. *Biophys J* 63:497–517
- Stern MD, Cheng H (2004) Putting out the fire: what terminates calcium-induced calcium release in cardiac muscle? *Cell Calcium* 35:591–601
- Stevens SC, Terentyev D, Kalyanasundaram A, Periasamy M, Gyorke S (2009) Intra-sarcoplasmic reticulum  $Ca^{2+}$  oscillations are driven by dynamic regulation of ryanodine receptor function by luminal  $Ca^{2+}$  in cardiomyocytes. *J Physiol* 587:4863–4872
- Strauss JD, Wagenknecht T (2013) Structure of glutaraldehyde cross-linked ryanodine receptor. *J Struct Biol* 181:300–306
- Sun J, Murphy E (2010) Protein S-nitrosylation and cardioprotection. *Circ Res* 106:285–296
- Sun J, Morgan M, Shen RF, Steenbergen C, Murphy E (2007) Preconditioning results in S-nitrosylation of proteins involved in regulation of mitochondrial energetics and calcium transport. *Circ Res* 101:1155–1163
- Tang H, Viola HM, Filipovska A, Hool LC (2011)  $Ca(v)1.2$  calcium channel is glutathionylated during oxidative stress in guinea pig and ischemic human heart. *Free Radic Biol Med* 51:1501–1511
- Terentyev D, Viatchenko-Karpinski S, Valdivia HH, Escobar AL, Gyorke S (2002) Luminal  $Ca^{2+}$  controls termination and refractory behavior of  $Ca^{2+}$ -induced  $Ca^{2+}$  release in cardiac myocytes. *Circ Res* 91:414–420
- Terentyev D, Gyorke I, Belevych AE, Terentyeva R, Sridhar A, Nishijima Y, de Blanco EC, Khanna S, Sen CK, Cardounel AJ, Carnes CA, Gyorke S (2008) Redox modification of ryanodine receptors contributes to sarcoplasmic reticulum  $Ca^{2+}$  leak in chronic heart failure. *Circ Res* 103:1466–1472
- Townsend DM (2007) S-glutathionylation: indicator of cell stress and regulator of the unfolded protein response. *Mol Interv* 7:313–324
- Tung CC, Lobo PA, Kimlicka L, Van PF (2010) The amino-terminal disease hotspot of ryanodine receptors forms a cytoplasmic vestibule. *Nature* 468:585–588
- Turrens JF (1997) Superoxide production by the mitochondrial respiratory chain. *Biosci Rep* 17:3–8
- Turrens JF (2003) Mitochondrial formation of reactive oxygen species. *J Physiol* 552:335–344
- van Petegem (2015) Ryanodine receptors: allosteric ion channel giants. *J Mol Biol* 427:31–53
- van Oort RJ, McCauley MD, Dixit SS, Pereira L, Yang Y, Respress JL, Wang Q, De Almeida AC, Skapura DG, Anderson ME, Bers DM, Wehrens XH (2010) Ryanodine receptor

- phosphorylation by calcium/calmodulin-dependent protein kinase II promotes life-threatening ventricular arrhythmias in mice with heart failure. *Circulation* 122:2669–2679
- Vanden Hoek TL, Shao Z, Li C, Zak R, Schumacker PT, Becker LB (1996) Reperfusion injury on cardiac myocytes after simulated ischemia. *Am J Physiol* 270:H1334–H1341
- Ventura-Clapier R, Garnier A, Veksler V (2004) Energy metabolism in heart failure. *J Physiol* 555:1–13
- Wehrens XH, Lehnart SE, Reiken SR, Marks AR (2004) Ca<sup>2+</sup>/calmodulin-dependent protein kinase II phosphorylation regulates the cardiac ryanodine receptor. *Circ Res* 94:e61–e70
- Werns SW, Fantone JC, Ventura A, Lucchesi BR (1992) Myocardial glutathione depletion impairs recovery of isolated blood-perfused hearts after global ischaemia. *J Mol Cell Cardiol* 24:1215–1220
- Xiao B, Zhong G, Obayashi M, Yang D, Chen K, Walsh MP, Shimoni Y, Cheng H, Ter KH, Chen SR (2006) Ser-2030, but not Ser-2808, is the major phosphorylation site in cardiac ryanodine receptors responding to protein kinase A activation upon beta-adrenergic stimulation in normal and failing hearts. *Biochem J* 396:7–16
- Xie LH, Weiss JN (2009) Arrhythmogenic consequences of intracellular calcium waves. *Am J Physiol Heart Circ Physiol* 297:H997–H1002
- Xing D, Chaudhary AK, Miller FJ Jr, Martins JB (2009) Free radical scavenger specifically prevents ischemic focal ventricular tachycardia. *Heart Rhythm* 6:530–536
- Xu L, Eu JP, Meissner G, Stamler JS (1998) Activation of the cardiac calcium release channel (ryanodine receptor) by poly-S-nitrosylation. *Science* 279:234–237
- Yamawaki H, Haendeler J, Berk BC (2003) Thioredoxin: a key regulator of cardiovascular homeostasis. *Circ Res* 93:1029–1033
- Yano M (2008) Ryanodine receptor as a new therapeutic target of heart failure and lethal arrhythmia. *Circ J* 72:509–514
- Yavuz S (2008) Surgery as early revascularization after acute myocardial infarction. *Anadolu Kardiyol Derg* 8(Suppl 2):84–92
- Zalk R, Clarke OB, des GA, Grassucci RA, Reiken S, Mancina F, Hendrickson WA, Frank J, Marks AR (2015) Structure of a mammalian ryanodine receptor. *Nature* 517:44–49
- Zaugg M, Lucchinetti E, Uecker M, Pasch T, Schaub MC (2003) Anaesthetics and cardiac preconditioning. Part I. Signalling and cytoprotective mechanisms. *Br J Anaesth* 91:551–565
- Zhang J, Jin B, Li L, Block ER, Patel JM (2005) Nitric oxide-induced persistent inhibition and nitrosylation of active site cysteine residues of mitochondrial cytochrome-c oxidase in lung endothelial cells. *Am J Physiol Cell Physiol* 288:C840–C849
- Zima AV, Blatter LA (2006) Redox regulation of cardiac calcium channels and transporters. *Cardiovasc Res* 71:310–321
- Zima AV, Terentyev D (2013) Sarcoplasmic reticulum Ca homeostasis and heart failure. In: *The biophysics of the failing heart*. Springer, pp 5–31
- Zima AV, Picht E, Bers DM, Blatter LA (2008) Termination of cardiac Ca<sup>2+</sup> sparks: role of intra-SR [Ca<sup>2+</sup>], release flux, and intra-SR Ca<sup>2+</sup> diffusion. *Circ Res* 103:e105–e115
- Zima AV, Bovo E, Bers DM, Blatter LA (2010) Ca<sup>2+</sup> spark-dependent and -independent sarcoplasmic reticulum Ca<sup>2+</sup> leak in normal and failing rabbit ventricular myocytes. *J Physiol* 588:4743–4757
- Zima AV, Bovo E, Mazurek SR, Rochira JA, Li W, Terentyev D (2014) Ca handling during excitation-contraction coupling in heart failure. *Pflugers Arch* 466:1129–1137
- Zissimopoulos S, Viero C, Seidel M, Cumbes B, White J, Cheung I, Stewart R, Jeyakumar LH, Fleischer S, Mukherjee S, Thomas NL, Williams AJ, Lai FA (2013) N-terminus oligomerization regulates the function of cardiac ryanodine receptors. *J Cell Sci* 126:5042–5051
- Zweier JL, Talukder MA (2006) The role of oxidants and free radicals in reperfusion injury. *Cardiovasc Res* 70:181–190
- Zweier JL, Flaherty JT, Weisfeldt ML (1987) Direct measurement of free radical generation following reperfusion of ischemic myocardium. *Proc Natl Acad Sci U S A* 84:1404–1407

# Electromagnetic Fields and Stem Cell Fate: When Physics Meets Biology

**Sara Hassanpour Tamrin, Fatemeh Sadat Majedi, Mahdi Tondar,  
Amir Sanati-Nezhad, and Mohammad Mahdi Hasani-Sadrabadi**

**Abstract** Controlling stem cell (SC) fate is an extremely important topic in the realm of SC research. A variety of different external cues mainly mechanical, chemical, or electrical stimulations individually or in combination have been incorporated to control SC fate. Here, we will deconstruct the probable relationship between the functioning of electromagnetic (EMF) and SC fate of a variety of different SCs. The electromagnetic (EM) nature of the cells is discussed with the emphasis on the effects of EMF on the determinant factors that directly and/or indirectly influence cell fate. Based on the EM effects on a variety of cellular processes, it is believed that EMFs can be engineered to provide a controlled signal with the highest impact on the SC fate decision. Considering the novelty and broad

---

S.H. Tamrin

Center of Excellence in Biomaterials, Department of Biomedical Engineering, Amirkabir University of Technology, Tehran, Iran

F.S. Majedi

Department of Bioengineering, University of California, Los Angeles, CA, USA

M. Tondar

Department of Biochemistry and Molecular & Cellular Biology, School of Medicine, Georgetown University, Washington, DC, USA

A. Sanati-Nezhad (✉)

BioMEMS and BioInspired Microfluidic Laboratory, Department of Mechanical and Manufacturing Engineering, Center for Bioengineering Research and Education, University of Calgary, Calgary, AB, Canada, T2N1N4  
e-mail: [amir.sanatinezhad@ucalgary.ca](mailto:amir.sanatinezhad@ucalgary.ca)

M.M. Hasani-Sadrabadi (✉)

Department of Chemistry & Biochemistry, and California NanoSystems Institute, University of California at Los Angeles, Los Angeles, CA 90095, USA

Parker H. Petit Institute for Bioengineering and Bioscience and G.W. Woodruff School of Mechanical Engineering, Georgia Institute of Technology, Atlanta, GA, USA

e-mail: [Mahdi.hasani@gatech.edu](mailto:Mahdi.hasani@gatech.edu)

applications of applying EMFs to change SC fate, it is necessary to shed light on many unclear mechanisms underlying this phenomenon.

**Keywords** Differentiation • Electromagnetic field • Self-renewal • Stem cell fate • Stem cell niche

## Contents

1	Introduction .....	64
2	Natural Endogenous EMFs .....	68
3	Externally Applied EMF .....	70
3.1	Natural Endogenous Fields Are Affected by External EMFs .....	72
3.2	Cell Fate Determinant Factors Are Affected by External EMFs .....	73
4	Conclusion .....	86
	References .....	87

## 1 Introduction

Research on SCs, one of the fascinating areas of biology and biophysics, has led to many discoveries and provided new ways of treatment for many diseases (Goldstein et al. 2015; Alwaal et al. 2015; Larsimont and Blanpain 2015; Wolff et al. 2015; Kemp et al. 2015; Harris and Sadiq 2015; Doyle et al. 2015). SCs are unspecialized cells that transmute into specialized cells to constitute different types of tissues (Fig. 1). These cells possess two important properties; differentiation into a variety of cell lineages and self-renewal as the ability to proliferate without the commitment in the lineage (Zhang and Wang 2008; Reya et al. 2001). It is known that fine balance between self-renewal and differentiation is crucial in regulating the dynamic states of tissue function, tissue maintenance during homeostatic conditions, and generation of differentiated progeny in response to injury (James et al. 2015; Li and Jiang 2011; Ramalho-Santos 2004; Celso et al. 2009). Undergoing self-renewing or differentiation, as the two possibilities for each SC during division, can be introduced as a phenomenon called cell fate decision (Fig. 2) (Morrison and Kimble 2006; Knoblich 2001, 2008; Neumüller and Knoblich 2009; Inaba and Yamashita 2012). Thereby, how differentiation and self-renewal in SCs can be controlled is the key question on controlling SC fate. Shedding light on the mechanisms underlying the balance between self-renewal and differentiation is a critical step in understanding the language of SCs and provides essential information for controlling SC fate.

An interesting aspect of physics interfacing with biology relates to the EM phenomena within the biological systems. An EM phenomenon is defined as the relation between electricity and magnetism, where an oscillating electric produces a magnetic field, and in consequence, the magnetic field can generate an electric field. This connection was discovered by Hans Christian Örsted in 1819 and theoretically

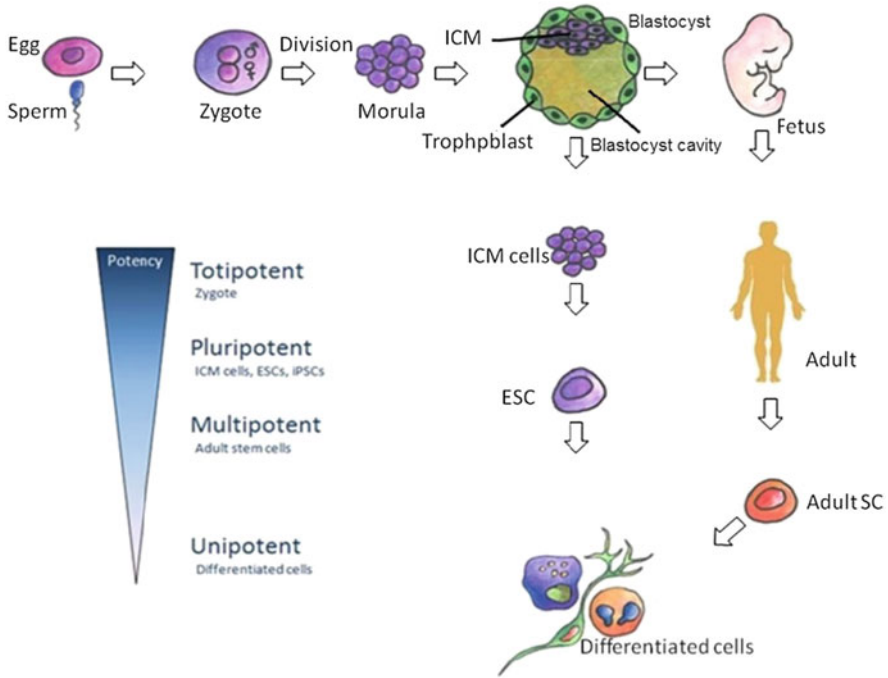


**Fig. 1** SCs and their differentiation potential (potency). SCs as unspecialized cells can undergo proliferation and differentiation to produce more SCs and constitute different types of cells and tissues. ESCs and adult SCs are two broad types of SCs. Potency, which describes the differentiation potential in SCs, decreases from the first cells in the embryo to the differentiated ones. Fertilization between two gamete cells (egg and sperm) produces Zygote, the earliest developmental stage of the embryo in multicellular organisms. The zygotes are totipotent and can form a complete viable organism. The zygote undergoes division and develops further to form morula consisting of many smaller cells, blastomeres. The morula's cell differentiates and forms blastocyst. It consists of a fluid-filled cavity, a cluster of cells on the interior called inner cell mass (ICM) and the outer layer, trophoblast, surrounding ICM. Blastocyst is a source of ESCs and is derived from ICM cells. ESCs, the descendants of totipotent cells, are pluripotent and can differentiate into nearly all cells. Differentiation potential is decreased in multipotent and unipotent cells. Multipotent SCs can differentiate into a number of cell types which are closely related family of cells, whereas unipotent cells can produce only one cell type. However, unipotent stem cells are different from non-SCs in their self-renewal property (Celso et al. 2009; Bernhard and Palsson 2004; Nichols 2001)

formulated by James Clerk Maxwell in 1864 (Malmivuo and Plonsey 1995). A combination of oscillating electric and magnetic fields, moving perpendicularly to each other, creates EM waves. The waves are characterized based on the wavelength and frequency or energy as their energy increases with the growing frequency (Fig. 3) (Gherardini et al. 2014). EM waves have covered our life and even exist within the biological systems (Malmivuo and Plonsey 1995; Levin 2003; Pokorný et al. 2001; Jelinek et al. 1999). During the last decades with advances in technology and growing introduction of electronic devices, the concerns about

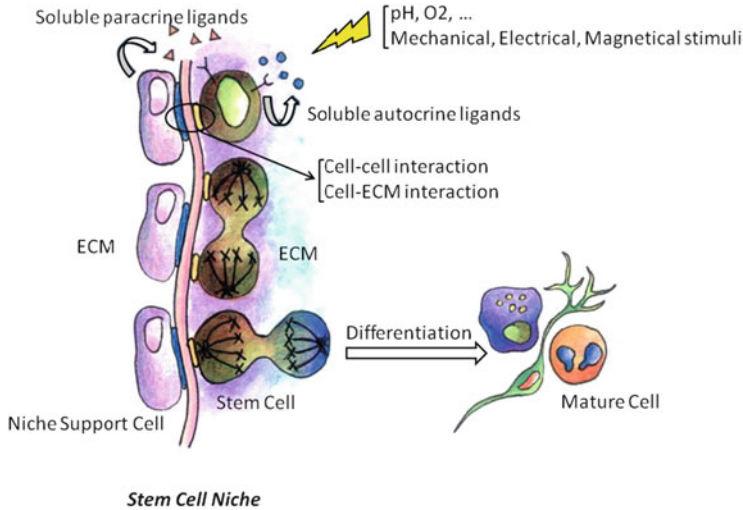


**Fig. 2** SC niche and its components. SC niche is an anatomic site for the maintenance of SCs, made up of supporting cells, ECM, soluble and surface bound signaling factors, cell–cell contacts, external mechanical and electrical forces, metabolites, and hormones, in which SCs differentiation is inhibited. During cell division, SCs can divide symmetrically or asymmetrically and SC fate decision is a choice between self-renewal and differentiation. The balance between HSC self-renewal and differentiation is thought to be controlled via the crosstalk between HSCs and their niches

the adverse effects of EM waves have been increased (Liu et al. 2013; Han et al. 2014; Megha et al. 2015). The EM waves are classified into EMFs/non-ionizing radiations and EM radiations/ionizing radiation. EMFs are low-level radiations among EM waves with the energy too low to break the electron bonds and consist of the ultraviolet, the visible light, the infrared radiation, the radiofrequency emissions, the microwave emissions, the extremely low-frequency (ELF) fields, and the static magnetic and electric fields (Gherardini et al. 2014). Although there are studies showing adverse effects of EM radiations on biological systems, much of the evidence, particularly those focusing on static or low-frequency fields, because of induced weak currents and ion redistribution through exposure, indicates that EMFs or non-ionizing radiations may have positive biological effects (Torres-Duran et al. 2007; Gerardi et al. 2008; Gaetani et al. 2009; Falone et al. 2007; Park et al. 2013; Kang et al. 2013; Yan et al. 2010; Soda et al. 2008).

Several studies have indicated that cells communicate with each other and with their environment through sending and receiving the EM signals (Malmivuo and Plonsey 1995; Levin 2003; Pokorný et al. 2001; Jelinek et al. 1999; Furse et al. 2009; Rahnama et al. 2011). Moreover, it is known that SC fate can be influenced via both specific intracellular signals (Pauklin and Vallier 2013; Orford and Scadden 2008; White and Dalton 2005; Singh and Dalton 2014) and extrinsic signals derived from SC's microenvironment or “niche” (Fig. 4) (Li and Jiang 2011;



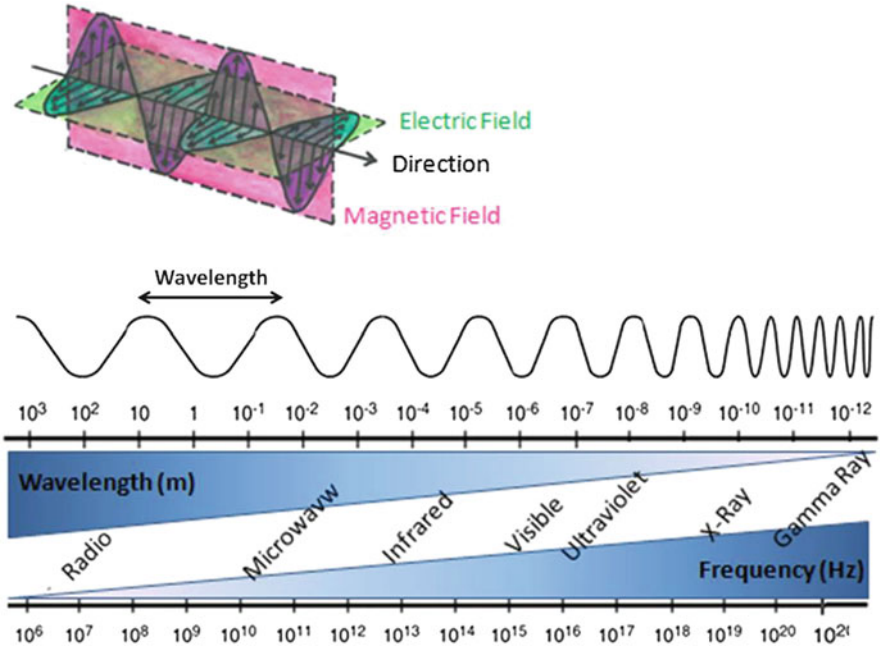


**Fig. 3** Electromagnetic (EM) field and EM radiation. Electric fields and magnetic fields are coupled together to form EM fields/waves. The frequency, wavelength, and energy describe the EM waves. The EM spectrum extends from Radio to Gamma radiation with the decreasing order of wavelength and increasing order of frequency and energy. (The wavelength increases from Gamma to Radio waves, while the frequency and energy decreases.)

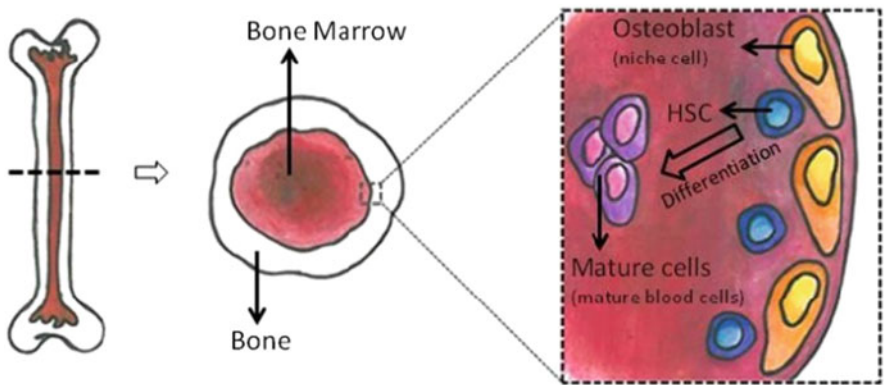


**Fig. 4** A schematic demonstration of the hematopoietic stem cell (HSC) niche. HSC niche is an anatomical location within the bone marrow consisting of hematopoietic and non-hematopoietic cells like osteoblasts, as well as extracellular components. HSCs within their niche located near the bone surfaces self-renew, and outside the niche commence the process of differentiation into mature blood cells (Dzierzak and Enver 2008; Papayannopoulou and Scadden 2008)

Watt and Huck 2013; Gattazzo et al. 2014; Spradling et al. 2001; Dzierzak and Enver 2008), as well as the interaction between these two signal groups (Fig. 2). Therefore, the possible roles of EMFs as environmental signals in the SC fate decision not only do not seem negligible, but also pose an interesting discussion in the SC field. In this article, we discuss determinant factors influencing the cell fate with a focus on the probable associations between cell fate decision and the EM energy.

## 2 Natural Endogenous EMFs

According to some reports, all living cells divulge EM signals through emitting the ultra-weak EM radiations (Malmivuo and Plonsey 1995; Levin 2003; Furse et al. 2009; Rahnama et al. 2011; Pokorný et al. 2001). In biological systems, these photon emissions (bio-photons) refer to “mitogenic radiation,” introduced to biological science by a Russian embryologist, Alexander Gurwitsch (Taylor and Harvey 1931). These EM radiations existing in the ultraviolet and infrared ranges are essential for the function of cells and their interactions (Taylor and Harvey 1931). Besides, the concept of “fields of life,” formulated by Harold Saxton Burr in 1937, can be a reason for the existence of EMFs in biological systems (Matthews 2007). It was also discovered that electro-dynamic fields, measurable with standard voltmeters, can organize and control the living systems (Levin 2003; Matthews 2007).

The natural endogenous EMFs have been detected in either extracellular matrix or within the cellular structures (Pokorný et al. 1997; Pokorný 2004). The most likely source of these fields is a mechanical vibration of polar biological structures that can be described by Fröhlich model (Pokorný et al. 1997; Pokorný 2004; Šrobár 2012, 2013). Briefly, electric dipoles and charges such as proteins, lipids, nucleic acids, and free ions exist in many structures within cells, and motility of these units generates an altering electric field and in consequence produces a varying magnetic field; Moreover, the altering magnetic field produces an electric field. Such coupled electrical and magnetic interactions lead to the generation of EMF in the cellular environment. For example, the solenoidal form of DNA seems to act physically as a conductive wire of nucleic acids with a core of histones, with a potential to generate EM force (Pienta and Hoover 1994). Motility of charges through DNA accounted as a current through a wire, thereby, has the potential to generate a magnetic field in the histones. Since DNA is a double-stranded molecule, a flux of current is created in DNA due to the movement of DNA and histones, leading to the generation of a mechanical force (Pienta and Hoover 1994), however there is no evidence reported on generation of EMF in DNA.

In several studies, the creation of EMFs by living cells (natural endogenous EMFs) has not only been reported (Levin 2003; Pokorný et al. 2001), but has also been quantified (Malmivuo and Plonsey 1995; Pokorný et al. 2001; Jelínek et al. 1999). The cell membrane is a serious candidate as the source of EM signals

and has a selective permeability, which acts selectively in the transportation of different ion species across it. This feature leads to accumulation of ions at the inner and outer membrane surfaces. A difference in the concentration of ions, including potassium ( $K^+$ ), chloride ( $Cl^-$ ), and ( $Na^+$ ) across the membrane produces a voltage difference in a bioelectrical gradient named transmembrane potential (TMP) (Malmivuo and Plonsey 1995; Panagopoulos et al. 2002). In reality, all cells generate bioelectrical signals correlated to the translocation of ions between the extracellular and intracellular spaces, meaning that there exist changes in TMP and ion fluxes. The ion channels and ion pumps are the sources of these gradients and assist in controlling the flow of ions and their concentrations. The channels are sensitive to TMP and correlated with the gates that are chemically or electrically activated or deactivated. These opening and closing of gates locally change TMP and produce an electric flow transmitted to other points in the membrane (Malmivuo and Plonsey 1995; Panagopoulos et al. 2002; Lim et al. 2009; Adams and Levin 2013).

In addition to the cell membrane, cytoskeleton consists of polar units. The cytoskeleton structure is composed of filaments like microtubules (MTs) that fulfill requirements for the Frohlich coherent vibrations and as a result generates EMF. MTs consist of electric dipoles,  $\alpha$ -tubulin and  $\beta$ -tubulin heterodimers (Pokorný et al. 1997; Bowne-Anderson et al. 2013). The synchronized oscillation of these subunits generates the natural endogenous field. The dynamic instability of MTs, convertible polymerization and depolymerization, has a correlative role in the formation of EMFs. It can be noted that the energy supply, which is a need for oscillation, is provided by hydrolysis of guanosine triphosphate to guanosine diphosphate in MTs (Pokorný et al. 1997, 2001; Bowne-Anderson et al. 2013; Ramalho et al. 2007; Havelka et al. 2011; Zhao and Zhan 2012). It is reasonable to state that cells have a high level of electro-dynamic activity during division due to the formation of the mitotic spindle and the rearrangement of MTs. The EM activity of yeast cells during mitosis has been measured, and an evident connection between MTs configuration and EM activity was detected (Pokorný et al. 2001; Šrobár 2013). It should be also underlined that a regulated generation of reactive oxygen species (ROS) and reactive nitrogen species due to natural metabolic processes can produce bio-photons (Rahnama et al. 2011; Vladimirov and Proskurnina 2009; Thar and Kühl 2004). In oxidative phosphorylation (OXPHOS), a strong electrochemical gradient is created upon mitochondrial driven pumping of protons from the matrix into the inter-membrane space (Šrobár 2013; Pokorný 2012). Transfer of protons across the inner membrane produces water ordering that leads to the generation of a strong static electric field (Pokorný 2012). This field is able to change the region of the MT oscillations due to the close association between mitochondria and cytoskeleton filaments. Therefore, MTs can immerse in the mitochondrial's electrostatic field (Šrobár 2013).

### 3 Externally Applied EMF

Living cells transmit not only EM signals, but also receive them (Levin 2003; Furse et al. 2009; Rahnama et al. 2011). Cells and their surrounding environment absorb energy when they are exposed to external EMFs (Fig. 5). Simeonova et al. (Simeonova et al. 2002) presented a method to calculate energy absorption

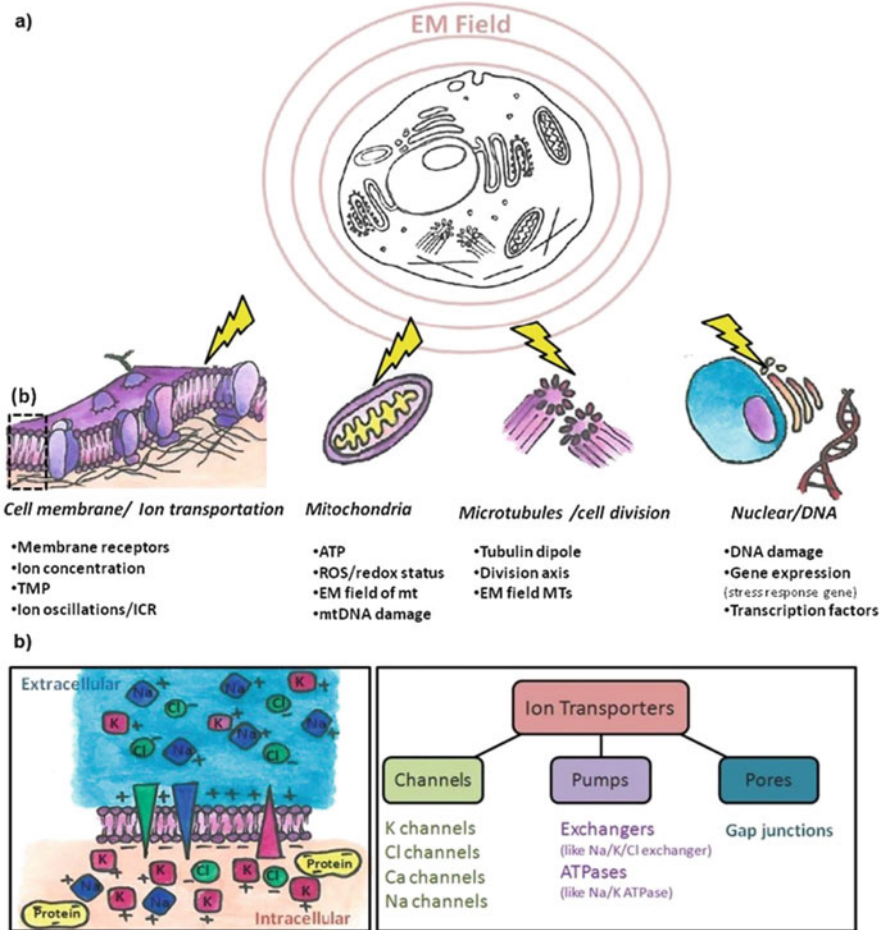


**Fig. 5** A schematic of the effects of externally applied EM fields. (a) A wide variety of biological processes can be influenced by EM fields. Cells exposed to the EM fields can absorb energy via their compartments and surrounding medium. Highlighted results: Alternation in cell membrane functions, stimulation of galvanotaxis and cell motion, change in cell cycle, cell division and spindle MT assembly, alternation of enzymes and their activities, changes in several metabolic parameters, and stimulation of an active status in the cells. (b) Motility of ions between the extracellular and intracellular spaces. The changes in ion fluxes and TMP are influenced by EM fields. Ionic channels, pumps, and pores control the ionic gradient and are sensitive to TMP

in a single human red blood cell. It is documented that various critical cellular systems can be regulated using EM energy. The Earth's geomagnetic field (GMF) and shielding from this field were shown active in many abnormalities of living systems. Malformed eyes and retarded/blocked development of larvae are some defects caused by shielding from GMF (Asashima et al. 1991). It was also reported that shielding from GMF influences the function of the immune system (Roman and Tombarkiewicz 2009). In Wistar rats, a long-term shielding of the GMF resulted in a decreased ability of macrophages to release NO and to synthesize O<sub>2</sub>, vital microbicidal molecules of macrophages in males and females, respectively. A single exposure (2 h) of ELF-EMF (60 Hz, 2.4 mT) on Wistar rats resulted in a drop in the total cholesterol content of liver and led to an elevated density of lipoproteins in blood serum and lipoperoxides (Torres-Duran et al. 2007). Additionally, long-term exposure to ELF-EMF (less than 100 Hz, by 50 days) in rats increased their body weight and blood glucose content and elevated the fatty acid metabolism (Gerardi et al. 2008). The changes observed in several metabolic parameters after exposure to ELF magnetic fields suggest that the external ELF electric fields have a significant impact on the metabolic processes and enzymatic activities (Torres-Duran et al. 2007). Electric fields are also capable of galvanotactic induction in the cells, a directional cellular movement towards the cathode or the anode; some cells, such as mouse embryo fibroblasts migrated towards the cathode, whereas some others like human granulocytes moved towards the anode (Mycielska and Djamgoz 2004; Brown and Loew 1994).

Spreading evidence demonstrates that the exposure to the EMF alters the proliferation and differentiation of cells under EMFs (Gaetani et al. 2009; Falone et al. 2007; Park et al. 2013; Kang et al. 2013; Serena et al. 2009; Tsai et al. 2009; Chen et al. 2000). For instance, exposure to EMF (15 Hz, 5 mT, by 21 days) increased collagen type II expression and glycosaminoglycan content of cultures in human mesenchymal stem cells (human MSCs), and thereby stimulated chondrogenic differentiation of SCs (Mayer-Wagner et al. 2011). In human, MSCs exposed to ELF-EMF (50 Hz, 1 mT) showed an increase in the expression of neural markers and indicated an enhanced neural differentiation (Park et al. 2013). Exposure of these cells to daily pulsed EMF (with a pulse duration of 300  $\mu$ s, and a constant rate of 7.5 Hz) showed that ELF-EM stimulation may modulate osteogenic differentiation of human MSCs (Tsai et al. 2009). Likewise, the stimulating effects of EMF (15 Hz, 1 mT, by 3 days) on osteoblast-specific mRNA expression in rat bone marrow MSCs indicated a promoted osteogenic differentiation of these cells (Yang et al. 2010). Stimulation of embryonic neural stem cell (NSC) with 50 Hz ELF-EMF (2 mT for 3 days) resulted in an alteration in the expression of genes regulating neuronal differentiation (Ma et al. 2014). In cardiac SCs, exposure to ELF-EMFs (7 Hz, 2.5  $\mu$ T), tuned at calcium (Ca<sup>2+</sup>) ion cyclotron energy resonance (Ca<sup>2+</sup>-ICR), showed an increase in the expression of cardiac markers after 5 days exposure, suggesting that this stimulation may drive a cardiac-specific differentiation with no pharmacological or genetic manipulation (Gaetani et al. 2009). Therefore, the influence of externally applied EMFs on cell behavior is undeniable.

Although there is a vast body of evidence regarding the understanding of the interaction of external EMFs with biological systems, the discussion about the degree of influence and safety of these fields on living systems has been remained unsettled. Overall, the cellular physiological state and the parameters related to the applied fields, such as frequency and exposure time, are strongly associated with the influence of the EMFs on the cells. It is not surprising to claim that EM energy emissions have a potential to affect the SC fate decision. However, the mechanisms underlying EMF effects are still poorly understood. In general, external EMFs can influence SC fate decisions via a direct EM interference with natural endogenous fields, or via affecting determinant factors affecting the SC fate.

### ***3.1 Natural Endogenous Fields Are Affected by External EMFs***

The direct interaction of external EMFs with natural endogenous fields or constituent components of endogenous fields may cause a change in the original pattern of natural fields (Panagopoulos 2014). In fact, polar biological structures like ions that make natural endogenous fields are likely magnetic targets for external fields. It is theoretically formulated that electric and magnetic fields interact with each other and also with polar structures as a target (Malmivuo and Plonsey 1995). Based on the Coulomb's law, electric charges are able to exert electric forces on each other along the line between the charges. Besides the electric force, a magnetic force is exerted by moving charges, although it is not parallel to the line between the charges (Furse et al. 2009; Lim et al. 2009). Thereby, EMFs as a combination of electric and magnetic fields can exert forces on polar units.

Theoretical studies confirmed that EMFs are able to rearrange the electric charges in cellular environments, including ECM, the cell membrane, and intracellular medium (Fig. 5). The oscillating electric and magnetic fields can exert forces to ions placed within the channel proteins and those existing on either side of the plasma membrane, thereby affecting the ion vibration and concentration (Halgamuge et al. 2009). The ion cyclotron resonance (ICR) theory confirms that ions can circle the vector of a static magnetic field such as GMF (Gerardi et al. 2008; Furse et al. 2009; Halgamuge et al. 2009). GMF may be utilized in biological systems through ICR-like mechanisms. The energy states of ions alter during the resonance, by which biological activities are regulated (Halgamuge et al. 2009). Therefore, the interaction of external fields with cellular targets may cause an oscillation at polar units' resonance frequency and an alteration in the magnitude, frequency, and direction of the original endogenous field. Also, since theoretical studies confirm the existence of a significant electric dipole moment along MTs' axes due to the permanent electric dipoles of tubulin heterodimers (Ramalho et al. 2007; Stracke et al. 2002), it is reasonable to acclaim that EMFs is able to target MTs and affect MTs dynamic instability. Dynamic instability of MTs



has a correlative role in the formation of endogenous EMFs due to the presence of tubulin dipoles (Pokorný et al. 1997, 2001; Bowne-Anderson et al. 2013; Ramalho et al. 2007; Havelka et al. 2011; Zhao and Zhan 2012); thereby external EMFs can impact the endogenous field.

Due to the correlation of natural endogenous fields with cellular functions, the claim of a direct impact of external fields on endogenous fields and their effects on cell functions is not unsubstantial. It has been shown that cellular processes and natural endogenous EMFs influence each other. In fact, the EM nature of biological systems is the reason that transmission of signals can affect the regulation of many cellular processes. According to Gurwitsch (Levin 2003), the association of endogenous fields with the developmental events seems reasonable, for instance, embryonic morphology is affected by altering the regular pattern of natural EMF. Natural endogenous electric fields of cells change during the developmental and regenerative states (Levin 2003; Matthews 2007). Characterization of the electric fields showed a correlation between the field parameters and corresponding biological events. It was also proposed that morphogenesis relies on an intricate pattern of direct electric fields (Levin 2003; Matthews 2007).

Some studies have indicated that EM activity within cells is associated with cell motion and cell division and that spindle MT assembly can be facilitated by MTs' electric fields (Pokorný et al. 2001; Zhao and Zhan 2012). The appearance of an abnormality in natural endogenous fields can result in an irregularity in cells function. For instance, cancer cells are directly influenced by a change in the electric fields of organisms (Levin 2003; Matthews 2007). It should be noted that as a result of the Warburg effect, cancer cells differ from healthy cells in their EM activity (Rahnama et al. 2011) and entropic state (Zhao and Zhan 2012). This implies that one source of energy for electric oscillation of MTs could be the overall entropic cellular environment (Zhao and Zhan 2012). Evidence shows that a disturbance in the mitochondria-MT network may lead to transfer to cancer states. The mitochondrial dysfunction of cancer cells increases the damping of MT oscillations and reduces the energy supply, thereby disturbing the power and coherence of EMFs (Pokorný 2012). Moreover, mitochondrial dysfunction in cancer cells may inhibit pyruvate pathways and suppress the proton transfer from the matrix into the inter-membrane space, leading to a drop in the level of water ordering and electric field (Pokorný 2012).

### ***3.2 Cell Fate Determinant Factors Are Affected by External EMFs***

Among a vast body of evidence indicating EMFs affect biological systems, determinant elements in SC self-renewal and differentiation affected by these fields directly and/or indirectly have highlighted the potential of EMF to regulate SC fate decision.

### 3.2.1 Ion Concentration and Transmembrane Potential (TMP)

The cellular response to external fields involves the vibration and transport of ions (Fig. 5) (Halgamuge et al. 2009). According to data on ICR recognized in the living organisms, the presence of a very weak magnetic field alters ion concentration within the cells by tuning the field's frequency with the characteristic frequency of the ions involved (Gerardi et al. 2008; Furse et al. 2009; Halgamuge et al. 2009). Ions like  $\text{Ca}^{2+}$  have mediatory roles in the effect of EMF on cell function (Levin 2003; Gaetani et al. 2009; Kang et al. 2013; Lim et al. 2009; Walleczek 1992; Morabito et al. 2010), for controlling the morphogenesis (Levin 2003), regulation of proliferation (Gaetani et al. 2009), differentiation (Gaetani et al. 2009; Gillo et al. 1993), and other cellular processes (Gaetani et al. 2009; Clapham 2007; Nicotera et al. 1989). A disruption in  $\text{Ca}^{2+}$ -dependent cell signalling and a modulation in the regulation of  $\text{Ca}^{2+}$  channels were reported for some neuronal cells exposed to EMF (50 Hz, 0.5–1 mT) for 24–72 h (Grassi et al. 2004). It was demonstrated that ELF magnetic fields as the combination of two static (ranging from 27 to 37 mT) and oscillatory (7–72 Hz, 13–114  $\mu\text{T}$ ) forms of magnetic fields can regulate the transport of  $\text{Ca}^{2+}$  through interaction with  $\text{Ca}^{2+}$  channels in the cell membrane (Bauréus Koch et al. 2003). In human MSCs, an increase in the extracellular  $\text{Na}^+/\text{K}^+$  concentration was detected upon exposure to ELF-magnetic fields (50 Hz, 20 mT); this exposure led to the activation of  $\text{Na}^+/\text{K}^+$  channels and thereby an increase in  $\text{Na}^+/\text{K}^+$  concentration (Yan et al. 2010).

Second messenger pathways involving small signalling molecules such as  $\text{Ca}^{2+}$  are strongly associated with the changes of TMP, depolarization, or hyperpolarization (Adams and Levin 2013; Cho et al. 1999). An asymmetric disturbance in TMP has been induced by an external electric field resulted in a hyperpolarization of the membrane surfaces faced to an anode and depolarization in other surfaces faced to a cathode (Brown and Loew 1994; Cho et al. 1999). Voltage-sensitive  $\text{Ca}^{2+}$  channels may be activated due to the depolarization of cathode-facing membrane surface, and thereby increases the concentration of intracellular free  $\text{Ca}^{2+}$  (Onuma and Hui 1988).

### 3.2.2 Intracellular Molecular Mechanisms

It is well known that cell fate is closely related to the signaling pathways (Fig. 5) (Li and Neaves 2006; Blank et al. 2008) and transcriptional factors (Orford and Scadden 2008; Young 2011; Ye et al. 2011; Pesce and Schöler 2000, 2001; Rodda et al. 2005; Mitsui et al. 2003). For example, Wnts, a family of protein ligands, are expressed in a variety of tissues and impact many processes such as tissue homeostasis, embryogenesis, and generation of cell polarity (Rattis et al. 2004; Nusse 2008; Huang et al. 2007). It has been seen that the activity of this pathway is required to control spindle orientation, for example in *C. elegans* (Watt and Hogan 2000). Additionally, this pathway is involved in OXPHOS (Reya et al. 2001;



Saretzki 2005) and can act as a niche factor. It has a regulatory role in the maintenance of self-renewing state, for example in HSCs (Blank et al. 2008; Rattis et al. 2004; Nusse 2008; Huang et al. 2007; Holland et al. 2013; Reya et al. 2003). Over-expression of the activated form of  $\beta$ -catenin (Nusse 2008) as a mediator of the Wnt signaling pathway can expand immature cells like HSCs and promote their self-renewal capacity. Over-expression of Wnt signaling inhibitors such as axin enhancing degradation of  $\beta$ -catenin causes HSCs to lose their capability to repopulate (Rattis et al. 2004; Huang et al. 2007; Reya et al. 2003). Additionally, Wnt signaling pathway in the skin was shown effective in promoting SC activation and expansion (Li and Neaves 2006). It should be implied that Wnts have a relationship with the genes involved in self-renewal; Wnt showed a repressing role on Nanog and over-expression of Oct4 caused an increase in the transcriptional activity of  $\beta$ -catenin (Nusse 2008). Moreover, an alteration in this pathway was shown to be related to an on/off switching in the expression of telomerase reverse transcriptase (TERT), a catalytic subunit of telomerase (Saretzki 2009). It has been reported that pulsed EMFs (8 Hz, 3.82 mT) in ovariectomized rat can activate Wnt/ $\beta$ -catenin signaling pathway and consequently, reveal positive effects on bone mass and trabecular bone microarchitecture and strength (Zhou et al. 2012a, b). The influence of pulsed EMFs on Wnt/ $\beta$ -catenin signaling has also been reported in osteoblasts after exposure (Zhai et al. 2016; Lin et al. 2015).

In addition to Wnt signaling pathways, MAPK signalings have regulatory impacts on many cellular processes such as proliferation, differentiation, and modulation of mitosis motility, metabolism, and apoptosis (Seger and Krebs 1995; Zhang and Liu 2002; Chang and Karin 2001) (details of MAPK pathway in Ref. (Zhang and Liu 2002) and Fig. 6). The elevated differentiation of human ESCs has been shown correlated with the activation of MAPKs family (Ji et al. 2010). Such activation via radiofrequency and ELF-EMF is a sign of EMFs' impact on intracellular molecular mechanisms (Blank and Goodman 2009; Li et al. 2013; Leszczynski et al. 2002). The MAPK and phosphatidylinositol 3-kinases (PI3Ks) pathways are known as the participants in the synthesis of enhanced collagen in mouse osteoblast-like MC3T3-E1 cells upon exposure to ELF-EMF (60 Hz, 3 mT) (Soda et al. 2008). Suppression of the PI3K pathway or activation of the MAPK pathway led to an increase in collagen content of the exposed cells (Soda et al. 2008).

Moreover, transcriptional factors such as Oct4, Nanog, c-Myc, and Sox2 can influence SC fate. The expression of these factors in differentiated cells differs from undifferentiated ones. The expression of a complex network of these factors has been appeared to maintain the self-renewing undifferentiated state in SCs (Orford and Scadden 2008; Pesce and Schöler 2000, 2001; Rodda et al. 2005; Mitsui et al. 2003) and developmental control of mammalian embryos (Pesce and Schöler 2000; Guo et al. 2004; Nichols et al. 1998). Surprisingly, these factors can reprogram somatic cells to induce pluripotent stem cells (iPSCs) (Kang et al. 2009a, b; Ryan and Rosenfeld 1997; (Hochedlinger and Plath 2009; Moon et al. 2011). Like ESCs, the reprogrammed cells have the potential to differentiate into three germ layers: endoderm, ectoderm, and mesoderm (Ryan and Rosenfeld 1997). There are

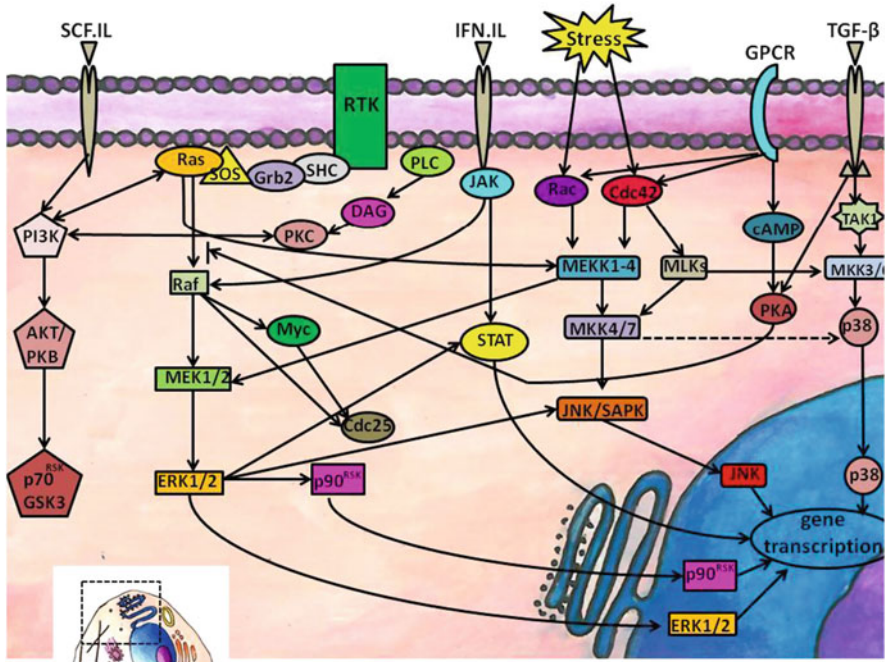


**Fig. 6** A schematic presentation of MAPK pathways in the signaling network in mammalian cells. Mitogen-activated protein kinase (MAPK) signalling pathway plays a key function in a variety of complex cellular processes such as proliferation, differentiation, apoptosis, and survival. MAPKs can be activated by a range of stimuli (mitogens, cytokines, growth factors, and environmental stress), causes a downstream signalling cascade, and consequently, leads to the transcription of genes that encode proteins. At least three MAPK families, including extracellular signal-regulated kinase (ERK), Jun kinase (JNK/SAPK), and p38 MAPK have been characterized in mammalian cells

several studies indicating that Oct4 is a key factor in the reprogramming (Okita et al. 2007; Nakagawa et al. 2007; Yu et al. 2007) and is one of the three proteins that are sufficient to reprogram differentiated adult cells to the ESCs in mouse and human (Okita et al. 2007; Nakagawa et al. 2007; Kang et al. 2009a, b). It has also been reported that exposure to EMFs enhances the reprogramming efficiency of somatic cells to pluripotency through inducing epigenetic alterations. In mouse somatic cells, a significant increase in Oct4, Sox2, and Nanog expressions after EL-EMF exposure (50 Hz, 1 mT) indicated an increased iPSC cell generation and confirmed that EL-EMF exposure promoted somatic cell reprogramming into pluripotency (Baek et al. 2014). The exposure of somatic cells to the radiofrequency energy via Radio Electric Asymmetric Conveyor stimulation increased the expression of Oct4, Sox2, c-Myc, and Nanog, and reprogrammed them towards pluripotency in fibroblasts (Maioli et al. 2013).

### 3.2.3 Redox Status and ROS

EMFs can affect ROS generation (Fig. 5), while ROS-induced signaling molecules play an essential role in many processes (Ji et al. 2010; Waypa et al. 2002; Chandel et al. 2000; Hamanaka and Chandel 2009, 2010; Bedard and Krause 2007; Lu et al. 2010; Zhang et al. 2011; Rafalski and Brunet 2011; Ezashi et al. 2005; Diehn et al. 2009; Hosokawa et al. 2007; Schmelter et al. 2006). ROS molecules are highly reactive molecules (oxygen radicals) such as superoxide, hydroxyl, peroxy, alkoxy, and even some non-radicals like hydrogen peroxide, with a potential to convert into free radicals (Vladimirov and Proskurnina 2009; Bedard and Krause 2007; Andreyev et al. 2005; Adam-Vizi and Chinopoulos 2006). The amount of ROS should be controlled since these molecules have two distinct roles; ROS not only act as an intermediary messenger (Hamanaka and Chandel 2009, 2010; Bedard and Krause 2007; Rehman 2010), but they also function as a toxic agent. Overproduction of ROS may lead to an alteration in redox status and oxidative stress in cells (Graziewicz et al. 2002; Guo et al. 2010; Ott et al. 2007). It is known that normal cellular activities require a balanced redox. Cells are usually able to prevent the accumulation of ROS at detrimental levels via antioxidant systems having a suppressive effect on ROS (Guo et al. 2004; Andreyev et al. 2005; Oktem et al. 2005; Zang et al. 1998; Cairns et al. 2011). A disequilibrium between the production of free radicals and the scavenging capacity of antioxidant compounds and enzymes such as peroxidases, catalase, vitamins, and superoxide dismutases (SOD) can lead to an oxidative stress to cells (Lee et al. 2004).

Cell fate determination was shown to be linked to the level of ROS and oxidative stress (Blank et al. 2008; Lu et al. 2010; Hosokawa et al. 2007; Suda et al. 2005). Several studies demonstrated that low ROS levels in SCs are linked to the progeny and maintenance of self-renewal. The ROS level was shown to be less in the early progenitors not only in ESCs but also in adult SCs (Ji et al. 2010; Zhang et al. 2011; Rafalski and Brunet 2011; Ezashi et al. 2005; Diehn et al. 2009; Hosokawa et al. 2007; Schmelter et al. 2006). The cardiovascular differentiation in ESCs was argued to be associated with the NADPH oxidase expression and ROS generation (Schmelter et al. 2006). The enhanced differentiation of human ESCs via ROS-involved signaling pathways resulted in an elevated expression of mesodermal and endodermal markers (Ji et al. 2010). Furthermore, ROS-inducing conditions reduce the expression of Oct4, Nanog, and Sox2 in human ESCs (Ji et al. 2010). Oxidative stress has been considered responsible for the oxidized low-density lipoprotein (ox-LDL) activity in biological systems (Lu et al. 2010; Chu et al. 2011). It was reported that the suppressed proliferation in bone marrow SCs and inhibited expression of Oct4 through ox-LDL is mediated by ROS generated from ox-LDL (Lu et al. 2010; Chu et al. 2011). The inhibitory function of antioxidants in the ROS-induced differentiation suggests that the promoted differentiation occur via high ROS levels. It was shown that an increase in the ROS production during ESCs differentiation is linked to an attendant increased antioxidant expression, whereas antioxidants are expressed at low levels in the

undifferentiated state (Rehman 2010). Treatment of free radical scavenger decreases ESCs differentiation and increases the expression of pluripotency markers such as Oct4 (Ji et al. 2010). Thioredoxin antioxidant has shown its pivotal role in the redox regulation of transcription factors like Oct4 (Guo et al. 2004; Nordberg and Arner 2001), and a probable regulatory role in totipotential property of ESCs (Guo et al. 2004; Kobayashi-Miura et al. 2002). Moreover, an increase in the Nanog expression related to ROS can be reduced through the suppressive effects of manganese-superoxide dismutase (MnSOD) on ROS (Fijalkowska et al. 2010).

Some cellular responses like proliferation and differentiation in response to EMFs are linked to the generation and activities of ROS (Falone et al. 2007; Serena et al. 2009; Blank and Goodman 2009; Schmelter et al. 2006; Oktem et al. 2005; Consales et al. 2012; Jelenković et al. 2006; Zwirska-Korczala et al. 2005; Simkó 2004; Simko 2007; Katsir and Parola 1998; Sauer and Wartenberg 2005; Sauer et al. 1999). It should be highlighted that different cell types, due to their particular redox status, display different reactions to the same stimulus (Simko 2007). Exposure to the radiofrequency EMFs (at 900 MHz) enhanced the production of ROS in murine L929 fibrosarcoma cells (Zeni et al. 2007). In contrast, in an experimental model of rat lymphocytes exposed to radiofrequency radiation at 900 MHz, results indicated that acute exposure after 5 and 15 min did not stimulate ROS production. Nevertheless, a combination of radiofrequency radiation and iron ions in the rat lymphocytes increased the level of ROS (Zmysłony et al. 2004). Stimulation of NADH-oxidase pathway with a consequent production of superoxide anion radicals upon exposure of mouse bone marrow-derived cells to ELF-MF (50 Hz, 1 mT) is another result emphasizing the EMF impact (Rollwitz et al. 2004). Surprisingly, EMFs can impact the activities of antioxidative enzymes (Zwirska-Korczala et al. 2005; Simko 2007; (Katsir and Parola 1998). The activation of antioxidant enzymes in rat liver mitochondria, upon exposure to EM pulse with the strength of 60 kV/m, prevented the generation of free radicals (Wang et al. 2013). A significant rise was detected in the activity of SOD enzymes in mice (Lee et al. 2004) and rat (Jelenković et al. 2006) brains after exposure to the ELF-magnetic field of 60 Hz and 50 Hz, respectively.

Redox-sensitive kinases can also impact signaling pathways like ROS activated signaling pathways (Ji et al. 2010; Waris and Ahsan 2006). These proteins play a modulating function in gene expression through the phosphorylation of transcription factors (Waris and Ahsan 2006). ROS and oxidative stress phosphorylated p38/MAPK in HSCs led to a defect in the self-renewal capacity (Blank et al. 2008; Bedard and Krause 2007; Suda et al. 2005). On the other hand, inactivation of p38 MAPK protects against the loss of self-renewal capacity in HSCs. Furthermore, the ROS-induced up-regulation of p16 and p19 in HSCs are blocked by the p38/MAPK inhibitor or an antioxidant, *N*-acetylcysteine (Suda et al. 2005). It has also been found that the intracellular ROS content of HSCs can be regulated by AKT, a family of serine/threonine-specific protein kinase. The combined loss of two isoforms of this kinase family has shown an impairment in self-renewal capacity of HSCs (Juntilla et al. 2010). Impairment of endothelial differentiation by Ox-LDL

has also been reported due to the inhibition of Akt phosphorylation (Chu et al. 2011). Moreover, AKT participates in controlling the cellular metabolisms and PI3Ks signaling cascade with a central role in the cell survival signaling (Soda et al. 2008; Cairns et al. 2011). The PI3K/AKT pathway can participate in self-renewing of the HSC. A faulty reconstitution and a reduced proliferative capacity were demonstrated with a decreased PI3K activity in these cells (Juntilla et al. 2010).

It is worthy to mention that the down-regulation of human TERT has been detected in human ESCs under ROS-induced conditions (Ji et al. 2010). The cells differentiated from TERT overexpressing SCs demonstrated a lower intracellular oxidative stress and a higher apoptosis resistance. These cells also maintained a high level of telomerase expression (Armstrong et al. 2005; Yang et al. 2008; Lee et al. 2005). A high telomerase activity level is a contributor to the immortality and self-renewal (Wesbuer et al. 2010; Ahmed et al. 2008). Different studies showed that the down-regulation of telomerase correlates significantly with the differentiation in embryonic and adult SCs (Saretzki et al. 2008; Li et al. 2005; Bagheri et al. 2006). In mouse and human ESCs, over-expression of the telomerase improved proliferation and ability for colony formation (Armstrong et al. 2005; Yang et al. 2008). Altogether, the concentration of ROS seems to be one of the vital factors regulating SC fate; EMFs are capable of influencing SC fate decision via affecting ROS generation.

### 3.2.4 Mitochondria

Mitochondria, the main sites of energy metabolism and ATP generation (Fig. 7) (Adam-Vizi and Chinopoulos 2006; Loureiro et al. 2013), play central roles in many cell processes such as differentiation, apoptosis, and metabolism of key cellular intermediates (Ye et al. 2011; Loureiro et al. 2013; Parker et al. 2009). They also act as a controller in concentrating  $\text{Ca}^{2+}$  ions (Parker et al. 2009; Scarpa and Graziotti 1973). It is a known fact that endoplasmic reticulum, an important site for  $\text{Ca}^{2+}$  ion storage, has a critical function in the  $\text{Ca}^{2+}$ -mediated signaling pathways (Clapham 2007). The physical association between mitochondria and endoplasmic reticulum not only emphasizes the  $\text{Ca}^{2+}$  signaling role in mitochondria but also corroborates that mitochondria play a temporary function in  $\text{Ca}^{2+}$  storage (Clapham 2007).

Based on the studies on mitochondrial features in the differentiated and undifferentiated states, the relationship between mitochondrial properties and stemness maintenance seems reasonable (St. John et al. 2005; Cho et al. 2006; Lonergan et al. 2006). During differentiation process, several physiological changes take place inside mitochondria, such as the alteration in the mitochondrial DNA copy number, ATP content, and oxygen consumption (Fig. 8). A reduction in mitochondrial number has been observed in undifferentiated SCs (Rehman 2010; Guo et al. 2010; Saretzki et al. 2008; Parker et al. 2009; St. John et al. 2005; Cho et al. 2006; Lonergan et al. 2006, 2007). Low mitochondrial DNA content might act



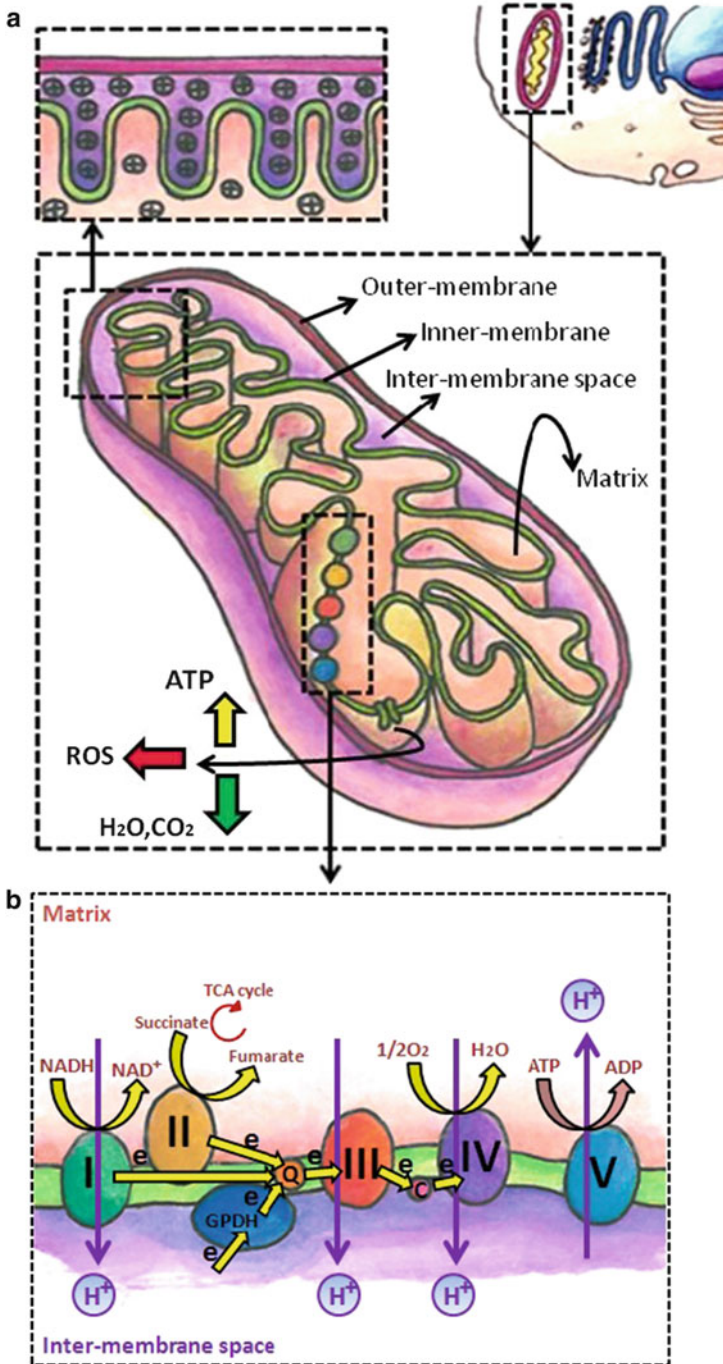


**Fig. 7** A schematic illustration of mitochondria and electron respiratory chain. (a) A mitochondrion consists of two membranes (outer membrane and a more complex inner membrane), the matrix, and the space between the two membranes, called the inter-membrane space. The inner

as an indicator of stemness. Up-regulation of ESCs' capacity to transcribe mitochondrial DNA as well as the increased mitochondrial DNA copies per cell has been detected in committed ESCs, losing their pluripotency. These all imply that there is a marked correlation between SC pluripotency and mitochondrial DNA (Lonergan et al. 2006, 2007; Facucho-Oliveira and John 2009). Moreover, low levels of ATP have been reported in undifferentiated ESCs. Mitochondrial activity and also mitochondrial DNA replication increase in ESCs undergoing differentiation. This represents that the mitochondrial DNA encodes ETC's components. Thus, an increased ATP content taking place with the increased mitochondrial activity might act as a signal to initiate the differentiation and decrease the stemness (Guo et al. 2010; Cho et al. 2006; Lonergan et al. 2006, 2007). Importantly, metabolic characterization showed that SCs prefer anaerobic metabolism (Rehman 2010; Loureiro et al. 2013). Studies on mouse epiblast SCs revealed that the respiration activity of mitochondria is lower in these cells, in contrast to the earlier stages of mouse SCs (Zhou et al. 2012a, b; Houghton 2006). Several studies indicated that undifferentiated cells are more glycolytic than differentiated ones. During the differentiation of ESCs, the energy production is switched to OXPHOS (Rehman 2010; Cho et al. 2006) which plays an essential function in the differentiation of ESCs to cardiomyocytes and creation of sarcomeres (Chung et al. 2007). Moreover, a more glycolytic nature of the undifferentiated cells has also been detected in adult SCs, like HSCs (Suda et al. 2011) and MSCs (Rehman 2010; Funes et al. 2007), demonstrating a high rate production of glycolysis and lactate. This phenomenon is in contrast to the condition of the differentiated cells. It is known that OXPHOS is linked to the mitochondrial DNA transcription. A limited mitochondrial DNA transcription has been reported in stemness situation, while mitochondrial mass and oxygen consumption increase with differentiation (Ye et al. 2011; St. John et al. 2005; Cho et al. 2006; Lonergan et al. 2006; Facucho-Oliveira and John 2009). Such alterations in mitochondria can be related to transcriptional factors. During differentiation of ESC, down-regulation of Oct4, Sox2, and Nanog has been reported in correlation with mitochondrial activities. However, in an undifferentiated state of SCs, the mitochondrial activities are suppressed (Ye et al. 2011; Facucho-Oliveira and John 2009). The decision between the oxidative and anaerobic glycolytic metabolisms can be mediated by these genes and their products (Kang et al. 2009a, b; Shakya et al. 2009). A connection between several common Oct (Oct4, Oct1) targets and energy



**Fig. 7** (continued) membrane contains the proteins involved in the electron transport and ATP synthesis. During the electron transport, protons are pushed from the matrix out to the cytosolic side of the inner mitochondrial membrane, creating a proton-motive force to synthesize ATP from ADP. At the end of this electron transport chain, ROS, H<sub>2</sub>O, and CO<sub>2</sub> are produced as by-products. **(b)** The components of the electron transport chain. The electron transport chain consists of four complexes. Each of the complexes is embedded in the inner mitochondrial membrane containing several different electron carriers. The electrons move along the electron transport chain from NADH to O<sub>2</sub>, while a proton is released at each step (Adam-Vizi and Chinopoulos 2006)

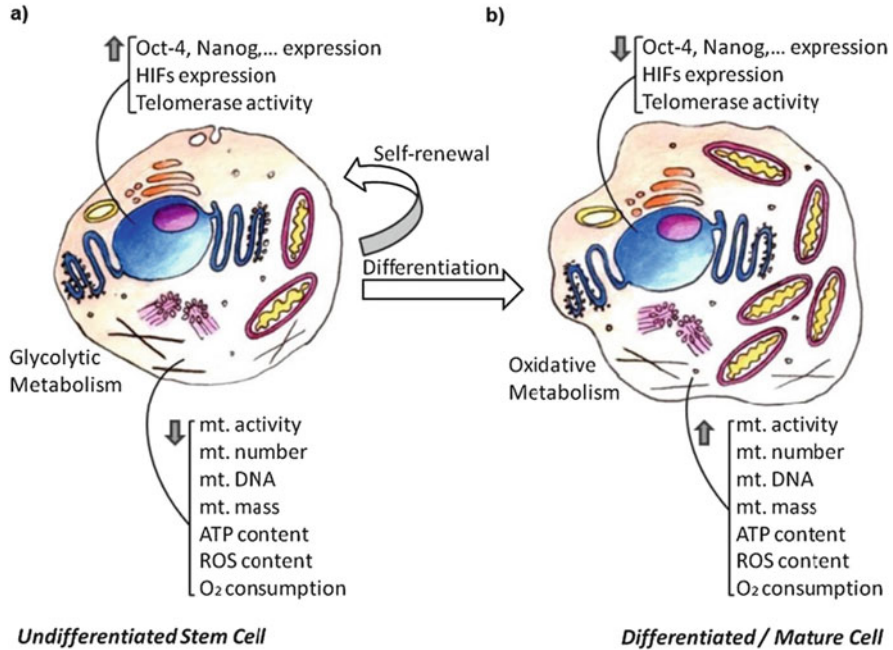


**Fig. 8** A schematic presentation of different characteristics between differentiated and undifferentiated states. **(a)** In undifferentiated states, cells are more glycolytic. Mitochondrial (mt) activity, mt. number, mt. mass, and mt. DNAs are low in contrast to the mature cells. ATP and ROS content as well as the O<sub>2</sub> consumption are less in these cells. However, the expression of some transcription factors, HIF factors (Heddleston et al. 2009; Forristal et al. 2010; Mathieu et al. 2011; Eliasson and Jönsson 2010), and also telomerase activity are high in these cells. **(b)** In mature cells, the activity of some factors like HIFs, telomerase, Oct4, and Nanog are lower than undifferentiated ones. In contrast, mt. activity, mt. number, mt. mass, mt. DNA, ATP content, ROS content and O<sub>2</sub> consumption are high in these cells. Oxidative phosphorylation in these cells is higher than glycolytic metabolism

metabolisms demonstrated that a small mitochondrial function and a high rate of glycolysis are the characterizations of the metabolic pattern (Kang et al. 2009a, b; Kondoh et al. 2007). Therefore, it is reasonable to claim that EMFs can influence the SC fate via direct or indirect effects on mitochondria.

It has been revealed that external fields are directly or indirectly capable of affecting the mitochondrial features such as the mitochondrial membrane potential ( $\Delta^{\varphi}m$ ) and consequently impact the factors controlling SC fate decision. The mobility of protons during mitochondrial OXPHOS for ATP generation produces an electrochemical gradient across the membrane, and the proton-motive force (PMF) is expressed in units of electrical potential including  $\Delta^{\varphi}m$  and  $\Delta pH$  (pH gradient) (Adam-Vizi and Chinopoulos 2006). In most circumstances,  $\Delta^{\varphi}m$  dominates pmf. This potential influences almost all activities in the mitochondria and is valued about 150–180 mV (Adam-Vizi and Chinopoulos 2006).  $\Delta^{\varphi}m$  as a



reflection of mitochondrial functional status is associated with the differentiation states (Ye et al. 2011).

Mitochondrial permeability transition is responsible for the release of several proteins (such as cytochrome c) from the mitochondrial inter-membrane space into the cytoplasm (Fig. 7) (Bernardi and Di Lisa 2015). In mitochondria, the control of bioenergetic parameters such as redox state of pyridine nucleotides is linked to  $\Delta^{\varphi}_m$  or pmf. The pyridine nucleotides, nicotinamide adenine dinucleotide (NAD), and nicotinamide adenine dinucleotide phosphate (NADP) participate in the energy transduction. They exist in two forms: oxidized ( $\text{NAD}^+$ ,  $\text{NADP}^+$ ) and reduced (NADH, NADPH). The balance between these two forms is central to the maintenance of the redox status and regulation of the ion channels and cell signaling, not only under the normal condition, but also in pathological states (Nakamura et al. 2012).  $\Delta^{\varphi}_m$  in differentiated cells, like fibroblasts, are maintained via ETC and form a proton gradient within the chain. However, in human pluripotent SCs this maintenance occurs through glycolysis. It should be noted that ATP hydrolysis maintains  $\Delta^{\varphi}_m$  upon an impairment of ETC in the differentiated cells (Zhang et al. 2011). Moreover, an increase in aerobic glycolysis and a drop in  $\Delta^{\varphi}_m$  have been detected in leukemia cells cultured over bone marrow-derived mesenchymal stromal cells. It was suggested that the Warburg effect in leukemia-stroma co-culture cells is promoted via mitochondrial uncoupling (Samudio et al. 2008). Mitochondrial uncoupling taking place under physiologic conditions is defined as the abrogation of ATP synthesis in response to  $\Delta^{\varphi}_m$  and mediated by uncoupling proteins (UCPs) as mitochondrial inner-membrane proteins regulating cell metabolism. In cancer cells, the increased dependency to glycolysis has been suggested to be possibly due to inability to synthesize ATP in response to  $\Delta^{\varphi}_m$  (Samudio et al. 2009).

In Jurkat cells upon induction of a nanosecond electric pulse (4 ns, 10 MV/m electrical pulses at a 1 kHz repetition rate) to the cells, an increase in both permeabilities of mitochondrial membrane and release of cytochrome c, and a decrease in  $\Delta^{\varphi}_m$  were reported (Napotnik et al. 2012).  $\Delta^{\varphi}_m$  was dropped in human cancer cells SMMC7721 upon exposure to electric pulses (120 ns, 600 V/cm). Notably, a significant decrease in  $\Delta^{\varphi}_m$  and release of cytochrome c into the cytoplasm act as a signal to apoptosis. The duration and intensity of electric pulses have a determinant function in regulatory effects of these pulses over cells (Jiang et al. 2008). Similar effects on mitochondrial permeability and release of cytochrome c were reported upon exposure of amniotic epithelial cells to 50 Hz magnetic field (0.4 mT) for 60 min. The transition of mitochondrial permeability and the release of cytochrome c were induced without any significant effect on  $\Delta^{\varphi}_m$  (Feng et al. 2016). However, neuroblastoma cells exposed to 50 Hz EMF with the intensity of above 0.8 mT showed a significant reduction in  $\Delta^{\varphi}_m$  (Calabrò et al. 2013).

EMFs can also indirectly impact the mitochondria via regulating the  $\text{Ca}^{2+}$  concentration. Also,  $\text{Ca}^{2+}$  concentration level can trigger mitochondrial permeability (Bernardi and Di Lisa 2015; Kristián et al. 2000; Vaseva et al. 2012; Moon et al. 2012). Interestingly, EMF-based ROS generation is another indirect route to

affect mitochondrial function (Fig. 7) (Adam-Vizi and Chinopoulos 2006). The mitochondrial activity and the amount of ROS production are closely related together (Adam-Vizi and Chinopoulos 2006). Researchers discovered that the rate of mitochondrial activity in undifferentiated NSCs is higher and the amount of ROS generation is lower in compared to differentiated neurons and glial cells (Zhang et al. 2011; Rafalski and Brunet 2011). ROS release in an undifferentiated state is less since glycolysis instead of OXPHOS predominately produces the cellular energy. The high levels of oxidative damage reported in some differentiating cells can be due to a rise in mitochondrial activity (Rehman 2010). The mitochondrial antioxidant MnSOD also influences mitochondrial ROS level (Fijalkowska et al. 2010). An increase in mitochondrial mass can be linked to the growing expression of antioxidant (Guo et al. 2004). Moreover, it was reported that ROS and oxidative stress have the ability to alter the activity of the antioxidative enzymes such as MnSOD and the copper- and zinc-containing superoxide dismutase (Cu/ZnSOD) (Zwirska-Korzala et al. 2005; Masri et al. 2008).

It should be noted that large amounts of oxidative stress can have an inhibitory function in the mitochondrial DNA polymerase activity via reducing its DNA binding efficiency (Graziewicz et al. 2002). ROS level can also influence ATP production. It has been shown that ATP generation in mitochondria is accompanied by a lower degree of oxidative stress (Saretzki 2009). Studies on isolated heart and brain mitochondria demonstrated that ROS production is related to  $\Delta^{\varphi}_m$ /pmf and the level of NADH. ROS production is succinate-supported, meaning that mitochondria need a high  $\Delta^{\varphi}_m$  to generate ROS. In other words, a small drop in  $\Delta^{\varphi}_m$  results in a decline in ROS production. On the other hand, the over-expression of UCPs might have a protective function against excessive ROS conditions. The reducer role of UCPs against ROS production may be dependent on a drop in NADH: NAD<sup>+</sup> ratio (Adam-Vizi and Chinopoulos 2006). UCP2 is capable of regulating energy metabolism. The regulatory function of UCP2 in human pluripotent SCs stimulated the aerobic glycolysis (Zhang et al. 2011). UCP2 not only regulates cell metabolism, but also impacts the ROS and differentiation (Saretzki 2009). In overall, UCP2 plays a regulatory function in the SC fate. Both in vivo and in vitro experiments indicated that the amount of UCP2 is less in differentiated cells in comparison with undifferentiated cells. In other words, the expression of UCP2 is repressed with differentiation (Zhang et al. 2011; Rafalski and Brunet 2011). The repression of UCP2 displays a necessary role in decreasing the glycolysis and maintaining or even increasing the mitochondrial glucose oxidation in differentiated human pluripotent SCs (Zhang et al. 2011).

### 3.2.5 MT Dynamic Instability

SCs can divide symmetrically or asymmetrically (Fig. 2) (Morrison and Kimble 2006; Bernhard and Palsson 2004). During symmetric cell division, both daughter cells attain the same fate. However, during asymmetric cell division, one daughter cell becomes a new SC, and the other differentiates. In other words, one cell leaves

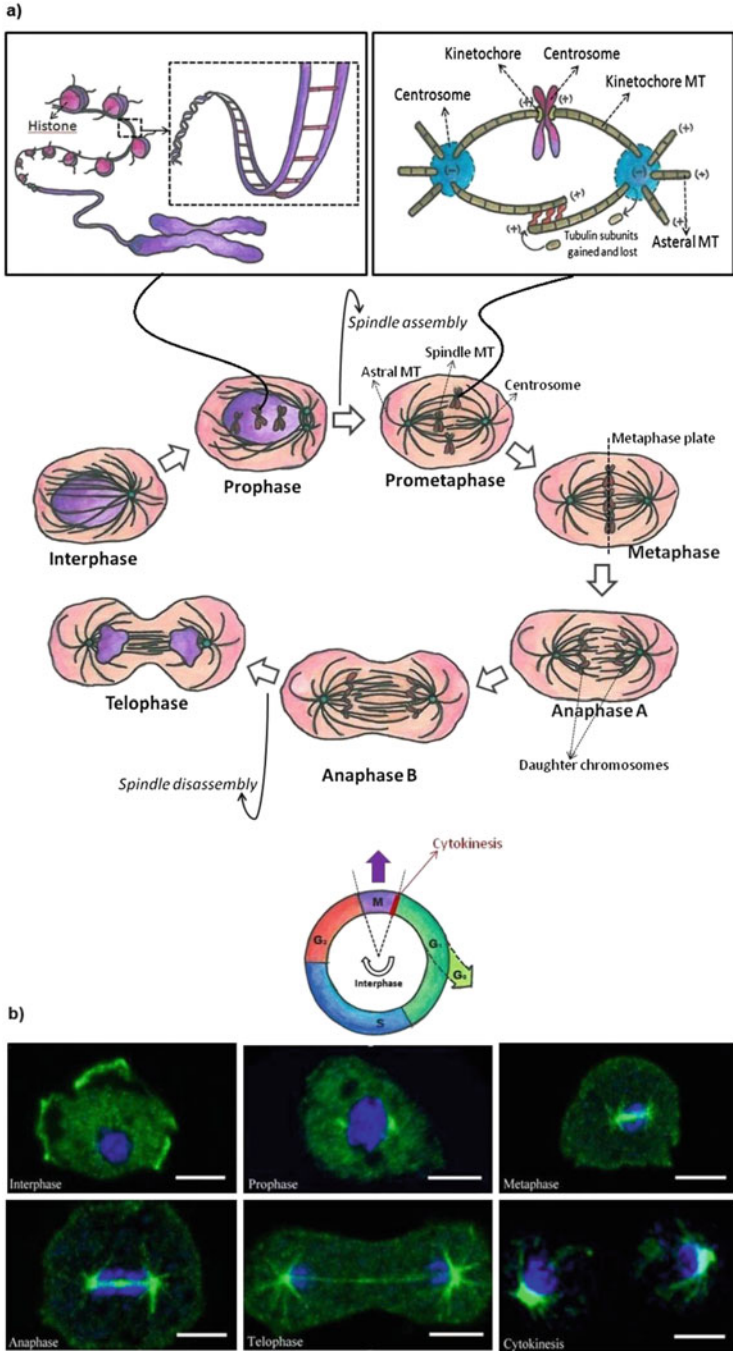


**Fig. 9** Cell cycle and cell division. **(a)** Stages of mitosis. Cell cycle consists of three periods: interphase, mitotic (M) phase, and cytokinesis. During interphase proceeding in three stages, synthesis (S) phase, and two gap phases (G<sub>1</sub> and G<sub>2</sub>), the cell grows and prepares for division. During M phase cell splits itself into two daughter cells, and in the cytokinesis stage, cell divides

the niche and produces a large number of progenies, whereas the other cell remains SC cell and receives the same niche signals (Fig. 2) (Morrison and Kimble 2006; Knoblich 2001). The control of symmetric and asymmetric divisions in SCs can be a valuable approach to balance self-renewal and differentiation. Importantly, the main subject in the control of cell division is related to the mitotic spindle and its orientation, establishing the symmetric or asymmetric SC division. The position of mitotic spindle determines the cleavage plane and the spatial arrangement of two daughter cells could be delimited thereupon. During the cell division, the segregation of chromosomes between daughter cells is performed by the mitotic spindle (Siller and Doe 2009). Cellular spindle consists of two spindle poles where MTs are nucleated by centrosomes at these ends (Fig. 9). Spindle MTs making up the mitotic spindle grow dynamically by polymerization and shrink by depolymerization, which refers to “dynamic instability” of MTs (Bowne-Anderson et al. 2013; Wang 2010; Walczak et al. 2010). Spindle alignment can be influenced by astral MT interactions with the cell cortex and cytoplasm. The plus-end depolymerization of astral MTs attaching to the cell cortex can generate the pulling forces, which influence the astral MTs. Similarly, these forces can be produced by cortically attached MT minus-end and translocation of MT plus-ends (Siller and Doe 2009; Trushko et al. 2013). Therefore, the productive spindle orientation is depended on the regulation of MT length. In other words, regulation of MT dynamic instability has a crucial role in the correct spindle positioning. EMFs can potentially influence MT dynamic instability, according to the claim that EMFs can target MTs because of the tubulin dipoles. Several studies referred to the regulatory function of electric (Ramalho et al. 2007; Zhao and Zhan 2012; Stracke et al. 2002; Zhao et al. 1999) and magnetic fields (Denegre et al. 1998; Valles 2002) in MT polymerization and cell division (Fig. 5).

## 4 Conclusion

SC functions rely on intrinsic genetic programs, extrinsic signals from their niche, and also the interaction between the two. The control of SC behavior and interactions between these cells together and with their niche can influence cell fate. Since the EMF was demonstrated to be an efficient approach to transporting energy between cells and also between the cells and their microenvironment, cells are able to communicate electromagnetically. In this article, the impact of both natural

---

**Fig. 9** (continued) completely. Besides, there is a resting phase ( $G_0$ ) in which the cell division is stopped (Orford and Scadden 2008; Bernhard and Palsson 2004). M phase/mitosis causes the chromosomes to be segregated between two daughter cells and consists of five stages; prophase, prometaphase, metaphase, anaphase, and telophase (Wang 2010) (b) Confocal images during interphase, mitosis stages, and cytokinesis in the *Dictyostelium discoideum* cells stained for chromatin (Reproduced with the permission from Ref. (Rump et al. 2011))

endogenous EMFs and external EMF in the regulation of cellular processes, particularly cell fate was emphasized. Two possible ways were proposed by which external EMFs potentially can influence SC fate decisions: (1) externally applied fields can affect determinant factors influencing the SC fate (i.e., by alteration of ROS generation and intracellular ionic concentrations), and (2) externally applied fields are capable of varying the natural endogenous EMF via a direct interference with endogenous fields, and consequently, cause a change in the corresponding functions of natural endogenous fields control. Since externally applied EMFs are able to regulate cellular processes corresponding to the SC fate decision, it is expected that novel strategies would be developed in the near future for the controlled delivery of EMFs to the cells for further modulating cell fate. In other words, given the fact that the niche provides a microenvironment composed of cellular and extracellular signals, and SCs and their niche components interact with each other, EMF as an external signal has the potential to be presented as a possible participating component in SC niche and consequently has an impact on SC fate. However, understanding how EMFs influence SC fate is related to how SCs sense and response to these fields. Further research is required to shed lights on the complex regulatory networks in SCs and their interactions with EMFs.

**Acknowledgments** The authors thank Dr. Mehran Solati for insightful discussions that greatly assisted the research.

## References

- Adams DS, Levin M (2013) Endogenous voltage gradients as mediators of cell-cell communication: strategies for investigating bioelectrical signals during pattern formation. *Cell Tissue Res* 352:95–122
- Adam-Vizi V, Chinopoulos C (2006) Bioenergetics and the formation of mitochondrial reactive oxygen species. *Trends Pharmacol Sci* 27:639–645
- Ahmed S, Passos JF, Birket MJ, Beckmann T, Brings S, Peters H, Birch-Machin MA, von Zglinicki T, Saretzki G (2008) Telomerase does not counteract telomere shortening but protects mitochondrial function under oxidative stress. *J Cell Sci* 121:1046–1053
- Alwaal A, Zaid UB, Lin C-S, Lue TF (2015) Stem cell treatment of erectile dysfunction. *Adv Drug Deliv Rev* 82:137–144
- Andreyev AY, Kushnareva YE, Starkov A (2005) Mitochondrial metabolism of reactive oxygen species. *Biochemistry* 70:200–214
- Armstrong L, Saretzki G, Peters H, Wappler I, Evans J, Hole N, Von Zglinicki T, Lako M (2005) Overexpression of telomerase confers growth advantage, stress resistance, and enhanced differentiation of ESCs toward the hematopoietic lineage. *Stem Cells* 23:516–529
- Asashima M, Shimada K, Pfeiffer CJ (1991) Magnetic shielding induces early developmental abnormalities in the newt, *Cynops pyrrhogaster*. *Bioelectromagnetics* 12:215–224
- Baek S, Quan X, Kim S, Lengner C, Park J-K, Kim J (2014) Electromagnetic fields mediate efficient cell reprogramming into a pluripotent state. *ACS Nano* 8:10125–10138
- Bagheri S, Nosrati M, Li S, Fong S, Torabian S, Rangel J, Moore DH, Federman S, LaPosa RR, Baehner FL (2006) Genes and pathways downstream of telomerase in melanoma metastasis. *Proc Natl Acad Sci* 103:11306–11311
- Bauréus Koch C, Sommarin M, Persson B, Salford L, Eberhardt J (2003) Interaction between weak low frequency magnetic fields and cell membranes. *Bioelectromagnetics* 24:395–402

- Bedard K, Krause K-H (2007) The NOX family of ROS-generating NADPH oxidases: physiology and pathophysiology. *Physiol Rev* 87:245–313
- Bernardi P, Di Lisa F (2015) The mitochondrial permeability transition pore: molecular nature and role as a target in cardioprotection. *J Mol Cell Cardiol* 78:100–106
- Bernhard O, Palsson SNB (2004) Tissue engineering. Pearson Prentice Hall
- Blank M, Goodman R (2009) Electromagnetic fields stress living cells. *Pathophysiology* 16:71–78
- Blank U, Karlsson G, Karlsson S (2008) Signaling pathways governing stem-cell fate. *Blood* 111:492–503
- Bowne-Anderson H, Zanic M, Kauer M, Howard J (2013) Microtubule dynamic instability: a new model with coupled GTP hydrolysis and multistep catastrophe. *Bioessays* 35:452–461
- Brown MJ, Loew LM (1994) Electric field-directed fibroblast locomotion involves cell surface molecular reorganization and is calcium independent. *J Cell Biol* 127:117–128
- Cairns RA, Harris IS, Mak TW (2011) Regulation of cancer cell metabolism. *Nat Rev Cancer* 11:85–95
- Calabrò E, Condello S, Currò M, Ferlazzo N, Vecchio M, Caccamo D, Magazù S, Ientile R (2013) 50 Hz electromagnetic field produced changes in FTIR spectroscopy associated with mitochondrial transmembrane potential reduction in neuronal-like SH-SY5Y cells. *Oxid Med Cell Longev* 2013:414393
- Celso CL, Wu JW, Lin CP (2009) In vivo imaging of hematopoietic stem cells and their microenvironment. *J Biophotonics* 2:619–631
- Chandel NS, McClintock DS, Feliciano CE, Wood TM, Melendez JA, Rodriguez AM, Schumacker PT (2000) Reactive oxygen species generated at mitochondrial complex III stabilize hypoxia-inducible factor-1 $\alpha$  during hypoxia: A mechanism of O<sub>2</sub> sensing. *J Biol Chem* 275:25130–25138
- Chang L, Karin M (2001) Mammalian MAP kinase signalling cascades. *Nature* 410:37–40
- Chen G, Upham BL, Sun W, Chang C-C, Rothwell EJ, Chen K-M, Yamasaki H, Trosko JE (2000) Effect of electromagnetic field exposure on chemically induced differentiation of friend erythroleukemia cells. *Environ Health Perspect* 108:967
- Cho MR, Thatte HS, Silvia MT, Golan DE (1999) Transmembrane calcium influx induced by ac electric fields. *FASEB J* 13:677–683
- Cho YM, Kwon S, Pak YK, Seol HW, Choi YM, Park DJ, Park KS, Lee HK (2006) Dynamic changes in mitochondrial biogenesis and antioxidant enzymes during the spontaneous differentiation of human embryonic stem cells. *Biochem Biophys Res Commun* 348:1472–1478
- Chu L, Hao H, Luo M, Huang Y, Chen Z, Lu T, Zhao X, Verfaillie CM, Zweier JL, Liu Z (2011) Ox-LDL modifies the behaviour of bone marrow stem cells and impairs their endothelial differentiation via inhibition of Akt phosphorylation. *J Cell Mol Med* 15:423–432
- Chung S, Dzeja PP, Faustino RS, Perez-Terzic C, Behfar A, Terzic A (2007) Mitochondrial oxidative metabolism is required for the cardiac differentiation of stem cells. *Nat Clin Pract Cardiovasc Med* 4:S60–S67
- Clapham DE (2007) Calcium signaling. *Cell* 131:1047–1058
- Consales C, Merla C, Marino C, Benassi B (2012) Electromagnetic fields, oxidative stress, and neurodegeneration. *Int J Cell Biol* 2012, 683897
- Denegre JM, Valles JM, Lin K, Jordan W, Mowry KL (1998) Cleavage planes in frog eggs are altered by strong magnetic fields. *Proc Natl Acad Sci* 95:14729–14732
- Diehn M, Cho RW, Lobo NA, Kalisky T, Dorie MJ, Kulp AN, Qian D, Lam JS, Ailles LE, Wong M (2009) Association of reactive oxygen species levels and radioresistance in cancer stem cells. *Nature* 458:780–783
- Doyle MJ, Lohr JL, Chapman CS, Koyano-Nakagawa N, Garry MG, Garry DJ (2015) Human induced pluripotent stem cell-derived cardiomyocytes as a model for heart development and congenital heart disease. *Stem Cell Rev Rep* 11:710–727
- Dzierzak E, Enver T (2008) Stem cell researchers find their niche. *Development* 135:1569–1573
- Eliasson P, Jönsson JI (2010) The hematopoietic stem cell niche: low in oxygen but a nice place to be. *J Cell Physiol* 222:17–22
- Ezashi T, Das P, Roberts RM (2005) Low O<sub>2</sub> tensions and the prevention of differentiation of hES cells. *Proc Natl Acad Sci U S A* 102:4783–4788

- Facucho-Oliveira J, John JS (2009) The relationship between pluripotency and mitochondrial DNA proliferation during early embryo development and embryonic stem cell differentiation. *Stem Cell Rev Rep* 5:140–158
- Falone S, Grossi MR, Cinque B, D'Angelo B, Tettamanti E, Cimini A, Di Ilio C, Amicarelli F (2007) Fifty hertz extremely low-frequency electromagnetic field causes changes in redox and differentiative status in neuroblastoma cells. *Int J Biochem Cell Biol* 39:2093–2106
- Feng B, Qiu L, Ye C, Chen L, Fu Y, Sun W (2016) Exposure to a 50-Hz magnetic field induced mitochondrial permeability transition through the ROS/GSK-3 $\beta$  signaling pathway. *Int J Radiat Biol* 92:148–155
- Fijalkowska I, Xu W, Comhair SA, Janocha AJ, Mavrakis LA, Krishnamachary B, Zhen L, Mao T, Richter A, Erzurum SC (2010) Hypoxia inducible-factor1 $\alpha$  regulates the metabolic shift of pulmonary hypertensive endothelial cells. *Am J Pathol* 176:1130–1138
- Forristal CE, Wright KL, Hanley NA, Oreffo RO, Houghton FD (2010) Hypoxia inducible factors regulate pluripotency and proliferation in human embryonic stem cells cultured at reduced oxygen tensions. *Reproduction* 139:85–97
- Funes JM, Quintero M, Henderson S, Martinez D, Qureshi U, Westwood C, Clements MO, Bourboulia D, Pedley RB, Moncada S (2007) Transformation of human mesenchymal stem cells increases their dependency on oxidative phosphorylation for energy production. *Proc Natl Acad Sci* 104:6223–6228
- Furse C, Christensen DA, Durney CH (2009) Basic introduction to bioelectromagnetics. CRC Press, Boca Raton
- Gaetani R, Ledda M, Barile L, Chimenti I, De Carlo F, Forte E, Ionta V, Giuliani L, D'Emilia E, Frati G (2009) Differentiation of human adult cardiac stem cells exposed to extremely low-frequency electromagnetic fields. *Cardiovasc Res* 82:411–420
- Gattazzo F, Urciuolo A, Bonaldo P (2014) Extracellular matrix: a dynamic microenvironment for stem cell niche. *Biochim Biophys Acta* 1840:2506–2519
- Gerardi G, De Ninno A, Prosdocimi M, Ferrari V, Barbaro F, Mazzariol S, Bernardini D, Talpo G (2008) Effects of electromagnetic fields of low frequency and low intensity on rat metabolism. *Biomagn Res Technol* 6:3
- Gherardini L, Ciuti G, Tognarelli S, Cinti C (2014) Searching for the perfect wave: the effect of radiofrequency electromagnetic fields on cells. *Int J Mol Sci* 15:5366–5387
- Gillo B, Ma Y-S, Marks A (1993) Calcium influx in induced differentiation of murine erythroleukemia cells. *Blood* 81:783–792
- Goldstein LS, Reyna S, Woodruff G (2015) Probing the secrets of Alzheimer's disease using human-induced pluripotent stem cell technology. *Neurotherapeutics* 12:121–125
- Grassi C, D'Ascenzo M, Torsello A, Martinotti G, Wolf F, Cittadini A, Azzena GB (2004) Effects of 50Hz electromagnetic fields on voltage-gated Ca<sup>2+</sup> channels and their role in modulation of neuroendocrine cell proliferation and death. *Cell Calcium* 35:307–315
- Graziewicz MA, Day BJ, Copeland WC (2002) The mitochondrial DNA polymerase as a target of oxidative damage. *Nucleic Acids Res* 30:2817–2824
- Guo Y, Einhorn L, Kelley M, Hirota K, Yodoi J, Reinbold R, Scholer H, Ramsey H, Hromas R (2004) Redox regulation of the embryonic stem cell transcription factor oct-4 by thioredoxin. *Stem Cells* 22:259–264
- Guo Y-L, Chakraborty S, Rajan SS, Wang R, Huang F (2010) Effects of oxidative stress on mouse embryonic stem cell proliferation, apoptosis, senescence, and self-renewal. *Stem Cells Dev* 19:1321–1331
- Halgamuge MN, Persson BR, Salford LG, Mendis P, Eberhardt J (2009) Comparison between two models for interactions between electric and magnetic fields and proteins in cell membranes. *Environ Eng Sci* 26:1473–1480
- Hamanaka RB, Chandel NS (2009) Mitochondrial reactive oxygen species regulate hypoxic signaling. *Curr Opin Cell Biol* 21:894–899

- Hamanaka RB, Chandel NS (2010) Mitochondrial reactive oxygen species regulate cellular signaling and dictate biological outcomes. *Trends Biochem Sci* 35:505–513
- Han J, Won E-J, Lee B-Y, Hwang U-K, Kim I-C, Yim JH, Leung KMY, Lee YS, Lee J-S (2014) Gamma rays induce DNA damage and oxidative stress associated with impaired growth and reproduction in the copepod *Tigriopus japonicus*. *Aquat Toxicol* 152:264–272
- Harris VK, Sadiq SA (2015) Stem cell therapy in multiple sclerosis: a future perspective. *Neurodegener Dis Manag* 5:167–170
- Havelka D, Cifra M, Kučera O, Pokorný J, Vrba J (2011) High-frequency electric field and radiation characteristics of cellular microtubule network. *J Theor Biol* 286:31–40
- Heddleston JM, Li Z, McLendon RE, Hjelmeland AB, Rich JN (2009) The hypoxic microenvironment maintains glioblastoma stem cells and promotes reprogramming towards a cancer stem cell phenotype. *Cell Cycle* 8:3274–3284
- Hochedlinger K, Plath K (2009) Epigenetic reprogramming and induced pluripotency. *Development* 136:509–523
- Holland JD, Klaus A, Garratt AN, Birchmeier W (2013) Wnt signaling in stem and cancer stem cells. *Curr Opin Cell Biol* 25:254–264
- Hosokawa K, Arai F, Yoshihara H, Nakamura Y, Gomei Y, Iwasaki H, Miyamoto K, Shima H, Ito K, Suda T (2007) Function of oxidative stress in the regulation of hematopoietic stem cell-niche interaction. *Biochem Biophys Res Commun* 363:578–583
- Houghton FD (2006) Energy metabolism of the inner cell mass and trophoblast of the mouse blastocyst. *Differentiation* 74:11–18
- Huang X, Cho S, Spangrude G (2007) Hematopoietic stem cells: generation and self-renewal. *Cell Death Differ* 14:1851–1859
- Inaba M, Yamashita YM (2012) Asymmetric stem cell division: precision for robustness. *Cell Stem Cell* 11:461–469
- James AW, Shen J, Zhang X, Asatrian G, Goyal R, Kwak JH, Jiang L, Bengs B, Culiati CT, Turner AS (2015) NELL-1 in the treatment of osteoporotic bone loss. *Nat Commun* 6
- Jelenković A, Janać B, Pešić V, Jovanović D, Vasiljević I, Prolić Z (2006) Effects of extremely low-frequency magnetic field in the brain of rats. *Brain Res Bull* 68:355–360
- Jelínek F, Pokorný J, Šaroč J, Trkal V, Hašek J, Palán B (1999) Microelectronic sensors for measurement of electromagnetic fields of living cells and experimental results. *Bioelectrochem Bioenerg* 48:261–266
- Ji A-R, Ku S-Y, Cho MS, Kim YY, Kim YJ, Oh SK, Kim SH, Moon SY, Choi YM (2010) Reactive oxygen species enhance differentiation of human embryonic stem cells into mesendodermal lineage. *Exp Mol Med* 42:175–186
- Jiang F-Y, Tang L-L, Zeng C, Liu H, Liang K-D, Mi Y, Sun C-X (2008) Effects of electric pulses on apoptosis induction and mitochondrial transmembrane potential of cancer cells. In: 7th Asian-Pacific conference on medical and biological engineering. Springer, pp 511–513
- Juntilla MM, Patil VD, Calamito M, Joshi RP, Birnbaum MJ, Koretzky GA (2010) AKT1 and AKT2 maintain hematopoietic stem cell function by regulating reactive oxygen species. *Blood* 115:4030–4038
- Kang J, Shakya A, Tantin D (2009a) Stem cells, stress, metabolism and cancer: a drama in two acts. *Trends Biochem Sci* 34:491–499
- Kang J, Gemberling M, Nakamura M, Whitby FG, Handa H, Fairbrother WG, Tantin D (2009b) A general mechanism for transcription regulation by Oct1 and Oct4 in response to genotoxic and oxidative stress. *Genes Dev* 23:208–222
- Kang KS, Hong JM, Kang JA, Rhie J-W, Jeong YH, Cho D-W (2013) Regulation of osteogenic differentiation of human adipose-derived stem cells by controlling electromagnetic field conditions. *Exp Mol Med* 45, e6
- Katsir G, Parola AH (1998) Enhanced proliferation caused by a low frequency weak magnetic field in chick embryo fibroblasts is suppressed by radical scavengers. *Biochem Biophys Res Commun* 252:753–756
- Kemp K, Redondo J, Mallam E, Scolding N, Wilkins A (2015) The use of mesenchymal stem cells for treating neurodegenerative diseases. In: *Stem cells and cancer stem cells*, vol 13. Springer, pp 3–20



- Knoblich JA (2001) Asymmetric cell division during animal development. *Nat Rev Mol Cell Biol* 2:11–20
- Knoblich JA (2008) Mechanisms of asymmetric stem Cell Division. *Cell* 132:583–597
- Kobayashi-Miura M, Nakamura H, Yodoi J, Shiota K (2002) Thioredoxin, an anti-oxidant protein, protects mouse embryos from oxidative stress-induced developmental anomalies. *Free Radic Res* 36:949–956
- Kondoh H, Leonart ME, Nakashima Y, Yokode M, Tanaka M, Bernard D, Gil J, Beach D (2007) A high glycolytic flux supports the proliferative potential of murine embryonic stem cells. *Antioxid Redox Signal* 9:293–299
- Kristián T, Gertsch J, Bates TE, Siesjö BK (2000) Characteristics of the calcium-triggered mitochondrial permeability transition in nonsynaptic brain mitochondria. *J Neurochem* 74:1999–2009
- Larsimont JC, Blanpain C (2015) Single stem cell gene therapy for genetic skin disease. *EMBO Mol Med* 7:366–367
- Lee B-C, Johng H-M, Lim J-K, Jeong JH, Baik KY, Nam TJ, Lee JH, Kim J, Sohn UD, Yoon G (2004) Effects of extremely low frequency magnetic field on the antioxidant defense system in mouse brain: a chemiluminescence study. *J Photochem Photobiol B* 73:43–48
- Lee MK, Hande MP, Sabapathy K (2005) Ectopic mTERT expression in mouse embryonic stem cells does not affect differentiation but confers resistance to differentiation-and stress-induced p53-dependent apoptosis. *J Cell Sci* 118:819–829
- Leszczynski D, Joenväärä S, Reivinen J, Kuokka R (2002) Non-thermal activation of the hsp27/p38MAPK stress pathway by mobile phone radiation in human endothelial cells: molecular mechanism for cancer-and blood-brain barrier-related effects. *Differentiation* 70:120–129
- Levin M (2003) Bioelectromagnetics in morphogenesis. *Bioelectromagnetics* 24:295–315
- Li L, Jiang J (2011) Stem cell niches and endogenous electric fields in tissue repair. *Front Med* 5:40–44
- Li L, Neaves WB (2006) Normal stem cells and cancer stem cells: the niche matters. *Cancer Res* 66:4553–4557
- Li S, Crothers J, Haqq CM, Blackburn EH (2005) Cellular and gene expression responses involved in the rapid growth inhibition of human cancer cells by RNA interference-mediated depletion of telomerase RNA. *J Biol Chem* 280:23709–23717
- Li H-J, Guo L-M, Yang L-L, Zhou Y-C, Zhang Y-J, Guo J, Xie X-J, Guo G-Z (2013) Electromagnetic-pulse-induced activation of p38 MAPK pathway and disruption of blood-retinal barrier. *Toxicol Lett* 220:35–43
- Lim K-T, Kim J-H, Seonwoo H, Son H-M, Baik S-J, Park J-Y, Jeon S-H, Kim E-S, Choung Y-H, Cho C-S (2009) In vitro effects of electromagnetic field stimulation on cells in tissue engineering. *Tissue Eng Regen Med* 6:675–684
- Lin CC, Lin RW, Chang CW, Wang GJ, Lai KA (2015) Single-pulsed electromagnetic field therapy increases osteogenic differentiation through Wnt signaling pathway and sclerostin downregulation. *Bioelectromagnetics* 36:494–505
- Liu C, Duan W, Xu S, Chen C, He M, Zhang L, Yu Z, Zhou Z (2013) Exposure to 1800MHz radiofrequency electromagnetic radiation induces oxidative DNA base damage in a mouse spermatocyte-derived cell line. *Toxicol Lett* 218:2–9
- Lonergan T, Brenner C, Bavister B (2006) Differentiation-related changes in mitochondrial properties as indicators of stem cell competence. *J Cell Physiol* 208:149–153
- Lonergan T, Bavister B, Brenner C (2007) Mitochondria in stem cells. *Mitochondrion* 7:289–296
- Loureiro R, Mesquita KA, Oliveira PJ, Vega-Naredo I (2013) Mitochondria in cancer stem cells: a target for therapy. *Recent Pat Endocr Metab Immune Drug Dis* 7:102–114
- Lu T, Parthasarathy S, Hao H, Luo M, Ahmed S, Zhu J, Luo S, Kuppusamy P, Sen CK, Verfaillie CM (2010) Reactive oxygen species mediate oxidized low-density lipoprotein-induced inhibition of oct-4 expression and endothelial differentiation of bone marrow stem cells. *Antioxid Redox Signal* 13:1845–1856

- Ma Q, Deng P, Zhu G, Liu C, Zhang L, Zhou Z, Luo X, Li M, Zhong M, Yu Z (2014) Extremely low-frequency electromagnetic fields affect transcript levels of neuronal differentiation-related genes in embryonic neural stem cells. *PLoS One* 9, e90041
- Maioli M, Rinaldi S, Santaniello S, Castagna A, Pigliaru G, Gualini S, Cavallini C, Fontani V, Ventura C (2013) Radio electric conveyed fields directly reprogram human dermal skin fibroblasts toward cardiac, neuronal, and skeletal muscle-like lineages. *Cell Transplant* 22:1227–1235
- Malmivuo J, Plonsey R (1995) *Bioelectromagnetism: principles and applications of bioelectric and biomagnetic fields*. Oxford University Press
- Masri FA, Comhair SA, Dostanic-Larson I, Kaneko FT, Dweik RA, Arroliga AC, Erzurum SC (2008) Deficiency of lung antioxidants in idiopathic pulmonary arterial hypertension. *Clin Transl Sci* 1:99–106
- Mathieu J, Zhang Z, Zhou W, Wang AJ, Heddleston JM, Pinna CM, Hubaud A, Stadler B, Choi M, Bar M (2011) HIF induces human embryonic stem cell markers in cancer cells. *Cancer Res* 71:4640–4652
- Matthews RE (2007) Harold burr's biofields measuring the electromagnetics of life. *Subtle Energies Energy Med J Arch* 18
- Mayer-Wagner S, Passberger A, Sievers B, Aigner J, Summer B, Schiergens TS, Jansson V, Müller PE (2011) Effects of low frequency electromagnetic fields on the chondrogenic differentiation of human mesenchymal stem cells. *Bioelectromagnetics* 32:283–290
- Megha K, Deshmukh PS, Banerjee BD, Tripathi AK, Ahmed R, Abegaonkar MP (2015) Low intensity microwave radiation induced oxidative stress, inflammatory response and DNA damage in rat brain. *Neurotoxicology* 51:158–165
- Mitsui K, Tokuzawa Y, Itoh H, Segawa K, Murakami M, Takahashi K, Maruyama M, Maeda M, Yamanaka S (2003) The homeoprotein Nanog is required for maintenance of pluripotency in mouse epiblast and ES cells. *Cell* 113:631–642
- Moon J-H, Heo JS, Kim JS, Jun EK, Lee JH, Kim A, Kim J, Whang KY, Kang Y-K, Yeo S (2011) Reprogramming fibroblasts into induced pluripotent stem cells with Bmi1. *Cell Res* 21:1305–1315
- Moon SH, Jenkins CM, Kiebish MA, Sims HF, Mancuso DJ, Gross RW (2012) Genetic ablation of calcium-independent phospholipase A2 $\gamma$  (iPLA2 $\gamma$ ) attenuates calcium-induced opening of the mitochondrial permeability transition pore and resultant cytochrome c release. *J Biol Chem* 287:29837–29850
- Morabito C, Rovetta F, Bizzarri M, Mazzoleni G, Fanò G, Mariggiò MA (2010) Modulation of redox status and calcium handling by extremely low frequency electromagnetic fields in C2C12 muscle cells: a real-time, single-cell approach. *Free Radic Biol Med* 48:579–589
- Morrison SJ, Kimble J (2006) Asymmetric and symmetric stem-cell divisions in development and cancer. *Nature* 441:1068–1074
- Mycielska ME, Djamgoz MB (2004) Cellular mechanisms of direct-current electric field effects: galvanotaxis and metastatic disease. *J Cell Sci* 117:1631–1639
- Nakagawa M, Koyanagi M, Tanabe K, Takahashi K, Ichisaka T, Aoi T, Okita K, Mochiduki Y, Takizawa N, Yamanaka S (2007) Generation of induced pluripotent stem cells without Myc from mouse and human fibroblasts. *Nat Biotechnol* 26:101–106
- Nakamura M, Bhatnagar A, Sadoshima J (2012) Overview of pyridine nucleotides review series. *Circ Res* 111:604–610
- Napotnik TB, Wu YH, Gundersen MA, Miklavčič D, Vernier PT (2012) Nanosecond electric pulses cause mitochondrial membrane permeabilization in Jurkat cells. *Bioelectromagnetics* 33:257–264
- Neumüller RA, Knoblich JA (2009) Dividing cellular asymmetry: asymmetric cell division and its implications for stem cells and cancer. *Genes Dev* 23:2675–2699
- Nichols J (2001) Introducing embryonic stem cells. *Curr Biol* 11:R503–R505

- Nichols J, Zevnik B, Anastassiadis K, Niwa H, Klewe-Nebenius D, Chambers I, Schöler H, Smith A (1998) Formation of pluripotent stem cells in the mammalian embryo depends on the POU transcription factor Oct4. *Cell* 95:379–391
- Nicotera P, Thor H, Orrenius S (1989) Cytosolic-free Ca<sup>2+</sup> and cell killing in hepatoma 1c1c7 cells exposed to chemical anoxia. *FASEB J* 3:59–64
- Nordberg J, Arner ES (2001) Reactive oxygen species, antioxidants, and the mammalian thioredoxin system. *Free Radic Biol Med* 31:1287–1312
- Nusse R (2008) Wnt signaling and stem cell control. *Cell Res* 18:523–527
- Okita K, Ichisaka T, Yamanaka S (2007) Generation of germline-competent induced pluripotent stem cells. *Nature* 448:313–317
- Oktem F, Ozguner F, Mollaoglu H, Koyu A, Uz E (2005) Oxidative damage in the kidney induced by 900-MHz-emitted mobile phone: protection by melatonin. *Arch Med Res* 36:350–355
- Onuma EK, Hui S-W (1988) Electric field-directed cell shape changes, displacement, and cytoskeletal reorganization are calcium dependent. *J Cell Biol* 106:2067–2075
- Orford KW, Scadden DT (2008) Deconstructing stem cell self-renewal: genetic insights into cell-cycle regulation. *Nat Rev Genet* 9:115–128
- Ott M, Gogvadze V, Orrenius S, Zhivotovsky B (2007) Mitochondria, oxidative stress and cell death. *Apoptosis* 12:913–922
- Panagopoulos DJ (2014) Electromagnetic interaction between environmental fields and living systems determines health and well-being. *Int J Condens Matter Adv Mater Superconductivity Res* 13:99
- Panagopoulos DJ, Karabarounis A, Margaritis LH (2002) Mechanism for action of electromagnetic fields on cells. *Biochem Biophys Res Commun* 298:95–102
- Papayannopoulou T, Scadden DT (2008) Stem-cell ecology and stem cells in motion. *Blood* 111:3923–3930
- Park J-E, Seo Y-K, Yoon H-H, Kim C-W, Park J-K, Jeon S (2013) Electromagnetic fields induce neural differentiation of human bone marrow derived mesenchymal stem cells via ROS mediated EGFR activation. *Neurochem Int* 62:418–424
- Parker GC, Acsadi G, Brenner CA (2009) Mitochondria: determinants of stem cell fate? *Stem Cells Dev* 18:803–806
- Pauklin S, Vallier L (2013) The cell-cycle state of stem cells determines cell fate propensity. *Cell* 155:135–147
- Pesce M, Schöler HR (2000) Oct-4: Control of totipotency and germline determination. *Mol Reprod Dev* 55:452–457
- Pesce M, Schöler HR (2001) Oct-4: gatekeeper in the beginnings of mammalian development. *Stem Cells* 19:271–278
- Pienta KJ, Hoover CN (1994) Coupling of cell structure to cell metabolism and function. *J Cell Biochem* 55:16–21
- Pokorný J (2004) Excitation of vibrations in microtubules in living cells. *Bioelectrochemistry* 63:321–326
- Pokorný J (2012) Physical aspects of biological activity and cancer. *AIP Adv* 2:011207
- Pokorný J, Jelínek F, Trkal V, Lamprecht I, Hölzel R (1997) Vibrations in microtubules. *J Biol Phys* 23:171–179
- Pokorný J, Hašek J, Jelínek F, Šaroch J, Palán B (2001) Electromagnetic activity of yeast cells in the M phase. *Electro- Magnetobiol* 20:371–396
- Rafalski VA, Brunet A (2011) Energy metabolism in adult neural stem cell fate. *Prog Neurobiol* 93:182–203
- Rahnama M, Tuszynski JA, Bokkon I, Cifra M, Sardar P, Salari V (2011) Emission of mitochondrial biophotons and their effect on electrical activity of membrane via microtubules. *J Integr Neurosci* 10:65–88
- Ramalho R, Soares H, Melo L (2007) Microtubule behavior under strong electromagnetic fields. *Mater Sci Eng C* 27:1207–1210
- Ramalho-Santos M (2004) Stem cells as probabilistic self-producing entities. *Bioessays* 26:1013–1016

- Rattis FM, Voermans C, Reya T (2004) Wnt signaling in the stem cell niche. *Curr Opin Hematol* 11:88–94
- Rehman J (2010) Empowering self-renewal and differentiation: the role of mitochondria in stem cells. *J Mol Med* 88:981–986
- Reya T, Morrison SJ, Clarke MF, Weissman IL (2001) Stem cells, cancer, and cancer stem cells. *Nature* 414:105–111
- Reya T, Duncan AW, Ailles L, Domen J, Scherer DC, Willert K, Hintz L, Nusse R, Weissman IL (2003) A role for Wnt signalling in self-renewal of haematopoietic stem cells. *Nature* 423:409–414
- Rodda DJ, Chew J-L, Lim L-H, Loh Y-H, Wang B, Ng H-H, Robson P (2005) Transcriptional regulation of *nanog* by OCT4 and SOX2. *J Biol Chem* 280:24731–24737
- Rollwitz J, Lupke M, Simkó M (2004) Fifty-hertz magnetic fields induce free radical formation in mouse bone marrow-derived promonocytes and macrophages. *Biochim Biophys Acta* 1674:231–238
- Roman A, Tombarkiewicz B (2009) Prolonged weakening of the geomagnetic field (GMF) affects the immune system of rats. *Bioelectromagnetics* 30:21–28
- Rump A, Scholz T, Thiel C, Hartmann FK, Uta P, Hinrichs MH, Taft MH, Tsiavaliaris G (2011) Myosin-1C associates with microtubules and stabilizes the mitotic spindle during cell division. *J Cell Sci* 124:2521–2528
- Ryan AK, Rosenfeld MG (1997) POU domain family values: flexibility, partnerships, and developmental codes. *Genes Dev* 11:1207–1225
- Samudio I, Fiegl M, McQueen T, Clise-Dwyer K, Andreeff M (2008) The Warburg effect in leukemia-stroma cocultures is mediated by mitochondrial uncoupling associated with uncoupling protein 2 activation. *Cancer Res* 68:5198–5205
- Samudio I, Fiegl M, Andreeff M (2009) Mitochondrial uncoupling and the Warburg effect: molecular basis for the reprogramming of cancer cell metabolism. *Cancer Res* 69:2163–2166
- Saretzki G (2005) Telomerase and oxidative stress in embryonic stem cells. Embryonic stem cells: the hormonal regulation of pluripotency and embryogenesis. Lippincott & Williams, Philadelphia
- Saretzki G, Walter T, Atkinson S, Passos JF, Bareth B, Keith WN, Stewart R, Hoare S, Stojkovic M, Armstrong L (2008) Downregulation of multiple stress defense mechanisms during differentiation of human embryonic stem cells. *Stem Cells* 26:455–464
- Saretzki G (2009) Telomerase, mitochondria and oxidative stress. *Exp Gerontol* 44:485–492
- Sauer H, Wartenberg M (2005) Reactive oxygen species as signaling molecules in cardiovascular differentiation of embryonic stem cells and tumor-induced angiogenesis. *Antioxid Redox Signal* 7:1423–1434
- Sauer H, Rahimi G, Hescheler J, Wartenberg M (1999) Effects of electrical fields on cardiomyocyte differentiation of embryonic stem cells. *J Cell Biochem* 75:710–723
- Scarpa A, Graziotti P (1973) Mechanisms for intracellular calcium regulation in heart I. Stopped-flow measurements of  $Ca^{++}$  uptake by cardiac mitochondria. *J Gen Physiol* 62:756–772
- Schmelter M, Ateghang B, Helmig S, Wartenberg M, Sauer H (2006) Embryonic stem cells utilize reactive oxygen species as transducers of mechanical strain-induced cardiovascular differentiation. *FASEB J* 20:1182–1184
- Seger R, Krebs EG (1995) The MAPK signaling cascade. *FASEB J* 9:726–735
- Serena E, Figallo E, Tandon N, Cannizzaro C, Gerech S, Elvassore N, Vunjak-Novakovic G (2009) Electrical stimulation of human embryonic stem cells: cardiac differentiation and the generation of reactive oxygen species. *Exp Cell Res* 315:3611–3619
- Shakya A, Cooksey R, Cox JE, Wang V, McClain DA, Tantin D (2009) Oct1 loss of function induces a coordinate metabolic shift that opposes tumorigenicity. *Nat Cell Biol* 11:320–327
- Siller KH, Doe CQ (2009) Spindle orientation during asymmetric cell division. *Nat Cell Biol* 11:365–374
- Simeonova M, Wachner D, Gimsa J (2002) Cellular absorption of electric field energy: influence of molecular properties of the cytoplasm. *Bioelectrochemistry* 56:215–218

- Simkó M (2004) Induction of cell activation processes by low frequency electromagnetic fields. *Scientific World Journal* 4:4–22
- Simko M (2007) Cell type specific redox status is responsible for diverse electromagnetic field effects. *Curr Med Chem* 14:1141–1152
- Singh AM, Dalton S (2014) Cell cycle regulation of pluripotent stem cells. *Stem cells: from basic research to therapy: basic stem cell biology, tissue formation during development, and model organisms* 1:3
- Soda A, Ikehara T, Kinouchi Y, Yoshizaki K (2008) Effect of exposure to an extremely low frequency-electromagnetic field on the cellular collagen with respect to signaling pathways in osteoblast-like cells. *J Med Invest* 55:267–278
- Spradling A, Drummond-Barbosa D, Kai T (2001) Stem cells find their niche. *Nature* 414:98–104
- Šrobár F (2012) Fröhlich systems in cellular physiology. *Prague Med Rep* 113:95–104
- Šrobár F (2013) Impact of mitochondrial electric field on modal occupancy in the Fröhlich model of cellular electromagnetism. *Electromagn Biol Med* 32:401–408
- St. John JC, Ramalho-Santos J, Gray HL, Petrosko P, Rawe VY, Navara CS, Simerly CR, Schatten GP (2005) The expression of mitochondrial DNA transcription factors during early cardiomyocyte in vitro differentiation from human embryonic stem cells. *Cloning Stem Cells* 7:141–153
- Stracke R, Böhm K, Wollweber L, Tuszyński J, Unger E (2002) Analysis of the migration behaviour of single microtubules in electric fields. *Biochem Biophys Res Commun* 293:602–609
- Suda T, Arai F, Hirao A (2005) Hematopoietic stem cells and their niche. *Trends Immunol* 26:426–433
- Suda T, Takubo K, Semenza GL (2011) Metabolic regulation of hematopoietic stem cells in the hypoxic niche. *Cell Stem Cell* 9:298–310
- Taylor GW, Harvey EN (1931) The theory of mitogenetic radiation. *Biol Bull* 61:280–293
- Thar R, Kühl M (2004) Propagation of electromagnetic radiation in mitochondria? *J Theor Biol* 230:261–270
- Torres-Duran PV, Ferreira-Hermosillo A, Juarez-Oropeza MA, Elias-Viñas D, Verdugo-Diaz L (2007) Effects of whole body exposure to extremely low frequency electromagnetic fields (ELF-EMF) on serum and liver lipid levels, in the rat. *Lipids Health Dis* 6:31
- Trushko A, Schäffer E, Howard J (2013) The growth speed of microtubules with XMAP215-coated beads coupled to their ends is increased by tensile force. *Proc Natl Acad Sci* 110:14670–14675
- Tsai M-T, Li W-J, Tuan RS, Chang WH (2009) Modulation of osteogenesis in human mesenchymal stem cells by specific pulsed electromagnetic field stimulation. *J Orthop Res* 27:1169
- Valles JM (2002) Model of magnetic field-induced mitotic apparatus reorientation in frog eggs. *Biophys J* 82:1260–1265
- Vaseva AV, Marchenko ND, Ji K, Tsirka SE, Holzmann S, Moll UM (2012) p53 opens the mitochondrial permeability transition pore to trigger necrosis. *Cell* 149:1536–1548
- Vladimirov YA, Proskurnina E (2009) Free radicals and cell chemiluminescence. *Biochemistry (Moscow)* 74:1545–1566
- Walczak CE, Cai S, Khodjakov A (2010) Mechanisms of chromosome behaviour during mitosis. *Nat Rev Mol Cell Biol* 11:91–102
- Walleczek J (1992) Electromagnetic field effects on cells of the immune system: the role of calcium signaling. *FASEB J* 6:3177–3185
- Wang B (2010) Phosphoproteome studies of human mitotic spindle proteins
- Wang C, Zhou H, Peng R, Wang L, Su Z, Chen P, Wang S, Wang S, Liu Y, Cong J (2013) Electromagnetic pulse reduces free radical generation in rat liver mitochondria in vitro. *Free Radic Res* 47:276–282
- Waris G, Ahsan H (2006) Reactive oxygen species: role in the development of cancer and various chronic conditions. *J Carcinog* 5:14
- Watt FM, Hogan B (2000) Out of Eden: stem cells and their niches. *Science* 287:1427–1430

- Watt FM, Huck WT (2013) Role of the extracellular matrix in regulating stem cell fate. *Nat Rev Mol Cell Biol* 14:467–473
- Waypa GB, Marks JD, Mack MM, Boriboun C, Mungai PT, Schumacker PT (2002) Mitochondrial reactive oxygen species trigger calcium increases during hypoxia in pulmonary arterial myocytes. *Circ Res* 91:719–726
- Wesbuer S, Lanvers-Kaminsky C, Duran-Seuberth I, Bolling T, Schafer K-L, Braun Y, Willich N, Greve B (2010) Association of telomerase activity with radio- and chemosensitivity of neuroblastomas. *Radiat Oncol* 5:66
- White J, Dalton S (2005) Cell cycle control of embryonic stem cells. *Stem Cell Rev* 1:131–138
- Wolff EF, Mutlu L, Massasa EE, Elsworth JD, Eugene Redmond D, Taylor HS (2015) Endometrial stem cell transplantation in MPTP-exposed primates: an alternative cell source for treatment of Parkinson's disease. *J Cell Mol Med* 19:249–256
- Yan J, Dong L, Zhang B, Qi N (2010) Effects of extremely low-frequency magnetic field on growth and differentiation of human mesenchymal stem cells. *Electromagn Biol Med* 29:165–176
- Yang C, Przyborski S, Cooke MJ, Zhang X, Stewart R, Anyfantis G, Atkinson SP, Saretzki G, Armstrong L, Lako M (2008) A key role for telomerase reverse transcriptase unit in modulating human embryonic stem cell proliferation, cell cycle dynamics, and in vitro differentiation. *Stem Cells* 26:850–863
- Yang Y, Tao C, Zhao D, Li F, Zhao W, Wu H (2010) EMF acts on rat bone marrow mesenchymal stem cells to promote differentiation to osteoblasts and to inhibit differentiation to adipocytes. *Bioelectromagnetics* 31:277–285
- Ye XQ, Li Q, Wang GH, Sun FF, Huang GJ, Bian XW, Yu SC, Qian GS (2011) Mitochondrial and energy metabolism-related properties as novel indicators of lung cancer stem cells. *Int J Cancer* 129:820–831
- Young RA (2011) Control of the embryonic stem cell state. *Cell* 144:940–954
- Yu J, Vodyanik MA, Smuga-Otto K, Antosiewicz-Bourget J, Frane JL, Tian S, Nie J, Jonsdottir GA, Ruotti V, Stewart R (2007) Induced pluripotent stem cell lines derived from human somatic cells. *Science* 318:1917–1920
- Zang L-Y, Cosma G, Gardner H, Vallyathan V (1998) Scavenging of reactive oxygen species by melatonin. *Biochim Biophys Acta* 1425:469–477
- Zeni O, Di Pietro R, d'Ambrosio G, Massa R, Capri M, Naarala J, Juutilainen J, Scarfi MR (2007) Formation of reactive oxygen species in L929 cells after exposure to 900 MHz RF radiation with and without co-exposure to 3-chloro-4-(dichloromethyl)-5-hydroxy-2 (5H)-furanone. *Radiat Res* 167:306–311
- Zhai M, Jing D, Tong S, Wu Y, Wang P, Zeng Z, Shen G, Wang X, Xu Q, Luo E (2016) Pulsed electromagnetic fields promote in vitro osteoblastogenesis through a Wnt/ $\beta$ -catenin signaling-associated mechanism. *Bioelectromagnetics* 37:152–162
- Zhang W, Liu HT (2002) MAPK signal pathways in the regulation of cell proliferation in mammalian cells. *Cell Res* 12:9–18
- Zhang H, Wang ZZ (2008) Mechanisms that mediate stem cell self-renewal and differentiation. *J Cell Biochem* 103:709–718
- Zhang J, Khvorostov I, Hong JS, Oktay Y, Vergnes L, Nuebel E, Wahjudi PN, Setoguchi K, Wang G, Do A (2011) UCP2 regulates energy metabolism and differentiation potential of human pluripotent stem cells. *EMBO J* 30:4860–4873
- Zhao Y, Zhan Q (2012) Electric fields generated by synchronized oscillations of microtubules, centrosomes and chromosomes regulate the dynamics of mitosis and meiosis. *Theor Biol Med Model* 9:26
- Zhao M, Forrester JV, McCaig CD (1999) A small, physiological electric field orients cell division. *Proc Natl Acad Sci* 96:4942–4946
- Zhou J, He H, Yang L, Chen S, Guo H, Xia L, Liu H, Qin Y, Liu C, Wei X (2012a) Effects of pulsed electromagnetic fields on bone mass and Wnt/ $\beta$ -catenin signaling pathway in ovariectomized rats. *Arch Med Res* 43:274–282

- Zhou W, Choi M, Margineantu D, Margaretha L, Hesson J, Cavanaugh C, Blau CA, Horwitz MS, Hockenbery D, Ware C (2012b) HIF1 $\alpha$  induced switch from bivalent to exclusively glycolytic metabolism during ESC-to-EpiSC/hESC transition. *EMBO J* 31:2103–2116
- Zmysłony M, Politanski P, Rajkowska E, Szymczak W, Jajte J (2004) Acute exposure to 930 MHz CW electromagnetic radiation in vitro affects reactive oxygen species level in rat lymphocytes treated by iron ions. *Bioelectromagnetics* 25:324–328
- Zwirska-Korczala K, Jochem J, Adamczyk-Sowa M, Sowa P, Polaniak R, Birkner E, Latocha M, Pile K, Suchanek R (2005) Effect of extremely low frequency of electromagnetic fields on cell proliferation, antioxidative enzyme activities and lipid peroxidation in 3T3-L1 preadipocytes—an in vitro study. *J Physiol Pharmacol* 56:101

# The Zebrafish Heart as a Model of Mammalian Cardiac Function

**Christine E. Genge, Eric Lin, Ling Lee, XiaoYe Sheng, Kaveh Rayani, Marvin Gunawan, Charles M. Stevens, Alison Yueh Li, Sanam Shafaat Talab, Thomas W. Claydon, Leif Hove-Madsen, and Glen F. Tibbits**

**Abstract** Zebrafish (*Danio rerio*) are widely used as vertebrate model in developmental genetics and functional genomics as well as in cardiac structure-function studies. The zebrafish heart has been increasingly used as a model of human cardiac function, in part, due to the similarities in heart rate and action potential duration and morphology with respect to humans. The teleostian zebrafish is in many ways a compelling model of human cardiac function due to the clarity afforded by its ease of genetic manipulation, the wealth of developmental biological information, and inherent suitability to a variety of experimental techniques. However, in addition to the numerous advantages of the zebrafish system are also caveats related to gene duplication (resulting in paralogs not present in human or other mammals) and fundamental differences in how zebrafish hearts function. In this review, we discuss the use of zebrafish as a cardiac function model through the use of techniques such as echocardiography, optical mapping, electrocardiography, molecular

---

CE Genge, E Lin and L. Lee contributed equally to the paper

C.E. Genge, E. Lin, K. Rayani, M. Gunawan, A.Y. Li, S.S. Talab, and T.W. Claydon  
Molecular Cardiac Physiology Group, Biomedical Physiology and Kinesiology, Simon Fraser University, Burnaby, BC, Canada, V5A 1S6

L. Lee and X. Sheng  
BC Children's Hospital Research Institute, Vancouver, BC, Canada, V5Z 4H4

C.M. Stevens and G.F. Tibbits (✉)  
Molecular Cardiac Physiology Group, Biomedical Physiology and Kinesiology, Simon Fraser University, Burnaby, BC, Canada, V5A 1S6

BC Children's Hospital Research Institute, Vancouver, BC, Canada, V5Z 4H4  
e-mail: [tibbits@sfu.ca](mailto:tibbits@sfu.ca)

L. Hove-Madsen  
Molecular Cardiac Physiology Group, Biomedical Physiology and Kinesiology, Simon Fraser University, Burnaby, BC, Canada, V5A 1S6

Cardiovascular Research Centre CSIC-ICCC, Hospital de Sant Pau, Barcelona, Spain



investigations of excitation-contraction coupling, and their physiological implications relative to that of the human heart. While some of these techniques (e.g., echocardiography) are particularly challenging in the zebrafish because of diminutive size of the heart (~1.5 mm in diameter) critical information can be derived from these approaches and are discussed in detail in this article.

**Keywords** Cardiac electrophysiology • Echocardiography • Electrophysiology • Excitation-contraction coupling • Optical mapping • Phylogeny

## Contents

1	Introduction to the Zebrafish as a Model .....	100
2	In Vivo Function of the Zebrafish Heart .....	104
3	Whole Heart Measurements .....	108
4	Isolated Cardiomyocytes .....	115
	4.1 Electrophysiology .....	115
	4.2 Excitation-Contraction (E-C) Coupling .....	119
	4.3 Contraction .....	121
5	Molecular Basis of Cardiac Function .....	125
6	Conclusions/Summary .....	127
	References .....	127

## 1 Introduction to the Zebrafish as a Model

The teleostian zebrafish (*Danio rerio*) is a widely used non-mammalian vertebrate model in developmental genetics and functional genomics as well as in cardiac structure-function studies (Bakkers 2011; Verkerk and Remme 2012; Asnani and Peterson 2014). Zebrafish hearts are increasingly used as a model of mammalian cardiac function, in part, due to the similarities in heart rate and action potential duration and morphology with respect to human hearts (Arnaout et al. 2007, p. 126; Nemtsas et al. 2010). The zebrafish is a compelling model of mammalian cardiac function due to the clarity afforded by its ease of genetic manipulation, the wealth of developmental biological information, and inherent suitability to a variety of experimental techniques. However, in addition to the numerous advantages of the zebrafish system are also caveats and fundamental differences in how zebrafish hearts function. In this review, we discuss the use of zebrafish in techniques such as echocardiography, optical mapping, electrocardiography, molecular investigations of excitation-contraction coupling, and their physiological implications to the human heart.

Historically, the zebrafish has been an important developmental model in part due to its transparency in its larval stages that allows not only for discerning developmental checkpoints but also for direct observation of cardiac function (Granato et al. 1996; Kane et al. 1996). More recently the role of zebrafish as a model organism has been expanded to include the adult zebrafish due to the

relative ease of genetic manipulation and a genome that bears similarity to humans (Bakkers 2011). Furthermore, zebrafish produce large numbers of offspring with short generation times and their upkeep is cost effective. This tropical fish is small, robust and survives well at temperatures close to room temperature (24–28°C) (Spence et al. 2008; Sidhu et al. 2014). The zebrafish genome is fully sequenced, publicly available, and was the third high-quality genome sequenced after those of mouse and human (Howe et al. 2013). Human Genome Wide Association Studies (GWAS) are limited to statistical association between a particular genetic variant and a given disease. Genetic variations associated with human disease often have a relatively minor phenotype, necessitating large amounts of sequencing data or testing in an alternative model system to elucidate the mechanism. Zebrafish as a vertebrate are closer genetically to humans than invertebrate models such as *Drosophila* or *C. elegans*. Hence they can be used as an animal model for mutations that have a strong phenotypic effect, and providing insight into the disease phenotype in humans.

The genetic similarity between humans and zebrafish enables the use of targeted mutagenesis techniques to systematically model human disease genes (Arnaout et al. 2007). Morpholino oligonucleotides (MOs) were the original standard technique for the generation of anti-sense knockdown mutations in zebrafish due to their time and cost effectiveness (Nasevicius and Ekker 2000; Bill et al. 2009); however, MOs were also susceptible to off-target inhibition (Law and Sargent 2014; Kok et al. 2015). Recently, MOs have been superseded for the most part by the application of clustered regularly interspaced palindromic repeats (CRISPRs) for targeted genetic modifications (Hwang et al. 2013). CRISPRs recently have been established as a powerful reverse genetic screening strategy in the zebrafish model (Shah et al. 2015) and are commonly used for both knock-outs and knock-ins. Through these gene screening and modification strategies, zebrafish can efficiently be used for the verification of candidate disease genes and functional characterization in human disease models. Further, high throughput sequencing technologies have also been used in zebrafish, including RNAseq for characterization of the transcriptome (Collins et al. 2012). Transcriptomic analysis provides the link between genotype and phenotype in zebrafish to better understand the underlying mechanisms of physiological responses (Qian et al. 2014). The combination of genomic, transcriptomic, and proteomic information available in the zebrafish provides a well-characterized platform for the exploration of many biological processes. An extensive freely available online database, ZEBRAFISHIN, integrates genetic, genomic, and developmental data for zebrafish as a model organism (Howe et al. 2013). This is closely linked to ZIRC, an NIH research facility that provides access to zebrafish lines, probes, and health services. These easily accessible services contribute to the appeal of the model.

There are important similarities between zebrafish and human cardiac physiology, including action potential morphology and basic contractile dynamics, making the zebrafish a robust model for cardiac function in experiments that focus on channelopathies and cardiomyopathies. The similarities in action potential (AP) morphology (Arnaout et al. 2007; Brette et al. 2008) contrast with other

model systems such as mice that possess fundamental differences from human hearts in terms of heart rates and repolarization characteristics. The similarities between mammals and zebrafish have made the zebrafish an ideal model, in some respects, for the study of channelopathy-causing mutations and the functional effects of electrophysiological abnormalities (Langheinrich et al. 2003; Langenbacher et al. 2005; Arnaout et al. 2007; Brette et al. 2008). Basic excitation-contraction (E-C) coupling is also conserved between teleosts and mammals with respect to fundamental features such as  $\text{Ca}^{2+}$  sparks and the ability of  $\text{Ca}^{2+}$  waves to trigger after-depolarizations (Llach et al. 2011; Bovo et al. 2013). This similarity is dictated by the conservation of key domains in several sarcomeric proteins (Fu et al. 2009). The use of transgenic zebrafish as models for cardiac function permits the manipulation of molecular components of the contractile apparatus. Transgenic studies allow the direct exploration of the genetic factors and molecular modifications that underlie human disease states. The application of these techniques makes the zebrafish particularly attractive for the study of human cardiac muscular diseases such as dilated or hypertrophic cardiomyopathies (Dahme et al. 2009).

Despite the many similarities, the zebrafish is a phylogenetically distant species from human. Fish are ectothermic with a morphologically distinct heart composed of two main contractile chambers working in series rather than the mammalian four-chambered heart as seen in Fig. 1. The two-chamber physiology as well as a lack of pulmonary circulation makes it difficult to completely integrate cardiovascular development and function. The end diastolic volume in the fish ventricle is greatly determined by atrial contraction rather than central venous pressure seen in mammals (Cotter et al. 2008). Fish typically show an early to late ventricular filling

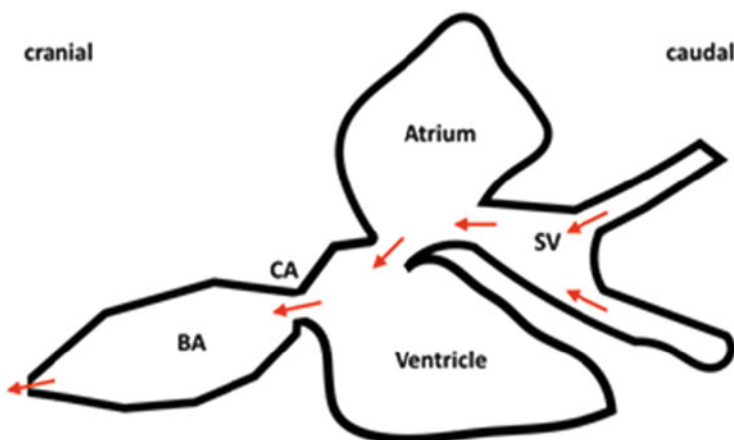


**Fig. 1** Schematic of the chambers of a typical fish heart. SV is the sinus venosus; BA is the bulbus arteriosus; CA is the conus arteriosus. The heart outflow tract (OFT) of fish is formed by two portions: a proximal conus arteriosus and a distal bulbus arteriosus. Although the form and function of the CA in teleosts such as the zebrafish remain somewhat controversial

ratio around 0.2, much lower than the typical healthy human and indicative of differential hemodynamics (Ho et al. 2002). For this reason, direct comparison of some parameters of whole heart function in zebrafish cannot be made with that of humans.

While the basics of cardiac excitation-contraction (E-C) coupling are conserved across vertebrates, differences between teleost and mammalian  $\text{Ca}^{2+}$  sources, myofilament  $\text{Ca}^{2+}$  sensitivities and/or spatial arrangement of the contractile element are essential for function in the environmental conditions in which teleosts exist. Ventricular myocytes from zebrafish more closely resemble myocytes from neonatal mammals rather than adults in terms of structure and function (Iorga et al. 2011). They are around 100  $\mu\text{m}$  in length, thin (around 5  $\mu\text{m}$ ) (Brette et al. 2008) with decreased diffusion distance to the center of the cell and generally lacking T-tubules (trout (Farrell and Jones 1992; Vornanen 1998); neonatal rabbit (Huang et al. 2005)). Critical processes such as cardiac E-C coupling must be adaptable to allow for the necessary cardiac scope due to the broad environmental conditions to which ectothermic teleosts are exposed. The evolution of variability in cardiac contractility is an important consideration in ectotherms. The underlying evolutionarily mechanism for producing these contractile changes involves differential expression of paralogs, particularly, key proteins guiding the  $\text{Ca}^{2+}$  signaling of sarcomeric function. The understanding of both conservation and modification of electrophysiology and contractile components is essential in the appropriate utilization of the zebrafish model.

About 71% of human genes have at least one corresponding gene in the zebrafish genome, known as an ortholog (Howe et al. 2013). Due to gene duplication events there may be two orthologs in the zebrafish genome for a given human gene. The zebrafish genome has several thousand unique genes without a corresponding ortholog in the mammalian genome. Gene duplication is thought to be one of the major driving forces in evolutionary innovation as it introduces the ability to have novelty without loss of the original function (Ohno 1993). While most genes are lost after a duplication event, tissue specific expression may lead to the retention of multiple copies of a given gene, known as paralogs. These copies can then divide ancestral functions (sub-functionalization) or develop new functions (neo-functionalization) (Ohno 1993; Meyer and Schartl 1999). Gene duplication has led to multiple copies of genes that code for sarcomeric proteins and ion channels, consequently there may be multiple genes in zebrafish that are orthologous to a given human gene. This is an evolutionary adaptation by the zebrafish that allows them to regulate cardiac contractility through the differential expression of functionally similar isoforms and paralogs (Karasinski et al. 2001; Sehnert et al. 2002; Rottbauer et al. 2006; Seeley et al. 2007; Zhao et al. 2008; Ohte et al. 2009; Sogah et al. 2010; Alderman et al. 2012; Genge et al. 2013, 2016; Zou et al. 2015; Singh et al. 2016). Certain channels that produce cardiac ion currents are regulated by non-orthologous genes in zebrafish and humans, for example the major repolarizing ( $I_{K1}$ ,  $I_{Kr}$ ) and depolarizing ( $I_{Na}$ ,  $I_{CaL}$ ) currents (Leong et al. 2010a, b; Vornanen and Hassinen 2016). While variation in zebrafish gene content may be a method of coping with varying environmental conditions, the

resulting unique gene content and expression in fish creates challenges in assigning a given function to a gene product that may be different between species.

Variation in ion currents due to genetic divergence between fish and humans due to this fish specific genome duplication can confound the selection of candidate molecules for medicinal drug development or in toxicological testing. With the increasing use of zebrafish as a model of vertebrate cardiac physiology (Milan et al. 2003; Arnaout et al. 2007; Scholz et al. 2009; Leong et al. 2010a, b; Nemtsas et al. 2010; Bovo et al. 2013; Dvornikov et al. 2014), the variation in paralog use must be considered due to the increased number of teleost-specific paralogous genes that code for cardiac proteins. Shared cardiac functions need to be distinguished as either derived or novel in zebrafish and humans. The discrepancies in gene content and cardiac function between humans and ectothermic models often originate in molecular adaptation to the native environment. Mammalian hearts function normally at a specific narrow temperature range (~37–38°C) while ectotherms must tolerate a broad range of environmental temperatures. Zebrafish must be able to maintain cardiac function between 6 and 38°C (Spence et al. 2008). The function of orthologous enzymes is conserved when the orthologous enzymes are at their typical physiological temperature (Somero and Hochachka 1969; Fields and Somero 1998; Somero 2005). As such there is variation in the biophysical properties of key proteins in the contractile element that are preferentially expressed by zebrafish at different temperatures. The substantial variation in cardiac function based on divergence in genetic background complicates the use of the zebrafish as a model. Even where commonalities are shared in whole-heart physiological measurements, the underlying mechanism may be divergent in teleosts. In this review, we will discuss both the conserved similarities in teleost and human hearts as well as the basis of variation that must be acknowledged when using this comparative model. While this can make the study of the ectothermic zebrafish difficult, zebrafish can be an excellent model for the study of mammalian cardiac systems when care is taken in the selection of appropriate techniques and questions.

## 2 In Vivo Function of the Zebrafish Heart

Visualization of *in vivo* heart function is important to identify the correlation between genotype and phenotype, to understand heart disease progression and/or treatment applied in longitudinal studies (Gemberling et al. 2015; Nair et al. 2016). High-resolution echocardiography has been used to examine cardiac structure and function of the *in vivo* adult zebrafish (Gerger et al. 2015; Lee et al. 2016). This accurate and non-invasive method allows real-time imaging *in vivo* for investigation of the many cardiac mutations available for zebrafish (Sun et al. 2008).

In echocardiographic imaging, two-dimensional (2D) bright (B)-mode image is considered the basic guide mode (Fig. 2). The zebrafish ventricle, atrium and bulbus arteriosus can be seen from a long-axis B-mode view. Functional parameters including stroke volume (SV), ejection fraction (EF), fractional shorting (FS),

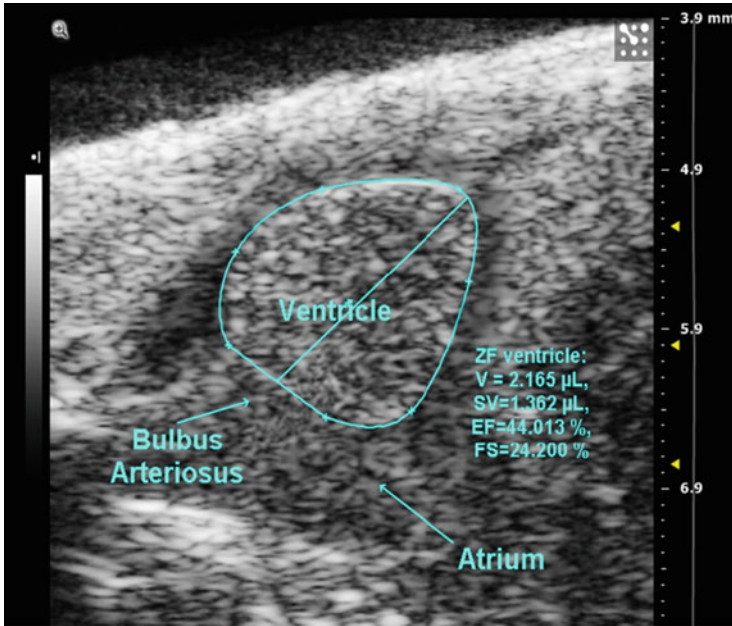


**Fig. 2** Echocardiographic long-axis B-mode of ZF ventricle. 2D B-mode long-axis view of a zebrafish ventricle. Zebrafish ventricle, atrium and bulbus arteriosus can be seen from this view. Tracing on the edge of the ventricle throughout diastole (d) and systole (s) allows an assessment of cardiac functional parameters. *V* volume, *SV* stroke volume, *EF* ejection fraction, *FS* fractional shortening

and fractional area change (FAC) can be calculated from this view (Gerger et al. 2015; Lee et al. 2016). Cardiac volumes can be calculated from 2D B-mode images, using the Simpson method, which has proved to give the best prediction for calculating fish ventricular volumes (Coucelo et al. 2000). The end diastolic volume (EDV) of zebrafish is typically around 2.3  $\mu\text{L}$  using these methods (Lee et al. 2016).

One-dimensional (1D) Motion (M)-mode images are acquired by a rapid sequence of B-mode scans along a single line and displayed as a function of time. This view is challenging to obtain in zebrafish due to the small heart size ( $\sim 1.5$  mm); also the compact layer and the sponge layer in the zebrafish heart are difficult to distinguish. However, Liu et al. developed a method of ultrahigh frame-rate (UHFR) echocardiography which can record M-mode images and measure zebrafish ventricular internal diameter (Liu et al. 2013). They reported the fractional shortening (FS) to be  $42 \pm 4\%$  (mean  $\pm$  SD) and  $60 \pm 13\%$  for the long axis and short axis of the ventricle, respectively, and fractional area change (FAC) was  $77 \pm 9\%$  (Liu et al. 2013). FS calculated from 1D M-mode is much higher than the 2D B-mode calculation, which is around 17–24% (Hein et al. 2015; Lee et al. 2016).

In the ectothermic zebrafish, acute temperature can be used as a perturbation on the whole animal model to quantify cardiac responses to stress, and thermal acclimation to alter cardiac function and morphology in similar-sized teleosts

(Johnson et al. 2014). In work done by our group, echocardiography with a high frequency probe (70 MHz) was used to observe cardiac function for warm-acclimated (WA) and cold-acclimated (CA) zebrafish at 28 and 18°C (Lee et al. 2016). Heart rate (HR) is the critical factor modulating the cardiac response to acute temperature change as it increases from  $78 \pm 6$  bpm at 18°C to  $162 \pm 10$  bpm at 28°C regardless of acclimation state. Stroke volume did not change in response to acute temperature change or acclimation (1.06–1.17  $\mu$ L). A similar lack of change in relative stroke volume measured with laser Doppler blood flow has been seen in other zebrafish undergoing the same temperature shift (Little and Seebacher 2013).

Doppler mode echocardiography is an important tool for studying hemodynamics, which is extremely useful for zebrafish heart imaging to identify the direction and velocity of blood flow from B-mode images (Ho et al. 2002). Parameters including heart rate (HR), ventricular inflow, ventricular outflow, the velocity time integral (VTI), isovolumic relaxation time (IVRT), isovolumic contraction time (IVCT), ejection time (ET), and myocardial performance index (MPI) can be clearly measured from the pulse wave (PW) Doppler mode (Sun et al. 2008; Lee et al. 2016).

One important parameter that can be determined in zebrafish heart by PW Doppler is the E/A ratio (Fig. 3). As there are two components of ventricular inflow: early (E) filling peak velocity during ventricular relaxation (passive filling) and the atrial (A) filling peak velocity that is the result of atrial contraction. Unlike mammals, the E velocities are significantly lower than the A velocities in fish hearts (Ho et al. 2002). This is consistent with the notion that the end diastolic volume in the fish ventricle is determined in large part by atrial contraction rather than central venous pressure as seen in mammals (Cotter et al. 2008). The increased importance of late ventricular filling by atrial contraction rather than the passive early filling of the ventricle is reflected in the early to late filling ratio (E/A ratio) of teleosts. Fish typically show an E/A ratio around 0.2, much lower than that of the healthy human

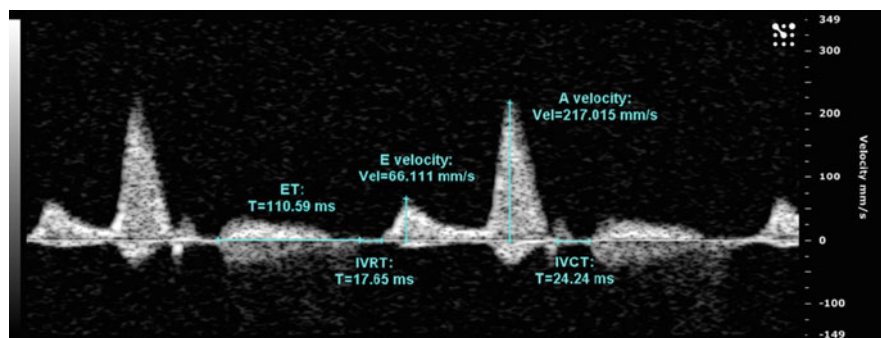


**Fig. 3** Zebrafish ventricular inflow velocity obtained by using pulse wave Doppler. The pulse wave Doppler mode of ventricular inflow. The velocity (in mm/s, y-axis) is shown over time (in ms, x-axis). Early filling peak velocity (E velocity), the atrial filling peak velocity (A velocity), ejection time (ET), isovolumic contraction time (IVCT) and isovolumic relaxation time (IVRT) can be measured from this view



( $1.5 \pm 0.4$ ) (Ho et al. 2002; Nagueh et al. 2009) under resting conditions. In our zebrafish study, E/A ratio was found to be 0.28 regardless of the acute or acclimated temperature state (Lee et al. 2016). This value corroborates previous zebrafish studies, which have shown similar E/A ratios at 15°C and 25°C (Ho et al. 2002; Sun et al. 2008). End systolic volume (ESV) of the fish heart is very small (Coucelo et al. 2000) relative to that of the mammalian heart even when normalized by body weight. This results in species such as zebrafish having relatively low systolic pressure generation (~2.5 mm Hg) in the ventricle (Hu et al. 2001).

One of the challenges for echocardiography in the zebrafish is the appropriate use of anesthetic. Tricaine methane sulfonate (MS-222) has been widely used as an anesthetic agent for zebrafish studies. It is known that the MS-222 doses normally used (100–200 ppm or mg/ml) are potent cardiac depressants and can result in heart rates less than 100 bpm or even death (Huang et al. 2010). A reasonable solution was proposed by Huang et al. in which they used a modified anesthetic protocol that was the combination of pH-adjusted MS-222 (45 ppm) and isoflurane (45 ppm), which showed significantly less impact on zebrafish cardiac function (Huang et al. 2010). We have found that using this drug combination, the zebrafish heart rate can be kept above 160 bpm at 28°C and achieved full recovery after long term exposure (up to 40 min) (Lee et al. 2016). Other anesthetics have been used that can also maintain cardiac function, or specifically for lacking a deleterious effect on SV, such as AQUI-S (Little and Seebacher 2013).

The zebrafish is an interesting model of cardiac regeneration that has been studied using *in vivo* echocardiography. It has been reported that zebrafish can remove scar tissue and regenerate its heart even after 20% ventricular resection (Poss et al. 2002). Non-invasive echocardiography is the most suitable tool for longitudinally observing the cardiac structure and function during recovery of adult zebrafish (Hein et al. 2015). Evaluation of ventricular recovery after cryo-cauterization and myocardial motion during heart regeneration has been done by Doppler imaging (Lee et al. 2014; Huang et al. 2015). Regeneration is of interest in the zebrafish model due to the insight it might offer for novel approaches to cardiac regeneration in humans.

Further advanced echocardiographic techniques have been used in zebrafish regeneration models, such as strain analysis using speckle-tracking applied on high-resolution B-mode images to assess the regional myocardial motion and deformation. It has been used to evaluate cardiac regeneration after myocardial cryoinjury (Hein et al. 2015). The imaging modalities evaluated both regional and global zebrafish ventricular functional changes and contribute to establish further adult zebrafish as cardiac disease model and regeneration process.

Amongst the numerous advantages of echocardiography and its hemodynamic measurements of the *in situ* heart are also significant limitations including a significant upfront investment in equipment and need for a highly skilled sonographer. By the very nature of making recordings from an intact organism, imaging quality is marred by the presence of movement artifact. Since bone is highly reflective to acoustical waves, there are a very limited number of probe positions and angles that give a clear view of the zebrafish heart. The combination of these



factors often limits recording lengths to several seconds and prevents the quantification of infrequent events such as errant beats by echocardiography. However, the use of whole animal *in vivo* cardiac function to characterize mutant phenotypes and to be able to do this non-invasively and longitudinally is invaluable, especially when coupled with other measures of cardiac function.

### 3 Whole Heart Measurements

One of the attractive elements of the zebrafish model is the similarity between the zebrafish and human ECG recordings, in large part, due to the similarities in heart rate and ventricular action potential durations. Developmentally, the transparency of zebrafish embryos allows heart rates to be manually observed (Granato et al. 1996). Additionally, embryonic ECGs are available from microelectrode recordings as early as 3 dpf, in which there can be diffusional drug delivery (Dhillon et al. 2013). In adult zebrafish, needle electrodes must be used and require anesthetic, which may be limited by the same cardiodepressive effects influencing echocardiographic measurements if appropriate anesthetic protocols are not employed (Milan et al. 2006; Chaudhari et al. 2013).

While hemodynamic measurements are invaluable, the absence of electrical information can make interpretation difficult. In particular, *in vitro* ECG recordings in the adult heart can show alteration of cardiac cycle components in response to drugs that exert electrophysiological effects on cardiomyocytes (Tsai et al. 2011). The addition of concurrent electrocardiography with hemodynamic measurements, which requires minimal additional equipment, gives a valuable physiological context and is ideally suited towards longer recordings. However, the insertion of the ECG electrodes greatly increases the invasiveness of the procedure, nullifying one of the key advantages of echocardiography. An additional limitation of ECG recordings in intact adult zebrafish is imprecise drug dosages with indirect delivery but this can be improved with intraperitoneal injections (Chaudhari et al. 2013). As well, continued gill movement in anesthetized fish contributes significant movement artifacts and signal noise. Averaging the ECG waveform over numerous cardiac cycles increases the signal integrity and further improvements in signal quality are possible with arrested gill movement and external perfusion but can introduce confounding effects (Milan et al. 2006).

An alternative approach to intact recordings is to excise the heart, which circumvents the complexities of anesthetization and motion artifacts, with the additional advantage of diffusional drug delivery (Tsai et al. 2011). In the excised preparation, neurohormonal regulation is lost and there is an increased risk of physical damage. However, peri-cardiac incisions can be made on a euthanized zebrafish to allow direct visualization of the heart prior to full heart isolation (Lin et al. 2015). Since rate and rhythm are observable by eye and rough handling of the heart has instantaneous deleterious effects, the health of the zebrafish heart can be continuously monitored to assess any possible damage during extraction. While the

excision process can initially be technically challenging, the result is an exceptionally stable preparation in which heart rate and rhythm can be stable ex-vivo for 12–24 h (Lin et al. 2014).

ECGs can be recorded using microelectrodes (Tsai et al. 2011) or by field-electrodes in which the heart is positioned within 1 mm, of two 0.5 mm silver-chloride electrodes (Lin et al. 2015). Embedding the electrodes into the bottom of a vinyl-terminated PDMS (e.g., Sylgard)-coated Petri dish allows for relatively high throughput screening since each heart only needs to be positioned between the recording electrodes for a short duration. One of the limitations of these arrangements is the difficulty in performing solution changes without changing the relative positioning of the heart and electrode positioning may contribute to variability observed in p- and t-wave polarity (Tsai et al. 2011). Since relative positioning can change the apparent conduction axis (Dhillon et al. 2013), cannulation of the zebrafish heart through the aortic-equivalent bulbus arteriosus facilitates precise relative positioning and the rotation of the heart can be manipulated to optimize the ECG recording (Lin et al. 2015). Cannulation also allows for superfusion with minimal movement artifact to improve signal quality.

The primary information available in an ECG recording is the temporal relationship of atrial depolarization, ventricular depolarization, and ventricular repolarization from which clinically relevant parameters such as heart rate, atrioventricular delay, and ventricular action potential duration can be derived (Tsai et al. 2011; Dhillon et al. 2013). Since ECG electrodes directly measure electrical activity, the length of an ECG recording is effectively unlimited making ECG especially well suited to investigating rare electrical events. Complementary techniques such as glass microelectrodes and optical mapping techniques are better suited to determining intermediate voltage kinetics. Impaled microelectrodes are one of the few techniques that can give absolute membrane voltages and rates of membrane depolarization and repolarization. The discrete nature of a microelectrode recording allows electrical signals to be precisely localized. However the size of a zebrafish heart makes multiple simultaneous recordings, such as for conduction velocity measurements or for assessing cell-to-cell variability, difficult (Lin et al. 2015).

Optical mapping recordings lack the ability to measure absolute membrane potentials but are able to capture relative changes from the atria and ventricles simultaneously, making it especially well suited to conduction velocity measurements and for investigating arrhythmogenicity (Efimov et al. 2004; Herron et al. 2012). Two common potentiometric dyes, di-4-ANEPPS (Sedmera et al. 2003; Tsai et al. 2011) and RH-237 (Lin et al. 2014) have been used in adult zebrafish hearts. While both dyes are prone to photobleaching, extended imaging using di-4-ANEPPS has been reported to have phototoxic effects (Sedmera et al. 2003) whereas no changes in rhythm were observed using RH-237 (Lin et al. 2014, 2015). However, it is unclear whether this result was due to the properties of the potentiometric dyes or due to other experimental parameters such as differences related to the use of cytochalasin D versus blebbistatin as the excitation-contraction uncoupler. Tsai et al. (2011) also used di-4-ANEPPS but

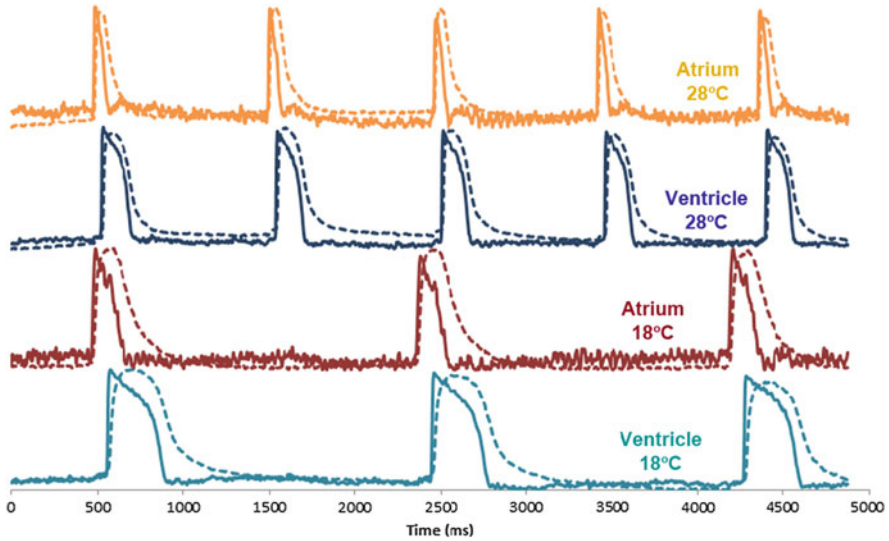


**Fig. 4** Fluorescent voltage and calcium recordings as a function of temperature. Atrial and ventricular recordings were made at 28°C (*top*) and 18°C (*bottom*). Voltage signals (*solid lines*) have a fast upstroke and rapid repolarization, resulting in a prominent peak. The upstroke of the calcium transient (*dotted lines*) is initially fast and then slows as it approaches peak calcium. The slow phase of the calcium upstroke coincides with early repolarization such that  $\text{Ca}^{2+}$  levels are increasing while voltage levels are decreasing. The slow approach to peak calcium followed by gradual relaxation results in a rounded calcium transient peak. Observable effects of changing temperature include changes to heart rate, atrioventricular delay, and voltage and calcium transient durations

made no mention of rhythm changes related to imaging. In rat hearts, effects of di-4-ANEPPS on AV conduction have been observed (Nygren et al. 2003) but no changes to AV conduction were reported in zebrafish (Sedmera et al. 2003).

Optical mapping can be extended to include simultaneous calcium measurements and the combination of the potentiometric dye RH-237 and the calcium-sensitive dye Rhod-2 is a powerful technique which has been used in zebrafish (Lin et al. 2015) (Fig. 4). As many indicator dyes are sensitive to the cell-specific microenvironment, it should be noted that the RH-237/Rhod-2 combination used in zebrafish contained spectral cross-talk (Lin et al. 2015) whereas no cross-talk was reported when used in guinea-pig (Choi and Salama 2000) or in rat myocyte cultures (Fast 2005). The species specific background may necessitate the use of possible alternative dye combinations (reviewed in Fast (2005) and Jaimes et al. (2016)).

Optical mapping recordings are considerably data rich. Thus, in one voltage-calcium recording of the zebrafish heart, measurable parameters include: heart rate, atrial action potential durations, atrial calcium transient, atrial conduction velocity, atrioventricular delay, ventricular action potential duration, ventricular calcium transient, and ventricular conduction velocity but can require extensive

data analysis. MATLAB-based processing and analysis tools are published and freely available (Laughner et al. 2012) as are additional methods of cycle averaging to increase signal quality (Ding et al. 2014; Lin et al. 2015).

In optical mapping experiments, larger hearts are associated with larger signal intensities and the advantages of working with a heart smaller than 1 mm<sup>2</sup> may appear to be counterintuitive. One advantage of the zebrafish model, that leverages its diminutive size, is its compatibility with common fluorescence microscopes. As the dyes used in optical mapping utilize common excitation and emission wavelengths, many fluorescence microscopes can be readily converted to optical mapping applications with the addition of a sufficiently fast digital camera. With care, confocal and spinning disk microscopes can also be used.

Conduction velocities in the zebrafish are relatively fast, with 20 ms and 25 ms conduction times in the atrial and ventricular compartments, respectively (Sedmera et al. 2003). Therefore, high-resolution conduction velocity measurements benefit from high speed cameras upwards of 500 fps. However, speed requirements for accurately measuring action potential and calcium transient kinetics is surprisingly low, with fast-Fourier analysis indicating few frequency components above 100 Hz (Mironov et al. 2006). Continuous developments in camera technology make high speed sensors increasingly affordable. A potential difficulty with using a microscope-based optical mapping system with lower-cost digital cameras is the smaller sensor sizes which limits the viewable area. This can be circumvented with lower magnification objectives and/or the addition of a demagnifying transfer lens in front of the camera sensor. Alternatively, a custom optical pathway can be constructed with simple lens (Lin et al. 2015) in a custom fashion and can be done more cost effectively.

The small size of the zebrafish heart has many pragmatic advantages for use in a simpler optical mapping set-up worth noting. The size of the zebrafish heart contributes to its ability to maintain cardiac function for many hours without external perfusion or oxygenation. This, in combination with the flexibility of the zebrafish heart to thrive under ambient temperature conditions, means that zebrafish optical mapping experiments can be conducted in the absence of perfusion pumps, gas bubblers, and temperature controllers. In mammalian optical mapping experiments, the stability of the preparation is heavily dependent on maintaining adequate coronary flow and pulsatile flow from the perfusion systems can contribute to movement artifact during image acquisition. As 37°C is significantly higher than ambient, maintaining sufficient warmth throughout the imaging system is also a non-trivial concern. Conversely, zebrafish hearts can function comfortably between 18 and 28°C (Spence et al. 2008) and do not require precise temperature regulation since cardiac cycles separated by 1°C are not statistically different. The relative indifference of zebrafish hearts to these rather large variations in temperature allows consumer aquarium-grade water heaters and coolers, which are typically accurate to ±1°C, to be used to good effect.

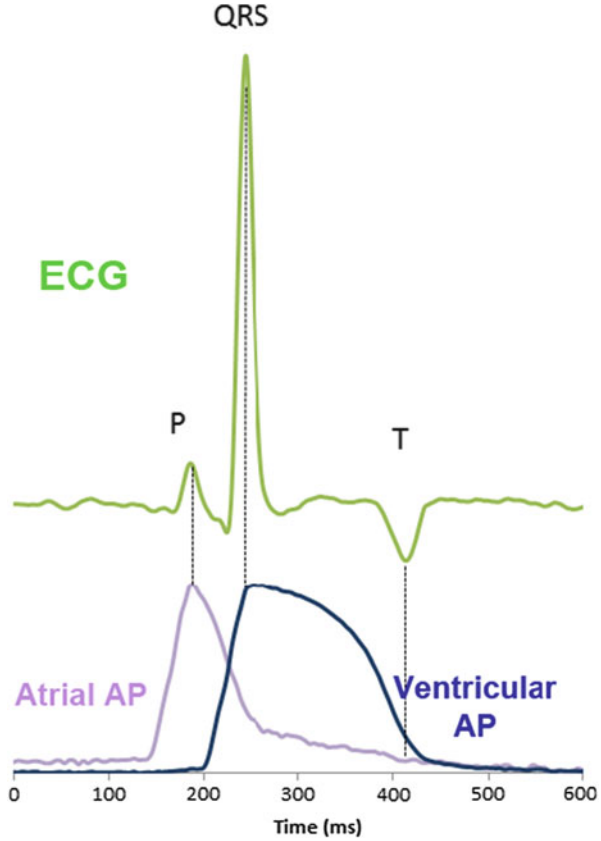
Further, the size of the zebrafish heart and the lack of an oxygenated perfusion system greatly decrease the rate of consumption of RH-237, Rhod-2 and, most importantly, blebbistatin per experiment. Blebbistatin, as a contractile inhibitor, is

necessary in modern optical mapping experiments to prevent muscle contraction, which would otherwise obscure the voltage and calcium dynamics recordings. As blebbistatin is typically supplied to mammalian hearts through the coronary circulation, the blebbistatin solution must be oxygenated and warmed prior to circulation, resulting in a circulating volume of hundreds of mL. As it is this recirculating volume that is used to deliver drugs to the coronary circulation, its volume can have a significant effect on the cost of each experiment. In a typical zebrafish optical mapping experiment, with no recirculating perfusion system, the imaging chamber holds 1.5 mL and RH-237 and Rhod-2 loading steps occur in 250  $\mu$ L chambers. These considerations all make the zebrafish a much more cost-effective model to work with.

In mammals, hypothermia reduces cardiac output primarily through negative chronotropic effects with complex effects on stroke volume (Wood and Thoresen 2015). Moderate hypothermia ( $37^{\circ}\text{C} - >29^{\circ}\text{C}$ ) is strongly inotropic due to changes in action potential duration and calcium handling (Shattock and Bers 1987) while more severe temperature reductions ( $>15^{\circ}\text{C}$ ) result in calcium overload and contracture (Liu et al. 1990; Wang et al. 1997). In zebrafish, reduced temperatures also reduce cardiac output primarily through negative chronotropic effects in which the transition from  $28^{\circ}\text{C}$  to  $>18^{\circ}\text{C}$  is associated with a 40% decrease in heart rate (Lin et al. 2014) while stroke volume is maintained (Lee et al. 2016). At  $28^{\circ}\text{C}$ , zebrafish heart rates vary across a wide range of values, from 50 bpm to over 200 bpm, and the average atrial and ventricular action potential duration ( $\text{APD}_{50}$ ) is 33 and 98 ms, respectively (Lin et al. 2014). In spontaneously beating hearts, the rate dependence of atrial and ventricular action potential durations was sufficiently shallow at  $28^{\circ}\text{C}$ , that the heart rate effect was comparable to inter-heart variability. Overall, there was a weakly correlated heart rate effect of 7 ms per 100 bpm for atrial  $\text{APD}_{50}$  and 14 ms per 100 bpm for ventricular  $\text{APD}_{50}$  at  $28^{\circ}\text{C}$ . The heart rate effect was also examined within hearts using field stimulation with similar effects (Lin et al. 2015).

Temperature strongly affects atrial and ventricular action potential durations, with  $Q_{10}$  values of 2.7 and 2.0, respectively, with additional effects on the action potential morphology. Because temperature has such a strong effect on heart rate, temperature-induced changes combine both the direct temperature effect together with indirect effects of reducing heart rate. For individual hearts, faster heart rates at  $28^{\circ}\text{C}$  would be expected to experience a larger indirect temperature effects due to the larger absolute change in heart rate. For example, a heart beating at 200 bpm at  $28^{\circ}\text{C}$  would experience a four-fold greater indirect temperature effect than a heart beating at 50 bpm upon cooling to  $18^{\circ}\text{C}$ . The average atrioventricular delay in zebrafish is 1 ms, with shallow rate dependence at  $28^{\circ}\text{C}$  but with a 70% increase in AV delay by cooling from  $28^{\circ}\text{C}$  to  $18^{\circ}\text{C}$ . Similar to mammalian hearts, zebrafish atrioventricular delays have decremental conduction, in which faster heart rates have longer atrioventricular delays. The absolute change experienced by a given heart will depend on the both on the starting heart rate at  $28^{\circ}\text{C}$  and the rate-dependence of AV delay at  $18^{\circ}\text{C}$ .

**Fig. 5** Simultaneous ECG and optical mapping. Silver chloride wire electrodes (0.5 mm) were placed 1 mm from the lateral aspects of the atria and ventricle and the ECG signal was acquired concurrently with optical mapping (RH-237). Average ECG (*green*), atrial AP (*lilac*), and ventricular AP (*blue*) cycles were created using the peak of the peak of the QRS-complex



Although no additional information is present in the ECG recording beyond what is available in the optical mapping recordings, ECG can have an important role in optical mapping experiments. Simultaneous recordings of ECG and optical mapping indicate that the peak of the P-wave aligns with the peak of the atrial action potential while atrial repolarization is absent from the ECG recording as is typically observed in the mammalian heart. For the ventricle, the exact relationship between the QRS complex and the ventricular action potential can vary with the AV delay and the peak of the R-wave roughly aligns with peak voltage while the end of the t-wave aligns with complete repolarization. However, even though rates of photobleaching and phototoxicity are limited even with 6 min of accumulated image acquisition time per heart (Lin et al. 2014), continuous illumination of the heart for several minutes results in movement artifact due to photo inactivation of blebbistatin activity. Therefore, the optical mapping approach is not as well suited for continuous monitoring as in ECG. Combining continuous ECG monitoring with episodic optical mapping recordings may be the ideal arrangement for imaging sporadic electrical events (Fig. 5).

Simultaneous voltage and calcium recordings using RH-237 and Rhod-2 can quantify the temporal differences in calcium handling between the atrial and ventricular compartments of the zebrafish heart (Lin et al. 2015). Atrial and ventricular calcium transients have distinctly separate relationships with respect to their voltage dynamics and changes in voltage kinetics produce parallel changes in the calcium dynamics. A variable rate stimulation protocol results in linear rate-dependent shortening of the action potentials. In the atrium, the calcium transient duration is 30 ms longer than the action potential duration over a 150 bpm difference in rate. In the ventricle, the calcium transient duration is 20 ms longer over the same range.

Another attractive feature in optical mapping technology is the potential use of genetically encoded voltage and calcium indicators, often referred to as optogenetic sensors, which can be brighter and inherently more photo-stable than fluorescent dyes, giving improved signal quality reviewed in Looger (2012) and Cohen (2016). The kinetics of optogenetic sensors may be slower than fluorescent dyes (Rose et al. 2014; Cohen 2016) but the high signal-to-noise ratio may yield higher effective temporal resolution. Optogenetic sensors are also not prone to leakage or compartmentalization and are more suitable for long imaging protocols (Broussard et al. 2014) and longitudinal studies. For example, one can conduct a time course study in tracking the development of the heart from embryo stage to adulthood and monitoring arrhythmogenesis in a mutant line. Perhaps more importantly, optogenetic sensors can have targeted expression opposed to the diffuse labeling associated with the incubation of fluorescent dyes, leading to far lower background signals, higher imaging contrast, and spatial resolution (Broussard et al. 2014). This targeted expression in the heart was recently demonstrated with a transgenic line carrying a dual function genetically encoded voltage and calcium indicators in which the reporter gene expression was driven by the cardiac specific promoter *cmlc2* (Hou et al. 2014). As zebrafish embryos are translucent and can be imaged under a conventional epifluorescent microscope, targeted expression in the heart also permits for ease in identifying potential founders that carry the optogenetic sensor of choice (Hou et al. 2014).

Numerous variants of optogenetic sensors have been developed in recent years. Typically, these sensors comprise a sensing domain tethered to one or two reporter fluorescent proteins (FPs), resulting in fluorescence readout either via Förster resonance energy transfer (FRET) or conformational change in monomeric FP. FRET-based sensors are ratiometric in nature, thus, less prone to motion artifact, making it the appropriate tool to image a moving heart (Lutcke et al. 2010). However, the signal-to-noise ratio of monomeric FP is higher than FRET-based indicators, leading to increased spatial and temporal resolution (Tian et al. 2009). For monomeric FP-based sensor, GFP is commonly used, although indicators with red-shifted fluorescent proteins are increasingly favored due to less phototoxicity (high wavelength excitation), deeper tissue penetrance, and less background autofluorescence (Shen et al. 2015; Abdelfattah et al. 2016).

Genetically encoded voltage indicators based on GFP include ArcLight and ASAP1. ArcLight reports action potential with high sensitivity ( $\Delta F/F = -35\%$  in



response to 100 mV depolarization) but with relatively slow upstroke (Jin et al. 2012). Comparatively, ASAP1 reliably reports AP with similar sensitivity ( $\Delta F/F = -30\%$  in response to 100 mV depolarization) and has faster on/off kinetics ( $\sim 2$  ms) (St-Pierre et al. 2014). For genetically encoded calcium indicators, extensive protein engineering in the GCaMP family has produced a whole line of indicators, with the most recent permutation GCaMP6 claimed to have highest sensitivity,  $\text{Ca}^{2+}$  binding affinity, larger dynamic range, and fastest kinetics (Chen et al. 2013). Furthermore, a derivative of GCaMP called GECO has been developed with a variety of FPs (Wu et al. 2014a, b; Zhao et al. 2014; Shen et al. 2015) resulting in the flexibility of choosing a calcium indicator with a range of  $K_d$  values for  $\text{Ca}^{2+}$  and spectral separation. This flexibility in the selection of fluorescent spectra enables multiplex imaging to determine the voltage and calcium dynamics using green- and red-shifted optogenetic sensors.

## 4 Isolated Cardiomyocytes

### 4.1 Electrophysiology

Zebrafish cardiac electrophysiology is comparable to mammals as they share major inward and outward currents resulting in similar action potential duration (APD) and morphology (Nemtsas et al. 2010). While optical mapping provides tangible advantages for exploring electrophysiology at multicellular and whole organ levels, it is complemented well by electrophysiological measurements on the individual cell. The use of patch clamping techniques on isolated zebrafish cardiomyocytes (Nemtsas et al. 2010; Zhang et al. 2011) or in heterologous expression systems expressing cloned ion channels (Scholz et al. 2009; Vornanen and Hassinen 2016) records individual channel activity critical for understanding the mechanism of function. Increased understanding can help to better predict the action of pharmacological agents when using the zebrafish heart as a model and is reviewed extensively elsewhere (Leong et al. 2010a, b; Alday et al. 2014; Vornanen and Hassinen 2016). However, as noted previously, due to whole genome duplication, as well as multiple orthologs and isoforms, the molecular mechanisms, function, and response to pharmacological agents of individual ion channels can be significantly different between the hearts of zebrafish and mammals (Verkerk and Remme 2012; Vornanen and Hassinen 2016). The following outlines current understanding of zebrafish cardiomyocyte ion channel currents with the view to highlight necessary caution in interpreting the results of APD and morphology when using zebrafish as a model of mammalian cardiac electrophysiology.

Similar to mammals, inwardly rectifying current ( $I_{k1}$ ) maintaining the cardiac resting membrane potential (phase 4) is present in both atria and ventricle of the zebrafish, along with higher  $I_{k1}$  density in the ventricle than atria (Nemtsas et al. 2010). However, six isoforms of Kir2 channels are expressed in zebrafish,



consequently driving  $I_{k1}$  mainly through orthologs of Kir2.4 and Kir2.2a which are not the main mammalian isoforms (Szuts et al. 2013; Hassinen et al. 2015), suggesting that  $I_{k1}$  is produced by divergent ion channels to those of mammals.

In zebrafish, the upstroke and the plateau phase of the AP are created by the depolarizing inward currents of  $\text{Na}^+$  ( $I_{\text{Na}}$ ) and  $\text{Ca}^{2+}$  ( $I_{\text{Ca}}$ ), respectively, (Nemtsas et al. 2010). The upstroke (phase 0) of the AP is driven by fast  $I_{\text{Na}}$  but with slower upstroke velocity than mammals (Warren et al. 2001). A more negative voltage dependence of inactivation seen in both cultured embryonic and freshly isolated adult zebrafish ventricular myocytes has been suggested to result in lower  $I_{\text{Na}}$  density and consequently the slower upstroke velocity (Warren et al. 2001; Nemtsas et al. 2010). Interestingly, whereas Nav1.5 channels, which underlie  $I_{\text{Na}}$  in mammalian cardiac tissue, are relatively TTX-insensitive compared to neuronal and skeletal muscle isoforms, zebrafish cardiac Nav1.5 channels display three times higher sensitivity to TTX than their mammalian counterpart (Nemtsas et al. 2010). It is intriguing as to how this is advantageous to the zebrafish, but it is due to the preservation of an aromatic residue, which is critical for TTX binding in mammalian neuronal and skeletal muscle channels, but which is substituted for cysteine in mammalian cardiac Nav1.5 channels (Haverinen and Vornanen 2007; Nemtsas et al. 2010). Another interesting discovery is the presence of two zebrafish orthologs (scn5Laa and scn5lab – identified as scn12aa and scn12ab on Ensembl) that share 60–65% amino acid identity with the human SCN5A gene encoding cardiac Nav1.5 channel (Novak et al. 2006; Chopra et al. 2010). Both of these genes are expressed in zebrafish hearts (Novak et al. 2006) and produce typical voltage-gated sodium currents when expressed in CHO cells (Chopra et al. 2010). The additional SCN5 gene is likely the result of the teleost-specific whole genome duplication based on linkage analysis (Novak et al. 2006).

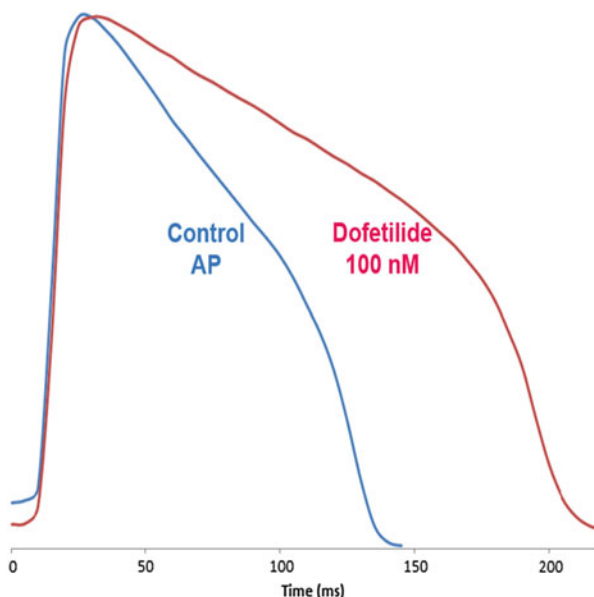
The L-type  $\text{Ca}^{2+}$  current ( $I_{\text{Ca,L}}$ ) is the primary contributor to the long plateau phase (phase 2) of the ventricular action potential in adult mammals, while T-type  $\text{Ca}^{2+}$  current ( $I_{\text{Ca,T}}$ ) is limited to pacemaker cells and immature cardiomyocytes (Mesirca et al. 2014). Careful pharmacological dissection of  $I_{\text{Ca,T}}$  and  $I_{\text{Ca,L}}$  using nifedipine and nickel showed that both currents are present in zebrafish atrial and ventricular myocytes (Nemtsas et al. 2010). L-type  $\text{Ca}^{2+}$  channel gene expression and robust  $I_{\text{Ca,L}}$  density was found in zebrafish ventricles, which contributes to the long plateau phase of AP and the resemblance of the mammalian AP phenotype (Rottbauer et al. 2001; Brette et al. 2008; Nemtsas et al. 2010). The dominant L-type  $\text{Ca}^{2+}$  channel  $\alpha 1$  subunit expressed in human hearts is  $\alpha 1\text{C}$  (Cav1.2), which when mutated in zebrafish, abolishes ventricular contraction (Rottbauer et al. 2001). However,  $\alpha 1\text{D}$  (Cav1.3) is also expressed in the adult zebrafish heart (Sidi et al. 2004). Furthermore, L-type  $\text{Ca}^{2+}$  channels are heteromeric protein complexes, which include a cytoplasmic  $\beta$  subunit that modulates electrophysiological activity. Two genes have been identified in zebrafish as orthologs for the primary  $\beta$  subunit expressed in human cardiac tissues, but the function of each is unclear based on morpholino studies in zebrafish embryos (Zhou et al. 2008). The presence of robust T-type  $\text{Ca}^{2+}$  current in mammals typically occurs in the developing heart, suggestive of a more immature phenotype of zebrafish cardiomyocytes.

The functional relevance of  $I_{Ca,T}$  in adult zebrafish myocytes is yet unknown (Verkerk and Remme 2012), but in embryos  $I_{Ca,T}$  blockade by NNC55-0396 reduces action potential generation (Alday et al. 2014). The T-type  $Ca^{2+}$  channels expressed in zebrafish hearts display properties likely to be consistent with the Cav3.1 subunit (Nemtsas et al. 2010), although immunofluorescence experiments suggest the additional presence of Cav3.2 (Alday et al. 2014). The genetic basis for these channels is unknown.

In mammals, the transient outward current ( $I_{to}$ ) constitutes the rapid repolarization (phase 1) of the AP, but the current is thought to be absent in the adult zebrafish heart (Nemtsas et al. 2010). The slow delayed rectifier  $K^+$  current ( $I_{ks}$ ), which accounts for the mammalian repolarization reserve that is necessary to adapt to stress conditions (Schmitt et al. 2014) may also not be expressed in zebrafish cardiomyocytes (Nemtsas et al. 2010; Alday et al. 2014). However, orthologs of mammalian KCNQ1 and KCNE1 are expressed at the transcript level in zebrafish (Tsai et al. 2011; Wu et al. 2014a, b), and in intact whole heart organ optical mapping experiments the  $I_{Ks}$  blocker chromanol 293B prolonged AP duration (Tsai et al. 2011). It is unclear why these studies differ in their reporting as to the presence of a functional  $I_{Ks}$  current. Given the prominent dependence of  $I_{Ks}$  current on stimulation rate and adrenergic tone (PKA levels), one possible reason is the difference between measurements made in isolated cells compared with intact hearts.

Analogous to mammals, the rapid delayed rectifier  $K^+$  current ( $I_{kr}$ ) is a dominant repolarization current in the zebrafish heart (Nemtsas et al. 2010). Cloned zebrafish ether-a-go-go-related gene (zERG) channels display comparable biophysical properties to human  $I_{kr}$  producing hERG channels (Scholz et al. 2009). Moreover, loss of function of  $I_{K_r}$  in zebrafish hearts recapitulates perturbed repolarization as observed in the human long QT syndrome (LQTS) leading to significant interest in the utility of zebrafish hearts as a model for studying and screening arrhythmogenic  $I_{K_r}$  gene mutation phenotypes (Arnaout et al. 2007). In zebrafish embryos Jou et al. knocked down the KCNH2 gene with morpholinos and then injected the wild-type or mutant hERG1 gene. The authors observed a high success rate for detecting LQTS causing mutations to produce repolarization disorders and bradycardia in the zebrafish embryos. In addition, Milan et al. applied a wide variety of pharmacological agents known to cause acquired LQTS to zebrafish embryos and demonstrated that the majority produced repolarization disorders, suggesting the system may be used as a high throughput screening tool (Milan et al. 2003). These studies present an exciting potential utility of the zebrafish model, but one key issue is that in zebrafish  $I_{kr}$  is not generated by the orthologous channel of hERG1, which is found in mammalian cardiomyocytes; but rather is produced by an ortholog of hERG2 (KCNH6) (Leong et al. 2010a, b). This presents a potential confounding factor when investigating hERG1 mutations that cause electrical disturbances such as LQTS as it is currently unclear whether mutations in the hERG1 ortholog of zebrafish fully recapitulate the disease (Arnaout et al. 2007). Further, the similarity between zebrafish orthologs of hERG may require further characterization of the appropriate gene to be used for mutation. Optical mapping of

**Fig. 6** Voltage recording of dofetilide effect using optical mapping. Observable 70 ms prolongation in  $APD_{50}$  45 min after application of 100 nM of the HERG (ZERG) channel blocker dofetilide (RED)



adult zebrafish hearts revealing AP and calcium handling information will also likely aid in the development of the zebrafish heart as a model for human electrical disorders.

In terms of pharmacological screening, understanding the molecular correlate is essential as different paralogs of zebrafish may produce ion channels with varying drug sensitivity (Abi-Gerges et al. 2011; Hassinen et al. 2015). However, functional relationship in pharmacology can still be established using optical mapping if appropriate care is taken given the caveats described above. Part of the importance of using zebrafish in pharmacological model is in monitoring the effects of drugs on the interdependence of ion channels, i.e. the entire depolarization and repolarization currents (Pugsley et al. 2015). Preliminary work using 100 nM dofetilide showed that the  $APD_{50}$  is elongated by 75 ms (Fig. 6) mimicking acquired long-QT syndrome. This work corroborates what has been done on individual channels with many compounds prolonging QT intervals in zebrafish (Langheinrich et al. 2003; Milan et al. 2003; Mittelstadt et al. 2008), suggesting that zebrafish can still be used in gross pharmacological screening.

Evidently, cardiac electrophysiology of zebrafish is quantitatively different from mammals, but the qualitative similarities allow the zebrafish heart to serve as a useful tool in modeling mammalian cardiac excitation, arrhythmogenesis, and pharmacological screening. With appropriate attention paid to characterization of the wild-type zebrafish, electrophysiological techniques will be important for understanding disease state models of mutants as well.

## 4.2 Excitation-Contraction (E-C) Coupling

The basic process of cardiac E-C coupling, converting the electrical signal of an action potential to the mechanical response of contraction, is conserved between humans and fish (Bovo et al. 2013). However, specifics of the mechanism are different. In mammalian cardiac excitation-contraction coupling, membrane depolarization activates voltage-gated L-type  $\text{Ca}^{2+}$  channel (LTCC or  $\text{Ca}_v1.2$ ) which, in turn, activates the opening of ryanodine receptors (RyR2) leading to a much greater calcium release from the sarcoplasmic reticulum (SR) via  $\text{Ca}^{2+}$ -induced calcium release (CICR). Proportionally, SR calcium release accounts for between 70 and 90% of the calcium necessary to activate contraction and extensive membrane invaginations of the transverse-tubule network allow this calcium release to occur deep within the cell.

In zebrafish cardiac E-C coupling, membrane depolarization also activates voltage-gated calcium channels, which in turn activates SR calcium release. However, the relative contribution of SR calcium release is thought to be far more limited, contributing to around 20% of the calcium transient and the majority of the calcium necessary to activate contraction comes directly through transsarcolemmal influx from extracellular sources (Zhang et al. 2011; Bovo et al. 2013). As in most fish, zebrafish cardiomyocytes lack an extensive T-tubular network (Brette et al. 2008; Di Maio and Block 2008), such that an apparent spatial separation exists between RyR and LTCC possibly explaining the reduction in SR  $\text{Ca}^{2+}$  release (Bovo et al. 2013). Interestingly, RyR phosphorylation by PKA shows that it acts similarly to the mammalian system (Bovo et al. 2013) but the RyR are apparently organized into release clusters with low cytosolic calcium sensitivity (Bovo et al. 2013). However, calcium sparks have been demonstrated in zebrafish that are quite similar in properties and frequency to trout, mammalian and human cardiomyocytes. Although zebrafish hearts may have similar heart rates and action potential durations with respect to humans, the underlying mechanisms of E-C coupling still need to be resolved.

These differences in E-C coupling have profound differences in the way that contractility is physiologically regulated in each system. Due to the dominant role of SR calcium release in mammalian systems, contractility is primarily controlled by modulating the amount of SR calcium release with lesser effects through increasing calcium influx. Since SR calcium release is affected by the SR calcium load, contractility is indirectly affected by the activity of SR-ATPases (SERCA).

In zebrafish myocytes, contractility is less reliant on CICR and is primarily regulated by modulating calcium entry, which occurs mainly through L-type and T-type calcium channels with secondary effects through reverse-mode sodium-calcium exchange (NCX) activity. In zebrafish ventricular myocytes,  $I_{\text{Ca,L}}$  accounts for 50% of calcium influx (Zhang et al. 2011). Zebrafish also maintain mammalian-like systems of response to  $\beta$  adrenergic receptor stimulation through LTCC-mediated increased cytosolic  $\text{Ca}^{2+}$  transient amplitude upon addition of the PKA activator forskolin (Bovo et al. 2013). Just as in mammalian hearts, increased heart

rate increases diastolic calcium and increases calcium-dependent inactivation. Increased diastolic calcium levels would also be expected to increase SR calcium loads in the zebrafish heart. However, because SR calcium release is unlikely to be a dominant source of activating calcium, the increase in SR calcium release is unable to compensate for the decreased calcium entry and zebrafish hearts exhibit a negative force-frequency response (Bovo et al. 2013). However, this interpretation is complicated by the fact that the murine heart, in which SR  $\text{Ca}^{2+}$  release plays a dominant role, often exhibits a negative force-frequency response. The apparent lesser importance of the SR for E-C coupling is reflected in a lack of arrhythmias with morpholino-knockdown of SERCA activity but defects in contractility in zebrafish embryos (Ebert et al. 2005).

Increased frequency directly reduces  $I_{\text{Ca}}$ , by limiting the time to recovery from voltage-dependent inactivation and indirectly reduces  $I_{\text{Ca}}$ , by increasing calcium-dependent inactivation through rising diastolic calcium levels. In combination, increasing the effective heart rate in single ventricular myocytes, from 30 bpm to 120 bpm, reduces  $I_{\text{Ca}}$  by 45% (Zhang et al. 2011). Yet, the magnitude of the calcium transient is relatively unaffected suggesting to some investigators that an alternative mechanism of calcium influx must be in place. However, this notion remains controversial in light of the comparable properties of the RYR2 and the  $\text{Ca}^{2+}$  sparks in zebrafish.

Contractility in mammalian cardiomyocytes varies with voltage and the relationship closely follows the voltage-dependence of activation of LTCC which peaks near 0 mV, reflecting an optimal balance between channel activation and driving force for calcium entry. However, in zebrafish myocytes, contractility continues to increase at more depolarized membrane potentials. In mammalian hearts the primary role of NCX is in relaxation, exchanging cytosolic calcium for extracellular sodium, which is favored by hyperpolarized membrane potentials and by high cytosolic calcium levels. However, due to the stoichiometry of  $3 \text{Na}^+:\text{Ca}^{2+}$ , strong depolarization can induce reverse-mode NCX activity resulting in calcium influx.

In fish, both  $I_{\text{Ca}}$  and reverse-mode NCX are capable of triggering  $\text{Ca}^{2+}$  release from the SR (Hove-Madsen et al. 2003). Reverse-mode NCX activity is most favorable when there is strong membrane depolarization, high cytosolic sodium concentration, and low cytosolic calcium – conditions that are present at the upstroke of the action potential (Birkedal and Shiels 2007). This is augmented by the fact that fish typically have a higher density of NCX than adult mammals. At high stimulation rates,  $I_{\text{Ca}}$  is reduced and  $[\text{Na}^+]_i$  may further increase, favoring increasing amounts of reverse-mode NCX. In general, a higher NCX activity is observed in teleost cardiomyocytes relative to mammalian (Vornanen 1999; Hove-Madsen et al. 2000; Zhang et al. 2011). Therefore, high NCX activity may contribute to the zebrafish heart's ability to maintain contractility at high heart rates despite the strong suppressive effects on  $I_{\text{Ca}}$ . Defective NCX activity leads to abnormal  $\text{Ca}^{2+}$  transients and de-synchronized contractions in the tremblor (tre) mutant, indicating the importance of NCX for proper rhythmicity of the zebrafish heart (Langenbacher et al. 2005).

It is likely that to some degree, the small volume and elongated shape of zebrafish ventricular myocytes (and the commensurate high surface-to-volume relationship) compensates for lack of T-tubules as in mammalian atrial cells (Blatter et al. 2003). This could relate to the impact of temperature on CICR. Mammalian hearts can induce rapid elevations in cytosolic  $\text{Ca}^{2+}$  via CICR, but it appears that zebrafish must rely primarily on direct  $\text{Ca}^{2+}$  influx (Verkerk and Remme 2012) as a slower but more robust mechanism of E-C coupling in a temperature variable environment. However this conclusion must be reconciled with the following facts: (1) the SR  $\text{Ca}^{2+}$  load and uptake rate (temperature adjusted) in many teleosts is comparable to or greater than that of mammals; (2) caffeine contractures are comparable in magnitude; (3) calcium can be released spontaneously from the SR and (4) the properties of sparks are similar to mammals. In some respects one could view the zebrafish as a model of immature human cardiac myocytes in many ways with the lack of t-tubules and reliance on extracellular  $\text{Ca}^{2+}$  (Huang et al. 2005). While this may not be the ideal model for E-C coupling to compare to mature humans, the similarities with immature human cardiomyocytes and overall developmental pathways allow zebrafish to be used in recapitulating disorders that occur at these stages of development.

### 4.3 Contraction

Work characterizing myofilament mechanical function is critical to understanding contractile dynamics of many zebrafish cardiomyopathy models. Several of these studies have concluded that cardiac myofibrils from zebrafish, like those from mice, are suitable contractile models to study cardiac function at the sarcomeric level (Iorga et al. 2011; Dvornikov et al. 2014). The proportions of the zebrafish cardiomyocyte make cardiac myofibrils ideally suited for force and sarcomere length measurements in response to changes in  $[\text{Ca}^{2+}]$ , as the entire cell can be perfused simultaneously (Stehle et al. 2002, 2009; Lionne et al. 2003). The fundamental mechanism of cardiac contraction is conserved across vertebrates. The basic contractile unit of the sarcomere is composed of thick and thin filaments, which form the characteristic striated pattern of cardiac muscle and regulate cardiac contraction and relaxation. As the cytosolic  $\text{Ca}^{2+}$  concentration increases, the regulatory  $\text{Ca}^{2+}$  binding site II of cTnC becomes occupied, leading to a conformational change that exposes a hydrophobic patch on cTnC. This hydrophobic patch then interacts with TnI and allows the TnI inhibitory peptide to withdraw from the actin filament (Parmacek and Solaro 2004). The cTnC- $\text{Ca}^{2+}$  binding interaction also interrupts the TnT-Tropomyosin (Tm) interaction, and permits actin/myosin cross-bridge formation and initiates muscle contraction. The modulation of twitch force by both extracellular  $[\text{Ca}^{2+}]$  and sarcomere length (SL), myofilament length-dependent activation, is an intrinsic property and critical mediator of contractile function of both mammalian and zebrafish cardiomyocytes (Dvornikov et al. 2014) (Fig. 7).

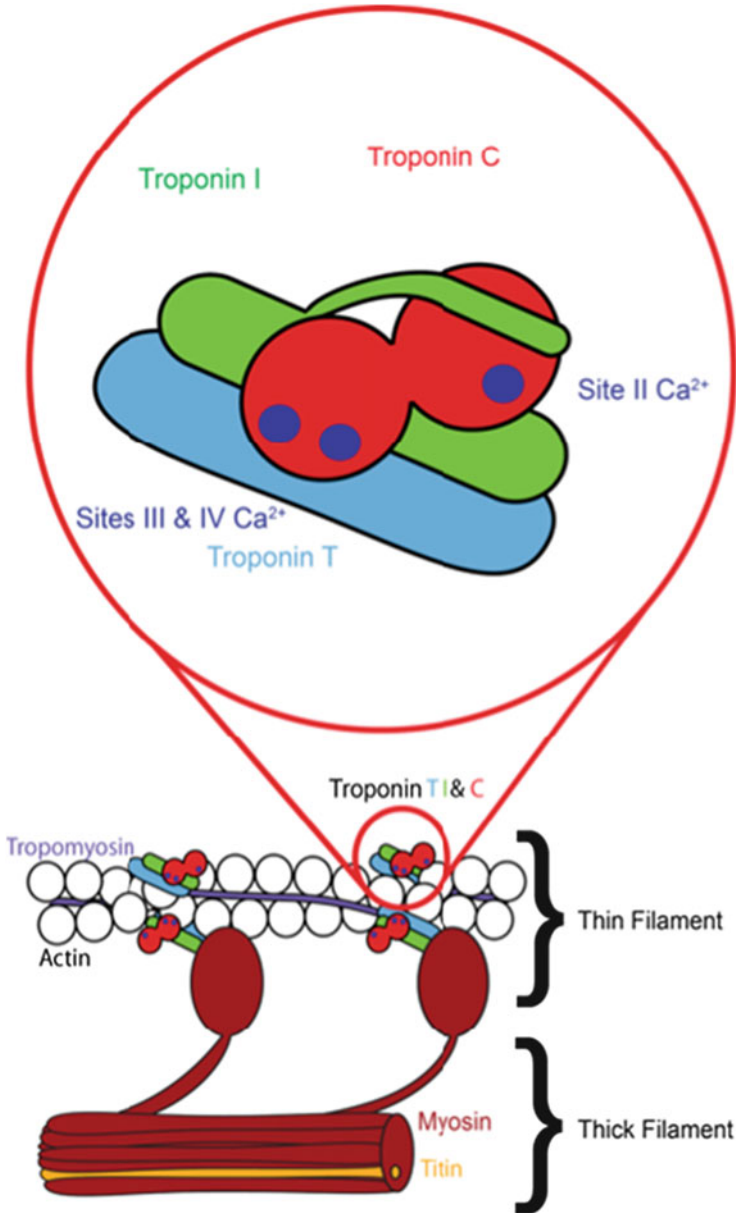


Fig. 7 Schematic of the role of troponin in muscle contraction

Similarities exist between the mammalian and zebrafish system in regulation of contractile force, namely a direct proportionality between extracellular  $[Ca^{2+}]$  and cytosolic  $Ca^{2+}$  transients (Dvornikov et al. 2014). As has been established in the mammalian system (Allen and Kurihara 1979; Janssen and de Tombe 1997) cell



length does not affect the magnitude of the cytosolic  $\text{Ca}^{2+}$  transient in the first twitch following cell stretch, just as in zebrafish (Dvornikov et al. 2014). The appearance of ventricular myofibrils from zebrafish is similar to mouse papillary muscles (Iorga et al. 2008, 2011). These myofibrils often branch just as in mammals (Iorga et al. 2011). The resting SL recorded in zebrafish (1.85  $\mu\text{m}$  in (Dvornikov et al. 2014); 2.12  $\mu\text{m}$  in (Iorga et al. 2011)) is comparable to that in all teleost species studied to date (Shiels et al. 2006; Patrick et al. 2011) as well as murine models ((SL =  $2.03 \pm 0.03 \mu\text{m}$ ) (Iorga et al. 2008)).

$\text{Ca}^{2+}$  sensitivity in cardiac myocytes is influenced much more by SL than skeletal myocytes (Hanft and McDonald 2010). In zebrafish,  $\text{Ca}^{2+}$ -dependent force of myotomal myofibrils is almost one order of magnitude lower (Iorga et al. 2011) than skeletal muscle of other teleosts (Altringham and Johnston 1982) and mammals (Edman 2005; Poggesi et al. 2005). The contractile element and thus cardiac TnC have an increased sensitivity for  $\text{Ca}^{2+}$  at longer sarcomere lengths (Granzier et al. 1991; de Tombe et al. 2010). Extracellular  $\text{Ca}^{2+}$ , cytosolic  $\text{Ca}^{2+}$ , and consequently twitch force are directly proportion in single cardiac myocytes isolated from adult zebrafish hearts (Dvornikov et al. 2014). The kinetics of force development in zebrafish were found to be dependent on  $[\text{Ca}^{2+}]$  but the relaxation was independent, neither of which was affected by SL (Dvornikov et al. 2014) in agreement with findings on the mammalian sarcomere (Poggesi et al. 2005). The rate constant of force development after  $\text{Ca}^{2+}$  activation, isometric force at maximal  $\text{Ca}^{2+}$  activation,  $\text{Ca}^{2+}$  sensitivity of force, and force response to an external stretch are all comparable in the zebrafish and mice models (Iorga et al. 2011). In mammalian systems, persistent stretch is concurrent over minutes with a slow increase in twitch force (Cingolani et al. 2011) known as the slow force response (SFR), which is poorly understood. This property is not present in either trout (Patrick et al. 2011) or zebrafish (Dvornikov et al. 2014), therefore the study of the mechanisms of SFR may not be possible in zebrafish.

The mammalian force–SL relationship is curvilinear and depends on extracellular  $[\text{Ca}^{2+}]$  (ter Keurs et al. 1980; Kentish et al. 1986). The slope of this relationship increases proportionally with stretch as does the twitch force in mammals (ter Keurs et al. 1980; Kentish et al. 1986; de Tombe and ter Keurs 1991). This forms the basis of the Frank-Starling response of the heart, in which the heart ejects a greater stroke volume at greater end diastolic volumes. This is an essential property of the myocardium which differentiates it from skeletal muscles and this response is intact in the zebrafish heart and individual myocytes. The force–pCa relationship is comparable in mice and zebrafish myofibrillar bundles, though maximal force may be slightly higher in the latter (Iorga et al. 2011). Both zebrafish skinned myofibrils and ventricular cells display a length-dependent force generation that is similar in magnitude to the mammalian sarcomere (Mateja and de Tombe 2012; Dvornikov et al. 2014). Increased sensitivity of the zebrafish sarcomere is thought to be causal as the changes occur at constant cytosolic  $[\text{Ca}^{2+}]$  (Dvornikov et al. 2014). The zebrafish is a good model for studying length dependent activation (LDA) as it shares this property as expected with other teleosts such as trout (Patrick et al. 2010) as well as mammals (Mateja and de Tombe 2012).



Passive stiffness is similar in zebrafish and mice myofibrils with low stretch (Iorga et al. 2011). Passive force at low stretch in rainbow trout and rats also shows similar levels of passive stiffness (Patrick et al. 2010). However, with extensive stretch (beyond  $\sim 2.5 \mu\text{m}$ ), passive forces in zebrafish and mice are very different (Iorga et al. 2011). Force decay upon  $\text{Ca}^{2+}$  removal is biphasic in zebrafish (Steffen et al. 2007; Iorga et al. 2011) and numerous species of mammals (Stehle et al. 2002; Poggesi et al. 2005). The initial slow decay of force can be used to estimate cross-bridge detachment, this phase occurs while SL is constant (Poggesi et al. 2005; Stehle et al. 2009); the rate constant corresponding to this phase is similar in zebrafish and mice when measured at  $10^\circ\text{C}$  (Iorga et al. 2011). A delay then occurs which is longer in zebrafish than that seen in mice at this common experimental temperature (Iorga et al. 2011). Following the delay is a faster force decay occurs as the sarcomeres lengthens accelerating cross-bridge detachment (Poggesi et al. 2005; Stehle et al. 2009); the rate constant corresponding to this phase of relaxation is smaller in zebrafish than in mice (Iorga et al. 2011). The overall effect is that zebrafish myofibrils relax more slowly than those isolated from mice, this makes sense in light of murine ( $\sim 600$  bpm at  $37^\circ\text{C}$ ) and zebrafish ( $\sim 150$  bpm at  $28.5^\circ\text{C}$ ) resting HR at their respective physiological temperatures (Iorga et al. 2011). While the molecular basis is currently unknown, it has been speculated that this is due to different titin isoforms and/or differential phosphorylation states of the contractile proteins in fish (Seeley et al. 2007; Patrick et al. 2010; Iorga et al. 2011; Zou et al. 2015) based on the weak contractile phenotype of the *pickwick* mutation (Driever et al. 1996) in zebrafish. A further benefit in using zebrafish myofibrils is their slower rate of contraction and relaxation compared to murine models such that kinetic parameters can be determined above  $10^\circ\text{C}$  (Iorga et al. 2011).

Variation in paralogs of contractile proteins can create variation in the mechanics of cardiac contraction present in zebrafish studies of cardiac myofibrils (Iorga et al. 2011; Dvornikov et al. 2014). In mammals, many of these sarcomeric proteins have muscle-specific paralogs that are expressed such that a single paralog is uniquely found in each muscle type (Huang and Jin 1999). Mutant zebrafish have been used to study cardiac specific orthologs of human sarcomeric proteins such as troponin T (Sehnert et al. 2002), troponin C (Ohte et al. 2009; Sogah et al. 2010), tropomyosin (Zhao et al. 2008), myosin light chain (Rottbauer et al. 2006), and titin (Seeley et al. 2007; Zou et al. 2015). However both the expression patterns and function of these same sarcomeric proteins may vary from humans due to retention of additional duplicated products in the zebrafish genome. Hence the phenotype of these mutants may not be directly translated to humans without knowledge of the fish-specific molecular basis. While the overall mechanism of contraction is conserved, the molecular basis of contraction in fish provides an interesting platform to understand the consequence of genome duplication in the zebrafish model.

## 5 Molecular Basis of Cardiac Function

With numerous mutations of zebrafish genes serving as both cardiomyopathy and channelopathy models, it becomes increasingly important to ensure that the correct zebrafish equivalent to the disease-causing human gene is found. Despite the fact that zebrafish have additional copies of many genes that are important to cardiac function, the wealth of knowledge available on the genomic level allows us to translate the physiological and biological conclusions that can be gleaned from zebrafish-based experiments effectively to mammalian systems. By addressing questions on the molecular level, one can better design experiments that are biologically appropriate to the model. An example of this can be seen in using genomic and phylogenetic analyses in conjunction with transcriptomic data, and integrating these findings with protein structure and functional data (e.g., molecular dynamics simulations and isothermal titration calorimetry) for exploration of troponin (Tn) paralogs (Genge et al. 2016; Stevens et al. 2016).

In mammalian cardiac cells co-expression of multiple variants of proteins composing the Tn complex can result in modified protein interactions and variation in  $\text{Ca}^{2+}$  sensitivity leading to non-uniform contraction (Wei and Jin 2011). Co-expression for Tn isoforms is often indicative of a diseased state of the mammalian heart (Anderson et al. 1991; Wei and Jin 2011). For example, the co-presence of multiple TnT splice variants in adult mammalian hearts reduces cardiac efficiency by desynchronizing the  $\text{Ca}^{2+}$  activation of the thin filaments (Jin et al. 2008). While mixed isoform usage of both TnT and TnI is found during fetal cardiac development, co-expression results in less contractile force (Fentzke et al. 1999; Yin et al. 2015). Many sarcomeric proteins also have multiple homologs expressed in the zebrafish heart (Alderman et al. 2012; Genge et al. 2013; Shih et al. 2015). Paralogs for transcripts of both TnC and TnI are expressed in a chamber- and temperature-specific manner in cardiac tissue of zebrafish (Sogah et al. 2010; Alderman et al. 2012; Genge et al. 2013, 2016). The presence of multiple fish-specific gene products of important components of the cardiac contractile element may be indicative of how fish have evolved mechanisms to thrive in variable environments. Incorporating the chamber-specific variation with temperature response reveals the complexity of these mechanisms in achieving survival, but may also be important to understanding variability in results in a zebrafish model.

TnC is a highly conserved protein across phylogeny, with few sequence changes maintained in any vertebrate ortholog. The cardiac contractile element in all species studied to date is less sensitive to  $\text{Ca}^{2+}$  when the temperature is decreased (Harrison and Bers 1989), therefore it is understandable that a higher relative TnC sensitivity is needed for teleosts to maintain proper cardiac function in colder environments (Gillis et al. 2005, 2007). The role of paralog usage likely creates functional differences in the atrium and ventricle through the use of chamber-specific isoforms of many contractile proteins (e.g., myosin heavy chain and myosin light chain (Karasinski et al. 2001)). In zebrafish, TnC1b and TnC1a transcripts are expressed

in a chamber-specific manner (Genge et al. 2013). This could possibly lead to changes in the  $\text{Ca}^{2+}$  affinity of the entire Tn complex.

The consequences of many gene products for Tn have been explored in some detail by our group on the protein function level (Genge et al. 2013, 2016; Stevens et al. 2016). These paralogs have very similar functions, but the differences between them involve the subtle manipulation of the energetic landscape of the transition between closed and open conformations. This has an effect on  $\text{Ca}^{2+}$  binding properties that is related to  $\text{Ca}^{2+}$  sensitivity, yet still maintains limited structural deviation between the structural models of each TnC paralog (Stevens et al. 2016). The expression of multiple TnC paralogs with minimal differences in  $\text{Ca}^{2+}$  sensitivity may allow flexibility in response to variable environmental conditions while still maintaining uniform cardiac contraction. While two paralogs of the cardiac TnC protein are not present in humans, the mechanism of initiation of cardiac contraction is conserved. Many disease-causing mutations are expected to increase  $\text{Ca}^{2+}$  sensitivity in a manner similar to the naturally occurring mutations in fish TnC (Gillis and Tibbits 2002), as a result, great care must be taken in the generalization of biological data. Additionally a more complete understanding of the molecular details of the contractile apparatus machinery across species will allow us to more accurately and efficaciously interpret and translate experimental designs and results between the zebrafish model and human disease.

Interaction sites that mediate important functions by binding regulatory proteins have strong evolutionary constraints on amino acid substitutions (Guharoy and Chakrabarti 2005). The conformation of TnC increases in degree of hydrophobic patch opening upon interaction with the switch region of TnI in mammalian models (Gagne et al. 1995; Li et al. 1999). The TnI switch peptide (TnI<sub>SW</sub>) will bind to and stabilize the open conformation of TnC, while simultaneously occluding the hydrophobic cleft (Li et al. 1999). To fully understand the dynamics between the open and closed state of TnC, TnI is necessary to stabilize the open conformation, which results in higher sensitivity. Having multiple paralogs in combination to form the Tn complex in teleost heart will change strength of interaction. A lower strength of interaction between mammalian cardiac TnC/TnI is responsible, at least in part, for the dependence of cardiac contractility on the formation of strong cross-bridges for full activation to occur. The increased dependence of strong cross-bridge formation has been suggested to be partially responsible for the steeper length dependence of force generation. Variability between contacts and residue distances between the TnI switch and TnC paralogs may promote faster sarcomeric relaxation and lower  $\text{Ca}^{2+}$  sensitivity (Palpant et al. 2010), as has been found in mammalian TnI3 (Genge et al. 2016). Correlated mutations suggest that compensatory changes that occur between interacting residues are crucial to maintain protein function (Ovchinnikov et al. 2014). Utilizing the teleost Tn complex thus provides an example of how compensatory substitutions to prevent loss of function and provide an important capacity to adapt, as well as emphasize the importance of looking at mutations in one protein in context with interacting proteins. An understanding of the interactions with other proteins is necessary for full understanding of variability in

function of Tn or any other sarcomeric protein in not only the zebrafish, but also all vertebrate models.

The work done on the evolution of paralogs of the contractile unit can contextualize the variation seen in zebrafish as a cardiac model. Certain paralogs may be utilized to recapitulate a mammalian model under certain conditions despite over differences in gene and protein structures. The co-evolution of Tn subunits can thus be used for the model of variation in contractile function as well as understanding the consequences of gene duplication on contractile function in the zebrafish. This work is by no means in isolation. Another example can be seen in work focused on the importance of transcriptional regulation for paralog usage and splice variation in titin in producing diseased phenotype in zebrafish cardiomyopathy models (Seeley et al. 2007; Zou et al. 2015). It may be necessary to understand the impact of retained duplicate gene products on the molecular level in order to accurately generate biological questions as well as explain a number of physiological mechanisms that occur in the zebrafish.

## 6 Conclusions/Summary

Although numerous caveats exist in using zebrafish to directly model human cardiac physiology, for specific questions the advantages of the zebrafish model are obvious. The relative ease of genetic manipulation and the conservation of many components of E-C coupling make the adult zebrafish an attractive model for cardiac function studies. This requires accurate knowledge of the molecular basis of the components of cardiac ionic currents and the contractile unit. Despite variation in the molecular basis, the conservation of the structure of critical domains of several ion channels and sarcomeric proteins does not preclude this model if appropriate attention is paid to evolutionary divergence. The assumption cannot be made that an orthologous gene in zebrafish will have the same function as it does in human so appropriate phylogenetic studies coupled with functional assays should be used.

## References

- Abdelfattah AS, Farhi SL, Zhao Y, Brinks D, Zou P, Ruangkittisakul A, Platasa J, Pieribone VA, Ballanyi K, Cohen AE, Campbell RE (2016) A bright and fast red fluorescent protein voltage indicator that reports neuronal activity in organotypic brain slices. *J Neurosci* 36(8):2458–2472
- Abi-Gerges N, Holkham H, Jones EM, Pollard CE, Valentin JP, Robertson GA (2011) hERG subunit composition determines differential drug sensitivity. *Br J Pharmacol* 164(2b):419–432
- Alday A, Alonso H, Gallego M, Urrutia J, Letamendia A, Callol C, Casis O (2014) Ionic channels underlying the ventricular action potential in zebrafish embryo. *Pharmacol Res* 84:26–31

- Alderman SL, Klaiman JM, Deck CA, Gillis TE (2012) Effect of cold acclimation on troponin I isoform expression in striated muscle of rainbow trout. *Am J Physiol Regul Integr Comp Physiol* 303(2):R168–R176
- Allen DG, Kurihara S (1979) Calcium transients at different muscle lengths in rat ventricular muscle [proceedings]. *J Physiol* 292:68P–69P
- Altringham JD, Johnston IA (1982) The pCa-tension and force-velocity characteristics of skinned fibres isolated from fish fast and slow muscles. *J Physiol* 333:421–449
- Anderson PA, Malouf NN, Oakeley AE, Pagani ED, Allen PD (1991) Troponin T isoform expression in humans. A comparison among normal and failing adult heart, fetal heart, and adult and fetal skeletal muscle. *Circ Res* 69(5):1226–1233
- Arnaut R, Ferrer T, Huisken J, Spitzer K, Stainier DY, Tristani-Firouzi M, Chi NC (2007) Zebrafish model for human long QT syndrome. *Proc Natl Acad Sci U S A* 104(27):11316–11321
- Asnani A, Peterson RT (2014) The zebrafish as a tool to identify novel therapies for human cardiovascular disease. *Dis Model Mech* 7(7):763–767
- Bakkers J (2011) Zebrafish as a model to study cardiac development and human cardiac disease. *Cardiovasc Res* 91(2):279–288
- Bill BR, Petzold AM, Clark KJ, Schimmenti LA, Ekker SC (2009) A primer for morpholino use in zebrafish. *Zebrafish* 6(1):69–77
- Birkedal R, Shiels HA (2007) High [Na<sup>+</sup>]<sub>i</sub> in cardiomyocytes from rainbow trout. *Am J Physiol Regul Integr Comp Physiol* 293(2):R861–R866
- Blatter LA, Kockskamper J, Sheehan KA, Zima AV, Huser J, Lipsius SL (2003) Local calcium gradients during excitation-contraction coupling and alternans in atrial myocytes. *J Physiol* 546(Pt 1):19–31
- Bovo E, Dvornikov AV, Mazurek SR, de Tombe PP, Zima AV (2013) Mechanisms of Ca<sup>2+</sup> handling in zebrafish ventricular myocytes. *Pflugers Arch* 465(12):1775–1784
- Brette F, Luxan G, Cros C, Dixey H, Wilson C, Shiels HA (2008) Characterization of isolated ventricular myocytes from adult zebrafish (*Danio rerio*). *Biochem Biophys Res Commun* 374(1):143–146
- Broussard GJ, Liang R, Tian L (2014) Monitoring activity in neural circuits with genetically encoded indicators. *Front Mol Neurosci* 7:97
- Chaudhari GH, Chennubhotla KS, Chatti K, Kulkarni P (2013) Optimization of the adult zebrafish ECG method for assessment of drug-induced QTc prolongation. *J Pharmacol Toxicol Methods* 67(2):115–120
- Chen TW, Wardill TJ, Sun Y, Pulver SR, Renninger SL, Baohan A, Schreiter ER, Kerr RA, Orger MB, Jayaraman V, Looger LL, Svoboda K, Kim DS (2013) Ultrasensitive fluorescent proteins for imaging neuronal activity. *Nature* 499(7458):295–300
- Choi BR, Salama G (2000) Simultaneous maps of optical action potentials and calcium transients in guinea-pig hearts: mechanisms underlying concordant alternans. *J Physiol* 529(Pt 1):171–188
- Chopra SS, Stroud DM, Watanabe H, Bennett JS, Burns CG, Wells KS, Yang T, Zhong TP, Roden DM (2010) Voltage-gated sodium channels are required for heart development in zebrafish. *Circ Res* 106(8):1342–50
- Cingolani HE, Ennis IL, Aiello EA, Perez NG (2011) Role of autocrine/paracrine mechanisms in response to myocardial strain. *Pflugers Arch* 462(1):29–38
- Cohen AE (2016) Optogenetics: turning the microscope on its head. *Biophys J* 110(5):997–1003
- Collins JE, White S, Searle SM, Stemple DL (2012) Incorporating RNA-seq data into the zebrafish Ensembl genebuild. *Genome Res* 22(10):2067–2078
- Cotter PA, Han AJ, Everson JJ, Rodnick KJ (2008) Cardiac hemodynamics of the rainbow trout (*Oncorhynchus mykiss*) using simultaneous Doppler echocardiography and electrocardiography. *J Exp Zool A Ecol Genet Physiol* 309(5):243–254

- Coucelo J, Joaquim N, Coucelo J (2000) Calculation of volumes and systolic indices of heart ventricle from *Halobatrachus didactylus*: echocardiographic noninvasive method. *J Exp Zool* 286(6): 585–595
- Dahme T, Katus HA, Rottbauer W (2009) Fishing for the genetic basis of cardiovascular disease. *Dis Model Mech* 2(1-2):18–22
- de Tombe PP, ter Keurs HE (1991) Sarcomere dynamics in cat cardiac trabeculae. *Circ Res* 68(2):588–596
- de Tombe PP, Mateja RD, Tachampa K, Ait Mou Y, Farman GP, Irving TC (2010) Myofilament length dependent activation. *J Mol Cell Cardiol* 48(5):851–858
- Dhillon SS, Doro E, Magyary I, Egginton S, Sik A, Muller F (2013) Optimisation of embryonic and larval ECG measurement in zebrafish for quantifying the effect of QT prolonging drugs. *PLoS One* 8(4), e60552
- Di Maio A, Block BA (2008) Ultrastructure of the sarcoplasmic reticulum in cardiac myocytes from Pacific bluefin tuna. *Cell Tissue Res* 334(1):121–134
- Ding W, Lin E, Ribeiro A, Sarunic MV, Tibbits GF, Beg MF (2014) Automatic cycle averaging for denoising approximately periodic spatiotemporal signals. *IEEE Trans Med Imaging* 33(8): 1749–1759
- Driever W, Solnica-Krezel L, Schier AF, Neuhauss SC, Malicki J, Stemple DL, Stainier DY, Zwartkuis F, Abdellah S, Rangini Z, Belak J, Boggs C (1996) A genetic screen for mutations affecting embryogenesis in zebrafish. *Development* 123:37–46
- Dvornikov AV, Dewan S, Alekhina OV, Pickett FB, de Tombe PP (2014) Novel approaches to determine contractile function of the isolated adult zebrafish ventricular cardiac myocyte. *J Physiol* 592(9):1949–1956
- Ebert AM, Hume GL, Warren KS, Cook NP, Burns CG, Mohideen MA, Siegal G, Yelon D, Fishman MC, Garrity DM (2005) Calcium extrusion is critical for cardiac morphogenesis and rhythm in embryonic zebrafish hearts. *Proc Natl Acad Sci U S A* 102(49):17705–17710
- Edman KA (2005) Contractile properties of mouse single muscle fibers, a comparison with amphibian muscle fibers. *J Exp Biol* 208(Pt 10):1905–1913
- Efimov IR, Nikolski VP, Salama G (2004) Optical imaging of the heart. *Circ Res* 95(1):21–33
- Farrell AP, Jones DR (1992) The heart. In: Hoar WS, Randall DJ, Farrell AP (eds) *Fish physiology*. Academic, San Diego
- Fast VG (2005) Simultaneous optical imaging of membrane potential and intracellular calcium. *J Electrocardiol* 38(4 Suppl):107–112
- Fentzke RC, Buck SH, Patel JR, Lin H, Wolska BM, Stojanovic MO, Martin AF, Solaro RJ, Moss RL, Leiden JM (1999) Impaired cardiomyocyte relaxation and diastolic function in transgenic mice expressing slow skeletal troponin I in the heart. *J Physiol* 517(Pt 1):143–157
- Fields PA, Somero GN (1998) Hot spots in cold adaptation: localized increases in conformational flexibility in lactate dehydrogenase A(4) orthologs of Antarctic notothenioid fishes. *Proc Natl Acad Sci U S A* 95(19):11476–11481
- Fu CY, Lee HC, Tsai HJ (2009) The molecular structures and expression patterns of zebrafish troponin I genes. *Gene Expr Patterns* 9(5):348–356
- Gagne SM, Tsuda S, Li MX, Smillie LB, Sykes BD (1995) Structures of the troponin C regulatory domains in the apo and calcium-saturated states. *Nat Struct Biol* 2(9):784–789
- Gemberling M, Karra R, Dickson AL, Poss KD (2015) Nrg1 is an injury-induced cardiomyocyte mitogen for the endogenous heart regeneration program in zebrafish. *Elife* 4
- Genge CE, Davidson WS, Tibbits GF (2013) Adult teleost heart expresses two distinct troponin C paralogs: cardiac TnC and a novel and teleost-specific ssTnC in a chamber- and temperature-dependent manner. *Physiol Genomics* 45(18):866–875
- Genge CE, Stevens CM, Davidson WS, Singh G, Peter Tieleman D, Tibbits GF (2016) Functional divergence in teleost cardiac troponin paralogs guides variation in the interaction of TnI switch region with TnC. *Genome Biol Evol* 8(4):994–1011

- Gerger CJ, Thomas JK, Janz DM, Weber LP (2015) Acute effects of beta-naphthoflavone on cardiorespiratory function and metabolism in adult zebrafish (*Danio rerio*). *Fish Physiol Biochem* 41(1):289–298
- Gillis TE, Tibbits GF (2002) Beating the cold: the functional evolution of troponin C in teleost fish. *Comp Biochem Physiol A Mol Integr Physiol* 132(4):763–772
- Gillis TE, Liang B, Chung F, Tibbits GF (2005) Increasing mammalian cardiomyocyte contractility with residues identified in trout troponin C. *Physiol Genomics* 22(1):1–7
- Gillis TE, Marshall CR, Tibbits GF (2007) Functional and evolutionary relationships of troponin C. *Physiol Genomics* 32(1):16–27
- Granato M, van Eeden FJ, Schach U, Trowe T, Brand M, Furutani-Seiki M, Haffter P, Hammerschmidt M, Heisenberg CP, Jiang YJ, Kane DA, Kelsh RN, Mullins MC, Odenthal J, Nusslein-Volhard C (1996) Genes controlling and mediating locomotion behavior of the zebrafish embryo and larva. *Development* 123:399–413
- Granzier HL, Akster HA, Ter Keurs HE (1991) Effect of thin filament length on the force-sarcomere length relation of skeletal muscle. *Am J Physiol* 260(5 Pt 1):C1060–C1070
- Guharoy M, Chakrabarti P (2005) Conservation and relative importance of residues across protein-protein interfaces. *Proc Natl Acad Sci U S A* 102(43):15447–15452
- Hanft LM, McDonald KS (2010) Length dependence of force generation exhibit similarities between rat cardiac myocytes and skeletal muscle fibres. *J Physiol* 588(Pt 15):2891–2903
- Harrison SM, Bers DM (1989) Influence of temperature on the calcium sensitivity of the myofilaments of skinned ventricular muscle from the rabbit. *J Gen Physiol* 93(3):411–428
- Hassinen M, Haverinen J, Hardy ME, Shiels HA, Vornanen M (2015) Inward rectifier potassium current (I<sub>K1</sub>) and Kir2 composition of the zebrafish (*Danio rerio*) heart. *Pflugers Arch* 467(12):2437–2446
- Haverinen J, Vornanen M (2007) Temperature acclimation modifies sinoatrial pacemaker mechanism of the rainbow trout heart. *Am J Physiol Regul Integr Comp Physiol* 292(2):R1023–R1032
- Hein SJ, Lehmann LH, Kossack M, Juergensen L, Fuchs D, Katus HA, Hassel D (2015) Advanced echocardiography in adult zebrafish reveals delayed recovery of heart function after myocardial cryoinjury. *PLoS One* 10(4), e0122665
- Herron TJ, Lee P, Jalife J (2012) Optical imaging of voltage and calcium in cardiac cells & tissues. *Circ Res* 110(4):609–623
- Ho YL, Shau YW, Tsai HJ, Lin LC, Huang PJ, Hsieh FJ (2002) Assessment of zebrafish cardiac performance using Doppler echocardiography and power angiography. *Ultrasound Med Biol* 28(9):1137–1143
- Hou JH, Kralj JM, Douglass AD, Engert F, Cohen AE (2014) Simultaneous mapping of membrane voltage and calcium in zebrafish heart in vivo reveals chamber-specific developmental transitions in ionic currents. *Front Physiol* 5:344
- Hove-Madsen L, Llach A, Tort L (2000) Na<sup>(+)</sup>/Ca<sup>(2+)</sup>-exchange activity regulates contraction and SR Ca<sup>(2+)</sup> content in rainbow trout atrial myocytes. *Am J Physiol Regul Integr Comp Physiol* 279(5):R1856–R1864
- Hove-Madsen L, Llach A, Tibbits GF, Tort L (2003) Triggering of sarcoplasmic reticulum Ca<sup>2+</sup> release and contraction by reverse mode Na<sup>(+)</sup>/Ca<sup>(2+)</sup> exchange in trout atrial myocytes. *Am J Physiol Regul Integr Comp Physiol* 284(5):R1330–R1339
- Howe DG, Bradford YM, Conlin T, Eagle AE, Fashena D, Frazer K, Knight J, Mani P, Martin R, Moxon SA, Paddock H, Pich C, Ramachandran S, Ruef BJ, Ruzicka L, Schaper K, Shao X, Singer A, Sprunger B, Van Slyke CE, Westerfield M (2013) ZFIN, the Zebrafish Model Organism Database: increased support for mutants and transgenics. *Nucleic Acids Res* 41(Database issue):D854–D860
- Hu N, Yost HJ, Clark EB (2001) Cardiac morphology and blood pressure in the adult zebrafish. *Anat Rec* 264(1):1–12

- Huang QQ, Jin JP (1999) Preserved close linkage between the genes encoding troponin I and troponin T, reflecting an evolution of adapter proteins coupling the Ca(2+) signaling of contractility. *J Mol Evol* 49(6):780–788
- Huang J, Hove-Madsen L, Tibbits GF (2005) Na<sup>+</sup>/Ca<sup>2+</sup> exchange activity in neonatal rabbit ventricular myocytes. *Am J Physiol Cell Physiol* 288(1):C195–C203
- Huang WC, Hsieh YS, Chen IH, Wang CH, Chang HW, Yang CC, Ku TH, Yeh SR, Chuang YJ (2010) Combined use of MS-222 (tricaine) and isoflurane extends anesthesia time and minimizes cardiac rhythm side effects in adult zebrafish. *Zebrafish* 7(3):297–304
- Huang CC, Su TH, Shih CC (2015) High-resolution tissue Doppler imaging of the zebrafish heart during its regeneration. *Zebrafish* 12(1):48–57
- Hwang WY, Fu Y, Reyon D, Maeder ML, Tsai SQ, Sander JD, Peterson RT, Yeh JR, Joung JK (2013) Efficient genome editing in zebrafish using a CRISPR-Cas system. *Nat Biotechnol* 31(3):227–229
- Iorga B, Blaudeck N, Solzin J, Neulen A, Stehle I, Lopez Davila AJ, Pfitzer G, Stehle R (2008) Lys184 deletion in troponin I impairs relaxation kinetics and induces hypercontractility in murine cardiac myofibrils. *Cardiovasc Res* 77(4):676–686
- Iorga B, Neacsu CD, Neiss WF, Wagener R, Paulsson M, Stehle R, Pfitzer G (2011) Micromechanical function of myofibrils isolated from skeletal and cardiac muscles of the zebrafish. *J Gen Physiol* 137(3):255–270
- Jaimes R 3rd, Walton RD, Pasdois P, Bernus O, Efimov IR, Kay MW (2016) A technical review of optical mapping of intracellular calcium within myocardial tissue. *Am J Physiol Heart Circ Physiol* 310(11):H1388–H1401
- Janssen PM, de Tombe PP (1997) Uncontrolled sarcomere shortening increases intracellular Ca<sup>2+</sup> transient in rat cardiac trabeculae. *Am J Physiol* 272(4 Pt 2):H1892–H1897
- Jin JP, Zhang Z, Bautista JA (2008) Isoform diversity, regulation, and functional adaptation of troponin and calponin. *Crit Rev Eukaryot Gene Expr* 18(2):93–124
- Jin L, Han Z, Platisa J, Woollorton JR, Cohen LB, Pieribone VA (2012) Single action potentials and subthreshold electrical events imaged in neurons with a fluorescent protein voltage probe. *Neuron* 75(5):779–785
- Johnson AC, Turko AJ, Klaiman JM, Johnston EF, Gillis TE (2014) Cold acclimation alters the connective tissue content of the zebrafish (*Danio rerio*) heart. *J Exp Biol* 217(Pt 11):1868–1875
- Kane DA, Maischein HM, Brand M, van Eeden FJ, Furutani-Seiki M, Granato M, Haffter P, Hammerschmidt M, Heisenberg CP, Jiang YJ, Kelsh RN, Mullins MC, Odenthal J, Warga RM, Nusslein-Volhard C (1996) The zebrafish early arrest mutants. *Development* 123:57–66
- Karasinski J, Sokalski A, Kilarski W (2001) Correlation of myofibrillar ATPase activity and myosin heavy chain content in ventricular and atrial myocardium of fish heart. *Folia Histochem Cytobiol* 39(1):23–28
- Kentish JC, ter Keurs HE, Ricciardi L, Bucx JJ, Noble MI (1986) Comparison between the sarcomere length-force relations of intact and skinned trabeculae from rat right ventricle. Influence of calcium concentrations on these relations. *Circ Res* 58(6):755–768
- Kok FO, Shin M, Ni CW, Gupta A, Grosse AS, van Impel A, Kirchmaier BC, Peterson-Maduro J, Kourkoulis G, Male I, DeSantis DF, Sheppard-Tindell S, Ebarasi L, Betsholtz C, Schulte-Merker S, Wolfe SA, Lawson ND (2015) Reverse genetic screening reveals poor correlation between morpholino-induced and mutant phenotypes in zebrafish. *Dev Cell* 32(1):97–108
- Langenbacher AD, Dong Y, Shu X, Choi J, Nicoll DA, Goldhaber JJ, Philipson KD, Chen JN (2005) Mutation in sodium-calcium exchanger 1 (NCX1) causes cardiac fibrillation in zebrafish. *Proc Natl Acad Sci U S A* 102(49):17699–17704
- Langheinrich U, Vacun G, Wagner T (2003) Zebrafish embryos express an orthologue of HERG and are sensitive toward a range of QT-prolonging drugs inducing severe arrhythmia. *Toxicol Appl Pharmacol* 193(3):370–382
- Laughner JI, Ng FS, Sulkin MS, Arthur RM, Efimov IR (2012) Processing and analysis of cardiac optical mapping data obtained with potentiometric dyes. *Am J Physiol Heart Circ Physiol* 303(7):H753–H765



- Law SH, Sargent TD (2014) The serine-threonine protein kinase PAK4 is dispensable in zebrafish: identification of a morpholino-generated pseudophenotype. *PLoS One* 9(6), e100268
- Lee J, Cao H, Kang BJ, Jen N, Yu F, Lee CA, Fei P, Park J, Bohlool S, Lash-Rosenberg L, Shung KK, Hsiai TK (2014) Hemodynamics and ventricular function in a zebrafish model of injury and repair. *Zebrafish* 11(5):447–454
- Lee L, Genge CE, Cua M, Sheng X, Rayani K, Beg MF, Sarunic MV, Tibbits GF (2016) Functional assessment of cardiac responses of adult zebrafish (*Danio rerio*) to acute and chronic temperature change using high-resolution echocardiography. *PLoS One* 11(1), e0145163
- Leong IU, Skinner JR, Shelling AN, Love DR (2010a) Identification and expression analysis of *kcnh2* genes in the zebrafish. *Biochem Biophys Res Commun* 396(4):817–824
- Leong IU, Skinner JR, Shelling AN, Love DR (2010b) Zebrafish as a model for long QT syndrome: the evidence and the means of manipulating zebrafish gene expression. *Acta Physiol (Oxf)* 199(3):257–276
- Li MX, Spyrapopoulos L, Sykes BD (1999) Binding of cardiac troponin-I147-163 induces a structural opening in human cardiac troponin-C. *Biochemistry* 38(26):8289–8298
- Lin E, Ribeiro A, Ding W, Hove-Madsen L, Sarunic MV, Beg MF, Tibbits GF (2014) Optical mapping of the electrical activity of isolated adult zebrafish hearts: acute effects of temperature. *Am J Physiol Regul Integr Comp Physiol* 306(11):R823–R836
- Lin E, Craig C, Lamothe M, Sarunic MV, Beg MF, Tibbits GF (2015) Construction and use of a zebrafish heart voltage and calcium optical mapping system, with integrated electrocardiogram and programmable electrical stimulation. *Am J Physiol Regul Integr Comp Physiol* 308(9):R755–R768
- Lionne C, Iorga B, Candau R, Travers F (2003) Why choose myofibrils to study muscle myosin ATPase? *J Muscle Res Cell Motil* 24(2-3):139–148
- Little AG, Seebacher F (2013) Thyroid hormone regulates cardiac performance during cold acclimation in Zebrafish (*Danio rerio*). *J Exp Biol*
- Liu B, Wohlfart B, Johansson BW (1990) Effects of low temperature on contraction in papillary muscles from rabbit, rat, and hedgehog. *Cryobiology* 27(5):539–546
- Liu TY, Lee PY, Huang CC, Sun L, Shung KK (2013) A study of the adult zebrafish ventricular function by retrospective Doppler-gated ultrahigh-frame-rate echocardiography. *IEEE Trans Ultrason Ferroelectr Freq Control* 60(9):1827–1837
- Llach A, Molina CE, Alvarez-Lacalle E, Tort L, Benitez R, Hove-Madsen L (2011) Detection, properties, and frequency of local calcium release from the sarcoplasmic reticulum in teleost cardiomyocytes. *PLoS One* 6(8), e23708
- Looger LL (2012) Running in reverse: rhodopsins sense voltage. *Nat Methods* 9(1):43–44
- Lutcke H, Murayama M, Hahn T, Margolis DJ, Astori S, Zum Alten Borgloh SM, Gobel W, Yang Y, Tang W, Kugler S, Sprengel R, Nagai T, Miyawaki A, Larkum ME, Helmchen F, Hasan MT (2010) Optical recording of neuronal activity with a genetically-encoded calcium indicator in anesthetized and freely moving mice. *Front Neural Circuits* 4:9
- Mateja RD, de Tombe PP (2012) Myofilament length-dependent activation develops within 5 ms in guinea-pig myocardium. *Biophys J* 103(1):L13–L15
- Mesirca P, Torrente AG, Mangoni ME (2014) T-type channels in the sino-atrial and atrioventricular pacemaker mechanism. *Pflügers Arch* 466(4):791–799
- Meyer A, Scharlt M (1999) Gene and genome duplications in vertebrates: the one-to-four (-to-eight in fish) rule and the evolution of novel gene functions. *Curr Opin Cell Biol* 11(6):699–704
- Milan DJ, Peterson TA, Ruskin JN, Peterson RT, MacRae CA (2003) Drugs that induce repolarization abnormalities cause bradycardia in zebrafish. *Circulation* 107(10):1355–1358
- Milan DJ, Jones IL, Ellinor PT, MacRae CA (2006) In vivo recording of adult zebrafish electrocardiogram and assessment of drug-induced QT prolongation. *Am J Physiol Heart Circ Physiol* 291(1):H269–H273

- Mironov SF, Vetter FJ, Pertsov AM (2006) Fluorescence imaging of cardiac propagation: spectral properties and filtering of optical action potentials. *Am J Physiol Heart Circ Physiol* 291(1): H327–H335
- Mittelstadt SW, Hemenway CL, Craig MP, Hove JR (2008) Evaluation of zebrafish embryos as a model for assessing inhibition of hERG. *J Pharmacol Toxicol Methods* 57(2):100–105
- Nagueh SF, Appleton CP, Gillebert TC, Marino PN, Oh JK, Smiseth OA, Waggoner AD, Flachskampf FA, Pellikka PA, Evangelisa A, Echocardiography AS (2009) Recommendations for the evaluation of left ventricular diastolic function by echocardiography. *Eur J Echocardiogr* 10(2):165–193
- Nair N, Geger C, Hatf A, Weber LP, Unniappan S (2016) Ultrasonography reveals in vivo dose-dependent inhibition of end systolic and diastolic volumes, heart rate and cardiac output by nesfatin-1 in zebrafish. *Gen Comp Endocrinol*
- Nasevicius A, Ekker SC (2000) Effective targeted gene ‘knockdown’ in zebrafish. *Nat Genet* 26(2):216–220
- Nemtsas P, Wettwer E, Christ T, Weidinger G, Ravens U (2010) Adult zebrafish heart as a model for human heart? An electrophysiological study. *J Mol Cell Cardiol* 48(1):161–171
- Novak AE, Jost MC, Lu Y, Taylor AD, Zakon HH, Ribera AB (2006) Gene duplications and evolution of vertebrate voltage-gated sodium channels. *J Mol Evol* 63(2):208–221
- Nygren A, Kondo C, Clark RB, Giles WR (2003) Voltage-sensitive dye mapping in Langendorff-perfused rat hearts. *Am J Physiol Heart Circ Physiol* 284(3):H892–H902
- Ohno S (1993) Patterns in genome evolution. *Curr Opin Genet Dev* 3(6):911–914
- Ohte N, Miyoshi I, Sane DC, Little WC (2009) Zebrafish with antisense-knockdown of cardiac troponin C as a model of hereditary dilated cardiomyopathy. *Circulation* 119(9):1595–1596
- Ovchinnikov S, Kamisetty H, Baker D (2014) Robust and accurate prediction of residue-residue interactions across protein interfaces using evolutionary information. *Elife* 3, e02030
- Palpant NJ, Houang EM, Delpont W, Hastings KE, Onufriev AV, Sham YY, Metzger JM (2010) Pathogenic peptide deviations support a model of adaptive evolution of chordate cardiac performance by troponin mutations. *Physiol Genomics* 42(2):287–299
- Parmacek MS, Solaro RJ (2004) Biology of the troponin complex in cardiac myocytes. *Prog Cardiovasc Dis* 47(3):159–176
- Patrick SM, Hoskins AC, Kentish JC, White E, Shiels HA, Cazorla O (2010) Enhanced length-dependent Ca<sup>2+</sup> activation in fish cardiomyocytes permits a large operating range of sarcomere lengths. *J Mol Cell Cardiol* 48(5):917–924
- Patrick SM, White E, Shiels HA (2011) Rainbow trout myocardium does not exhibit a slow inotropic response to stretch. *J Exp Biol* 214(Pt 7):1118–1122
- Poggesi C, Tesi C, Stehle R (2005) Sarcomeric determinants of striated muscle relaxation kinetics. *Pflügers Arch* 449(6):505–517
- Poss KD, Wilson LG, Keating MT (2002) Heart regeneration in zebrafish. *Science* 298(5601): 2188–2190
- Pugsley MK, Curtis MJ, Hayes ES (2015) Biophysics and molecular biology of cardiac ion channels for the safety pharmacologist. *Handb Exp Pharmacol* 229:149–203
- Qian X, Ba Y, Zhuang Q, Zhong G (2014) RNA-Seq technology and its application in fish transcriptomics. *OMICS* 18(2):98–110
- Rose T, Goltstein PM, Portugues R, Griesbeck O (2014) Putting a finishing touch on GECIs. *Front Mol Neurosci* 7:88
- Rottbauer W, Baker K, Wo ZG, Mohideen MAPK, Cantiello HF, Fishman MC (2001) Growth and function of the embryonic heart depend upon the cardiac-specific L-type calcium channel alpha 1 subunit. *Dev Cell* 1(2):265–275
- Rottbauer W, Wessels G, Dahme T, Just S, Trano N, Hassel D, Burns CG, Katus HA, Fishman MC (2006) Cardiac myosin light chain-2: a novel essential component of thick-myofilament assembly and contractility of the heart. *Circ Res* 99(3):323–331
- Schmitt N, Grunnet M, Olesen SP (2014) Cardiac potassium channel subtypes: new roles in repolarization and arrhythmia. *Physiol Rev* 94(2):609–653

- Scholz EP, Niemer N, Hassel D, Zitron E, Burgers HF, Bloehs R, Seyler C, Scherer D, Thomas D, Kathofer S, Katus HA, Rottbauer WA, Karle CA (2009) Biophysical properties of zebrafish ether-a-go-go related gene potassium channels. *Biochem Biophys Res Commun* 381(2): 159–164
- Sedmera D, Reckova M, deAlmeida A, Sedmerova M, Biermann M, Volejnik J, Sarre A, Raddatz E, McCarthy RA, Gourdie RG, Thompson RP (2003) Functional and morphological evidence for a ventricular conduction system in zebrafish and *Xenopus* hearts. *Am J Physiol Heart Circ Physiol* 284(4):H1152–H1160
- Seeley M, Huang W, Chen Z, Wolff WO, Lin X, Xu X (2007) Depletion of zebrafish titin reduces cardiac contractility by disrupting the assembly of Z-discs and A-bands. *Circ Res* 100(2): 238–245
- Sehnert AJ, Huq A, Weinstein BM, Walker C, Fishman M, Stainier DYC (2002) Cardiac troponin T is essential in sarcomere assembly and cardiac contractility. *Nat Genet* 31(1):106–110
- Shah AN, Davey CF, Whitebirch AC, Miller AC, Moens CB (2015) Rapid reverse genetic screening using CRISPR in zebrafish. *Nat Methods* 12(6):535–540
- Shattock MJ, Bers DM (1987) Inotropic response to hypothermia and the temperature-dependence of ryanodine action in isolated rabbit and rat ventricular muscle: implications for excitation-contraction coupling. *Circ Res* 61(6):761–771
- Shen Y, Lai T, Campbell RE (2015) Red fluorescent proteins (RFPs) and RFP-based biosensors for neuronal imaging applications. *Neurophotonics* 2(3):031203
- Shiels HA, Calaghan SC, White E (2006) The cellular basis for enhanced volume-modulated cardiac output in fish hearts. *J Gen Physiol* 128(1):37–44
- Shih YH, Zhang Y, Ding Y, Ross CA, Li H, Olson TM, Xu X (2015) Cardiac transcriptome and dilated cardiomyopathy genes in zebrafish. *Circ Cardiovasc Genet* 8(2):261–269
- Sidhu R, Anttila K, Farrell AP (2014) Upper thermal tolerance of closely related *Danio* species. *J Fish Biol* 84(4):982–995
- Sidi S, Busch-Nentwich E, Friedrich R, Schoenberger U, Nicolson T (2004) *gemin1* encodes a zebrafish L-type calcium channel that localizes at sensory hair cell ribbon synapses. *J Neurosci* 24(17):4213–4223
- Singh AR, Sivadas A, Sabharwal A, Vellarikal SK, Jayarajan R, Verma A, Kapoor S, Joshi A, Scaria V, Sivasubbu S (2016) Chamber specific gene expression landscape of the zebrafish heart. *PLoS One* 11(1), e0147823
- Sogah VM, Serluca FC, Fishman MC, Yelon DL, Macrae CA, Mably JD (2010) Distinct troponin C isoform requirements in cardiac and skeletal muscle. *Dev Dyn* 239(11):3115–3123
- Somero GN (2005) Linking biogeography to physiology: evolutionary and acclimatory adjustments of thermal limits. *Front Zool* 2(1):1
- Somero GN, Hochachka PW (1969) Isoenzymes and short-term temperature compensation in poikilotherms: activation of lactate dehydrogenase isoenzymes by temperature decreases. *Nature* 223(5202):194–195
- Spence R, Gerlach G, Lawrence C, Smith C (2008) The behaviour and ecology of the zebrafish, *Danio rerio*. *Biol Rev Camb Philos Soc* 83(1):13–34
- Steffen LS, Guyon JR, Vogel ED, Beltre R, Pusack TJ, Zhou Y, Zon LI, Kunkel LM (2007) Zebrafish orthologs of human muscular dystrophy genes. *BMC Genomics* 8:79
- Stehle R, Kruger M, Scherer P, Brixius K, Schwinger RH, Pfister G (2002) Isometric force kinetics upon rapid activation and relaxation of mouse, guinea pig and human heart muscle studied on the subcellular myofibrillar level. *Basic Res Cardiol* 97(Suppl 1):I127–I135
- Stehle R, Solzin J, Iorga B, Poggesi C (2009) Insights into the kinetics of Ca<sup>2+</sup>-regulated contraction and relaxation from myofibril studies. *Pflugers Arch* 458(2):337–357
- Stevens CM, Rayani K, Genge CE, Liang B, Roller JM, Li C, Singh G, Li YA, Tieleman DP, van Petegem F, Tibbits GF (2016) Functional characterization of cardiac and slow skeletal troponin C paralogs in zebrafish by MD simulation and isothermal titration calorimetry. *Biophys J* 111:38–49

- St-Pierre F, Marshall JD, Yang Y, Gong Y, Schnitzer MJ, Lin MZ (2014) High-fidelity optical reporting of neuronal electrical activity with an ultrafast fluorescent voltage sensor. *Nat Neurosci* 17(6):884–889
- Sun L, Lien CL, Xu X, Shung KK (2008) In vivo cardiac imaging of adult zebrafish using high frequency ultrasound (45–75 MHz). *Ultrasound Med Biol* 34(1):31–39
- Szuts V, Menesi D, Varga-Orvos Z, Zvara A, Houshmand N, Bitay M, Bogats G, Virag L, Baczko I, Szalontai B, Geramipour A, Cotella D, Wettwer E, Ravens U, Deak F, Puskas LG, Papp JG, Kiss I, Varro A, Jost N (2013) Altered expression of genes for Kir ion channels in dilated cardiomyopathy. *Can J Physiol Pharmacol* 91(8):648–656
- ter Keurs HE, Rijnsburger WH, van Heuningen R, Nagelsmit MJ (1980) Tension development and sarcomere length in rat cardiac trabeculae. Evidence of length-dependent activation. *Circ Res* 46(5):703–714
- Tian L, Hires SA, Mao T, Huber D, Chiappe ME, Chalasani SH, Petreanu L, Akerboom J, McKinney SA, Schreiter ER, Bargmann CI, Jayaraman V, Svoboda K, Looger LL (2009) Imaging neural activity in worms, flies and mice with improved GCaMP calcium indicators. *Nat Methods* 6(12):875–881
- Tsai CT, Wu CK, Chiang FT, Tseng CD, Lee JK, Yu CC, Wang YC, Lai LP, Lin JL, Hwang JJ (2011) In-vitro recording of adult zebrafish heart electrocardiogram – a platform for pharmacological testing. *Clin Chim Acta* 412(21-22):1963–1967
- Verkerk AO, Remme CA (2012) Zebrafish: a novel research tool for cardiac (patho)electrophysiology and ion channel disorders. *Front Physiol* 3:255
- Vornanen M (1998) L-type Ca<sup>2+</sup> current in fish cardiac myocytes: effects of thermal acclimation and beta-adrenergic stimulation. *J Exp Biol* 201(Pt 4):533–547
- Vornanen M (1999) Na<sup>+</sup>/Ca<sup>2+</sup> exchange current in ventricular myocytes of fish heart: contribution to sarcolemmal Ca<sup>2+</sup> influx. *J Exp Biol* 202(Pt 13):1763–1775
- Vornanen M, Hassinen M (2016) Zebrafish heart as a model for human cardiac electrophysiology. *Channels* 10(2):101–110
- Wang SQ, Huang YH, Liu KS, Zhou ZQ (1997) Dependence of myocardial hypothermia tolerance on sources of activator calcium. *Cryobiology* 35(3):193–200
- Warren KS, Baker K, Fishman MC (2001) The slow mo mutation reduces pacemaker current and heart rate in adult zebrafish. *Am J Physiol Heart Circ Physiol* 281(4):H1711–H1719
- Wei B, Jin JP (2011) Troponin T isoforms and posttranscriptional modifications: evolution, regulation and function. *Arch Biochem Biophys* 505(2):144–154
- Wood T, Thoresen M (2015) Physiological responses to hypothermia. *Semin Fetal Neonatal Med* 20(2):87–96
- Wu C, Sharma K, Laster K, Hersi M, Torres C, Lukas TJ, Moore EJ (2014a) Kcnq1-5 (Kv7.1-5) potassium channel expression in the adult zebrafish. *BMC Physiol* 14:1
- Wu J, Prole DL, Shen Y, Lin Z, Gnanasekaran A, Liu Y, Chen L, Zhou H, Chen SR, Usachev YM, Taylor CW, Campbell RE (2014b) Red fluorescent genetically encoded Ca<sup>2+</sup> indicators for use in mitochondria and endoplasmic reticulum. *Biochem J* 464(1):13–22
- Yin Z, Ren J, Guo W (2015) Sarcomeric protein isoform transitions in cardiac muscle: a journey to heart failure. *Biochim Biophys Acta* 1852(1):47–52
- Zhang PC, Llach A, Sheng XY, Hove-Madsen L, Tibbits GF (2011) Calcium handling in zebrafish ventricular myocytes. *Am J Physiol Regul Integr Comp Physiol* 300(1):R56–R66
- Zhao L, Zhao XY, Tian T, Lu QL, Skrbo-Larssen N, Wu D, Kuang Z, Zheng XF, Han YC, Yang SY, Zhang CM, Meng AM (2008) Heart-specific isoform of tropomyosin4 is essential for heartbeat in zebrafish embryos. *Cardiovasc Res* 80(2):200–208
- Zhao Y, Abdelfattah AS, Zhao Y, Ruangkittisakul A, Ballanyi K, Campbell RE, Harrison DJ (2014) Microfluidic cell sorter-aided directed evolution of a protein-based calcium ion indicator with an inverted fluorescent response. *Integr Biol (Camb)* 6(7):714–725

- Zhou W, Horstick EJ, Hirata H, Kuwada JY (2008) Identification and expression of voltage-gated calcium channel beta subunits in Zebrafish. *Dev Dyn* 237(12):3842–3852
- Zou J, Tran D, Baalbaki M, Tang LF, Poon A, Pelonero A, Titus EW, Yuan C, Shi C, Patchava S, Halper E, Garg J, Movsesyan I, Yin C, Wu R, Wilsbacher LD, Liu J, Hager RL, Coughlin SR, Jinek M, Pullinger CR, Kane JP, Hart DO, Kwok PY, Deo RC (2015) An internal promoter underlies the difference in disease severity between N- and C-terminal truncation mutations of Titin in zebrafish. *Elife* 4, e09406